ΕΘΝΙΚΟ ΚΑΙ ΚΑΠΟΔΙΣΤΡΙΑΚΟ ΠΑΝΕΠΙΣΤΗΜΙΟ ΑΘΗΝΩΝ
ΣΧΟΛΗ ΕΠΙΣΤΗΜΩΝ ΥΓΕΙΑΣ
ΙΑΤΡΙΚΗ ΣΧΟΛΗ

Τομέας Κοινωνικής Ιατρικής, Ψυχιατρικής και Νευρολογίας

Εργαστήριο Κλινικής, Πειραματικής Χειρουργικής και Μεταφραστικής Έρευνας του Ιδρύματος Ιατροβιολογικών Ερευνών της Ακαδημίας Αθηνών (Ι.ΙΒ.Ε.Α.Α)

Α' Νευρολογική Κλινική, Αιγινήτειο Νοσοκομείο
Διευθυντής: Στεφανής Λεωνίδας, Καθηγητής Νευρολογίας-Νευροβιολογίας

ΔΙΔΑΚΤΟΡΙΚΗ ΔΙΑΤΡΙΒΗ

Διερεύνηση της επίδρασης του στρες στις νευροεκφυλιστικές διεργασίες επαγόμενες από την πρωτεΐνη α-συνουκλεΐνη

Investigation of the effect of stress on neurodegenerative processes induced by the protein alpha-synuclein

Μόδεστος Νάκος Μπίμπος

Βιολόγος

Αθήνα, 2024

«Η υλοποίηση της Διδακτορικής Διατριβής συγχρηματοδοτήθηκε από την Ελλάδα και την Ευρωπαϊκή Ένωση (Ευρωπαϊκό Κοινωνικό Ταμείο) μέσω του Επιχειρησιακού Προγράμματος «Ανάπτυξη Ανθρώπινου Δυναμικού, Εκπαίδευση και Δια Βίου Μάθηση», 2014-2020, στο πλαίσιο της Πράξης «Ενίσχυση του ανθρώπινου δυναμικού μέσω της υλοποίησης διδακτορικής έρευνας- Υποδράση 2: Πρόγραμμα χορήγησης υποτροφιών ΙΚΥ σε υποψηφίους διδάκτορες των ΑΕΙ της Ελλάδας».

Ευρωπαϊκή Ένωση
Ευρωπαϊκό Κοινωνικό Ταμείο

Επιχειρησιακό Πρόγραμμα
Ανάπτυξη Ανθρώπινου Δυναμικού, Εκπαίδευση και Διά Βίου Μάθηση
Με τη συγχρηματοδότηση της Ελλάδας και της Ευρωπαϊκής Ένωσης

ΕΣΠΑ 2014-2020

ΕΘΝΙΚΟ ΚΑΙ ΚΑΠΟΔΙΣΤΡΙΑΚΟ ΠΑΝΕΠΙΣΤΗΜΙΟ ΑΘΗΝΩΝ
ΣΧΟΛΗ ΕΠΙΣΤΗΜΩΝ ΥΓΕΙΑΣ
ΙΑΤΡΙΚΗ ΣΧΟΛΗ

Τομέας Κοινωνικής Ιατρικής, Ψυχιατρικής και Νευρολογίας

Εργαστήριο Κλινικής, Πειραματικής Χειρουργικής και Μεταφραστικής Έρευνας του Ιδρύματος Ιατροβιολογικών Ερευνών της Ακαδημίας Αθηνών (Ι.ΙΒ.Ε.Α.Α)

Α' Νευρολογική Κλινική, Αιγινήτειο Νοσοκομείο
Διευθυντής: Στεφανής Λεωνίδας, Καθηγητής Νευρολογίας-Νευροβιολογίας

ΔΙΔΑΚΤΟΡΙΚΗ ΔΙΑΤΡΙΒΗ

Διερεύνηση της επίδρασης του στρες στις νευροεκφυλιστικές διεργασίες επαγόμενες από την πρωτεΐνη α-συνουκλεΐνη

Investigation of the effect of stress on neurodegenerative processes induced by the protein alpha-synuclein

Μόδεστος Νάκος Μπίμπος

Βιολόγος

Αθήνα, 2024

«Η υλοποίηση της Διδακτορικής Διατριβής συγχρηματοδοτήθηκε από την Ελλάδα και την Ευρωπαϊκή Ένωση (Ευρωπαϊκό Κοινωνικό Ταμείο) μέσω του Επιχειρησιακού Προγράμματος «Ανάπτυξη Ανθρώπινου Δυναμικού, Εκπαίδευση και Δια Βίου Μάθηση», 2014-2020, στο πλαίσιο της Πράξης «Ενίσχυση του ανθρώπινου δυναμικού μέσω της υλοποίησης διδακτορικής έρευνας- Υποδράση 2: Πρόγραμμα χορήγησης υποτροφιών ΙΚΥ σε υποψηφίους διδάκτορες των ΑΕΙ της Ελλάδας».

Ημερομηνία αίτησης υποψηφίου: **26/10/2018**

Ημερομηνία ορισμού τριμελούς συμβουλευτικής επιτροπής: **18/12/2018**

Ημερομηνία ορισμού θέματος: **15/03/2019**

Ημερομηνία κατάθεσης Διδακτορικής Διατριβής: **15/10/2024**

Τριμελής Συμβουλευτική Επιτροπή

1. (Επιβλέπων) **ΣΤΕΦΑΝΗΣ ΛΕΩΝΙΔΑΣ**
Καθηγητής, Ιατρική Σχολή, ΕΚΠΑ και Συνεργαζόμενος Ερευνητής Ι.ΙΒ.Ε.Α.Α

2. (Μέλος) **ΑΝΤΩΝΙΟΥ ΑΙΚΑΤΕΡΙΝΗ**
Καθηγήτρια, Ιατρική Σχολή, Πανεπιστήμιο Ιωαννίνων

3. (Μέλος) **ΔΑΛΛΑ ΧΡΙΣΤΙΝΑ**
Καθηγήτρια, Ιατρική Σχολή, ΕΚΠΑ

Ημερομηνία ορισμού 7μελούς εξεταστικής επιτροπής: **31/10/2024**

Ημερομηνία υποστήριξης διδακτορικής διατριβής: **22/11/2024**

Μέλη επταμελούς εξεταστικής επιτροπής

1. **ΧΡΟΥΣΟΣ ΓΕΩΡΓΙΟΣ** Καθηγητής, Ιατρική Σχολή, ΕΚΠΑ, Ελλάδα

2. **ΣΤΕΦΑΝΗΣ ΛΕΩΝΙΔΑΣ** Καθηγητής, Ιατρική Σχολή, ΕΚΠΑ, Ελλάδα

3. **ΔΑΛΛΑ ΧΡΙΣΤΙΝΑ** Καθηγήτρια, Ιατρική Σχολή, ΕΚΠΑ, Ελλάδα

4. **ΑΝΤΩΝΙΟΥ ΑΙΚΑΤΕΡΙΝΗ** Καθηγήτρια, Ιατρική Σχολή, Πανεπιστήμιο Ιωαννίνων, Ελλάδα

5. **LASHUEL HILAL** Assoc. Proffessor, Life Sciences, Swiss Federal Institute of Technology Lausanne, Switzerland

6. **ΒΛΑΧΟΥ ΣΤΥΛΙΑΝΗ** Assoc. Proffessor, School of Psychology, Dublin City University, Ireland

7. **ΠΑΛΗΚΑΡΑΣ ΚΩΝΣΤΑΝΤΙΝΟΣ** Επικ. Καθηγητής, Ιατρική Σχολή, ΕΚΠΑ, Ελλάδα

Πρόεδρος της Ιατρικής Σχολής: ΝΙΚΟΛΑΟΣ Φ. ΑΡΚΑΔΟΠΟΥΛΟΣ

Βαθμός: «ΑΡΙΣΤΑ»

Όρκος του Ιπποκράτη

"Ορκίζομαι στον Απόλλωνα τον Ιατρό και στον Ασκληπιό και στην Υγεία και στην πανάκεια και σ΄ όλους τους Θεούς επικαλούμενος την μαρτυρία τους, να τηρήσω πιστά κατά τη δύναμη και την κρίση μου αυτό τον όρκο και το συμβόλαιό μου αυτό. Να θεωρώ αυτόν που μου δίδαξε αυτή την τέχνη ίσο με τους γονείς μου και να μοιραστώ μαζί του τα υπάρχοντά μου και τα χρήματά μου αν έχει ανάγκη φροντίδας. Να θεωρώ τους απογόνους του ίσους με τ΄ αδέλφια μου και να τους διδάξω την τέχνη αυτή αν θέλουν να τη μάθουν, χωρίς αμοιβή και συμβόλαιο και να μεταδώσω με παραγγελίες, οδηγίες και συμβουλές όλη την υπόλοιπη γνώση μου και στα παιδιά μου και στα παιδιά εκείνου που με δίδαξε και στους άλλους μαθητές που έχουν κάνει γραπτή συμφωνία μαζί μου και σ΄ αυτούς που έχουν ορκισθεί στον ιατρικό νόμο και σε κανέναν άλλο και να θεραπεύω τους πάσχοντες κατά τη δύναμή μου και την κρίση μου χωρίς ποτέ, εκουσίως, να τους βλάψω ή να τους αδικήσω. Και να μη δώσω ποτέ σε κανένα, έστω κι αν μου το ζητήσει, θανατηφόρο φάρμακο, ούτε να δώσω ποτέ τέτοια συμβουλή. Ομοίως να μη δώσω ποτέ σε γυναίκα φάρμακο για ν΄ αποβάλει. Να διατηρήσω δε τη ζωή μου και την τέχνη μου καθαρή και αγνή. Και να μη χειρουργήσω πάσχοντες από λίθους αλλά ν΄ αφήσω την πράξη αυτή για τους ειδικούς. Και σ΄ όποια σπίτια κι αν μπω, να μπω για την ωφέλεια των πασχόντων αποφεύγοντας κάθε εκούσια αδικία και βλάβη και κάθε γενετήσια πράξη και με γυναίκες και με άνδρες, ελεύθερους και δούλους. Και ό,τι δω ή ακούσω κατά την άσκηση του επαγγέλματός μου, ή κι εκτός, για τη ζωή των ανθρώπων, που δεν πρέπει ποτέ να κοινοποιηθεί, να σιωπήσω και να το τηρήσω μυστικό. Αν τον όρκο μου αυτό τηρήσω πιστά και δεν τον αθετήσω, είθε ν΄ απολαύσω για πάντα την εκτίμηση όλων των ανθρώπων για τη ζωή μου και για την τέχνη μου, αν όμως παραβώ και αθετήσω τον όρκο μου να υποστώ τα αντίθετα από αυτά".

Curriculum Vitae

Education

December 2018: PhD candidate at the **Medical School of the National and Kapodistrian University of Athens** under the supervision of **Prof. Leonidas Stefanis MD, PhD** and Dr. **Alexia Polissidis, PhD** studying the **effect of stress in alpha synuclein-induced neurodegenerative processes.**

September 2016 – August 2018: Fundamental Neuroscience, Research Master in Cognitive and Clinical Neuroscience, Maastricht University, The Netherlands [Grade: **7.89/10**].

2010 – 2015: Degree in Biology, Aristotle University of Thessaloniki [Grade: **8.38/10**].

Research Experience

1. October 2020 – May 2021: Volunteer (part time) in the BRFAA's **Covid-19 diagnostic center in collaboration with the Hellenic National Public Health Organization.**

2. June – August 2019: Visiting PhD student at the Mailman School of Public Health, Department of Environmental Health Sciences at **Columbia University** under the supervision of **Dr. Diane Re.**

3. November 2017 – August 2018: Research Internship titled: **"Re-engineering a CRISPR-based epigenetic editing toolbox to study the role of 5-HT neurons in Alzheimer's Disease in an in vitro model of human neural progenitor cells"** at the Laboratory of Cancer Epigenetics and Biology Program (PEBC) in the **Bellvitge Institute for Biomedical Research** (IDIBELL), under the supervision of **Dr. Raul Delgado Morales** and **Dr. Daniël van den Hove**.

4. October – November 2017: Course on Laboratory Animal Science, (ex. Art.9 Experiments on Animals Act, FELASA A and B accredited) in The Netherlands.

5. February – May 2015: Erasmus Mobility for Placement Project at the Centre for Integrative Physiology (School of Biomedical Sciences) of the **University of Edinburgh**, under the supervision of **Dr. Emanuel Busch**, studying the physiology of neural circuits and behaviour in Caenorhabditis elegans.

6. August – October 2014: Practical training at the Laboratory of Experimental Neurology and Neuroimmunology, 2nd Department of Neurology of the **University Hospital "AHEPA"**, Thessaloniki, under the supervision of **Dr. Nikolaos Grigoriadis.**

Distinctions

- **Highest grade** in the Summer Graduation (1st among 30) **and 5th highest grade** among the 100 graduates of the academic year 2014 – 2015 **during my Bachelor's studies.**
- In June, 2022, I was awarded a **scholarship by the State Scholarships Foundation (IKY)** until the completion of my PhD.
- **Travel Award from the Japan Neuroscience Society** to participate and make an oral presentation at the 46th Annual Meeting.

- ❖ **Travel Award from the Mediterranean Neuroscience Society** to attend CISS2024 Catania International Summer School of Neuroscience 2024

Participation in Seminars / Conferences

- **FENS Featured Regional Meeting** (Thessaloniki, Greece, 2015)
- **EuroTau Meeting 2018** (Lille, France, 2018)
- **Synuclein meeting** (Porto, Portugal, 2019) [poster presentation]
- **28th Meeting of the Hellenic Society for Neuroscience** (Heraklion, Greece, 2019) [poster presentation]
- **15th International Conference on Alzheimer's & Parkinson's Diseases (AD/PD** (online, 2021) [e-poster presentation]
- **29th Meeting of the Hellenic Society for Neuroscience** (online, 2021) [e-poster presentation]
- **Neurobiology of Brain Disorders Conference GRC** (Barcelona, Spain, 2022) [poster presentation]
- **The 46th Annual Meeting of the Japan Neuroscience Society** (Sendai, Japan 2023) [oral presentation]
- **30th Meeting of the Hellenic Society for Neuroscience** (Athens, Greece 2023) [poster presentation]

Publications in peer-reviewed journals

1. **Nakos-Bimpos, M.**, Karali, K., Antoniou, C., Palermos, D., Fouka, M., Delis, A., Tzieras, I., Chrousos, G.P., Koutmani, Y., Stefanis, L. & Polissidis, A. (**2024**). Alpha-synuclein-induced stress sensitivity renders the Parkinson's disease brain susceptible to neurodegeneration. *Acta Neuropathologica Communications*, *12*(1), 100.
2. Nikolopoulos, D., **Nakos-Bimpos, M.**, Manolakou, T., Polissidis, A., & Boumpas, D. T. **(2024)**. Impaired serotonin synthesis in hippocampus of murine lupus represents an early neuropsychiatric event. *Lupus, 33*(2), 166-171.
3. Kowalczyk, J., **Nakos-Bimpos, M.**, Polissidis, A., Dalla, C., Kokras, N., Skalicka-Woźniak, K., & Budzyńska, B. (**2022**). Imperatorin Influences Depressive-like Behaviors: A Preclinical Study on Behavioral and Neurochemical Sex Differences. *Molecules*, *27*(4), 1179.
4. Tsoupri, E., Kostavasili, I., Kloukina, I., Tsikitis, M., Miliou, D., Vasilaki, E., Varela, A., **Nakos-Bimpos, M.**, ... & Capetanaki, Y. (**2021**). Myospryn deficiency leads to impaired cardiac structure and function and schizophrenia-associated symptoms. *Cell and Tissue Research*, *385*(3), 675-696.
5. Polissidis, A., Koronaiou, M., Kollia, V., Koronaiou, E., **Nakos-Bimpos, M.**, Bogiongko, M., ... & Stefanis, L. (**2021**). Psychosis-Like Behavior and Hyperdopaminergic Dysregulation in Human α-Synuclein BAC Transgenic Rats. *Movement Disorders*, *36*(3), 716-728.
6. Kowalczyk, J., **Nakos-Bimpos, M.**, Polissidis, A., Dalla, C., Kokras, N., Skalicka-Wozniak, K., & Budzynska, B. (**2021**). Xanthotoxin affects depression-related behavior and neurotransmitters content in a sex-dependent manner in mice. *Behavioural Brain Research*, *399*, 112985.
7. Polissidis, A., Petropoulou-Vathi, L., **Nakos-Bimpos, M.**, & Rideout, H. J. (**2020**). The Future of Targeted Gene-Based Treatment Strategies and Biomarkers in Parkinson's Disease. *Biomolecules*, *10*(6), 912.

Ευχαριστίες

Για την ολοκλήρωση της παρούσας διδακτορικής διατριβής χρειάστηκε η βοήθεια και η συμβολή πολλών ανθρώπων ανά τα χρόνια. Φτάνοντας στο τέλος της διαδρομής και κοιτάζοντας πίσω, νιώθω αρκετά τυχερός για τον τρόπο με τον οποίο εξελίχθηκε η πορεία μου στο εργαστήριο. Παρότι οι παράγοντες που συντέλεσαν σε αυτό ήταν πολλοί και διαφορετικοί, όπως θα αναφέρω και παρακάτω, όλα ξεκίνησαν και φυσικά επιστρέφουν στην επιστημονική μου υπεύθυνη, Δρ. Αλεξία Πολυσίδη. Από το γεγονός ότι με επέλεξε και με εμπιστεύτηκε για την πραγματοποίηση της ερευνητικής πρότασης που η ίδια είχε συλλάβει, μέχρι τον χρόνο που αφιέρωσε για να με εκπαιδεύσει, την εργασιακή της ηθική και τις πολυάριθμες ευκαιρίες για συνεργασίες και για την περαιτέρω επιστημονική εξέλιξη που μου προσέφερε, η Αλεξία ήταν πάντα εκεί. Μέσω της αλληλεπίδρασής μας όλα αυτά τα χρόνια, αυτό που αποκόμισα ήταν μια σχέση που βασιζόταν στην ειλικρινή επικοινωνία, την εμπιστοσύνη και την κατανόηση.

Στη συνέχεια, θα ήθελα να ευχαριστήσω θερμά τον επιβλέποντά μου, Δρ. Λεωνίδα Στεφανή, που μου έδωσε την ευκαιρία να εκπονήσω τη διατριβή μου σε ένα τόσο καλό — από επιστημονική καθώς και από άποψη ανθρώπινου δυναμικού — εργαστήριο. Επιπλέον, η προσήλωσή του και το ενδιαφέρον του για την έρευνα και την επιστήμη, σε συνδυασμό με την άμεση και αμέριστη υποστήριξή του, δε θα μπορούσαν παρά να αποτελέσουν πρότυπο κατά τη διάρκεια του διδακτορικού μου. Σε αυτό το σημείο, θα ήθελα επίσης να ευχαριστήσω και τα δύο άλλα μέλη της τριμελούς μου επιτροπής, ξεκινώντας από την Χριστίνα Δάλλα — η οποία πρώτη με έφερε σε επαφή με την Αλεξία — και την Κατερίνα Αντωνίου, τις οποίες εκτιμώ για την επιστημονική τους κατάρτιση και τον χαρακτήρα τους. Αμφότερες βοήθησαν στην ολοκλήρωση του διδακτορικού με τα σχόλιά και τις υποδείξεις τους, αλλά και εμπράκτως, ενώ χάρη σε αυτές είχα την ευκαιρία να γνωρίσω και τους εξαιρετικούς φοιτητές τους, Παυλίνα Παυλίδη, Χάρη Μπρακατσέλο και Γιώργο Ντούλα.

Επίσης, ευχαριστώ πολύ τα υπόλοιπα μέλη της επταμελούς εξεταστικής μου επιτροπής, που δέχτηκαν να συμμετάσχουν και να με τιμήσουν με την παρουσία και τις παρατηρήσεις τους σχετικά με τη διατριβή μου, τους Δρ. Χρούσο Γεώργιο, Lashuel Hilal, Βλάχου Στυλιανή και Παληκαρά Κωνσταντίνο. Εδώ θα ήθελα να κάνω ειδική μνεία στον Δρ. Χρούσο για τις πολύτιμες συμβουλές του και τα ενθαρρυντικά του λόγια, καθώς και στην ερευνήτρια Γιασεμή Κουμάνη για την καθοριστική τους συνεισφορά στη δημοσίευση ενός κομματιού από τη δουλειά που παρουσιάζεται εδώ. Θα ήθελα επίσης να ευχαριστήσω τους συνεργάτες μας Yogesh Singh (University of Tübingen), καθώς και τους Χριστίνα Μαντζουράνη και Γεώργιο Κόκοτο (Εθνικό και Καποδιστριακό Πανεπιστήμιο Αθηνών). Τέλος, δεν θα μπορούσε να λείπει η αναφορά στον φίλο — και εσχάτως συνεργάτη — Ραφαήλ Στρογγυλό, του οποίου η προθυμία και η προσφορά ήταν καθοριστικές σε πολλά κομμάτια της διατριβής.

Το διδακτορικό αυτό όμως δε θα είχε ολοκληρωθεί χωρίς τη βοήθεια και τη συνεργασία μιας σειράς ανθρώπων που θεωρώ ότι αποτελούν τη ραχοκοκαλιά του IIBEAA. Αναφέρομαι φυσικά στο προσωπικό της Μονάδας Ζωικών Προτύπων: Βαγγέλη Μπαλάφα, Βάσω Ρίζου, Παύλο Αλεξάκο, Νίκο Κουτσογιώργο, Κώστα Πασχίδη, Μαξιμιλιανό Χόρχε, Ευθύμη Παρώνη και Γιάννη Απέργη, με τους οποίους πέρασα πολλές εβδομάδες κάτω από

τη γη και οι οποίοι ήταν πάντα διαθέσιμοι και πρόθυμοι να με διευκολύνουν και φυσικά να μου συμπαρασταθούν σε οποιαδήποτε δυσκολία ανέκυπτε. Επιπλέον, ένα τεράστιο ευχαριστώ στους εργαζόμενους της Μονάδας Μικροσκοπίας, Δελή Τάσο, Παγκάκη Σταμάτη και Ελένη Ρηγανά, για τις αμέτρητες φορές που με βοήθησαν, την αδιάλειπτη προσοχή, την υπομονή και τον επαγγελματισμό τους.

Φυσικά, η καθημερινότητα στο εργαστήριο δε θα ήταν η ίδια χωρίς τους ανθρώπους με τους οποίους συνυπήρξαμε, εργαστήκαμε πλάι πλάι, χαρήκαμε για τα πειράματα που πήγαν καλά και απογοητευτήκαμε και πεισμώσαμε για αυτά που δεν πέτυχαν. Έχοντας περάσει από διαφορετικά εργαστήρια — σε Ελλάδα και εξωτερικό — κατά τη διάρκεια των σπουδών μου, είμαι σίγουρος ότι είναι σπάνιο σε ένα τόσο πολυπληθές εργαστήριο να περιτριγυρίζεσαι από τόσα αξιόλογα άτομα. Από την Φρόσω Κορωναίου, που αποτελεί την προσωποποίηση της συναδελφικότητας, τη Μαρία Φούκα με την ατελείωτη υπομονή, τα ανεξάντλητα κρυφά στοκ και την ικανότητα να έχει το νου της σε όποιο πείραμα τρέχει στους γειτονικούς πάγκους πέρα από τα δικά της, τον Μιχάλη Κέντρο και την Λίλιαν Πετροπούλου, των οποίων η βοήθεια, από τη μεμβρανοκοπτική έως τις ELISAs, υπήρξε σωτήρια, την απομονωμένη στον πάγκο της — αλλά άμεσα δίπλα σου σε περίπτωση ανάγκης — Μανού Λεάνδρου, έως τα πιο έμπειρα μέλη του εργαστηρίου, τη Μαρίνα Παπαδοπούλου, την Κατερίνα Μελαχροινού, την Μάντια Καραμπέτσου, πάντα διαθέσιμα να συμβουλεύουν και να συνεισφέρουν με τις γνώσεις τους. Φυσικά, δε θα μπορούσα να μην αναφερθώ στα ασταμάτητα μέλη της ομάδας Ξυλούρη, Φαίδρα, Μαρία, Δήμητρα, όπως και στην ίδια την Μαρία Ξυλούρη, αλλά και στους ερευνητές Hardy Rideout, Ευαγγελία Εμμανουηλίδου και Κώστα Βεκρέλη, καθώς και στην τεχνικό/σημείο αναφοράς του εργαστηρίου, Ματίνα Μανιάτη. Ακόμα, ένα ιδιαίτερο ευχαριστώ στην Γεωργία Ντερμεντζάκη για την υποστήριξη και την καθοδήγησή της κατά το σύντομο πέρασμά μου από τη Νέα Υόρκη. Τέλος, ένα τεράστιο ευχαριστώ στα μέλη του γκρουπ μας, Διονύση Παλέρμο, Κατερίνα Κάραλη και Χριστίνα Αντωνίου, με τους οποίους πέρασα αμέτρητες ώρες και των οποίων η δουλειά, η αδιαπραγμάτευτη προσφορά και βοήθεια συνέβαλαν καθοριστικά στην επιτυχή ολοκλήρωση του διδακτορικού.

Τέλος, θα ήθελα να ευχαριστήσω τους ανθρώπους που με στηρίζουν με κάθε δυνατό τρόπο και είναι εκεί σε κάθε μου βήμα: τη μητέρα μου Ιωάννα, τη σύντροφό μου Ελισάβετ, καθώς και τους φίλους μου στην Ελλάδα και στο εξωτερικό. Για όλους αυτούς τους ανθρώπους νιώθω ευγνωμοσύνη πέρα από κάθε πλαίσιο, αλλά η ολοκλήρωση του διδακτορικού σίγουρα αποτελεί μια πρώτης τάξεως ευκαιρία να τους εκφράσω την αγάπη μου.

Στο σωματείο και σε όλους τους ανθρώπους που αγωνίστηκαν
και αγωνίζονται για καλύτερες συνθήκες στην έρευνα

Abbreviations

3MT: 3-methoxytyramine

6-OHDA: 6-hydroxydopamine

Asyn: alpha-synuclein

AU: arbitrary units

BAC: bacterial artificial chromosome transgene (overexpressing the human full-length wildtype alpha-synuclein protein)

CMS: chronic mild stress

CNS: central nervous system

CORT: corticosterone

CRUST: chronic unpredictable stress

CUMS: chronic unpredictable mild stress

CRF: corticotropin releasing factor

DA: dopamine

DAB: diaminobenzidine

DAPI: 4',6-diamidino-2-phenylindole

DL: dorsolateral

DLB: dementia with Lewy bodies

DM: dorsomedial

DOPAC: 3,4-dihydroxyphenylacetic acid

ENS: enteric nervous system

EPM: elevated plus maze

FST: forced swim test

GABA: gamma-aminobutyric acid

GC: glucocorticoid

GFAP: glial fibrillary acidic protein

GI: gastrointestinal tract

GR: glucocorticoid receptor

HPA: hypothalamic-pituitary-adrenal

HVA: homovanillic acid

Iba1: ionized calcium binding adaptor molecule 1

IBD: inflammatory bowel disease

IBS: irritable bowel syndrome

IM: intramuscular

IP: intraperitoneal

KO: knock-out

LB: Lewy body

L-DOPA: levodopa

LC: locus coeruleus

LPS: lipopolysaccharide

METH: methamphetamine

MPTP: 1-methyl-4-phenyl-1,2,3,6-tetrahydropyridine

MR: mineralocorticoid receptor

NA: noradrenaline

NOS: nitric oxidase synthase

OF: open field

PD: Parkinson's disease

PFC: prefrontal cortex

PFF: pre-formed fibrils

PPI: prepulse inhibition

RN: raphe nucleus

ROS: reactive oxygen species

pS129: serine 129 phosphorylation

SDS: sodium dodecyl sulfate

SNg: substantia nigra

SNpc: substantia nigra pars compacta

Tg: transgenic

TH: tyrosine hydroxylase

Tx100: triton-x-100

V: ventral

VTA: ventral tegmental area

WT: wild type

Table of Contents

Περίληψη

Μία σύνδεση μεταξύ του χρόνιου στρες και της παθογένεσης της νόσου του Πάρκινσον (ΝΠ) έχει αρχίσει να αναδύεται. Πληθώρα στοιχείων υποστηρίζουν ότι η α-συνουκλεΐνη, μια πρωτεΐνη που εντοπίζεται στις συνάψεις των νευρωνικών κυττάρων, σχετίζεται άμεσα με την παθογένεση της ΝΠ. Ωστόσο, δεν είναι ακόμα γνωστό εάν το σύστημα του στρες δυσλειτουργεί πριν ή/και κατά τη ΝΠ, αν η α-συνουκλεΐνη εμπλέκεται σε αυτή τη δυσλειτουργία και αν συμβάλλουν από κοινού στη νευροεκφύλιση που χαρακτηρίζει τη νόσο.

Προκειμένου να διερευνήσουμε τα παραπάνω ερωτήματα, αξιολογήσαμε τη λειτουργία του άξονα του στρες σε διαγονιδιακούς επίμυες που υπερεκφράζουν την πλήρους μήκους ανθρώπινη α-συνουκλεΐνη (asyn BAC επίμυες) και πραγματοποιήσαμε μια πολύπλευρη φαινοτυπική αξιολόγηση της λειτουργίας του συστήματος του στρες και της ΝΠ έπειτα από την έκθεση σε χρόνιο στρες. Η υπερέκφραση της ανθρώπινης α-συνουκλεΐνης οδηγεί σε δυσλειτουργία του άξονα υποθαλάμου-υπόφυσης-επινεφριδίων (HPA) στους επίμυες, ενώ το χρόνιο απρόβλεπτο στρες καθως και η χρόνια χορήγηση κορτικοστερόνης επιδεινώνουν σημαντικά την εκφύλιση που παρατηρείται κατά μήκος του άξονα μέλαινας ουσίας – ραβδωτού σώματος, την έκφραση της φωσφορυλιωμένης α-συνουκλεΐνης στη θέση 129 (pS129) και τη νευροφλεγμονή, οδηγώντας στη μετάβαση - από ένα προδρομο σε έναν εμφανή - κινητικό φαινότυπο που σχετίζεται με τη ΝΠ. Ιδιαίτερο ενδιαφέρον παρουσιάζει το ότι η χρόνια χορήγηση κορτικοστερόνης στους asyn BAC επίμυες προκαλεί διπλασιασμό της έκφρασης της pS129 στον υποθάλαμο, μια περιοχή του εγκεφάλου που αποτελεί τον κύριο ρυθμιστή της αντίδρασης στο στρες, ενώ ο ιππόκαμπος, περιοχή που λειτουργεί τόσο ως ρυθμιστής όσο και ως στόχος της αντίδρασης στο στρες, παρουσιάζει επίσης αυξημένα επίπεδα pS129 και οδηγεί σε αλλαγές σε δείκτες σηματοδότησης του στρες.

Στον ιππόκαμπο των BAC ζώων, η αλληλεπίδραση μεταξύ του χρόνιου στρες και της ανθρώπινης α-συνουκλεΐνης διαταράσσει την έκφραση γονιδίων και κυτταρικών μονοπατιών που σχετίζονται με την ανάπτυξη των νευρώνων, τη λειτουργία των συνάψεων και τη νευροδιαβίβαση, αλλαγές που υποδεικνύουν εξασθενημένη εγκεφαλική συνδεσιμότητα και συναπτική επικοινωνία και απαντώνται στις νευροεκφυλιστικές διαταραχές. Επιπλέον, το χρόνιο στρες ενέτεινε περαιτέρω αυτές τις διαταραχές, οδηγώντας σε υπερέκφραση αντιοξειδωτικών καθώς και μονοπατιών που σχετίζονται με τη λειτουργία των μιτοχονδρίων προκειμένου να αντισταθμιστεί το αυξημένο κυτταρικό στρες.

Τα παραπάνω αποτελέσματα υποδηλώνουν ότι ο συνδυασμός στρες και παθολογίας που οφείλεται στην α-συνουκλεΐνη, επιταχύνει τη δυσλειτουργία των συνάψεων και την εξέλιξη της ΝΠ.

Τέλος, ενώ η υπερέκφραση της α-συνουκλεΐνης στους BAC επίμυες οδηγεί σε ένα προφίλ μικροβιώματος και μεταβολιτών παρόμοιο με αυτό που απαντάται σε ασθενείς με ΝΠ, και τα δύο πρωτόκολλα πρόκλησης στρες οδηγούν στην υπερέκφραση των ίδιων πληθυσμών μικροβίων τόσο στους BAC όσο και στους αγρίου τύπου (WT) επίμυες. Επιπλέον, το στρες αλληλεπιδρά με το BAC γονότυπο, αποκαλύπτοντας σημαντικές μεταβολές στους πληθυσμούς *Subdoligranulum* και *Peptococcus*. Παρότι η επίδραση του συστήματος του εντέρου καθώς και οι παρατηρούμενες αλλαγές στα επίπεδα των μεταβολιτών και των διαφορετικών πληθυσμών του μικροβιώματος είναι πολύπλοκες και πολυεπίπεδες, τα ευρήματα αυτά παρουσιάζουν την ευκαιρία να ταυτοποιηθούν, να απομονωθούν και να αξιολογηθούν συγκεκριμένα βακτηριακά είδη για τις επιζήμιες ή ευεργετικές επιδράσεις τους στην αποκατάσταση της φυσιολογικής λειτουργίας του εντέρου και της ευβίωσης, και έμμεσα, η επίδρασή τους στη νευροεκφύλιση.

Συνολικά, τα αποτελέσματά μας συνδέουν την επίδραση του στρες μέσω της αναδυόμενης δυσλειτουργίας του άξονα μικροβιώματος-εντέρου-εγκεφάλου με την α-συνουκλεΐνη και παρέχουν στοιχεία για το ότι τα αυξημένα επίπεδα γλυκοκορτικοειδών μπορούν να συμβάλουν στη νευροεκφύλιση που προκαλείται από την α-συνουκλεΐνη, οδηγώντας τελικά από ένα προδρομο σε έναν εμφανή παρκινσονικό φαινότυπο.

Abstract

An emerging connection between chronic stress and the pathogenesis of Parkinson's disease (PD) is gaining increased attention. Despite the plethora of evidence linking the presynaptic neuronal protein alpha-synuclein (asyn) to PD pathogenesis, it remains unclear whether stress system dysfunction is present in PD, if asyn is involved, and if both together promote neurodegeneration.

To explore these questions, we evaluated stress axis function in transgenic rats overexpressing full-length human asyn (asyn BAC rats) and performed multi-level stress and PD phenotyping following two different paradigms of chronic stress exposure. While the transgenic rats overexpressing human wildtype asyn are characterized by hypothalamic-pituitary-adrenal (HPA) axis dysregulation, chronic unpredictable stress and corticosterone exposure further intensify nigrostriatal degeneration, increased serine129 phosphorylated asyn (pS129), and neuroinflammation, ultimately leading to phenoconversion from a prodromal to an overt motor PD phenotype. Notably, chronic corticosterone in asyn BAC rats leads to a robust, twofold increase in pS129 levels in the hypothalamus, the master regulator of the stress response, while the hippocampus, both a regulator and target of stress, also shows elevated pS129 asyn and altered stress signaling.

In BAC rats, chronic stress and human asyn disrupt genes and cellular pathways linked to neuronal development, synaptic function, and neurotransmitter signaling in the hippocampus, indicating impaired brain connectivity and synaptic function—archetypal features of neurodegenerative diseases. Chronic stress further amplifies these disruptions, leading to compensatory upregulation of mitochondrial and detoxification pathways, highlighting increased cellular stress suggesting that the combination of stress and asyn pathology accelerates synaptic dysfunction and the progression of PD.

Additionally, asyn overexpression in BAC rats reproduces a microbiota profile of genera and metabolites similar to those observed in PD patients, with both stress paradigms leading to the upregulation of the same microbiota populations in BAC and WT rats. Stress interaction with the BAC genotype, reveals significant changes in *Subdoligranulum* and *Peptococcus* populations. While the impact of enteric system changes and microbiome shifts is complex, these findings provide an opportunity to identify and evaluate specific bacterial species for their potential protective or harmful effects on restoring normal gut function and eubiosis, and indirectly, on neurodegeneration.

Taken together, our findings link stress to asyn through microbiota-gut-brain axis dysregulation and provide evidence that elevated circulating glucocorticoids can contribute to asyn-induced neurodegeneration, ultimately triggering phenoconversion from prodromal to overt PD.

I. Introduction

1. Epidemiology & symptoms of Parkinson's disease

On an aging planet where neurological disorders have become the major cause of disability, Parkinson's disease (PD) notoriety grows along with the number of patients worldwide (Carroll, 2019). It is estimated that the prevalence of PD has more than doubled since 1990, thus exceeding the growth of Alzheimer's disease (Dorsey et al., 2018). PD is a neurodegenerative disorder characterized by the loss of dopaminergic neurons in the substantia nigra pars compacta (SNpc) and by the presence of cytoplasmic alpha-synuclein (asyn)-rich inclusions termed Lewy bodies (LBs) (Illus. 1). The hallmark motor symptoms of PD are bradykinesia, rigidity, resting tremor, and late postural instability (Bloem et al., 2021). While the incidence of PD rises with age, along with the manifestation of the characteristic motor symptoms, a prodromal phase of the disease may be lurking for up to two decades before diagnosis (Schapira et al., 2017). A number of non-motor symptoms, such as autonomic, sleep, neuropsychiatric, cognitive, olfactory and gastrointestinal (GI) dysfunctions, manifest years before the onset of the more typical motor symptoms and might even inflict a heavier burden than motor symptoms, especially in late stage PD patients (Prakash et al., 2016; Hermanowicz et al., 2019). Interestingly, male sex is associated with higher disease incidence, prevalence, earlier onset, more severe motor symptoms, faster progression and more frequent cognitive decline (Meoni et al., 2020).

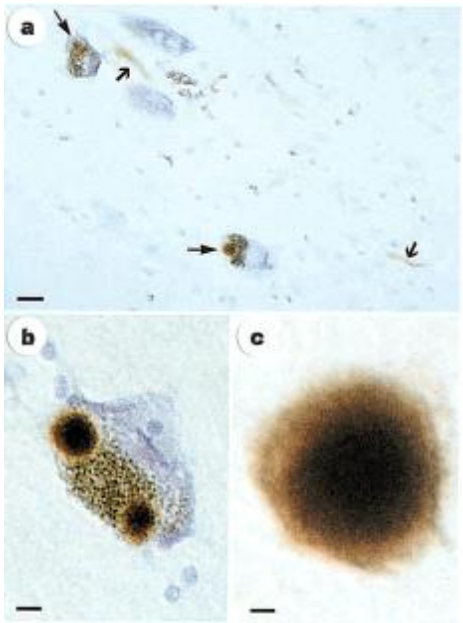

Illustration 1. Substantia nigra from PD patients stained for asyn; a) Pigmented nerve cells, each containing an asyn-positive LB (thin arrows). Lewy neurites (thick arrows) are also immunopositive (scale bar, 20 mm). b) A pigmented nerve cell with two asyn-positive LBs. Scale bar, 8 mm. c) Asyn positive, extracellular LB (scale bar, 4 mm). Source: Spillantini et al., 1997.

2. Key moments in PD research highlighting the role of asyn in the disease

The year 1997 was seminal for PD research since the protein asyn was identified as a main component of LBs (Spillantini et al., 1997) while a mutation in *SNCA* - the gene encoding asyn - was characterized as the first genetic locus causing PD (with a penetrance of approximately 85%) in a well-studied Italian family, the Contursi kindred (Polymeropoulos et al., 1997). Since the discovery of the A53T mutation (Polymeropoulos et al., 1997), seven more point mutations located in the *SNCA* gene have been linked with PD pathogenecity in an autosomal dominant manner; A30P (Krüger et al., 1998), E46K (Zarranz et al., 2004), G51D (Lesage et al., 2013), H50Q (Appel-Cresswell et al., 2013), A53E (Pasanen et al., 2014), A53V (Yoshino et al., 2017) and A30G (Liu et al., 2021). While in some of these highly penetrant PD mutations symptoms appear early and the disease has a rapid progression taking a heavy toll on cognition, the total number of mutation carriers is rather low. Apart from point mutations in the asyn gene, duplication and triplication of *SNCA* were also found to cause PD (Chartier-Harlin et al., 2004; Singleton et al., 2003). Though the etiology of PD is multifaceted, ample evidence point towards complex interactions of genetic variants with environmental risk factors and aging, with the majority of cases being idiopathic (iPD) and familial cases accounting for approximately 10% of all cases (Van Den Eeden et al., 2003; Gasser, 2009). While over 20 disease-causing gene loci have been linked to PD, genome-wide association studies (GWAS) and next generation sequencing (NGS) studies have identified 90 independent variants - many of which are of unknown significance - that increase the risk of iPD (Blauwendraat et al., 2019; Cali et al., 2019). While it was suspected that genetic variability in the promoter of the gene encoding asyn contributes to the risk of developing PD, a GWAS identified *SNCA* as a major risk locus across Caucasian and Asian populations of iPD patients (Farrer et al., 2001; Simón-Sánchez et al., 2009). Additionally, polymorphisms associated with PD adjacent to the *SNCA* locus may increase neuronal asyn expression levels (Soldner et al., 2016). In 2003, asyn was first traced in culture media and in extracellular biological fluids (including CSF and plasma), showing that asyn is normally secreted both *in vitro* and *in vivo* (El-Agnaf et al., 2003). Following the identification of asyn-positive LBs in grafted fetal mesencephalic DA neurons years after transplantation in PD patients, it was found that asyn can spread via endocytosis to neighboring neurons, thus providing the first evidence of cell-to-cell asyn propagation (Kordower et al., 2008; J.-Y. Li et al., 2008; Desplats et al., 2009). Around the same time, it was shown for the first time - *in vitro* - that asyn can be secreted by exosomes in a calcium-dependent manner, aggravating PD-related pathology (Emmanouilidou et al., 2010). Moreover, synthetic asyn fibrils (PFFs)

efficiently seed the aggregation and fibrillization of soluble endogenous asyn *in vivo*, leading to transynaptic spreading of pathological asyn in anatomically interconnected regions, recapitulating a neurodegenerative cascade and the main pathological features of the disease (Luk et al., 2012; Karampetsou et al., 2017). A year following the discovery that asyn can cross the BBB in both directions (Sui et al., 2014), it was reported that following intravenous (IV) injection, different asyn strains spread to the CNS, displaying different seeding and pathology-inducing capacities resembling traits of different synucleinopathies (Peelaerts et al., 2015). Apart from discoveries regarding the genetics or spreading of asyn, the recent development of the seeding amplification assay (SAA) is a breakthrough in the field of diagnostics thanks to the ability of the method to detect PD with high sensitivity and specificity by amplifying small amounts of misfolded asyn aggregates in CSF from PD patients, even before the onset of clinical symptoms. The SAA was able to detect sporadic PD with a sensitivity of 88% and a specificity of 96% among normal controls, also displaying high sensitivity in detecting PD among individuals with prodromal conditions such as rapid eye movement (REM), sleep behavior disorder and loss of smell. This advancement in diagnostic capability is crucial as it allows for earlier [than traditional methods like DaTscans (de la Fuente-Fernández, 2012)] detection and intervention, potentially leading to better patient outcomes (Siderowf et al., 2023). Finally, performance of a SAA for misfolded asyn in CSF and brain tissue, detected most patients with LB pathology at Braak stages 3 and all the patients at stage >3, also enabling the assessment of the severity and progression of the disease providing information regarding pathology burden (Bentivenga et al., 2024).

The existence of pathogenic variants and of multiplications in the *SNCA* gene suggests that asyn plays a causal role in PD. A deeper understanding of native asyn function is essential, not only to enhance therapeutic approaches aiming at the reduction of extracellular and/or intracellular asyn or to promote the native over the pathological states, but also to decipher the initiation and development of the disease. Findings from the use of various KO cell and animal models, such as triple KO mice lacking all the members of the synuclein family (alpha-, beta- and gamma-synuclein) (Greten-Harrison et al., 2010; Anwar et al., 2011) or conditional KO mice (Ninkina et al., 2020), converge toward the fact that loss of asyn does not lead to neurodegeneration. Additionally, findings from population-based studies support the notion that lower asyn levels are associated with a lower risk of developing PD; individuals with deletion of one *SNCA* allele do not exhibit features of PD motor symptoms or dementia (Blauwendraat et al., 2019).

On the other hand, genetic, pathological and molecular evidence support the hypothesis that elevated asyn levels are central to the misfolding process, with increased protein accumulation driving aggregation through oligomerization, fibril formation and eventually creation of the characteristic inclusions (Courte et al., 2020; Vasili et al., 2022). Characteristically, *SNCA* gene triplication cases have a more severe disease phenotype compared to duplication cases providing support for a gain-of-function effect of asyn (Singleton et al., 2003). However, it is also possible that misfolding and aggregation can occur through mechanisms that are not directly related to protein levels with these alternative theories not being necessarily mutually exclusive.

At this point, it is important to note that since spontaneous pathology has not been replicated neither in genetic nor in environmental models showing aggregation, current modeling relies on either genetic modifications or experimental conditions that induce aggregation artificially. Most PD models rely on overexpressing asyn or using external triggers to induce aggregation, rather than replicating the spontaneous aggregation observed in human disease (Lázaro et al., 2014; Giráldez-Pérez et al., 2014). Despite the lower occurrence of genetic PD, the advantage of studying these cases - from a molecular perspective - is that they offer valuable insights into the pathoetiology and the development of the disorder. For this reason, animal models based on mutations and/or multiplications of disease-causing genes such as *SNCA* are more accurate in terms of translatability and can be used as a starting point from where researchers can study PD by incorporating other important aspects of the disease, such as aging or environmental factors.

While the involvement of asyn in PD cannot be disputed, a deeper understanding of its contribution to the disease will be significantly enhanced by elucidating its normal physiological functions.

3. Introduction to asyn and its physiological roles

Asyn is a small, natively unfolded protein, consisting of 140 amino acids divided into three main protein regions: the N terminus (residues 1–60), the non-amyloid-β component (NAC) region (residues 61–95), known for its tendency to form aggregates and the C terminus (residues 96–140) (Illus. 2). Despite being abundant in pre-synaptic terminals across the CNS (Maroteaux et al., 1988; Iwai et al., 1995), asyn is also present in various other locations including the gut (Qualman et al., 1984; Wakabayashi et al., 1988, 1990; Braak et al., 2006), the red blood cells (Barbour et al., 2008), the heart (Iwanaga et al., 1999; Orimo et al., 2008; Fujishiro et al., 2008), the muscles (Askanas et al., 2000), but also in

different subcellular compartments, including the nucleus (Pinho et al., 2019). *In vivo* targeted expression of asyn in the nucleus results in a more pronounced PD-like phenotype, compared to cytoplasmic asyn expression. Nuclear expression of asyn is characterized by increased loss of dopaminergic neurons along with greater motor impairments as well as formation of inclusions containing high molecular weight (HMW) asyn species (Du et al., 2024). Moreover, asyn nuclear inclusions lead to transcriptomic changes such as increased expression of p21 -a master regulator of senescence whose overexpression promotes cell death (Mansour et al., 2023)- and of genes related with senescence-associated secretory phenotype, gliosis, inflammation and DNA damage (Du et al., 2024).

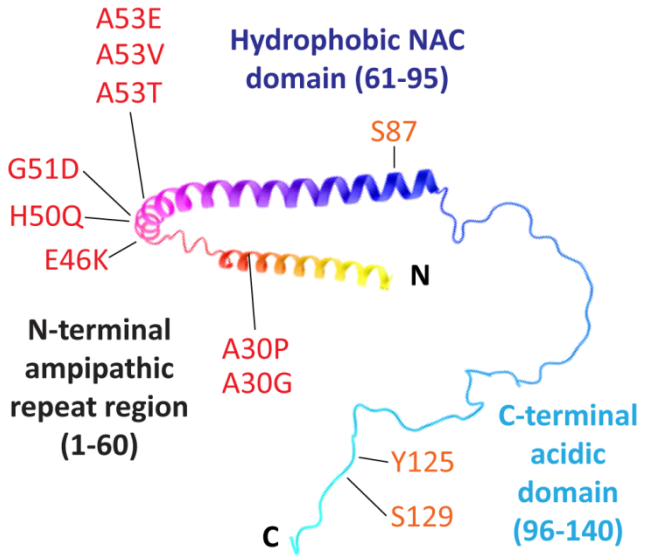

Illustration 2. Schematic representation of the asyn protein structure, consisting of 140 amino acids and three distinct regions: the N-terminal amphipathic domain, where PD mutations (A30P/G, E46G, H50Q, G51D, A53T/V/E) are located, the central NAC region, responsible for aggregate formation and the C-terminal domain, which is involved in post-translational modifications (Y125, S129).

A number of studies focusing on the physiological role of asyn in the nerve terminals provide evidence that it is involved in maintaining synaptic integrity and plays an important role in the regulation of dopamine (DA) biosynthesis and pre-synaptic release (Abeliovich et al., 2000; Perez et al., 2002; S. Chandra et al., 2004), as well as of other neurotransmitters such as norepinephrine (Yavich et al., 2006) and glutamate (Gureviciene et al., 2007). A number of the proposed roles for asyn in synapses, such as regulating synaptic plasticity, DA levels and synaptic vesicles trafficking, are related to asyn's ability to interact with cell membranes (Burré et al., 2018). Despite being structurally disordered in solution, asyn

adopts a partially structured form when bound to membranes. Presynaptically, asyn binds to synaptobrevin-2 (VAMP2), a key component of the SNARE complex, to promote its assembly. This interaction facilitates the docking and fusion of synaptic vesicles; essential processes for the release of neurotransmitters (Burré et al., 2010). Additionally, asyn shows a particular preference for small, highly curved synthetic vesicles through its N terminus (Bell & Vendruscolo, 2021). Both N and C termini interactions are regulated by calcium which facilitates the localization of asyn at the presynaptic terminal. Calcium or asyn levels imbalance can lead to synaptic vesicle clustering *ex vivo* and *in vitro* (Lautenschläger et al., 2018). While clathrin-mediated endocytosis is the physiological mechanism of vesicle retrieval (Granseth et al., 2006), asyn and poly-unsaturated fatty acids also contribute to endocytosis by the recycling of synaptic vesicles upon neuronal stimulation (Ben Gedalya et al., 2009).

Moreover, asyn is physiologically involved in maintaining DA homeostasis by regulating the levels of DA transporter (DAT) between cell surface and intracellular compartments via clathrin-mediated endocytosis (Kisos et al., 2014). While asyn localization in the nerve terminals is well documented, asyn KO in animals has little to no effect on synaptic neurotransmission, while asyn overexpression leads to decreased synaptic vesicle density at the active zone and impaired re-clustering of synaptic vesicles after endocytosis. Interestingly, the aforementioned physiological defect in synaptic vesicle recycling is observed before any obvious signs of neuropathology (Nemani et al., 2010). Recently, a long sought physiological action of asyn was observed *in vivo* as the protein was found to both facilitate and depress DA release, depending on the length of the intervals between bursts of action potentials. These findings, influenced by specific temporal patterns of neuronal activity, seem to be independent of the presence of other members of the synuclein family or of presynaptic calcium levels. Rapid facilitation of DA release is hypothesized to rely on enhanced fusion of synaptic vesicles at active zones during exocytosis while depression is attributed to synaptic exhaustion (Somayaji et al., 2020).

DAT is responsible for the reuptake of DA from the synaptic cleft back into the presynaptic neuron, a process critical for the termination of DA signaling and recycling. Transient interaction between DAT and asyn at the plasma membrane leads to increased DAT-mediated membrane depolarization and DA efflux leading to decreasing the uptake of the neurotransmitter (Swant et al., 2011; Butler et al., 2015). Additionally, cellular stress and damage induced by asyn aggregates can further reduce DA; in a Drosophila model of

synucleinopathy, human asyn accumulated in presynaptic terminals causing a reduction in key synaptic proteins like cysteine string protein, synapsin and syntaxin 1A. These alterations impair neuronal function, resulting in behavioral deficits in Drosophila and dopaminergic neuron degeneration both in aging Drosophila and in brain samples of dementia with LB patients. These findings suggest that asyn-induced presynaptic dysfunction initiates synaptopathy, contributing to behavioral deficits and eventual dopaminergic neuron loss akin to synucleinopathies' early stages (Bridi et al., 2021). Localization of DAT on the plasma membrane or in the intracellular space is frequently influenced by interactions with trafficking and regulatory proteins. Under physiological conditions, asyn regulates DAT activity by anchoring the transporter to the microtubular network while in early stages of PD pathogenesis, asyn finely modulates the dopaminergic synapse by controlling the subcellular distribution of key proteins, including DAT (Wersinger & Sidhu, 2005; Bellucci et al., 2011; Butler et al., 2015).

Studies have shown that the abundance and composition of cell surface N-methyl-D-aspartate (NMDA) receptors (NMDARs) are altered in experimental Parkinsonism models and in PD patients. The involvement of asyn in promoting clathrin-mediated endocytosis implies the protein's potential role in regulating NMDAR trafficking from the cell surface to intracellular compartments (Ben Gedalya et al., 2009). The first evidence of asyn and NMDARs interaction were reported following the discovery that asyn can induce endocytosis of surface NR1 subunits of the NMDARs through a mechanism involving clathrin and RAB5B, resulting in NMDA-induced cell death in dopaminergic cell cultures *in vitro* (Cheng et al., 2011). Moreover, asyn oligomers, especially those present in the plasma of PD patients, enhance the ability of asyn to induce GluN1 subunit internalization, potentially via a clathrin-mediated endocytosis pathway (Yu et al., 2019). In the striatum, asyn levels increase with age, showing a negative correlation with GluN1 expression while cells treated with asyn oligomers exhibit a greater reduction in NMDA-evoked calcium influx compared to those treated with monomers, with this reduction being reversed by a clathrin inhibitor. These findings suggest that age-related accumulation of asyn monomers and oligomers affects the reduction of surface NMDAR expression differently in specific brain regions (W. Yang et al., 2020). Oligomeric asyn can directly impact synaptic transmission and plasticity in PD models by reducing NMDAR-mediated synaptic currents and impairing corticostriatal long-term potentiation of striatal spiny projection neurons (SPNs), with injections of asyn in the striatum, leading to selective targeting of the NMDR subunit GluN2A both *in vitro* and *ex vivo* (Durante et al., 2019). Rabphilin-3A (Rph3A) is a synaptic protein originally identified as

being associated with synaptic vesicles, playing a role in regulating exocytosis and endocytosis at presynaptic sites. In excitatory dendritic spines, Rph3A is necessary for maintaining synaptic NMDARs by directly interacting with the GluN2A regulatory subunit (Burns et al., 1998). While intrastriatal injection of asyn PFFs in mice leads to an early loss of striatal synapses accompanied by reduced synaptic levels of Rph3A and disrupted interaction between Rph3A and NMDARs, both Rph3A overexpression and the use of a small molecule disrupting the Rph3A/asyn complex, prevent the loss of dendritic spines in SPNs and the early motor defects. The involvement of Rph3A in mediating asyn-induced synaptic toxicity across different brain regions is also confirmed in primary hippocampal neurons in vitro (Ferrari et al., 2022). These findings support the hypothesis that asyn selectively impacts the function of specific NMDARs across different neuronal subtypes, suggesting that the unique characteristics of postsynaptic receptors may play a crucial role in determining synaptic vulnerability of different neuronal populations (Calabresi et al., 2023).

4. Post-translational modifications of asyn

While asyn found in LBs is predominantly hyperphosphorylated, there is a number of post-translational modifications including nitration (Paxinou et al., 2001), ubiquitination (Nonaka et al., 2005) and C-terminal truncation (W. Li et al., 2005) affecting asyn's properties. While phosphorylation at the serine-129 site (pS129) of asyn is the most commonly studied phosphorylation (Anderson et al., 2006), other sites such as serine-87 (S87) (Paleologou et al., 2010) and tyrosine-125 (Y125) (Lu et al., 2011) are additional sites that can be phosphorylated and have been detected in LBs.

4a. Serine-129 phosphorylation of asyn

Phosphorylation of asyn at the serine-129 (Ser129) is a known pathological hallmark of synucleinopathies, significantly impacting its aggregation, toxicity, and interaction with cellular membranes. Under normal physiological conditions, only a small fraction of asyn is phosphorylated in different brain regions, indicating intrinsic regulation. Neuronal activity increases pS129 asyn, triggering essential protein-protein interactions at synapses while preventing pS129 blocks asyn activity-dependent synaptic function. It is suggested that pS129 induces conformational changes that facilitate interactions with binding partners (Parra-Rivas et al., 2023). Over 20 years ago, mass spectrometry measurements found pS129 to be significantly elevated in synucleinopathy lesions. Moreover, pS129 promotes the formation of fibrils *in vitro*, suggesting a crucial role for this modification in the pathogenesis of neurodegenerative disorders characterized by filamentous protein aggregation (Fujiwara

et al., 2002). Mutation of serine (Ser129) to alanine (S129D) (preventing phosphorylation at this site) suppresses dopaminergic neuronal loss induced by human asyn expression in a Drosophila model. Conversely, substituting Ser129 with aspartate (S129D) (mimicking constitutive phosphorylation) intensifies asyn toxicity. Inhibition of pS129 significantly enhances aggregate formation, highlighting its critical role in pathology development. Interestingly, increased inclusion bodies pathology correlated with reduced toxicity, potentially shielding neurons from asyn's detrimental effects (L & Mb, 2005). While small amounts of pS129 asyn are present in the soluble fraction of both healthy and PD brains, ubiquitination is solely observed in LBs and mainly on phosphorylated synuclein, suggesting it occurs after the accumulation of pS129 asyn in LBs. This pattern of phosphorylation, truncation and ubiquitination is also consistently seen across the brains of PD patients carrying the A53T mutation and in Multiple Systems Atrophy (MSA), indicating a common pathogenic pathway for both genetic and sporadic LB diseases where the preferential accumulation of naturally occurring pS129 asyn is the primary mechanism leading to LB formation (Anderson et al., 2006). A direct *in vivo* link between pS129 asyn and disease progression was uncovered using an adeno-associated virus (AAV) to overexpress human WT asyn and two different human asyn mutants (S129A and S129D). Notably, following AAVs injections in the substantia nigra (SNg), the non-phosphorylatable form of asyn (S129A) worsened nigral pathology, whereas phosphorylation of Ser129 prevented asyn-induced degeneration along the nigrostriatal pathway (Gorbatyuk et al., 2008). Detailed analysis of the amino acid sequence of all the synucleins across humans and other species, indicates that most of the potential phosphorylation sites are highly conserved, suggesting that phosphorylation may be crucial for regulating physiological functioning in both healthy and diseased states (Oueslati et al., 2010). *In vitro* experiments reported that pS129 increases the conformational flexibility of asyn and prevents fibrillogenesis, without affecting its membrane-bound structure. However, phosphorylation mimicking mutants S129A or S129D do not reproduce the effects of actual phosphorylation at the Ser129 site on the structural and aggregation properties of asyn, indicating that results obtained using these mimics should be interpreted cautiously (Paleologou et al., 2008). In rats injected with recombinant AAVs expressing either WT human or asyn mutants S129A/D, both WT and mutant asyn led to significant dopaminergic cell loss, with only minor reductions in nigrostriatal terminal density and tyrosine hydroxylase (TH) expression without any further differences among the different conditions. Additionally, there were no differences observed in asyn aggregation or distribution between WT and Ser129 mimicking mutants (McFarland et al., 2009). These

findings, suggesting that both Ser129 mutants and WT asyn induce dopaminergic neurotoxicity with the same intensity, differ from previously reported results, possibly due to neuronal toxicity linked to AAV-mediated over-expression of GFP in the SNg. Another factor possibly obscuring the differences in neuronal loss caused by asyn and the S129 mutants is that the immunohistological analysis was conducted in an earlier time point compared to other studies (Oueslati et al., 2010). More recently, a study comparing the pathogenecity among WT, pS129 and phosphorylation incompetent fibers reported that phosphorylated fibrils promoted greater formation of asyn inclusions in the SNpc, worsening cortical pathology, DA neuron loss and fine motor deficits at an earlier time point additionally triggering early changes in the innate immune response and enhancing asyn fibrils uptake by neurons (Karampetsou et al., 2017).

Most studies investigating the pathogenesis and development of PD typically focus on the presence of pS129 asyn in specific brain regions. However, this approach neglects recent findings elucidating both the physiological properties of pS129 asyn (Parra-Rivas et al., 2023) and its appearance throughout the progression of the disease. In PD and DLB brain homogenates, pS129 asyn was found to inhibit fibril formation and seed aggregation, while results from cell culture experiments support a lower seeding propensity and an attenuated toxicity upon treatment with pS129 asyn, compared to non-phosphorylated asyn (Ghanem et al., 2022). Additionally, asyn PFF-injected mice were characterized by aggregated WT asyn with relatively little pS129 asyn, at least during earlier time points (Ghanem et al., 2022).

5. Role of asyn in neurodegenerative pathology

Overall, asyn's structural flexibility and neurophysiological complexity are reflected in its multitude of roles. Its ability to undergo post-translational modifications and rapid conformational changes, and interact with a wide range of protein partners makes it challenging to decipher the molecular consequences of asyn aggregation at synaptic sites, particularly during the early stages of synucleinopathies (Longhena et al., 2019). In the following section, the role and contribution of asyn in the pathophysiology of PD will be reviewed.

5a. Lysosomal effects of asyn

While asyn is degraded in the lysosomes, at the same time lysosomal functions appear to be hindered by the presence of asyn. Under physiological conditions, WT asyn is translocated to the lysosomal membrane where it binds to *LAMP2A*, a selective receptor for

chaperone-mediated autophagy (CMA). Overexpression of *LAMP2A in vitro* leads to CMA upregulation, decreased asyn turnover and selective protection against WT asyn neurotoxicity while overexpression of the lysosomal receptor *in vivo*, in the SNg protects the nigrostriatal axis against asyn-induced dopaminergic neurodegeneration (Xilouri et al., 2013). On the other hand, *LAMP2A* downregulation in the SNg of adult rats, resulted in progressive loss of TH+ neurons, severe reduction in DA levels/terminals in the striatum, increased gliosis and motor deficits further supporting that CMA dysfunction may underlie PD pathogenesis (Xilouri et al., 2016). *SNCA* gene mutations A53T and A30P, along with DA-modified asyn, appear to inhibit degradation by resisting internalization due to stronger binding, thus blocking CMA not only for asyn but also for the rest of the substrates which follow this pathway for degradation (Cuervo et al., 2004; Martinez-Vicente et al., 2008; Xilouri et al., 2009). In this case, macroautophagy increases but in the presence of elevated asyn levels, unlike in other situations, this compensatory degradation mechanism appears to be harmful, resulting in neuronal death (Xilouri et al., 2009). Macroautophagy is the major lysosomal pathway used by cells to degrade proteins within the cytoplasm. It differs from CMA since it handles nonspecific, large-scale degradation of cytoplasmic materials and relies on vesicular trafficking rather than directly importing substrates into lysosomes. Asyn overexpression impairs macroautophagy in mammalian cells and in transgenic (Tg) mice via Rab1a inhibition (Winslow et al., 2010). Overexpression of Rab1a restores Golgi body structure, trafficking and activity of hydrolases (which is disrupted by asyn in synucleinopathies reflecting lysosomal dysfunction) and decreases pathological asyn in iPS midbrain neurons (Mazzulli et al., 2016).

Gaucher's disease is the most common lysosomal storage disorder, with Parkinsonism being one of its most characteristic features (Neudorfer et al., 1996; Sidransky & Lopez, 2012). The *GBA1* gene encodes the lysosomal enzyme glucocerebrosidase (GCase) that breaks down glucosylceramide (GlcCer) into glucose and ceramide. When *GBA1* mutations occur, they lead to GCase a deficiency or malfunction. As a result, GlcCer accumulates within cells, particularly in macrophages, leading to the symptoms and tissue damage associated with Gaucher's disease (Lwin et al., 2004; Sidransky & Lopez, 2012). The severity of Gaucher's disease can vary depending on the specific mutations in the *GBA1* gene (Sidransky et al., 2009). Interestingly, heterozygous mutations in the *GBA1* gene are among the most prevalent genetic risk factors for PD, with an estimated occurrence rate of 7% to 10% in PD patients (Neumann et al., 2009; Schapira, 2015). Reduced GCase activity and subsequent lysosomal dysfunction leads to asyn accumulation and subsequent

oligomerization of the protein. In turn, increased concentration of asyn oligomers may disrupt ER-Golgi trafficking of WT GCase, further inhibiting the activity of the enzyme, creating a pathogenic loop (Cooper et al., 2006; Mazzulli et al., 2011; Bae et al., 2015).

While the normal function of the leucine-rich repeat kinase 2 (LRRK2) protein remains elusive, LRRK2 mutations are the most common, known cause of autosomal dominant PD (Singleton et al., 2013). The G2019S LRRK2 mutation induces modest but significant changes in lysosomal morphology and acidification, decreasing autophagic activity, accumulation of insoluble asyn and increasing asyn release. These changes are reversed by LRRK2 kinase activity inhibitors, providing new evidence regarding the possibility of LRRK2 involvement in late-onset pathogenesis of familial PD via mechanisms regulating lysosome functioning and asyn homeostasis (Schapansky et al., 2018). Finally, lysosomal dysfunction results in higher levels asyn release through exosomes and associates with an increase in asyn transmission to neighboring cells (Alvarez-Erviti et al., 2011).

5b. Effects of asyn on mitochondria

Mitochondrial dysfunctions inducing bioenergetic imbalance, calcium signaling dysregulation and morphological changes, may significantly contribute to the onset and progression of PD. Recessive mutations associated with early-onset forms of PD include loss-of-function mutations in the genes PINK1 (encoding PTEN-induced putative kinase 1), PARK2 (encoding parkin) and PARK7 (encoding protein deglycase DJ1) (Surmeier et al., 2017). The loss of function in each of these genes has been linked to impairments in mitochondrial function and mutation carriers typically develop levodopa (L-DOPA)-responsive PD, indicative of mitochondria-dependent degeneration of dopaminergic neurons in the SNpc (Bonifati, 2012). Since endogenous asyn closely interacts with mitochondria in many different sites, it is possible that asyn plays a role in the regulation of mitochondrial function under both normal and pathological conditions (Vicario et al., 2018). Overexpression of asyn leads to mitochondrial fragmentation, resulting in a greater ratio of mitochondria removal through mitophagy (Chinta et al., 2010; Choubey et al., 2011). Monomeric and oligomeric forms of asyn accumulate both in the outer and the inner mitochondrial membranes of mitochondria (Kamp et al., 2010; Nakamura et al., 2011; Robotta et al., 2014). There, they firmly interact with cardiolipin, a phospholipid enriched in mitochondrial membranes, strictly required for asyn interaction (Ghio et al., 2016). Additionally, asyn in the inner mitochondrial membrane directly interacts with complex I of the respiratory chain, inhibiting its activity (Chinta et al., 2010; Devi et al., 2008; Liu et al., 2009; Nakamura et al., 2011;

Stichel et al., 2007). Mitochondrial fragmentation and complex I activity inhibition, disrupt the potential of the mitochondrial membrane resulting in increased production of reactive oxygen species (ROS) and subsequently in neuronal cell death (Vekrellis et al., 2011). WT forms of Parkin and PINK1 can inhibit the adverse effects of mitochondrial fragmentation caused by asyn, but still lead to increased mitophagy (Kamp et al., 2010). More recently, a new conformationally distinct pS129 asyn species was identified not only in a cell culture model treated with asyn PFFs but also in the brain of PFF-injected mice and in PD patients' brains. This species was generated following incomplete autophagic degradation of pS129 asyn and was characterized by high neurotoxicity leading to mitochondrial damage, fission and mitophagy, thus highlighting the importance of both lysosomal pathways and proper mitochondria functioning in PD (Grassi et al., 2018). Similarly, in exogenously PFF-seeded primary neurons, the majority of pS129 asyn was membrane-bound and associated with mitochondria and cellular respiration defects, thus revealing a connection between two major pathogenic events. These findings were reproduced both in neuronal and animal models not requiring exogenous PFFs as well as in postmortem brain tissues of patients from a range of alpha-synucleopathies, apart from PD (Wang et al., 2019). A mitochondria-targeted asyn construct in differentiated human dopaminergic neurons leads to severe ultrastructural deformation of the inner mitochondrial cristae membranes, swelling and depletion of respiratory function, while asyn overexpression results in loss of mitochondrial membrane potential and production of ROS (Ganjam et al., 2019). Interestingly, caspase inhibition ameliorates mitochondrial respiratory function and cellular ATP levels, negating the asyn-induced cell death (Ganjam et al., 2019; Vekrellis et al., 2009). Apart from the caspases, another potential therapeutic target for PD is the protein SIRT3, member of the sirtuins family, which is deemed essential for cell survival, metabolism and longevity. Downregulation of SIRT3 results in increased ROS and mitochondrial dysfunction (Park et al., 2020).

5c. Effects of asyn on the cytoskeleton

Several lines of evidence converge on the hypothesis that oligomerization of asyn could affect the stability of the cytoskeleton, possibly leading to the neuronal degeneration which characterizes PD (Vekrellis et al., 2011). Addition of asyn oligomers in cell medium results in decreased tubulin polymerization and alterations in mitochondria function and cell morphology. While internalization of the exogenously added asyn is deemed as a critical step for these adverse effects, direct interaction between the oligomers and tubulin is not

observed (Chen et al., 2007). Evidence from studies performed both *in vitro* and *in vivo*, attest that asyn interacts with tubulin, possibly through the region spanning from residue 60 to 100 to bind to this microtubule-forming protein (Zhou et al., 2010; Amadeo et al., 2021). Interaction of the two proteins in murine striatal boutons might be substantial for the normal functioning of synapses (Amadeo et al., 2021). While asyn oligomers seem to selectively affect tubulin sparing actin microfilaments and intracellular trafficking unrelated to microtubules in degenerating neurites (Lee et al., 2006), WT asyn binds actin, contributing to its depolymerization while A30P asyn increases actin polymerization, disrupting physiological cell functions such as cell migration and endo- / exo-cytic trafficking, altering cytoskeletal dynamics (Sousa et al., 2009). Moreover, increased asyn in the extracellular environment leads to heightened presence of glucose-related protein (GRP78) in the plasma membrane of neurons. Asyn interaction with GRP78 activates a signaling cascade ultimately dysregulating actin turnover and subsequently synapse function, possibly initiating the pathogenic process that eventually advances to neurodegeneration (Bellani et al., 2014).

Since we have already reviewed the effects of asyn in mitochondria, it is interesting to examine how asyn can additionally disrupt cell energy metabolism through new mechanistic routes, once again involving proper mitochondrial functioning. Transfer of mitochondria from PD patients to healthy neuronal cells, in which endogenous mitochondrial DNA was depleted, led to reduced ATP levels, increased ratio of free/polymerized tubulin and accumulation of asyn oligomers. This phenotype was normalized following the use of a microtubule-stabilizing drug (Esteves et al., 2010). Additionally, in a Drosophila model overexpressing human WT asyn, the actin filament network was destabilized by mislocalization of the critical mitochondrial fission protein Drp1, which in turn led to mitochondrial dysfunction and neuronal death. Interestingly, the same actin cytoskeletal abnormalities were present in the brains of asyn Tg mice and alpha-synucleinopathy patients (Ordonez et al., 2018). Following the identification of microtubule-associated protein tau as an asyn ligand -with the interacting domains being localized to the C terminus- it was proposed that asyn further catalyzes the phosphorylation of tau at residues Ser262 and Ser356 via protein kinase A (PKA), indirectly destabilizing the axonal microtubules (Jensen et al., 1999). Intriguingly, the existence of abundant filamentous tau in the postmortem brain tissues of PD patient has been reported repeatedly (Duda et al., 2002; Kotzbauer et al., 2004). PD linked asyn mutations A30P, E46K and A53T but also MPTP exposure were found to promote tau Ser262 phosphorylation, possibly via GSK3β, causing microtubule instability (Duka et al., 2006; Qureshi & Paudel, 2011). Importantly, the

presence of asyn was mandatory to observe MPTP-induced increases in phosphorylated Tau levels (Duka et al., 2006). Apart from mutations or environmental insults, overexpression of human asyn in old Tg mice was also accompanied by progressively greater levels of phosphorylated tau and subsequent tau and MAP1 dissociation from the cytoskeleton, along with increased levels of free tubulin and actin, all signs indicating cytoskeleton remodeling and destabilization (Haggerty et al., 2011).

Finally, LRRK2 overexpression promotes abnormal asyn aggregation and accumulation only in A53T but not in WT mice, synergistically leading to disruption of microtubule dynamics, Golgi organization and the ubiquitin-proteasome pathway, possibly playing a role in regulating the progression of A53T asyn-induced neuropathological abnormalities (Lin et al., 2009).

5d. Effects of asyn on calcium homoeostasis

Excessive influx of calcium into cells leads to cytotoxicity through multiple pathways. High intracellular calcium levels activate various enzymes, such as proteases, phospholipases and endonucleases. Proteases like calpains degrade essential cytoskeletal and structural proteins, disrupting cellular integrity. Phospholipases break down membrane lipids, leading to loss of membrane integrity and function. Endonucleases can cause DNA fragmentation, resulting in genetic damage. Additionally, elevated calcium levels disturb mitochondrial function by opening the mitochondrial permeability transition pore, leading to a loss of mitochondrial membrane potential, decreased ATP production and release of pro-apoptotic factors. This cascade of events can initiate apoptotic or necrotic cell death pathways, ultimately resulting in cytotoxicity and tissue damage (Berridge et al., 2003).

Interestingly enough, autosomal dominant A30P and A53T *SNCA* mutations may promote the formation of ion-permeable pore-like oligomeric structures, termed protofibrils. In contrast to monomeric or fibrillar asyn, these pore-like oligomers have the ability to bind synthetic vesicles with a β-sheet-rich structure, leading to membrane permeabilization with deleterious effects for the cells, offering a possible mechanistic explanation for the appearance of early-onset PD due to the aforementioned mutations (Volles et al., 2001; Lashuel et al., 2002). Moreover, L-DOPA-treated PC12 cells overexpressing A30P or A53T *SNCA* were characterized by disrupted vesicular pH, compared with those expressing WT asyn, leading to a marked increase in the levels of cytosolic catechol transmitters; an effect that may in turn trigger cellular oxyradical damage

(Mosharov et al., 2006). Following the development of new protocols to synthesize different types of asyn oligomers, it was found that heterogeneous oligomer populations coexist in equilibrium under physiological conditions *in vitro*, contributing to cell damage in different ways (Danzer et al., 2007). Data from Danzer and colleagues support the amyloid pore hypothesis formulated by Lashuel and Lansbury based on their own experimental results with the use of synthetic vesicles, showing a pore-forming mechanism of asyn protofibrils (Volles et al., 2001; Lashuel et al., 2002; Lashuel & Lansbury, 2006; Danzer et al., 2007). The influx of extracellular calcium indicates that asyn may form pores in living cells similarly to the formation of membrane-spanning pores created by pore-forming toxins (Bouillot et al., 2018). These findings imply that asyn oligomers disrupt the homeostasis of cellular ions, leading to caspase activation and cell death through the formation of membrane pores, a pathogenic mechanism that could also occur *in vivo*. Large asyn oligomers have also been found to increase synaptic transmission mediated by AMPA receptors both pre- and post-synaptically, leading to exacerbation of intracellular calcium imbalance and subsequent excitotoxic nerve cell death (Hüls et al., 2011).

As previously discussed, susceptible neuronal populations such as catecholaminergic neurons may be particularly susceptible to calcium level fluctuations due to their distinct reliance on L-type Cav1.3 calcium channels to maintain their constant, rhythmic pacemaking (Chan et al., 2007). The activation of L-type calcium channels in the plasma membrane during regular autonomous pacemaking causes oxidative stress, leading to a transient, mild mitochondrial depolarization or uncoupling that was specific to the susceptible dopaminergic neurons in the SNg (Guzman et al., 2010). Additionally, apart from the calcium-buffering calbindin, other intracellular machinery such as the sarcoendoplasmic reticulum Ca^{2+}-ATPase (SERCA) pump is affected. SERC is an ATP-driven enzyme essential for actively transporting calcium ions back into the sarcoplasmic or endoplasmic reticulum, thus regulating intracellular calcium homeostasis. Mitochondrial uncoupling leading to reduced ATP production or carbonylation due to oxidative stress, has been found to significantly reduce SERCA enzymatic activity in DJ-1β mutant flies as well as in a human cell PD model based on DJ-1-deficiency (Solana-Manrique et al., 2021).

5e. Effects of asyn on neuroinflammation

Postmortem analyses of PD patients' brains are characterized by signs of widespread inflammation, displaying increased glial activation along with infiltration of immune cells originating from the periphery (Weiss et al., 2022). Despite the undoubtly central role of

neuronal cell death in the disease, today PD is perceived as a multi-system disorder, with characteristic non-motor symptoms. Symptoms such as gastrointestinal (GI) tract dysfunction, among others, are now known to be linked to neuroinflammation. Thus, immune system dysfunction and glial cell activation are examined as significant contributors to the pathogenic environment and not as a mere response to neurodegeneration (Tansey et al., 2022). Inflammatory features most likely originate from GI dysbiosis, resulting in gut permeability and increased circulation of pro-inflammatory cytokines and microbial metabolites which in turn activate both the innate and the adaptive peripheral immune systems (S. Lim et al., 2016; Tansey et al., 2022).

There is substantial evidence indicating that microgliosis and astrogliosis play a major role in the development of synucleinopathies. Mutant or aggregated forms of asyn are known to cause enhanced activation of microglial and astroglial cells, leading to the release of cytokines and oxidative stress (Klegeris et al., 2006; E.-J. Lee et al., 2010; H.-J. Lee et al., 2010; Rojanathammanee et al., 2011; Roodveldt et al., 2010). Additionally, recent findings indicate that the reactivity of microglial and astroglial cells contributes to dopaminergic degeneration and may mediate the progression of neurodegeneration (Fellner et al., 2011; G. M. Halliday & Stevens, 2011). Even though the mechanisms driving microglial and astroglial activation are not well understood, toll-like receptors (TLRs) are suspected to play a role based on their upregulated levels in PD (Fellner et al., 2013). TLRs belong to the family of pattern recognition receptors and are crucial components of the innate immune response. They recognize pathogen-associated molecular patterns and endogenous molecules, including misfolded proteins. TLRs are expressed on innate immune system cells, including microglial and astroglial cells. While TLR4 is upregulated in alpha-synucleinopathy postmortem brain tissue, *in vivo* experimental TLR4 deficiency leads to decreased asyn clearance by microglia (Stefanova et al., 2011). Evidence shows that both unaggregated and aggregated forms of asyn can activate TLR4 receptors on microglia and astroglia, triggering a pro-inflammatory response. This activation leads to chronic neuroinflammation in PD, potentially contributing to the degeneration of dopaminergic neurons (Fellner et al., 2013). Dysfunction of dopaminergic neurons in PD is believed to be partly due to pro-inflammatory responses from glial cells (Béraud et al., 2013). TLR4 has been shown to facilitate the microglial clearance of asyn which might be neuroprotective in certain situations (Stefanova et al., 2011). Asyn also activates Toll-like receptor 2 (TLR2) on microglia, leading to the production of inflammatory cytokines while in various brain regions of PD patients, TLR2 expression is reported to be increased (Dzamko et al., 2017). Apart from being involved in

the innate immunity by recognizing pathogens, TLR2 also participates in neuronal autophagy regulation and asyn clearance. TLR2 activation leads to the accumulation of asyn aggregates in neurons by inhibiting autophagic activity via the AKT/mTOR pathway. Conversely, TLR2 inactivation lead to activation of autophagy, enhanced clearance of neuronal asyn and consequently lower levels of neurodegeneration, both *in vivo* and *in vitro* (Kim et al., 2015). Interestingly, only β-rich oligomers of asyn, and not other forms of the protein, activate glial TLR2 receptors (Kim et al., 2013). This may account for the stronger pro-inflammatory response of microglia to DA-aggregated asyn compared to unaggregated asyn (Béraud et al., 2013).

By further exploring the role of microglia in the pathogenesis of PD, it was recently reported for the first time that A53T human iPSC-derived microglia show an increased intrinsic tendency for pro-inflammatory activation, following exposure to LPS and interferon-γ *in vitro* (Krzisch et al., 2024). Transplantation of these mutant human microglial cells to mouse brains under non-inflammatory conditions, results in a strong decrease of catalase expression leading to increased oxidative stress (Krzisch et al., 2024). Catalase is a key antioxidant enzyme that reduces oxidative stress by breaking down cellular hydrogen peroxide into water and oxygen. Deficiency or malfunction in catalase levels is believed to contribute to the pathogenesis of numerous degenerative diseases associated with aging (Nandi et al., 2019).

Finally, following correlation of hyper-phosphorylated asyn oligomers, but not monomers, with sustained inflammatory responses, both *in vitro* and in postmortem brain samples of PD patients, it was reported that *in vivo* activation of the p38/ATF2 signaling pathway in microglia and of the NF-κB pathway in astrocytes results in the upregulation of astrocytic T-type Cav3.2 calcium channels, altering the astrocytic secretome and promoting the expression of the anti-inflammatory and neuroprotective protein IGFBPL1 (Leandrou et al., 2024).

6. Asyn aggregation and propagation

Apart from the existence of brain banks, often lacking complete medical histories of patients, current knowledge about the development of pathology in clinical PD (L-DOPA-responsive, with typical clinical characteristics without any markers suggestive of other disease) relied on sparser, smaller collection of brains from well-documented individuals who have been followed over time (Surmeier et al., 2017). These patients are characterized

by an over 50% loss of SNpc dopaminergic neurons while the majority also displays Lewy pathology, consisting of cytoplasmic spherical eosinophilic inclusions in the perikarya of nerve cells, known LBs and spindle or thread-like inclusions, termed Lewy neurites, located within neuronal processes (Gibb & Lees, 1988). Interestingly, Lewy pathology can also be present in the brain of individuals without clinical PD symptoms (Berg et al., 2014). In late-stage patients pathology appears within specific nuclei in the caudal medulla, i.e. the dorsal motor nucleus of the vagus (DMV) and the intermediate reticular zone, while pathology is also frequently found in the nucleus tractus solitarius, gigantocellular reticular nucleus, raphe magnus, locus coeruleus (LC) and subcoeruleus. Further rostrally, Lewy pathology is found in the dorsal and the median raphe nuclei, in the pedunculopontine nucleus, the SNpc, and in the ventral tegmental area (VTA). In the diencephalon and telencephalon, pathology is commonly observed in the magnocellular nuclei of the basal forebrain, the tuberomammillary nucleus of the hypothalamus, the lateral hypothalamus, the intralaminar nuclei of the thalamus, the olfactory and basolateral portions of the amygdala, the anterior olfactory nucleus, the insular, the cingulate and prefrontal cortices, and the CA2 area of the hippocampus.

According to the hypothesis proposed by Braak and colleagues, PD pathogenesis may begin in the peripheral nervous system and subsequently spread to the CNS (Illus. 3) (Braak et al., 2003). This hypothesis suggests that the initial pathological changes, characterized by the formation of LBs containing asyn, occur in the enteric nervous system (ENS) (specifically, in the dorsal vagal nucleus), the olfactory bulb (in the anterior olfactory nucleus) and the lower brainstem. Non-motor symptoms such as constipation and olfaction deficits often occurring during the early stages of PD support this notion of peripheral involvement. Presence of LBs in the ENS of PD patients was first reported following the identification of inclusions in the esophagus and the colon of two different PD patients (Qualman et al., 1984). Since then, Lewy pathology has been reported in numerous studies, being present in almost the entire gut of PD patients, including the myenteric (Auerbach's) plexus and the submucosal (Meissner's), following a rostrocaudal gradient within the GI tract, with more pathological aggregates found in the upper, compared to the lower gut (Wakabayashi et al., 1988, 1990; Braak et al., 2006). Interestingly, LBs are already present in the intestinal perikarya and neurites from 2 to 5 years or even up to 8 years prior to the onset of PD (Shannon et al., 2012; Hilton et al., 2014). More recently, a group of enteroendocrine cells named neuropods were discovered expressing asyn and forming direct synaptic connections with vagal afferents (Chandra et al., 2017; Kaelberer et al.,

2018). These connections create a synaptic pathway to the SNg and the striatum, suggesting that asyn fibrils might originate in enteroendocrine cells, spread to the myenteric plexus and eventually reach the CNS (Han et al., 2018).

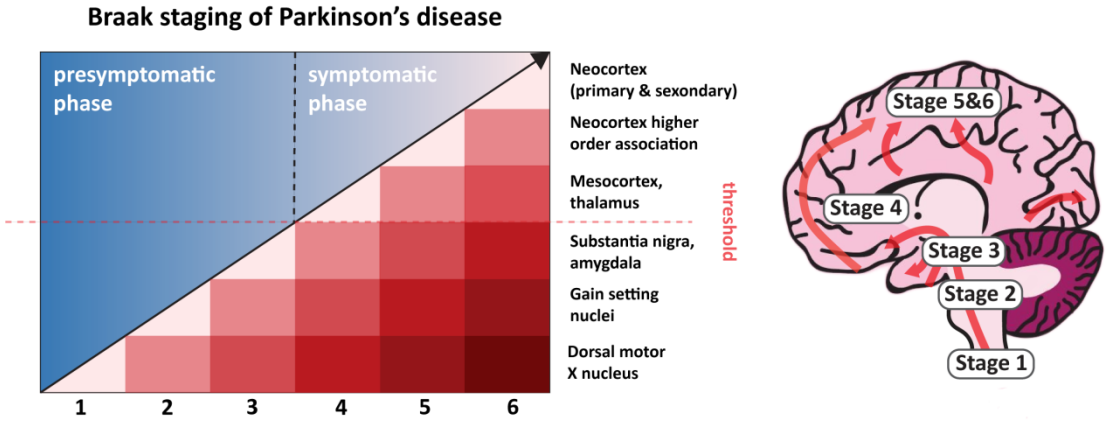

Illustration 3. Braak staging of PD: The presymptomatic phase is characterized by the presence of Lewy neurites and bodies in the brains of individuals who have not yet shown symptoms. During the symptomatic phase, the neuropathological threshold is surpassed (represented by the dashed red line). The increasing slope and intensity of the colored areas below the diagonal indicate the progression and worsening of pathology in susceptible brain regions (right), while the severity of the pathology is represented by the darker shading. Adapted from Braak et al., 2004.

The vagus nerve, the major component of the "axis" bridging the brain with the gut, has been shown to engage in active retrograde transport of recombinant asyn forms in preclinical studies. Following injection of recombinant asyn into the intestinal wall, the protein is first detected in the DMV (Holmqvist et al., 2014) before further spreading in brain areas involved in the pathophysiology of PD, leading to loss of dopaminergic neurons, motor and non-motor symptoms. Intriguingly, the aforementioned PD-like symptoms were absent from vagotomized asyn deficient (*SNCA* -/-) animals (Kim et al., 2019). The possible involvement of the vagus nerve in the pathogenesis of PD is corroborated by findings of asyn accumulation in the bowel of pre-clinical patients (Hilton et al., 2014) and by studies in cohorts of Danish (Svensson et al., 2015) and Swedish (Holmqvist et al., 2014; Liu et al., 2017) patients having undergone total truncal vagotomy, with a potentially protective effect.

As we have already discussed, Braak and others have proposed that distribution of Lewy pathology evolves over time from specific starting points evolving alongside the symptoms (Braak et al., 2004; Beach et al., 2009); pathology spreading is characterized by six

different stages progressing from pre-symptomatic (1 & 2) to early (3 & 4) and finally late symptomatic stages (5 & 6). However, in only about half of clinical PD patients, LBs are distributed according to Braak's staging model (Kalaitzakis et al., 2008; Halliday et al., 2012). Additionally, in PD with typical clinical characteristics, patients with familial and patients with idiopathic PD have distinct patterns of Lewy pathology or, in other cases, little to no presence of LBs (Doherty et al., 2013). This is noteworthy; however, it underscores that, despite substantial research and comprehensive mapping of brain regions susceptible to Lewy pathology, the precise sequence and extent of their involvement in disease progression are still not fully understood (Surmeier et al., 2017).

While the body-first hypothesis aligns with the Braak staging system, in many cases pathology initially appears in structures within the CNS (most likely in the amygdala, followed by the SNg and LC) with no prior involvement of the ANS (Borghammer et al., 2021). Based on human post-mortem neuropathological datasets and summarizing clinical, imaging and other findings, Borghammer and colleagues proposed the body-first (caudo-rostral) and brain-first (amygdala-centered) subtypes of LB disorders. In the body-first subtype, autonomic symptoms and REM sleep behavior disorder appear in the prodromal phase along with sympathetic and parasympathetic denervation and LC degeneration, at time of diagnosis, hyposmia is very frequent, dopaminergic denervation and motor symptoms are more symmetrical, and the progression rate of dementia and motor symptoms is faster of diagnosis. On the other hand, in the brain-first subtype, autonomic symptoms and REM sleep behavior disorder first appear after diagnosis along with sympathetic and parasympathetic denervation and LC degeneration, and at the time of diagnosis, hyposmia is less frequent, dopaminergic denervation and motor symptoms are more asymmetrical and the progression rate of dementia and motor symptoms is slower (Borghammer et al., 2021).

Luk and colleagues were the first to provide *in vivo* evidence that upon inoculation of asyn PFFs into the brains of mice, pathology can propagate from one neuron to another and lead to cell death (Luk et al., 2012). Since then, it has been shown multiple times that asyn PFFs, either synthetic or extracted from human PD patient LBs, can propagate from the site of stereotaxic injection to synaptically connected neighboring structures, leading to the formation of Lewy-like pathology (Masuda-Suzukake et al., 2013; Peelaerts et al., 2015; Recasens et al., 2014). These observations gave rise to the idea that PD is a prion-like disorder (Olanow & Prusiner, 2009; Olanow & Brundin, 2013). This hypothesis is appealing

because it suggests a unified mechanism for the development of Lewy pathology in PD, aligning with Braak's hypothesis that Lewy pathology spreads retrogradely through the brain's synaptic connections. The idea that asyn spreads retrogradely in proportion to synaptic connection strength, does not align with actual patterns of Lewy pathology. For example, despite strongly innervating LC, regions like the cerebellum or midbrain reticular nucleus show little to no Lewy pathology in human PD patients (Surmeier et al., 2017). Similarly, brain areas with strong connections to the SNg such as the striatum and the globus pallidus externa, do not display significant pathology, challenging the notion that connectivity predicts the spread of pathology (Watabe-Uchida et al., 2012). On the other hand, a new Tg mouse model that expresses human A53T SynGFP shows that aggregation begins in axons and spreads retrogradely to the cell body along with clear evidence of retrograde, trans-synaptic propagation through connected motor system pathways. Furthermore, the model reveals a progression from neuronal to astrocytic inclusions, with astrocytes outliving their neuronal counterparts (Schaser et al., 2020). Supporting this, another study found that asyn aggregates first appear in the olfactory system and vagus nerve before spreading to other brain regions in PD. Using a mathematical model based on mouse brain connectivity, researchers showed that this spread follows neural networks, initially retrograde and later anterograde, accurately predicting the progression of asyn pathology (Mezias et al., 2020).

Interestingly, endogenous asyn seems to hold a crucial role in the process of fibrillary asyn spreading, using the latter as a template (Luk et al., 2012; Masuda-Suzukake et al., 2013; Volpicelli-Daley et al., 2011). In numerous *in vitro* and *in vivo* synucleinopathy models, PFF-induced toxicity spreading is dependent on the endogenous asyn, with *SNCA* expression levels closely correlating with the relative vulnerability of different hippocampal neuron subtypes. Additionally, only early therapeutic intervention with ASOs resulted in neuroprotection, indicating that neurotoxicity occurs once a critical threshold of pathological burden is surpassed in vulnerable neurons. Taken together, these findings revealed that endogenous asyn heterogeneity may play a role in explaining the selective vulnerability seen in synucleinopathies (Luna et al., 2018). On the other hand, while endogenous asyn does not play a role in the effect toxic stimuli such as PFFs have in the cargo of exosomes, its presence as exosomal cargo is essential for the facilitation of disease transmission (Melachroinou et al., 2024).

Today we know that synthetic asyn PFFs can induce asyn pathology (detected by pS129) spreading retrogradely and anterogradely, arguing that pathology propagation in humans could be bidirectional (Arotcarena et al., 2020; Schaser et al., 2020; Uemura et al., 2021; Wang, Shinkai, et al., 2021). But while pathology propagation can be independent of cell type, its persistence and toxicity may be cell-type specific (Henrich et al., 2020).

Finally, on the debate of whether greater levels or more insoluble/aggregated asyn are responsible for the pathogenesis of PD, a study using laser-capture micro-dissection in surviving TH+ neurons in the SNg of sporadic PD patients, found that *SNCA* mRNA levels are significantly higher (Gründemann et al., 2008). Additionally, a more recent study examining the effects of seeding human iPSC-derived dopaminergic neurons with endogenous asyn PFFs amplified in the presence of PD brain homogenates, reported an increase in *SNCA* mRNA levels (Tanudjojo et al., 2021). These findings indicate that protein aggregation upregulates asyn expression, further promoting aggregation and creating a self-perpetuating pathogenic cycle (Burré et al., 2024).

These *in vivo* findings were recapitulated by an SAA study examining CSF and brain tissue from patients with LB pathology, showing that brain deposition of misfolded asyn precedes the formation of LBs and Lewy neurites (Bentivenga et al., 2024).

7. Factors influencing neuronal vulnerability, disease progression and development

The mystery still remains as to why some neuronal populations are more vulnerable (e.g., SNpc dopaminergic neurons) while others (e.g., VTA dopaminergic neurons) tolerate pathology without succumbing (Burré et al., 2024). Neuropathology studies of brains from individuals with mutations in *PARK2*, the gene encoding the Parkin protein causing the most common form of autosomal recessive young-onset PD (Periquet et al., 2003), reveal severe neuronal loss in the SNg, variable neuronal loss in the LC and relatively rare LB pathology (Doherty et al., 2013). In animal models of PD, replicating Lewy pathology - specifically the formation of LBs and Lewy neurites - poses significant challenges. While some Tg mice expressing human asyn do develop asyn the aggregates formed tend to be more diffuse and less organized compared to those seen in human patients (Lim et al., 2011). Moreover, in a different study, Tg mice carrying a bacterial artificial chromosome with the human *SNCA* gene exhibit an age-related loss of DA neurons, without the presence of inclusions (Janezic et al., 2013). This suggests that physiological abnormalities or even neuronal loss can occur without the need for protein aggregation. Traditional toxin-based models inducing

dopaminergic neuron death generally do not produce Lewy pathology. These models are primarily focused on replicating the neurodegeneration and motor symptoms of PD rather than the underlying protein aggregation (Bové & Perier, 2012). In animal models where viral vectors are used to overexpress asyn in the brain, LB-like inclusions can form, though these inclusions also often differ in structure and distribution compared to those found in human PD (Luk et al., 2012). These observations challenge the idea that neuronal degeneration is driven by the spread of Lewy pathology through a neuronal network defined by synaptic connections and suggests that degeneration of neurons in the SNg may not necessarily rely on Lewy pathology.

One of the most distinct characteristics of the neurons susceptible to degeneration is their long, highly branched axons containing a great number of transmitter release sites that serve to coordinate spatially distributed networks (e.g., the basal ganglia or the spinal cord). However, not all neuronal populations characterized by long axons with extensive arborization are vulnerable in PD. For example, despite their highly branched axons with as many release sites as SNg DA neurons, striatal cholinergic interneurons do not degenerate or show Lewy pathology, suggesting that there are more contributing factors leading to the disease (Surmeier et al., 2017). Another common trait among vulnerable neuronal groups in PD is their distinctive physiology characterized by slow, tonic activity *in vivo* (Surmeier et al., 2012). As expected, the most extensively studied neurons of this type are the dopaminergic neurons in the SNg, which generate broad action potentials without any excitatory synaptic input . Their only difference compared to DA neurons in the VTA - which are significantly less vulnerable despite also being characterized by autonomous broad spiking - is that SNg located DA neurons are characterized by greater voltage-dependent Cav1 channel currents and weaker intrinsic calcium buffering due to lower levels of calbindin. Calbindin is a critical calcium-binding protein that helps regulate intracellular calcium levels by binding free Ca^{2+} and preventing calcium overload (Chan et al., 2007; Foehring et al., 2009; Guzman et al., 2009; Philippart et al., 2016). The combination of large oscillations in intracellular calcium concentrations - due to broad neuronal spiking - accompanied by relatively free interaction with other intracellular proteins, low calcium buffering capacity and high metabolic activity, make these neuronal populations particularly vulnerable to oxidative stress, mitochondrial dysfunction and disrupted calcium homeostasis; all of which are key factors in the pathogenesis of PD.

Recently, a new conceptual model for PD pathogenesis was proposed, categorizing all the disease-associated factors into three categories, depending on their potency and importance for the onset and/or the development of the disease. Thus, agents or events capable of initiating the disease were characterized as “triggers”. Triggers such as viral infections or environmental toxins are necessary to spark the disease process in the brain and/or peripheral tissues but are not enough on their own for the spreading of the disease. For this next stage, factors such as aging or leaky gut barrier enabling the disease to develop, that is to spread and significantly affect the CNS, are termed “facilitators”. Finally, “aggravators” directly promote the neurodegenerative process (e.g., asyn cell-to-cell propagation) and often have a domino effect that exacerbates pathology and spreads the disease beyond the basal ganglia (Johnson et al., 2019). Thus, it becomes clear that apart from the initial event leading to asyn aggregation, there is a much bigger landscape of factors contributing to the development of the disease which should be taken into account during the planning of the experiments for higher translatability and relevance in the results.

8. The gut-brain axis: A key player in PD

Despite the seminal discoveries in the field of neurobiology regarding asyn and PD, the aforementioned research fields can further benefit from studying the gut microbiome (i.e., the genetic material of the trillions of microorganisms we host in our gastrointestinal tract). Since the original observations of digestive problems (e.g., constipation) preceding the manifestation of the characteristic motor symptoms of PD (Adams-Carr et al., 2016) and the formulation of Braak’s hypothesis proposing the enteric route as the gateway of the pathology into the CNS (Braak et al., 2003), recent years have seen a surge of publications underlying the importance of the bidirectional communication between microbiota and the brain and the adverse results of disrupting this symbiosis (from 161 publications/year in 2013 to more than 1600 in 2023 according to PubMed using the keywords: “gut brain axis”). To put this interaction between different organisms in perspective, human bodies are comprised of more microbial than human cells while in terms of genetic material, revised estimations support that human genes consist less than the 1% of the total genes in the human organism (Sender et al., 2016). Based on continuous technological advances in the fields of sequencing and “big data” sciences, recent preliminary studies report that analyzing the biodiversity of microbes in the gut can reveal the presence of various common diseases – including PD – more accurately than human genomics (i.e., GWAS) (Tierney et al., 2020) and can also be used as a predictor for clinical risk (Salosensaari et al., 2021).

With multiple studies qualitatively and quantitatively mapping the gut microbiome of patients in search of a microbiota - composition characteristic of PD, consensus has yet to be reached (for a detailed review, please see Cryan et al., 2020). For this reason, meta-analyses play a crucial role in synthesizing data from multiple studies, providing clarity and helping to establish consistent patterns and conclusions in this rapidly expanding field (Nishiwaki et al., 2020). Apart from the composition of the microbiome, short chain fatty acids (SCFAs), one of the main metabolic products by some gut microbiota, are also being investigated (Unger et al., 2016). SCFAs are organic fatty acids with less than six atoms of carbon atoms mostly represented by acetic (C2:0), propionic (C3:0) and butyric (C4:0) acid, in a proportion of approximately 3:1:1 (Cummings et al., 1987). SCFAs are produced through the fermentation of dietary fibers and serve several essential functions in the gut, including regulating inflammation, maintaining intestinal barrier integrity and influencing the nervous system through the gut-brain axis (Duan et al., 2024). In PD, alterations in SCFA levels have been observed, with decreased concentrations of fecal SCFAs, particularly butyrate, being linked to increased gut permeability, inflammation and potential disruptions in the gut-brain axis (Unger et al., 2016; Aho et al., 2021; X. Yang et al., 2022). SCFAs can also influence brain function directly by crossing the BBB and modulating neurotransmitter synthesis and signaling (Oldendorf, 1973; Dalile et al., 2019). For instance, they can affect DA metabolism by interacting with receptors in the CNS (Sharma et al., 2015; Hamamah et al., 2022). Furthermore, the imbalance of SCFAs in the gut may be associated with motor and non-motor symptoms of PD (Chen et al., 2022; Wu et al., 2022). An animal study has shown that oral administration of SCFAs to germ-free mice promotes asyn mediated activation of the microglia and motor symptoms. Additionally, colonizing asyn-overexpressing mice with fecal samples of PD patients leads to neuroinflammation and motor deficits; a phenotype that is ameliorated after treatment with antibiotics (Sampson et al., 2016).

Given their diverse roles in inflammation, gut permeability and brain function, gut microbiota are considered a potential target for therapeutic intervention in PD. The field is still in its early stages and interpreting data can be challenging because microbiome composition is affected by numerous factors, including diet and exercise (Cryan et al., 2020). Since alterations in the human microbiome represent a risk factor for PD, prospective longitudinal studies in big cohorts and population-wide microbiome sequencing might elucidate the mechanisms and the dynamics of the microorganisms colonizing the GI tract and their metabolites. Such knowledge will serve a dual role; early diagnostics, before

pathophysiological events can lead to - possibly irreversible - changes, and therapeutics, via diet alterations or the use of antibiotics or super-donor fecal microbiota transplantations.

9. A brief introduction to stress and its physiological response

While the physiological and endocrinological mechanisms underlying the stress response have always existed, the term “stress” per se, is surprisingly recent. While Hans Selye first described the “Diseases of adaptation” and the general adaptive syndrome in 1936, it was only after the Second World War that the term “stress” prevailed (Hutmacher, 2021). Despite the many different scientific fields sharing the same term, in biomedical sciences, stress is defined as the disruption of homeostasis by an external factor or perceived stressor. This definition encompasses a wide range of stressors, including physical, chemical, or psychological factors that can trigger a biological response and is attributed to Selye. The stress response is shaped by a mix of genetic, developmental and environmental factors. Both the intensity and duration of the exposure to stressors are crucial. When a stressor surpasses certain limits and disrupts the state of dynamic equilibrium of the organism, adaptive homeostatic systems are activated and triggers compensatory responses to facilitate the restoration of the equilibrium (Chrousos, 2009).

10. Acute stress response and the role of the CNS

Acute stressors exert a well studied “fight or flight” response in an organism, which is based on a series of well-studied changes in physiological processes, guided by the CNS and affecting multiple organs. Briefly, this standardized innate response results in the focus of attention, the arousal of the brain, the heart and the skeletal muscles through increased flow of oxygen and nutrients and the concurrent suppression of appetite, growth and reproduction. Focusing on the CNS, various stress centers – such as the sensory cortex – relay the stimulus perceived as a stressor to the LC in the brainstem, through the hypothalamus. This leads to an increased rate of noradrenergic (NA) activity, contributing to heightened alertness and attentiveness, particularly within the LC/NA system. When a stimulus is perceived as a threat, the stress response intensifies. This includes a more pronounced and prolonged activation of the LC and a simultaneous activation of the sympathetic nervous system. In this process, preganglionic neurons release acetylcholine (ACh) which in turn binds to receptors on the cells of the adrenal medulla, leading to the

release of adrenaline, and to a lesser extent, NA, contributing to the “fight or flight” stress response.

11. Adaptation to prolonged stress and the HPA axis

Apart from the effects of adrenaline and NA release, which constitute the immediate response, if the stressor persists, the body attempts to adapt via a physiological response orchestrated by the activation of the HPA axis (Illus. 4). Corticotropin-releasing factor (CRF) neurons located in the paraventricular nucleus (PVN) of the hypothalamus, innervate the pituitary gland, which is not covered by the BBB. The release of CRF in the pituitary gland stimulates the synthesis and secretion of adrenocorticotropic hormone (ACTH), which in turn is released in the bloodstream, marking the initiation of the endocrine response of the HPA axis. Through the blood circulation, ACTH reaches the adrenal cortex, resulting in the synthesis and release of glucocorticoids (GCs) into the bloodstream. While humans produce cortisol as the main GC, rats produce corticosterone due to their lack of the adrenocortical zona fasciculata enzyme 17-α hydroxylase (CYP17). Thus, taken together, the hypothalamus, pituitary and adrenal glands constitute the 3 parts of the axis and are the key players in the organism’s response to physical or psychogenic stressors. GC secretion has a systemic effect on the body, affecting multiple tissues and causing changes in the physiology and behavior of the organism.

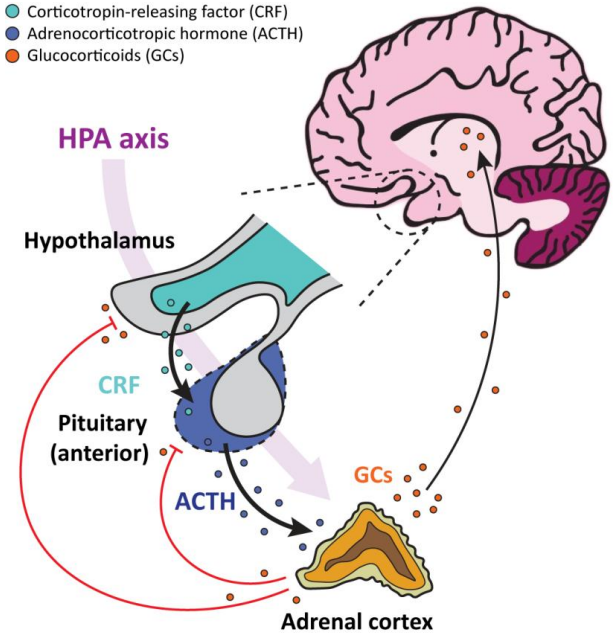

Illustration 4. Activation of the HPA axis begins when the hypothalamus releases CRF in response to stress. CRF stimulates the pituitary gland to secrete ACTH, which then triggers the adrenal glands to release GCs (cortisol in humans, corticosterone in rodents). GCs act on various tissues to regulate metabolism, immune responses, and help the body adapt to stress. Once sufficient cortisol levels are reached, negative feedback mechanisms inhibit further activation of the HPA axis (red lines), maintaining balance.

12. Circadian regulation and variability in GC secretion

GC hormones are not released by the organism only when under stress; under physiological conditions, GC secretion is synchronized by the circadian rhythm, being released following hourly ultradian pulses with higher levels of the hormone released to ensure there is energy at the start of each active period (being diurnal, humans tend to be active when the sun is up and rest when it's down, while the opposite is seen in nocturnal rodents commonly used as animal models in biomedical studies). Thus, increased GC levels avert the onset of sleep. The frequency and the amplitude of the GC pulses are altered due to pathological events such as infections or injuries followed by inflammation, neuropsychological disorders (e.g., depression), or during the natural course of aging. Naturally, GC secretion is mediated by the response to a stressor which can have either a physical aspect, i.e., environmental (e.g., extreme temperatures), physiological (e.g., illness or injury), biological (e.g., pathogens or parasites), chemical (e.g., toxins) or a psychogenic aspect, i.e., psychological (e.g., novel environment), social (e.g., social isolation), or reproductive (e.g., changes in mating availability). Thus, to assess the physiological stress response, the easiest way is to measure the GCs, having previously taken into consideration the temporal and mechanistic aspects that govern its secretion.

13. Mediators and effects of GCs in the CNS

In the CNS, GCs act at many different levels, ranging from gene transcription and cell signaling to behavioral changes. Their actions are mediated by two receptors; namely the mineralocorticoid (MR) and the glucocorticoid (GR) receptor. MR and GR belong to a superfamily of nuclear receptors of transcription factors. While GR is ubiquitously expressed throughout most of the brain regions and different cell types, MR displays a more limited expression pattern, in structures of the limbic system (such as the hippocampus, the amygdala, the prefrontal cortex and the paraventricular nucleus (PVN) of the hypothalamus) and in neurons of the solitary nucleus in the medulla oblongata of the brainstem. MR is also expressed in glial and ependymal cells of the choroid plexus.

14. Negative feedback and termination of the stress response

When the stressor is no longer posing a threat, GCs are also responsible for the attenuation of the stress response via the activation of a negative feedback loop which acts in different centers of the brain and the stress axis. As we have already discussed, this loop closes via the binding of the GCs on the GRs and MRs. Since the MRs are already occupied due to their much higher affinity for GCs and their more limited distribution, it is up to the

GR expressing cells to restore GC levels back to normal. The main brain region regulating the release of GCs is the hippocampus. Given the excitatory nature of the major hippocampal efferent projections, it has been suggested that inhibition might be facilitated by groups of inhibitory neurons located in the hypothalamus or other areas. Indeed, the hypothesis that these brain areas would be excited by connections from the hippocampus and send signals to CRF cells in the PVN were corroborated by functional evidence showing that the connection between the hippocampus and the BNST plays a role in inhibiting the HPA axis (Cole et al., 2022). Interestingly, the role of higher limbic structures in regulating the HPA axis seems to be limited to the response to psychological stressors, rather than physiological stressors. This conclusion is based on various studies involving lesion experiments and Tg mice with conditional KO of the GR in the forebrain cortical and limbic regions (Diorio et al., 1993; Furay et al., 2008). Apart from the hippocampus, CRH neurons located in the PVN play a crucial role in initiating the activation of the HPA axis, making them the expected target for GC negative feedback. Experiments in the hypothalamic PVN have shown that corticosterone and the synthetic GC, dexamethasone, can quickly suppress excitatory glutamatergic synaptic inputs to the parvocellular neurosecretory neurons. These findings shed light on the mechanism of rapid GC feedback inhibition of hypothalamic hormone secretion, which occurs through endocannabinoid release in the PVN (Di et al., 2003). Interestingly, while endogenous GCs exert their self-suppressing role through the PVN, synthetic GCs such as dexamethasone, which is a GR agonist, elicit negative feedback through the ACTH cells of the anterior pituitary gland (Chong et al., 2017). By inhibiting the secretion of CRH and ACTH, the body can effectively limit the duration of tissue exposure to GCs. This helps to minimize the negative effects of these hormones – e.g., catabolism, lipogenesis, reproductive issues and immune suppression- since the stressor is no longer threatening homeostasis. Naturally, it takes up to 2 hours to restore homeostasis since GRs are intracellular nuclear receptors which exert their functions through the alteration of gene expression; while on the other hand, GC levels peak within the first 30 minutes following a stressful event (Spencer & Deak, 2017).

15. Evolutionary perspective on the stress system

From an evolutionary perspective, every vertebrate produces corticosteroids and possesses proopiomelanocortin, the precursor molecule of ACTH. Peptide sequences akin to those of human ACTH can be found in a wide range of organisms, including mammals, amphibians, reptiles, insects, mollusks, and marine worms. ACTH has been extensively linked to other signaling molecules, including CRH, epinephrine, norepinephrine, cortisol, and

cytokines, all of which play a vital role in defensive systems. It's fascinating how the genetic sequences for these molecules have remained unchanged for millions of years, while still playing important roles in the immune system (Nesse et al., 2016). The stress responce system is capable of responding to a wide range of stimuli, including both threats and challenges, as well as novel stimuli and positive social opportunities. However, today, most aspects of the stress response tend to be linked more strongly with negative rather than positive arousal. The main reasons are that stress response can be energetically costly, it disrupts other beneficial behaviors and that certain adaptations providing an advantage in the presence of threats, can also result in tissue damage (Nesse et al., 2016). In other words, the harm caused by stress responses does not always stem from "abnormal" stress. For example, the advantages of a stress response that enhances the chances of capturing prey can sometimes outweigh the drawbacks. However, a stress response making sure that prey will manage to escape from a predator, is worth any potential costs. On average, a well-designed regulatory mechanism will activate a stress response when the benefits outweigh the costs. According to a signal detection analysis, the principle of the "smoke detector" explains why many stress responses may appear excessive or unnecessary. This analysis is based on how natural selection shapes the mechanisms that regulate defense responses (Nesse, 2005). In the environment of our ancestors, where stressors were mostly physical, the stress response system proved to be more valuable than it is in our modern world. Today, societies are primarily confronted with social and mental challenges, resulting in the HPA system's actions often leading to more negative outcomes (Nesse et al., 2016).

16. Implications of stress system dysregulation

Having reviewed the physiological role of the stress system in restoring homeostasis and preserving the dynamic equilibrium which characterizes living organisms, it is time to examine the adverse effects of the stress response system dysregulation. By now, we have seen that the stress system has both a circadian activity and also reacts to stimuli when needed. An optimal level of baseline activity, along with precise and timely reaction of the stress system to stressors, is crucial for experiencing a state of well-being, achieving task performance and fostering social interactions (eustasis). Conversely, if the stress system's basal activity and/or responsiveness are incorrect, both in terms of intensity and duration, this could hinder growth, development and physiologic body composition. This could also be a contributing factor to various behavioral, endocrine, metabolic, cardiovascular, autoimmune and allergy problems (allostasis/cacostasis) (Illus. 5). The progression and intensity of these conditions are influenced by (epi)genetics or by the resilience of

individuals to stress, their exposure to stressors during crucial stages of development, the presence of detrimental or beneficial environmental factors and the timing, magnitude and duration of stress. Stress, when mediated by certain factors, can cause either acute or chronic pathological, physical and mental problems in susceptible individuals. Acute stress can induce allergic reactions, abnormal blood vessel activity, hyper/hypo-tension, various types of discomfort, gastrointestinal symptoms, as well as panic attacks and psychotic episodes. Chronic stress can lead to various physical, behavioral or neuropsychiatric symptoms. These may include anxiety, depression, difficulties with thinking and decision making, cardiovascular system problems, metabolic disorders, degenerative brain diseases, osteo-penia/porosis and sleep disorders (for a thorough review of the disorders of the stress system, including the conditions stemming from altered HPA axis activity, please see Chrousos, 2009).

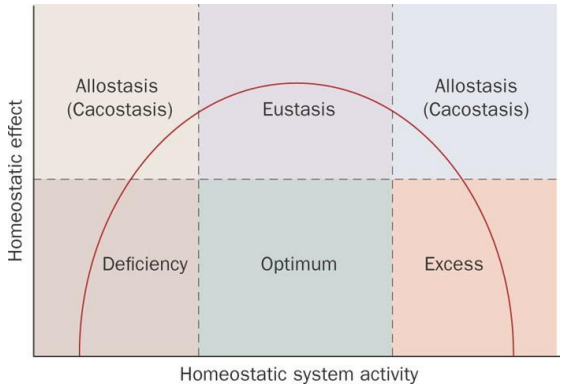

Illustration 5. Homeostatic systems follow an inverse U-shaped dose-response curve, with eustasis representing the optimal, balanced state in the middle. On either side of this optimal range, suboptimal effects can occur, leading to poor adaptation, referred to as allostasis or more accurately, cacostasis. These suboptimal adaptations may be detrimental to the organism in both the short and long term. Source: Chrousos, 2009.

17. The role of stress in neuronal vulnerability and PD

The hypothesis that stress may trigger PD by increasing the vulnerability of certain types of neurons to an early cell death has been around for a long time and has received renewed consideration since it affects the CNS at many different levels (Smith et al., 2002). In 1886, the renowned neurologist Sir William Gowers noted in his book "Manual of Diseases of the Nervous System" that “prolonged anxiety and severe emotional shock often precede the onset of tremor", a prominent motor symptom of Parkinson's disease (then referred to as "paralysis agitans") (Gowers, 1887). Today, it is understood that chronic stress and stress hormones impact the CNS at various levels, including transcriptional regulation, cellular signaling, synaptic function, neurotransmission, glial function and behavior (Carroll et al.,

2011). As I tried to convey earlier in the introduction, stress is one of the most significant influences on behavior and performance. As it was nicely reviewed by Metz (2007), while traditionally stress was thought to primarily impact the limbic system, affecting learning, memory and emotions, recent findings show that stress also influences motor system function and can affect movement disorders since GRs are found throughout the motor system, in brain regions such as the striatum and motor cortex, making these circuits particularly sensitive to stress hormones. Stress and GCs can alter various aspects of motor performance, with skilled movements being particularly vulnerable to disruptions, though stress can also impact locomotion and posture, while the activation of the HPA axis can also affect movement and lead to emotional changes. The dopaminergic system plays a key role in how stress affects motor function, potentially linking stress to dopamine-related motor diseases like PD (Metz, 2007). Clinical observations suggest that stress can trigger or worsen Parkinsonian symptoms. In the case of the first known instance of early-onset PD following major stress, an otherwise healthy 38-year-old woman without prior neurological issues or trauma, developed a sudden resting tremor in her left forearm one week after discovering her husband's affair, with EMG and PET test results being indicative of early PD and symptoms significantly improving with anti-parkinsonian medication (Zou et al., 2013). Similar results were acquired following chronic severe restraint stress of otherwise healthy adult WT rats. After two weeks of stress, young adult WT rats had a significant reduction in the number of DA and noradrenergic neurons in the SN and the LC, respectively, with the neuronal loss reaching up to 61% after 16 weeks in the SN, along with increased microglial activation and oxidative stress (Sugama et al., 2016). Regarding the worsening of symptoms, a study comparing stress-resilient to stress-sensitive PD patients during the COVID-19 pandemic, found that high stress-reactive patients had greater anxiety and non-motor symptoms while resilient patients had better quality of life, social support and cognitive abilities. Disease-specific factors like motor severity and medication use did not affect stress response. In addtion, while the pandemic did not accelerate PD progression, it worsened depressive symptoms in highly stress-reactive patients (van der Heide et al., 2024). Moreover, while chronic stress has been definitively linked to the development of neuropsychiatric conditions such as depression (Hill et al., 2012), it may also lead to dopaminergic neurodegeneration, a hallmark of PD, in vulnerable individuals (Djamshidian & Lees, 2014), and could accelerate this degeneration in PD animal models (Hemmerle et al., 2014; Wu et al., 2016). Currently, no study has thoroughly examined the risk that chronic stress poses to PD, nor determined if it should be viewed as a trigger, facilitator, or

aggravator of the disease (Johnson et al., 2019). Clinical observations suggest an abnormal stress response, such as HPA axis dysregulation, but direct evidence of molecular and glucocorticoid-related pathologies is lacking (Du & Pang, 2015). Asyn might be a significant factor, however, it is still unclear whether the increased asyn burden directly contributes to stress dysregulation or if the relationship is reciprocal. Table 1 summarizes all the animal studies examining the interplay of PD and stress. Naturally, in the course of roughly four decades spanning from the first publication in 1985 by Snyder and colleagues until this dissertation, along with the scientific paper which is included here and was published in 2024 by Nakos Bimpos and colleagues, there has been a tremendous progress in the fields of neurodegeneration and stress (Snyder et al., 1985; Nakos Bimpos et al., 2024). The growing evidence that stress can elicit neurodegeneration provides the impetus for expanding our understanding of the mechanisms underlying PD pathogenesis and discovering novel future therapeutic avenues.

Table 1. Overview of animal studies exploring the interaction between stress and Parkinson's disease.

Study	Species, sex, age, N	PD model	Stress Protocol (and duration)	PD and HPA axis related pathology	Proposed mechanism
(Snyder et al., 1985)	Sprague-Dawley male rats, N=194 (age NA: animals weighted 250-280 g)	6-OHDA (150 – 250 µg) single lesion in cisterna magna or bilaterally in the lateral ventricles	Chronic acute stress (two weeks after regaining normal weight post lesion): Glucoprivation and food deprivation, osmotic dehydration and water deprivation, tail shock or cold exposure stress. (Duration: NA, once/week)	6-OHDA lesions led to decreased dopaminergic nerve terminals but transient motor deficits manifested only after stressing lesioned animals. Decreased norepinephrine levels in the hippocampus are not related with stress induced neurological deficits.	6-OHDA lesioned animals could manifest akinetic symptoms following the effects – and depending on the severity – of stress in the striatum, due to inhibition of DA release or exhaustion of DA reserves.
(Urakami et al., 1988)	Young adult C57BL/6J mice at 6-8 weeks of age, N=20 (sex NA)	MPTP IP injections (30mg/kg); everyday for 3 consecutive days	Severe stress (one week post MPTP injection): single immersion immobilization stress for 15h in a water bath with a temperature of 25^{o}C (Duration: single event)	A trend of decreased locomotor activity was more apparent following stress in MPTP, than in saline mice. No differences in striatal DA between saline and MPTP treated groups but transient decrease of DA in the striatum of MPTP mice following stress. DA turnover significantly higher following stress with a greater increase in the MPTP treated group.	Akinetic phenotype following stress in MPTP mice could be attributed to decreased DA levels and enhanced DA turnover in the striatum. DA and DA turnover might be enhanced only after stress due to increased production or release of DA.
(Keefe et al., 1990)	Sprague-Dawley male rats (N and age NA: animals weighted 200-300 g)	6-OHDA (175 – 200 µg) lesion bilaterally in the lateral ventricles	Intermittent tail-shock (27 days post lesion):constant current pulses for 1 s every 10 s for a duration of 1 min was repeated every 5 min for a total of 30 min) (Duration: single event)	After stress, 6-OHDA treated rats showed a significantly increased extracellular DA, DOPAC and HVA release in the striatum. Post-stress catalepsy test was negatively correlated with the amount of extracellular fluid DA.	Stressed 6-OHDA-treated rats have a greater relative release of DA possibly due to neurochemical compensation combining a reduction of high-affinity reuptake and increased synthesis and release of DA.

Table 1. continued

Study	Species, sex, age, N	PD model	Stress Protocol (and duration)	PD and HPA axis related pathology	Proposed mechanism
(Howells et al., 2005)	Long Evans male rats, N=31 (age NA: animals weighted 222-405 g)	6-OHDA (10 µg) unilateral lesion into the medial forebrain bundle of the left hemisphere	Chronic mild stress (one week post lesion); Immobilization of their running wheel for 1 h per day, a single 24h long food restriction and a single 7h shift in the light/dark cycle (Duration: 2 weeks)	Apomorphine-induced running test to evaluate the severity of the neurotoxic lesion showed that runner group rotated significantly less than non-runners and stressed runners. TH staining in the SNg showed a trend of increased destruction of DA neurons in the non-runners and stressed runners compared to the runners.	Voluntary exercise exerts neuroprotective action through gene transcription, neurotrophic factor release and upregulation of DA receptors in the striatum.
(L. K. Smith et al., 2008)	Long Evans adult female rats, N=71 (age NA)	6-OHDA (8 µg) unilateral lesion of the nigrostriatal bundle	Chronic restraint stress (20 min/day) or CORT administration (5 mg/day) (Duration: 46 days, lesion was at day 17)	While both stress and CORT treatments elevate open field activity, stress causes a significant increase of Fluoro-Jade positive cells early after lesion and a significant acceleration of cell death. CORT treatment leads to consistently increased plasma CORT levels and a significantly increased GFAP intensity in the non-lesioned SNg.	Stress associated changes, such as disruption of pro/anti-apoptotic & neurotrophic factors and alteration of DA neurons metabolism, leading to altered susceptibility to 6-OHDA, might be independent to GC regulation. Attenuated neurodegeneration following CORT treatment could be dose-dependent inflammatory response or delayed cell death.
(Barnum et al., 2008)	Adult Sprague-Dawley male rats, N=73 (age NA: animals weighted 225-250 g)	6-OHDA (12 µg) unilateral lesion of the left medial forebrain bundle	Chronic exogenous CORT administration (three weeks post lesion); Low (1.25 mg/kg), or high (3.75 mg/kg) dose of CORT (Duration: 9 days)	Abnormal involuntary movements were reduced in rats receiving the high CORT dose on day 1 and in rats receiving either the high or the low dose of CORT on days 3 & 5. No changes in ipsilateral rotations. IL-1β gene expression increased in the lesioned side of L-DOPA treated rats.	Exogenous CORT administration attenuated both the expression and development of L-DOPA-induced dyskinesia possibly through neuroinflammation signaling, without modulating DA metabolism.

Table 1. continued

Study	Species, sex, age, N	PD model	Stress Protocol (and duration)	PD and HPA axis related pathology	Proposed mechanism
(Kelly et al., 2012)	Young C57BL/6J male mice at 4-6 weeks of age, N=25	Single dose of meth-amphetamine (20 mg/kg)	Acute (20 mg/kg) or chronic (400 mg/L in drinking water) pre-treatment with CORT prior to METH injection (Duration: single event or one week)	Chronic CORT enhances the meth-amphetamine induced expression of pro-inflammatory cytokines/ chemokines (TNF-α, CCL-2, IL-1β, LIF), activation of microglia (Isolectin B), astrogliosis (GFAP), dopaminergic neurotoxicity (significant decrease of TH+ neurons) in the striatum. Chronic CORT pre-treatment also affects frontal cortex and hippocampus.	Chronic CORT administration affects multiple areas of the CNS and may have a pro-inflammatory effect enhancing the neuro-inflammatory response to a neurotoxic dose of methamphetamine, along with signs of increasing microgliosis and astrogliosis.
(Hemmerle et al., 2014)	Adult Sprague Dawley male rats, N=36-40 (age NA: animals weighted 250-405 g)	6-OHDA (10 µg each); two unilateral lesions into the right striatum	Chronic unpredictable stress; two stressors/day (at three different time points; pre/post/mid-lesion): cold exposure, restraint, vibration, hypoxia, cold/warm swim, crowding, isolation (Duration: 4 weeks)	Four weeks after the 6-OHDA treatment, only the rats that were stressed concurrently with the lesion displayed a worse motor phenotype and increased degeneration of TH+ cells in the SNg, compared to the non-stressed lesioned rats or with the rats that were stressed either prior or after the lesion.	Chronic stress concurrent with the neurotoxic insult induced neurodegeneration and worsens motor symptoms, implicating cellular mechanisms regulating resistance and reactivity to neurotoxic threats.
(de Pablos et al., 2014)	Wistar male rats (N and age NA: animals weighted 250-270 g)	LPS (2 µg); single intranigral unilateral injection	Chronic variate stress; one stressor/day (following the LPS injection): forced swimming, restraint, restrain at 4^{o}C, isolation, food deprivation, water deprivation (Duration: 9 days)	Combination of LPS and stress significantly exacerbates damage inflicted in the SNg via microglia activation in a GC-dependant manner. A GR antagonist exerts a protective role confining the degeneration of TH+ neurons in the SNg in the same levels as in the animals that were only treated with LPS.	Stress could be involved in PD pathogenesis via dysregulation of the HPA axis, which is further burdened with increased age. Stress could be inflicting greater damage in brain regions with higher GR density while in parallel DAergic neurons become more susceptible to damage.

Table 1. continued

Study	Species, sex, age, N	PD model	Stress Protocol (and duration)	PD and HPA axis related pathology	Proposed mechanism
(Lauretti et al., 2016)	Adult C57BL/6 male and female mice at 7 months of age, N=40	MPTP IP injections (25 mg/kg); once a day for 7 consecutive days	Chronic restraint/isolation stress (before the administration of MPTP): restraint for 6h/day (Duration: 31 days)	Pre-exposure to stress exacerbates MPTP-induced motor deficits (rotarod test), TH+ neurons depletion and astocytosis (GFAP) in the SNg. In the striatum, DA and DOPAC levels, and TH signal are reduced in MPTP animals, regardless of previous exposure to stress. D2DR increased solely in the stressed group.	Stress has a pro-inflammatory role in the onset and development of the Parkinsonian phenotype since DA system appears to be stress-susceptible.
(Wu et al., 2016)	Adult Tg and WT, male and female WT mice at 6 months of age, N=90	Tg mouse line that over-expresses the human A53T mutant asyn (A53T mice)	Chronic variable mild stress; one stressor/day: food and water deprivation, wet bedding-, overnight illumination, cage rotation, restrain at 4°C and tail pinch (Duration: 31 days)	Stress increases CORT levels and anhedonia in both WT and A53T mice while it exacerbates motor impairments, olfactory deficits, nigrostriatal DA degeneration, neuroinflammation (IL-1β, IL-6, IFN-γ) and microgliosis (Iba1) and increased asyn aggregates solely in Tg males.	Mutations and/or neurotoxins disrupt neuronal functioning while stress triggers or exacerbates PD progression by increasing oxidative stress inflammatory processes. Female mice either display estrogen-related resilience to stress-induced neurodegeneration or slower progression of pathology.
(Janakiraman et al., 2017)	C57BL/6J male mice, N=96 (age NA: animals weighted 25-30 g)	MPTP IP (25 mg/kg) and probenecid (250 mg/kg) injections twice per week for 5 weeks	Chronic mild stress (before, amidst and after MPTP): cage tilting, wet bedding, empty cage, empty cage with water, light/dark cycle inversion, food or water deprivation and lights on during the dark phase (Duration: 4 weeks)	Stress worsened the MPTP/p induced motor and non-motor symptoms, antioxidant imbalance and molecular expressions (diminishes BDNF levels and pTrkB, p-ERK/ERK, p-AKT/AKT and p-CREB expression in nigrostriatal regions). Stress following MPTP/p had the most detrimental effect, further worsening the symptoms.	Stress alone cannot incite inflammatory processes along the nigrostriatal axis. There is an additive or synergistic interaction between stress and PD exerting the combined insults via oxidative stress and various other signaling molecules.

Table 1. continued

Study	Species, sex, age, N	PD model	Stress Protocol (and duration)	PD and HPA axis related pathology	Proposed mechanism
(Hao et al., 2017)	Young adult Long-Evans male rats, N=24 (age NA)	6-OHDA (8 µg) unilateral lesions of the nigrostriatal bundle	Chronic restraint stress (pre- and post- lesion) for 20 min/day (Duration: 6 weeks) or bilateral surgical removal of adrenal glands and CORT administration (5 ml/day)	Restraint stress increases open field activity and impairs skilled reaching accuracy, while restraint stress and clamped CORT partially protect TH expression in both SNg and VTA and differentially modulate the expression of SYN, calcyon and GR mRNA in midbrain and cortical areas.	Apart from the alterations of DA-related proteins involved in synaptic and neuronal plasticity induced by stress, GR upregulation in SNg, VTA, striatum and motor cortex could exert a protective effect as transcription factor or involved in mitochondria functioning.
(Z. Zhang et al., 2018)	Adult Tg and WT male mice at 10 months of age, N=64	Tg mice line that over-expresses the human A53T mutant asyn (A53T Tg mice)	Chronic restraint test for 4 hours/day (Duration: 4 weeks)	Stress accelerated non-motor (olfactory disorder), motor (rotarod and pole climb) and pathological PD process (increased mono/oligomeric asyn, decreased TH+ neurons in the SNg and decreased DA & DOPAC in the striatum) in Tg mice, along with decreased proteasome degradation of protein RTP801.	After stress, levels of protein RTP801 were found to be increased especially in DA neurons in the SNg. Elevated RTP801 reportedly blocked autophagy, leading to the accumulation of oligomeric asyn and ER stress. Inhibition of RTP801 alleviated the symptoms of neurodegeneration.
(Mitsumoto & Mori, 2018)	Adult C57BL/6 male mice at 8 weeks of age, N=20	MPTP IP injection (20 mg/kg) single dose	Acute restraint stress (following MPTP injection): single event (Duration: 2 hours)	In the mice that underwent stress following treatment with MPTP, decreased DAT and DA levels implicate a severe loss of nerve terminals in the striatum due to increased MPP+, while MAO-B activity remained unaffected.	Enhanced MPTP neurotoxicity in the striatum with the same levels of MAO-B activity suggest increased presence of the neurotoxin via CRF induced increased BBB permeability.

Table 1. continued

Study	Species, sex, age, N	PD model	Stress Protocol (and duration)	PD and HPA axis related pathology	Proposed mechanism
(Wassouf et al., 2019)	Adult C57BL/6N female mice Tg and WT at four months of age, N=32-40	Tg mouse model with a BAC containing the entire human *SNCA* gene (including the 5'/3' flanking regions)	Chronic unpredictable mild stress: restraint, cage tilt, rat confrontation, food restriction, water restriction, extended light exposure and reversed light/dark cycle (Duration: 8 weeks)	Stress causes hyperlocomotion while Tg animals show increased anxiety in the light/dark box, regardless of treatment. In stressed Tg mice, exploratory activity increases in the EPM. In the striatum of Tg mice, genes related to GABA & cholinergic signaling, alcohol metabolism and other environment-induced metabolic responses involved in PD are altered.	*SNCA*-overexpressing mice may have a prolonged response to acute stressors compared to the WTs leading to altered emotional processing. The limited impact of stress in the transcriptome of the striatum and hippocampus may be attributed to the absence of chronic cortisol elevation in the blood after stress.
(Kong et al., 2019)	Sprague Dawley male rats, N=48 (age NA: animals weighted 220-250 g)	LPS single intranigral unilateral injection (5 µg)	Chronic unpredictable mild stress (before or after LPS): tail pinch, foot shock, high speed agitation, water deprivation, forced swimming in 4 °C cold water, food deprivation, reversed light/dark cycle (Duration: 1-3 weeks)	Only the LPS and the 2 weeks stress followed by LPS groups show a robust increase of IL-1β, IL-6, TNF-α, NLRP-3, ASC and Caspase-1 expression, along with microglia (Iba1) activation and TH+ cell loss in the SNg. Stress increases CORT in the serum and decreases GR and MR in the SNg after the first two weeks.	When the LPS model of DA neurons degeneration (an animal model of brain inflammation) is combined with chronic stress, acceleration of the inflammatory response and activation of NLRP3 inflammasome may be based on different CORT levels and GC mediated microglia priming.
(Rudyk et al., 2019)	Adult C57BL6/J male mice at 3.5 months of age, N=48	Paraquat IP injections (10 mg/kg) (twice per week for 3 weeks)	Chronic unpredictable stress (3 weeks before paraquat injections begin): rat odor, lights on during dark phase, hair dryer air, social stress, empty cage, tail hang, cage tilting, tail pinch, restraint (Duration: 6 weeks)	Stress leads to lower locomotion and higher blood CORT (further increased by paraquat). Stress and paraquat synergistically reduce SPT and motor coordination. Stress does not alter paraquat induced DA neuron loss or regional microglia activation in SNg and reverses the paraquat reduction of hippocampal GR levels.	The adverse effects of paraquat are similar to those of an environmental stressor in terms of behavioral outcomes, HPA activity and hippocampal functioning, affecting both motor and non-motor aspects of PD in non-additive or synergistic interaction with other stressors.

Table 1. continued

Study	Species, sex, age, N	PD model	Stress Protocol (and duration)	PD and HPA axis related pathology	Proposed mechanism
(Burtscher et al., 2019)	Adult C57BL/6JRj male mice at 3 months of age, N=36	WT asyn PFFs (5 mg) unilateral injection into the right dorsal striatum	Chronic CORT (35 mg/L) administration in drinking water starting 4 weeks before PFFs stereotactic injection until sacrifice (Duration: 90 days)	PFF-induced hypoanxious phenotype is reversed by CORT, which also leads to decreased ipsi vs contra TH+ cells in SNg, while no TH+ cell loss is observed in saline-injected PFF mice. PFF-caused brain asyn pathology is most notably exacerbated in the entorhinal cortex following CORT.	In PFF mice, while SNg and motor phenotype are not affected, CORT aggravates neuronal degeneration. Entorhinal cortex was found to be particularly vulnerable to asyn pathology in the case of GC imbalance. Asyn PFFs may have a preconditioning role exerting a hormesis effect.
(Mitsumoto et al., 2019)	Adult C57BL/6 male mice at 8 weeks of age, N=14	MPTP IP single dose (20 mg/kg)	Confrontational housing stress (single event, followed by MPTP injection) (Duration: 24 h)	MPTP treated stressed mice display decreased DAT and TH and increased GFAP protein levels in the striatum, suggesting a dysregulation in nerve terminal functions and signs of astrogliosis.	Abnormal monoamine neurotransmission renders the DA neurons vulnerable while psycho-social stress induces a pro-inflammatory profile via HPA axis activation, suggesting that stress-related disorders could be a PD risk factor.
(Dodiya et al., 2020)	Young adult C57BL/6 male mice at 6-8 weeks of age, N=28	Rotenone (10 mg/kg/day) orally for 6 weeks	Chronic unpredictable restraint stress (starting 6 weeks before treatment with rotenone begins) for 2 h/day at different times (Duration: 12 weeks)	During the first 6 weeks, stress increases colonic permeability and disrupts key tight junction proteins (ZO-1, occludin, claudin-1) while rotenone alone reduces ZO-1. Stress and rotenone synergistically disrupt tight junctions leading to hyper-permeability-induced endotoxemia and change gut microbiota, reducing Firmicutes and Actinobacteria and increasing Verrucomicrobia.	Stress and rotenone-induced intestinal hyper-permeability leads to endotoxemia in the SNg and peripherally along with an altered microbiota profile. The decrease of putative “anti-inflammatory” and increase of “pro-inflammatory” bacteria may contribute to neuro inflammation / degeneration via a mechanism including TLR4 signaling.

Table 1. continued

Study	Species, sex, age, N	PD model	Stress Protocol (and duration)	PD and HPA axis related pathology	Proposed mechanism
(Diwakarla et al., 2020)	Adult Tg and WT, male and female mice at 5 months of age, N=40	Tg mouse line that over-expresses the human A53T mutant asyn (A53T Tg mice)	Chronic isolation stress: single-housed conditions (Duration: 10 months)	Stress increases plasma CORT levels, exacerbates motor deficits and GI dysfunction. Tg animals have increased large asyn particles in ganglion and enteric neurons and less nNOS neurons in myenteric ganglia of the ileum. Stressed Tg mice have less Hu+ neurons / ganglion in the colon.	While Tg mice have reduced anxiety-like behaviors and lower baseline CORT, stress-increased CORT levels may be involved in exacerbated gut and motor PD phenotype through inhibitory effects in the colon and DA system imbalance respectively.
(Grigoruţă et al., 2020)	Adult Tg and WT male and female Long-Evans rats at 9-11 weeks of age, N=58	PINK1-KO rats	Predator-induced psychological distress (Duration: 3 or 10 days)	Stress increases anxiety-like behavior, motor dysfunction and alters BDNF and expression of antioxidants in WT and Tg rats alike, without signs of SNg neurodegeneration. Plasma CORT increases only in WT rats. Stress and mitochondrial dysfunction, modestly interact to exacerbate rotarod performance. Stressed female rats show less bioenergetic alterations.	Stress phenocopies PD neuro-pathology aspects by disrupting brain energy production. Unchanged CORT levels in Tg rats indicate dysregulation of HPA axis, presumably due to the absence of endogenous PINK1. Female rats are more resilient possibly due to neuroprotective effects of estrogen.
(Tuon et al., 2021)	Adult Wistar male rats, N=40-48 (age NA)	6-OHDA (20 µg) unilateral lesion in the striatum	Chronic mild stress (CMS) consisting of one stressor/ day at different times every day (starting 32 days before 6-OHDA lesion); food deprivation, water deprivation, restraint (+ at 4 °C), flashing light and isolation (Duration: 40 days)	In the open field, crossings and rearings increase only in the stress & 6-OHDA group, along with an increase in nitrite/nitrate concentrations in the striatum, decreased SOD in the hippocampus and increased myeloperoxidase activity in both regions. Striatum is mainly affected by 6-OHDA, PFC by stress while hippocampus is affected by both.	Both CMS and 6-OHDA models show neurotransmitter system alterations, with oxidizing substances increasing in brain areas related to MDD and PD, potentially being involved in neurodegenerative and mood disorder processes.

Table 1. continued

Study	Species, sex, age, N	PD model	Stress Protocol (and duration)	PD and HPA axis related pathology	Proposed mechanism
(Wang, Xu, et al., 2021)	Adult C57BL/6 male mice at 8-10 weeks of age, N=105	MPTP IP injections (30 mg/kg/day) consecutively for five days	Chronic mild (one stressor/day) or strong (two stressors/day) stress (10 days after MPTP); cage tilting, sawdust dampening, immersion in ice water, tail clamping, inversion of light/dark cycle, food or water deprivation and lights on for 24h (Duration: 21 days)	MPTP leads to a 50% loss of TH+ neurons in the SNpc but has non-significant effects to mobility and depression symptoms. Stress impairs learning (MWM) while motor deficits (open field and rotarod), depressive symptoms (FST), GFAP in the striatum, 5-HT & DA levels, oxidation & inflammation markers and 5-HT & GABA receptors mRNA are further altered depending on stress severity.	Motor deficits and depression in PD may be due to alterations of the brain functional network and neurotransmitters other than dopaminergic impairment. Based on FST positive correlation with 5-HT receptors expression, 5-HT1bR and 5-HT2cR are speculated to have a role in the development of the depressive phenotype in PD.
(Idrissi et al., 2023)	Young adult Wistar male rats at 7 to 8 weeks of age, N=32	6-OHDA (5 µg) injection into the left medial forebrain bundle	Restraint stress (one week after the 6-OHDA lesion) (Duration: 7 days)	Stress exacerbates motor deficits (open field, beam walking and rotarod tests) and anxiety in 6-OHDA. In the striatum, 6-OHDA decreases DA levels, increases iron accumulation and induces caspase-3, AChE and p53 overexpression while after stress, p53 remains unaffected in PD animals.	Stress may aggravate apoptosis by increasing caspase-3 and AChE in 6-OHDA rats, later aggravating motor coordination, possibly through HPA axis hyper-activity and increased GC release. Anxiety might be due to monoamines - especially DA - system imbalance.
(Alwani et al., 2023)	Adult C57BL/6J male mice at 12 weeks of age, N=48-76	Bilateral injections of asyn preformed (length of PFFs ~50 nm) into the striatum	Chronic social defeat stress 90 days post-PFFs injection (Duration: 10 days)	Asyn aggregation led to increased locomotion (open field test), reduced anxiety (light-dark box) and immobility (tail suspension). Asyn aggregation was more prominent in amygdala, PFC and SNg, with minimal aggregation in the RN and LC and there was only modest DA neuron loss along the nigrostriatal axis in PFF groups.	Progressive bilateral asyn aggregation might lead to increased compensatory activity and alterations in emotionally regulated behavior. At this point, modest DA neuron loss and asyn aggregation at the brain regions of amygdala and PFC do not affect stress susceptibility.

18. PD and stress animal models

Three years after the identification of the *SNCA* gene mutation in 1997 (Polymeropoulos et al., 1997), the first Tg mouse expressing WT human asyn was generated. This was a pivotal moment in PD research as alterations characterized by the formation of intra-nuclear deposits and cytoplasmic inclusions were associated with loss of dopaminergic terminals in the basal ganglia and with motor impairments, thus providing the first direct evidence of asyn's role in neurodegeneration in a Tg animal model (Masliah et al., 2000). Sixteen more years had to pass by before a group used Tg animals to study the effects of chronic variable mild stress in adult animals of both sexes reporting that stress triggers or exacerbates PD progression by increasing oxidative stress and inflammatory processes predominantly in male Tg mice, leading to an exacerbation of motor impairment, olfactory deficits, nigrostriatal DA degeneration, neuroinflammation and microgliosis, along with increased asyn aggregation (Wu et al., 2016). Before that, all the studies relied on the use of neurotoxic agents of varying concentrations, applied either directly in the brain of the animal models or administered peripherally. The two most commonly used substances are MPTP (1-methyl-4-phenyl-1,2,3,6-tetrahydropyridine) and 6-OHDA (6-hydroxydopamine).

The neurotoxins MPTP and 6-OHDA were selected to create animal models of PD due to their ability to selectively destroy dopaminergic neurons in the SNg, mimicking the dopaminergic degeneration characterizing PD. MPTP, when administered to non-human primates, mice, or other species, crosses the BBB and is metabolized by astrocytes to MPP+ (1-methyl-4-phenylpyridinium), which is then taken up by dopaminergic neurons via the DA transporter (DAT). This leads to mitochondrial dysfunction, oxidative stress and subsequent cell death, effectively replicating the motor symptoms and neurochemical deficits characteristic of PD (Langston et al., 1983). Similarly, 6-OHDA is commonly injected directly into specific brain regions, such as the SNg or striatum. 6-OHDA is selectively taken up by catecholaminergic neurons through DAT and norepinephrine transporters, causing oxidative stress and mitochondrial damage, thereby inducing dopaminergic neuron loss and behavioral deficits (Ungerstedt, 1968). While both MPTP and 6-OHDA models are crucial for testing potential neuroprotective and neurorestorative therapies it is understood that, although they replicate the pathophysiological hallmarks of PD (Bové & Perier, 2012), they offer little to no insight regarding the pathogenesis, the development, the progression or the early diagnosis of the disease.

Compared to the rest of the studies using 6-OHDA to model PD pathophysiology, the earlier studies appear to have used a much greater amount of the neurotoxin. 6-OHDA lesions led to decreased dopaminergic nerve terminals and norepinephrine levels in the hippocampus. Transient motor deficits manifested only after chronically acute stressing the lesioned animals, with the authors of the study hypothesizing that the manifestation of akinetic symptoms following the effects – and depending on the severity – of stress in the striatum, resulted either due to inhibition of DA release or due to the exhaustion of DA reserves (Snyder et al., 1985). Intriguingly, in a different study published five years later using the same amount of 6-OHDA, the lesioned rats showed a significantly increased extracellular DA, DOPAC and HVA release in the striatum. On the other hand, a single stress event in the 6-OHDA-treated rats led to greater release of DA, possibly due to neurochemical compensation combining a reduction of high-affinity reuptake and increased synthesis and release of DA, with post-stress catalepsy being negatively correlated with the amount of extracellular fluid DA (Keefe et al., 1990).

A number of studies included in Table 1, using a more moderate amount of 6-OHDA, employ chronic restraint as a stressor. Restraint stress, whether acute or chronic, involves confining an animal in a restricted space, which can significantly elevate stress hormone levels and affect psychological well-being. Restraint stress has been extensively studied to understand both the physical and psychological impacts of confinement, with findings indicating alterations in neuroinflammatory pathways and behavioral changes such as increased anxiety and depressive-like symptoms (Bains et al., 2015). Following an increase in open field activity after 6-OHDA lesion, restraint stress causes a significant increase of Fluoro-Jade positive cells early along with acceleration of cell death. Additionally, restrain stress disrupts pro/anti-apoptotic & neurotrophic factors and affects the metabolism of dopaminergic neurons, altering susceptibility to 6-OHDA, possibly in a way independent of GC regulation (Smith et al., 2008). A different study notes an increase in open field activity and impaired skilled reaching accuracy only after restraint stress was applied to 6-OHDA lesioned rats, along with a further decrease of synaptophysin TH levels in SNg and VTA (Hao et al., 2017). Finally, in a study published last year, chronic restraint stress following 6-OHDA lesion exacerbates motor deficits and anxiety, while it influences apoptosis by increasing caspase-3 and AChE, though without further affecting p53 expression, possibly through HPA axis hyper-activity and increased GC release (Idrissi et al., 2023).

While natural stress response involves a complex systemic response that begins with the activation of the HPA axis resulting in the stimulation of the adrenal glands to produce CORT, this cascade reflects just one aspect of the stress response (McEwen, 2007). Simultaneously, there is activation of the sympathetic-adrenal-medullary (SAM) axis, which leads to increased epinephrine and norepinephrine levels, affecting cardiovascular and energy metabolism (Herman et al., 2016). Moreover, stress induces alterations in immune function and neurotransmitter systems, which can influence behavior and cognitive processes. This complex response ensures that the organism adapts to the stressor, but it also introduces variability in experimental outcomes due to the multiple pathways and feedback mechanisms involved (Sapolsky, 1992). Direct CORT administration provides a focused approach by isolating the effects of this GC hormone. When CORT is administered externally, it bypasses the upstream components of the HPA axis, leading directly to changes in GCR activation without the concurrent activation of the SAM axis or initial CRH and ACTH release. This method allows for precise control over the timing, dose and duration of CORT exposure, enabling researchers to study its direct effects on target cells and tissues (de Kloet et al., 2005).

The effects of CORT administration were also examined as an alternative to the restraint stress. In both cases, CORT administration either attenuated neurodegeneration in a dose-dependent inflammatory response or by delaying cell death (Smith et al., 2008), or spared mobility and had rather the opposite effect than restraint stress, by increasing synaptophysin (a synaptic marker) and TH levels and GR upregulation in SNg, VTA striatum and motor cortex, possibly exerting a protective effect (Hao et al., 2017). Chronic administration of different concentrations of CORT three weeks after 6-OHDA unilateral lesion leads to attenuation of both the expression and development of L-DOPA-induced dyskinesia, possibly through neuroinflammation signaling, without modulating DA metabolism (Barnum et al., 2008).

The remaining three studies using 6-OHDA to model PD employ the chronic unpredictable stress (CRUST) protocol. The CRUST protocol can be better understood by separately analyzing each component of the term, which reveals insights into the protocol's duration and predictability. Chronic stress involves repeated exposure to a stressor over a prolonged period, leading to sustained activation of the HPA axis. Chronic stress exposure has been shown to result in various long-term physiological and neurological effects, including changes in neuroplasticity and increased vulnerability to psychiatric disorders

(McEwen, 2007). Severe (or acute) stress, in contrast, typically involves a brief but intense exposure to a stressor that triggers a robust activation of the hypothalamic-pituitary-adrenal (HPA) axis and the sympathetic nervous system. This acute activation results in a rapid release of stress hormones such as CORT, which can be measured to assess stress response (Herman et al., 2016). For instance, severe stress can be induced by acute foot shock or forced swim tests, which are commonly used in studies investigating the immediate physiological and behavioral effects of stress (Koolhaas et al., 2011). Predictable vs. unpredictable stress protocols differ primarily in whether the timing and nature of the stressor are known to the animal. Predictable stress, which allows animals to anticipate the stressor, generally leads to less pronounced physiological responses compared to unpredictable stress. Unpredictable stress, involving random exposure to various stressors, is particularly effective in studying the effects of stress unpredictability on mental health, as it prevents habituation and induces a more pronounced activation of stress-related pathways (Grissom & Bhatnagar, 2009).

Applying CRUST at three different time points, pre/post and mid-lesion, combined with two unilateral lesions into the right striatum revealed that the rats that were stressed concurrently with the lesion displayed a worse motor phenotype and increased degeneration of TH+ cells in the SNg, compared to the non-stressed lesioned rats or with the rats that were stressed either prior or after the lesion (Hemmerle et al., 2014). In experimental studies of PD, the timing of neurotoxin administration relative to stress exposure can significantly influence research outcomes, reflecting different hypotheses about disease progression and vulnerability. Administering a neurotoxin, such as 6-OHDA or MPTP, before introducing stress models the scenario where an individual already exhibiting PD pathology encounters additional environmental stressors. This approach is akin to what many patients experience, where pre-existing neurological decline may be exacerbated by subsequent stress, potentially accelerating disease progression. This sequence helps researchers explore how stress might further the neurodegenerative process or impact symptom severity in already compromised neurological systems, focusing on identifying therapeutic interventions to mitigate these effects (Sulzer, 2007). Voluntary exercise exerts neuroprotective actions through gene transcription, neurotrophic factor release and upregulation of DA receptors in the striatum in another study applying CRUST one week post 6-OHDA lesion (Howells et al., 2005). Interestingly, application of a CRUST protocol followed by 6-OHDA insult results in increased crossings and rearings in the open field test, along with an increase in nitrite/nitrate concentrations in the striatum, decreased SOD in the

hippocampus and increased myeloperoxidase activity in both regions. Overall, CRUST and 6-OHDA models show neurotransmitter system alterations with oxidizing substances increasing in brain areas related to MDD and PD potentially being involved in neurodegenerative and mood disorder processes (Tuon et al., 2021).

When MPTP was used to model PD, half of publications presented in Table 1 used a single event of severe stress. Following stress, the MPTP-treated animals presented an akinetic phenotype and a bigger trend of decreased locomotor activity (compared to mice treated with saline), along with a transient decrease of DA in the striatum and increased DA turnover (Urakami et al., 1988). After a smaller dose of MPTP, decreased toxicity was followed by acute restraint stress leading to a decrease of DAT and DA levels while MAO-B activity remains unaffected, suggesting an increase in the presence of the neurotoxin via CRF-induced increased BBB permeability (Mitsumoto & Mori, 2018). Work by the same group, this time applying acute psychological stress before the administration of MPTP, reports that mice display decreased DAT and TH and increased GFAP protein levels in the striatum. This abnormal monoamine neurotransmission possibly renders the DA neurons vulnerable while psycho-social stress induces a pro-inflammatory profile via HPA axis activation, affirming stress-related disorders as a PD risk factor (Mitsumoto et al., 2019).

Pre-exposure to chronic acute restraint before the administration of MPTP exacerbates the neurotoxic-induced motor deficits, TH+ neurons depletion and astocytosis in the SNg. In the striatum, DA and DOPAC levels along with TH signal are reduced in MPTP-treated animals, regardless of previous exposure to stress, while D2DR increased solely in the stressed group (Lauretti et al., 2016). When MPTP administration is combined with probenecid, a drug potentiating MPTP toxicity (Alvarez-Fischer et al., 2013), subsequent CRUST protocol further worsens the MPTP/p induced motor and non-motor symptoms, antioxidant imbalance and molecular expressions. MPTP/p followed by CRUST is reported to have the most detrimental effect, further worsening the symptoms while CRUST alone cannot incite inflammatory processes along the nigrostriatal axis. Thus, it is hypothesized that there is an additive or synergistic interaction between stress and PD, exerting the combined insults via oxidative stress and various other signaling molecules (Janakiraman et al., 2017). Finally, a different study marked a 50% loss of TH+ neurons in the SNpc following five consecutive days of MPTP injections, though without significant effects to mobility and depression symptoms. Motor deficits, depressive-like symptoms , GFAP in the striatum, 5-HT & DA levels, oxidation & inflammation markers and 5-HT & GABA receptors mRNA are

further altered depending on a CRUST protocol of varying intensity. Moreover, based on forced swim test results, correlation with 5-HT receptors expression, it is hypothesized that depression in PD may be due to alterations of the brain functional network and neurotransmitters other than dopaminergic impairment (Wang, Xu, et al., 2021).

A different study aiming to examine the interaction of PD with stress, used a single dose of methamphetamine (METH) to model PD pathophysiology (Kelly et al., 2012). METH is a potent psychostimulant known to increase the release and inhibit the reuptake of DA, leading to elevated DA levels in the synaptic cleft. This excess DA can undergo auto-oxidation or be metabolized into toxic reactive oxygen species (ROS), causing oxidative stress and subsequent damage to dopaminergic neurons (Cadet & Krasnova, 2009). In animal studies, a single high dose of METH increases DA release and inhibits its reuptake, leading to elevated synaptic DA levels. This process induces oxidative stress and neuronal damage, particularly in dopaminergic neurons in regions such as the striatum and SNg (Kita et al., 2003). METH neurotoxicity involves not only direct damage to DA neurons, but also significant neuroimmune activation. METH activates microglia and astrocytes in the brain, leading to the release of pro-inflammatory cytokines (such as TNF-α, IL-1β, and IL-6), ROS and nitric oxide (NO) (Flora et al., 2002; Thomas et al., 2004). This inflammatory response creates a neurotoxic environment further damaging neurons due to the combined activation of microglia and astrocytes amplifying the neurotoxic effects of METH, promoting dopaminergic neuron degeneration similar to that seen in PD (Loftis & Janowsky, 2014). Indeed, in the study we present in Table 1, chronic CORT administration enhances the METH-induced expression of pro-inflammatory cytokines/ chemokines and the activation of microglia and astrogliosis further decreasing the amount of TH+ neurons in the striatum (Kelly et al., 2012).

Lipopolysaccharide (LPS), a bacterial endotoxin, is frequently used in PD research to induce neuroinflammation and study its effects on dopaminergic neurons. When injected into the brain, particularly in the SNg as in the studies we examined (de Pablos et al., 2014; Kong et al., 2019), LPS activates microglia resulting in a robust inflammatory response characterized by the release of pro-inflammatory cytokines such as TNF-α, IL-1β, and IL-6, leading to oxidative stress and selective degeneration of dopaminergic neurons, mimicking aspects of PD pathology (Castaño et al., 1998; Gao et al., 2002). Both studies used adult rats of approximately the same age, based on their weights. In contrast to the earlier study that only used less than half of the amount of LPS with CRUST preceding the unilateral

intrastriatal injection, the latest study applied CRUST of varying duration at many different time points, reporting that only the group that solely received LPS and the group that was stressed two weeks prior to the LPS injection show a robust increase of IL-1β, IL-6, TNF-α, NLRP-3, ASC and Caspase-1 expression, along with microglia activation and TH+ cell loss in the SNg (Kong et al., 2019). In the first study, combination of LPS followed by CRUST significantly exacerbated damage inflicted in the SNg (de Pablos et al., 2014). Both studies postulate that damage is exacerbated based on different CORT levels and GC mediated microglia priming, further validating the value of LPS-induced models for investigating the role of neuroinflammation in PD progression (de Pablos et al., 2014; Kong et al., 2019).

Paraquat, a widely used herbicide, is utilized in PD research due to its ability to induce dopaminergic neurodegeneration, thereby mimicking key aspects of PD pathology. Paraquat generates ROS through redox cycling, leading to oxidative stress and mitochondrial dysfunction, both of which selectively damage dopaminergic neurons in the SNg. Studies using paraquat in animal models, particularly rodents, have demonstrated that exposure to this herbicide causes progressive motor deficits and dopaminergic neuron loss, similar to the neurodegenerative process observed in PD patients (Brooks et al., 1999). Additionally, mice exposure to paraquat has been associated with increased asyn expression and aggregation, a hallmark of PD pathology (Manning-Bog et al., 2002), while in a Drosophila model expressing human asyn and exposed chronically to paraquat, fly mortality rates along with soluble, misfolded asyn not prone to fibril aggregation increased (Arsac et al., 2021). Paraquat administration in adult male mice combined with a 6-weeks long CRUST protocol, results to lower locomotion and higher blood CORT which is further increased by paraquat. Stress and paraquat synergistically reduce SPT and motor coordination, while stress does not alter paraquat induced DA neuron loss or regional microglia activation in SNg, but interestingly reverses the paraquat reduction of hippocampal GR levels (Rudyk et al., 2019).

Rotenone is a widely used pesticide that has been employed in PD research as a tool to model the disease in various animal species. Rotenone is a potent inhibitor of mitochondrial complex I, which is a key component of the electron transport chain in mitochondria. When rotenone is systemically administered, it leads to selective degeneration of dopaminergic neurons in the SNg. This model mimics several key features of PD, including motor deficits, dopaminergic neuron loss and the formation of LB-like inclusions within surviving neurons (Betarbet et al., 2000). The neurotoxic effects of rotenone are attributed to its ability to induce oxidative stress, mitochondrial dysfunction

and impair energy metabolism. These mechanisms lead to increased production of ROS and reduced ATP production, which are detrimental to the health of neurons. Chronic exposure to rotenone in animal models can induce a progressive and irreversible Parkinsonian syndrome, making it a valuable model for studying the pathophysiology of PD and for testing neuroprotective therapies (Sherer et al., 2003). Interestingly, in the study we reviewed, young adult mice received low oral doses of rotenone for 6 weeks while they were undergoing a 12-week long chronic unpredictable restraint stress protocol. Restraint stress and rotenone synergistically disrupt tight junctions leading to hyper-permeability-induced endotoxemia and changes in the gut microbiome, reducing the population of the phyla *Firmicutes* and *Actinobacteria* and increasing *Verrucomicrobia*. Stress and rotenone-induced intestinal hyper-permeability leads to endotoxemia in the SNg and peripherally along with an altered microbiota profile. The decrease of putative "anti-inflammatory" and increase of "pro-inflammatory" bacteria may contribute to neuro- inflammation / degeneration via a mechanism including TLR4 signaling (Dodiya et al., 2020).

While the rest of the publications up until today are based on Tg animal models, two recently new studies use instead asyn PFFs to model PD. Interestingly, the more recent study by Alwani and colleagues reported that bilateral injections of asyn PFFs in the striatum lead to increased locomotion, reduced anxiety and immobility with more prominent asyn aggregation in the amygdala, PFC and SNg and minimal aggregation in the RN and the LC. Since there was only modest dopaminergic neuronal loss along the nigrostriatal axis in the PFF groups, they hypothesize that compensatory mechanisms accompanied by alterations in emotionally regulated behavior could have been activated, without any further susceptibility to the chronic stress that took place 3 months after the stereotaxic injections (Alwani et al., 2023). The other study using PFFs had considerable methodological differences despite the use of adult male mice of around the same age. There, asyn PFFs were injected solely into the right dorsal striatum with the injection being performed while the stress protocol, consisting of chronic CORT administration in drinking water, was ongoing (Burtscher et al., 2019). Unilateral PFF injections also lead to a hypoanxious phenotype which is reversed by CORT and results to decreased ipsi *vs*. contra TH+ cells in SNg. While no TH+ cell loss is observed in saline-injected mice, PFF-caused brain asyn pathology is most notably exacerbated in the entorhinal cortex, following CORT. While SNg and motor phenotype are not affected, CORT administration aggravates neuronal degeneration leading the authors to hypothesize that asyn PFFs may have a preconditioning role exerting a hormesis effect (Burtscher et al., 2019). As previously noted, the seminal paper that detailed the injection of

asyn PFFs as a PD animal model was published by Virginia Lee and her team in 2012, more than a decade after the creation of the first Tg animal model (Luk et al., 2012). In terms of translatability, once again this approach only serves as a model of the pathological hallmarks of the disease, representing only cases of brain-first PD, ignoring the processes that are involved from the pathogenesis of the disease until the onset of the symptoms as well as introducing an extra variability due to the differences in structure, morphology and seeding capacity of the PFFs (Burtscher et al., 2019; Alwani et al., 2023).

One of the most commonly used Tg animal in PD research is the A53T asyn mouse model, which overexpresses the human A53T mutant form of asyn (A53T mice). This model exhibits many PD-like features, including the accumulation of pS129 asyn within neurons and the development of severe motor impairments. These features appear in a progressive manner, closely mimicking the human disease, which has made this model highly valuable for research (Giasson et al., 2002). In A53T mice, stress accelerated non-motor, motor and pathological PD processes, while inhibition of RTP801 alleviated the symptoms of neurodegeneration, proposing that autophagy dysregulation is implicated in the disease (Zhang et al., 2018). The GI track of old A53T Tg mice is characterized by increased amounts of large asyn particles in ganglion and enteric neurons and less nNOS neurons in myenteric ganglia of the ileum. While Tg rats have reduced anxiety-like behaviors and lower baseline CORT, stress-induced increase of CORT levels may be involved in exacerbated gut and motor PD phenotype through inhibitory effects in the colon and DA system imbalance, respectively (Diwakarla et al., 2020).

Of course, other models are also created or chosen based on how well they replicate the particular features of PD that researchers are keen on investigating, such as LB pathology, motor symptoms or specific genetic mutations. For this reason, among the Tg animals used to investigate the interplay of PD with stress, PINK1-KO rats are also included (Grigoruţă et al., 2020). The PINK1 gene mutation is closely associated with PD, particularly affecting early-onset forms. PINK1 plays a critical role in mitochondrial maintenance, primarily through regulating mitophagy and mutations disrupting this function lead to the accumulation of dysfunctional mitochondria, contributing to neuronal stress and death (Valente et al., 2004). Additionally it has been shown that PINK1 mutations can result in complex I deficiencies and impaired respiration in mitochondria, exacerbating dopaminergic cell loss in PD (Clark et al., 2006). In PINK1-KO rats, stress increases anxiety-like behavior, motor dysfunction and alters BDNF and expression of antioxidants in WT and Tg rats alike,

without signs of SNg neurodegeneration. Unchanged CORT levels in Tg rats following stress indicate dysregulation of HPA axis, presumably due to the absence of endogenous PINK1 (Grigoruţă et al., 2020). A different Tg mouse, carrying a BAC containing the entire human *SNCA* gene, displayed baseline increased exploratory activity increases in the elevated plus maze. The limited impact of CUMS in the transcriptome of the striatum and hippocampus of the *SNCA*-overexpressing mice may be attributed to the absence of chronic cortisol elevation in the blood following the stress protocol. Remarkably, this was the one of the few studies where a chronic stress protocol had little-to-no effect and the animals that participated in the experiments were female (Wassouf et al., 2019). Likewise, only old female - but not male - A53T mice that underwent CUMS display estrogen-related resilience to stress-induced neurodegeneration or slower progression of pathology (Wu et al., 2016).

19. Sex-specific variations in stress and PD response

Incorporating both sexes in animal models for PD research is crucial for a comprehensive understanding of the disease, particularly because non-motor symptoms often manifest differently between males and females. This approach ensures that findings are more broadly applicable and can guide more effective, gender-specific treatments. The importance of using both sexes in PD research is underscored by the differences in how non-motor symptoms - such as depression, anxiety and cognitive decline - appear and progress. For instance, women with PD may experience more pronounced depression and anxiety compared to men (Picillo et al., 2017). Additionally, hormonal influences, which vary significantly between sexes, can affect disease pathology and response to treatments, necessitating a sex-specific analysis to optimize therapeutic strategies (Gillies et al., 2014). Despite the clear differences in symptomatology and progression between sexes, PD is more prevalent in males. This higher incidence in males has been linked to several factors, including environmental exposures, lifestyle choices and biological differences in neuroprotection and neurodegeneration mechanisms. Men are more likely to be exposed to certain environmental risk factors, such as pesticides and heavy metals, which are associated with higher PD risk (Van Den Eeden et al., 2003). Moreover, estrogen has been suggested to play a neuroprotective role in women, potentially delaying the onset or progression of PD, which might contribute to the lower incidence in females until post-menopausal years when estrogen levels decline (Rocca et al., 2008; Shulman & Bhat, 2006). A study investigating the impact of estrogen on DA neuron health in postmenopausal women with untreated PD found indications that higher estrogen exposure was linked to better preservation of DAT in

the brain and less severe motor symptoms. Additionally, those with higher estrogen exposure required slower increases in PD medication suggesting a protective role for estrogens on the dopamine system in PD (Lee et al., 2019).

Experimental groups consisting of both male and female animals is definitely a move in the right direction (Lauretti et al., 2016; Diwakarla et al., 2020), but it is still a risky approach since experimental procedures might activate different mechanisms between the two sexes that could generate confounding results. In the case of Diwakarla et al., the stress applied in the A53T male and female mice consisted of chronic isolation achieved by single-housed conditions (Diwakarla et al., 2020). A number of studies have shown that stress enhances HPA axis baseline activity in males and isolated females, but this response is mitigated in group-housed females, suggesting that social environment can lessen the perception and physiological impact of stress (Brown & Grunberg, 1995; Westenbroek et al., 2003; McCormick et al., 2005). Additionally, Diwakarla and associates reported that old A53T mice had less nNOS neurons in myenteric ganglia of the ileum (Diwakarla et al., 2020). In a different study of PD-like neurodegeneration caused by MPTP, young females had a greater recovery in DA levels compared to males following the neurotoxic insult. However, in older mice of both sexes, reduced DA levels persisted indicating that age and sex influence DA concentrations along with the expression of inducible (iNOS) and neuronal NOS synthase enzymes, highlighting increased MPTP's toxic effects and a slower recovery process in males and older animals (Joniec et al., 2009). On the other hand, after using MPTP to model PD Lauretti and colleagues report an increase in the steady-state levels of GFAP across the nigrostriatal axis, which are further exacerbated in the groups that are stressed prior to MPTP administration (Lauretti et al., 2016). While estrogen receptors are notably sparse within the mouse striatum and SNpc and their distribution remains unchanged following MPTP intoxication, suggesting that estrogen's protective mechanism on DA neurons may act via nuclear receptor independent mechanisms (Shughrue, 2004), MPTP induced toxicity on astrocytes varies depending on sex and brain region, mostly affecting male mesencephalic astrocytes. MPTP exerts its neurotoxic effects specifically through changes in the expression of cytochrome c oxidase isoform, leading to reduced energy production and increased oxidative stress, both key features of neurodegenerative diseases (Sundar Boyalla et al., 2011). Only two more - out of the remaining twenty-four studies [one study fails to report on the sex of the animals participating (Urakami et al., 1988)] - separately examine the interplay of PD and stress on both sexes (Wu et al., 2016; Grigoruţă et al., 2020). These two studies, using both male and female Tg animal models of PD, highlight neuroinflammatory,

oxidative and bioenergic alterations between males and females while in each case, females display greater resilience (Wu et al., 2016; Grigoruţă et al., 2020). In females, estrogens modulate microglia reactivity promoting an anti-inflammatory state that may confer neuroprotection after the use of 6-OHDA (Siani et al., 2017). Moreover, male mesencephalic neurons exposed to 6-OHDA have reduced expression of selected mitochondrial proteins, lower ATP levels and higher ROS levels compared to female neurons (Misiak et al., 2010). Finally, there was only a single publication included in the Table 1 where the experiments were performed solely on female animals, though without any further comments about the sex or the age of the rats (Smith et al., 2008).

20. The critical role of aging in neurodegenerative disease research

Considering age in PD research is crucial, due to its strong association with the disease's onset and progression. PD primarily affects older adults, with the risk increasing significantly after the age of 60 (Pang et al., 2019). This age-related prevalence suggests that biological changes inherent to aging, such as increased oxidative stress, mitochondrial dysfunction and protein accumulation, are integral to the disease's pathogenesis (Collier et al., 2011; Pang et al., 2019). These factors underscore the necessity of age-specific approaches in both the study and treatment of PD since age is not just a risk factor but a critical element that shapes the entire landscape of PD from diagnosis to treatment. As it is greatly reviewed by Klæstrup and colleagues, despite aging being the main risk factor for idiopathic PD, most studies use young animals, neglecting age-related cellular and molecular mechanisms. Recent research shows that aged animals are more susceptible to PD pathology and neurodegeneration and exhibit a faster and more extensive disease progression than younger ones, highlighting the importance of using aged animal models to better reflect the clinical presentation of PD in older adults, despite the challenges involved (Klæstrup et al., 2022). Since 3 months old (mo) rats and mice correspond to young adults, 10-14 mo rats and 12 mo mice correspond to middle-aged and 18 mo rats and 19mo mice correspond to aged animals, the animals used in the vast majority of the studies presented in Table 1, fall within the young adult range. More specifically, out of the 27 studies, 16 explicitly mention the age of the animals while in 8 studies the weight is mentioned as an indirect way of roughly calculating the age of the animals. Three studies provide neither direct nor indirect information regarding the age of the animals.

Based on the weights and the age provided in the study only four studies exceed the 6 months at the time when the animals are sacrificed (Lauretti et al., 2016; Wu et al., 2016;

Wassouf et al., 2019; Burtscher et al., 2019) while the animals reach the age where the animals are considered to be young adults only in two (Zhang et al., 2018; Diwakarla et al., 2020). Despite some drawbacks of using older animals, such models would ultimately be more advantageous in accurately reflecting the clinical disease in older adults, enhancing the translational value, and reducing the likelihood of therapeutic failures in clinical trials.

21. Aims

Overall, the emerging microbiota-gut-brain (MGB) axis is sustained by mechanisms of bidirectional communication involving endocrine, neural, metabolic and immune pathways. The HPA axis plays a central role in stress response with the GCs traveling through the bloodstream, modulating immune function, gut microbiome composition and gut permeability. Conversely, gut microbiota influence the stress response via the secretion of cytokines activating the HPA axis. Apart from the direct neural communication occurring through the vagus nerve and the ENS - where microbes play a key role through the production or metabolism of neurotransmitters or their precursors - microbial metabolites, such as SCFAs, can reach to the CNS via the circulation and additionally affect it by interacting with immune cells exerting pro-/anti-inflammatory effects.

To date, no study has comprehensively addressed the risk chronic stress confers, and whether it should be considered a trigger, a facilitator or an aggravator of PD (Johnson et al., 2019). Clinical evidence alludes to an abnormal stress response, i.e. hypothalamic–pituitary–adrenal (HPA) axis dysregulation, however, direct evidence of molecular and glucocorticoid-mediated pathologies is lacking (Du & Pang, 2015). Asyn poses a likely culprit as exacerbated asyn pathology has been demonstrated in the A53T mouse model following chronic mild stress (Wu et al., 2016) and in a model of seeded asyn pathology in mouse striatum following corticosterone administration (Burtscher et al., 2019). However, it is currently unknown if enhanced asyn burden itself is involved in stress dysregulation and vice versa. To address this issue, we assessed HPA axis function in bacterial artificial chromosome Tg rats that overexpress human full-length wildtype asyn (BAC). Nine month-old BAC rats model a premotor hyperdopaminergic phenotype, representing a state prior to overt neurodegenerative phenoconversion (Polissidis et al., 2021). Furthermore, we examined the pathological and phenotypic consequences of both CRUST and chronic exogenous CORT administration to explore whether chronic stress can act additively or synergistically with asyn to incite changes related to asyn pathology, neuroinflammation, nigrostriatal neurodegeneration, non-motor and motor behavioral deficits as well as changes in

neurotransmission and in the microbiome. Finally, upon finding transcriptomic and molecular perturbations in hippocampal stress signaling in BAC rats, we sought to investigate if such changes are conserved in PD patient brains and could potentially be involved in altered sensitivity to chronic stress in the context of PD.

II. Methods & Materials

1. Animals and ethics approval

All experiments were approved by the Ethical Committee for Use of Laboratory Animals at the BRFAA (Permit no. 1043/20.02.2019) and complied to the ARRIVE guidelines. Middle-aged (9 mo) male wild type and BAC Sprague–Dawley rats were housed in pairs in individually ventilated cages, on a 12-h light/dark cycle (lights on at 7:00 am), at a constant room temperature of 21 ± 1 °C and had unlimited access to food and water. Upon computation of appropriate sample sizes, animals were randomly assigned to the experimental groups. The interaction between sex, environment and genetics is complex and understudied, thus, for this first study of ours exploring the interaction between genetics and stress, male animals were chosen due to higher overall incidence and prevalence of PD, earlier disease onset, worse motor symptoms and progression, and more frequent cognitive decline in males (Polissidis et al., 2020). We based this decision on ours and others' animal studies that revealed a significant PD phenotype only in male rats (Polissidis et al., 2021) and chronic stress PD exacerbation only in male A53T mice (Wu et al., 2016).

2. Stress protocols

Rats were semi-randomly assigned to 4 treatment groups: wild type control group (WT CTL), BAC CTL, WT stress (either CORT or CRUST) and BAC stress (either CORT or CRUST). Animals were handled for one week prior to the start of the stress protocols. Following this, they were exposed to one of two distinct stress protocols: a pharmacological stress protocol or a psychological stress protocol, for a total period of 14 days. Animals from the CTL groups were handled similarly but were placed back in their home cages without exposure to any stress protocols.

2a. Chronic corticosterone administration (CORT)

CORT (Corticosterone, 27840, Sigma Aldrich) was initially dissolved in absolute ethanol and then added at a concentration of 50 μg/ml to the drinking water (1%). The animals were designated to one of four treatment groups: (1) wildtype control (WT CTL), (2) wildtype CORT (WT CORT), (3) BAC control (BAC CTL) and BAC CORT (BAC CORT) groups. Either CORT or a vehicle solution (drinking water with 1% ethanol) was administered to the CORT and the CTL groups, respectively, for two weeks (Ding et al., 2018). Fresh solutions

were prepared every two days in tinfoil-covered water bottles to protect CORT from light-induced degradation. There were no differences in daily water consumption among groups. Average water intake of 35 ml/rat/day corresponded to a daily dose of approximately 1.75 mg of CORT per animal. Fecal pellets were collected from all animals during morning hours (9.00 – 14.00) before and after the pharmacological stress protocol.

2b. Chronic unpredictable stress (CRUST)

Stressors were randomly interspersed throughout the two weeks period. Two stressors were applied every day in an unpredictable, random manner, to avoid habituation (Table 2). The CRUST stressors included: cage tilting (45° for 6 h), wet bedding (500ml water; 6 h), cold swim (16-18°C for 10 min) and warm swim (31-34°C for 20 min), cage crowding (4 animals/cage; 12 h), restraint in a plexiglass restrainer (1 h), cage isolation (1 animal/cage; 12 h), cage vibration (100 rpm for 1 h), placement on a brightly lit elevated platform (BLEP) (5 min), and light cycle reversal (48 h). Body weight was monitored weekly for the duration of the protocol. Fecal pellets were collected from all animals during morning hours (9.00 – 14.00) before and after the psychological stress protocol.

Table 2. Daily program of the two-week long ChRonic Unpredictable STress (CRUST) protocol.

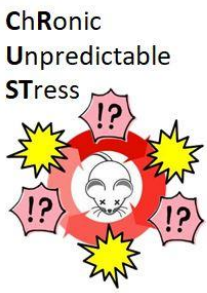

Week 1	D1	D2	D3	D4	D5	D6	D7
am	Restraint	Wet bedding	Cage tilting	Restraint	Vibration	Day/night	BLEP
pm	Crowding	BLEP	Cold swim	Warm swim	Crowding	reversal	Isolation
Week 2	D8	D9	D10	D11	D12	D13	D14
am	Vibration	Wet bedding	Cage tilting	Wet bedding	Vibration	Day/night	Cold swim
pm	Cold swim	Crowding	Warm swim	BLEP	Restraint	reversal	Isolation

3. Behavioral testing

All behavioral testing was carried out during the light phase, between 9:00 and 17:00 upon the completion of the stress protocols. All animals stress cohorts were tested in a behavioral test battery of motor and non-motor tests, at 9 months including in sequential order: open field, elevated plus maze, pre-pulse inhibition, gait analysis and postural instability. Each behavioral task was separated by at least 24h.

3a. Open field

The open field test was employed to evaluate locomotion and anxiety-related behaviors in a square acrylic open field arena (40 x 40 x 30 cm). Placed in the arena's center (20 cm x 20 cm), each rat was allowed to freely explore the arena for one hour. Activity was tracked by an overhead camera [Panasonic WV-BP332] and analyzed using specialized video tracking software [Ethovision XT 9.0, Noldus, The Netherlands]. The parameters evaluated were locomotor activity, as measured by the total distance travelled (cm), exploration, as measured by the rearing frequency (when the animal stands on its hind legs) and anxiety-related behavior, as measured by the total amount of time the rat spent in the central area of the arena (s).

3b. Elevated plus maze (EPM)

Anxiety-related behaviors were assessed in a polyvinyl chloride EPM apparatus over a five-minute period, according to previously established protocols (Polissidis et al., 2021). Briefly, at the beginning of the experiment, each rat was placed in the central square with its head facing an open arm and was allowed to freely explore the apparatus while the activity of each animal was tracked using the same overhead camera and specialized video tracking software that was used in the open field test. The parameters evaluated were the percentage of time spent in the open arms (vs. total time in closed and open arms) and the locomotor activity (measured as the total distance travelled, cm).

3c. Pre-pulse inhibition (PPI)

Prepulse inhibition (PPI) was conducted according to previously established protocols (Polissidis 2020). Briefly, on the first day, habituation of the animals began with 5 minutes of 70-dB white noise, followed by a series of sound pulses of varying amplitude (70, 80, 90, 100, 110 and 120 dB, in pseudorandom order, 1 s apart; 20 s intertrial interval; five times each). The average startle response of the five trials, termed acoustic startle response (ASR) was calculated. The next day, the animals were once more restrained, placed in the startle chamber and introduced to a PPI protocol consisting of a 5-min habituation (background white noise 70 dB), 10 pulse-alone (115 dB) trials, 10 prepulse (each of 75, 80, 85 and 90 dB) plus pulse trials in pseudorandom order (1 sec apart; 20 sec intertrial interval) and 10 no stimulus (white noise) trials. PPI was calculated as a percentage score: % PPI = [1 - (PreS)/S)] * 100, where “PreS” denotes the mean startle response for prepulse plus trials and “S” the mean startle response for the startle pulse-alone trials.

3d. Olfaction deficit test

Olfactory function was assessed based on the preference of rodents for bedding impregnated with their own odor (familiar compartment) versus fresh bedding (novel compartment) (Carr et al., 1976; Prediger et al., 2006). Regarding the experimental procedure, for the first session, each rat was placed in the neutral compartment of a rectangular apparatus divided into three compartments and was left to habituate for 5 minutes. In the second session, one of the side compartments was filled with 3-day-old bedding from the rat's home-cage while the other side compartment was filled with fresh bedding and the rat was re-introduced, in the neutral compartment and allowed to freely explore for 5 min. The time the animal spent in each compartment was recorded for a 5-min period(s).

3e. Gait analysis

Gait analysis was assessed with footprinting. Each rat had its forelimbs and hindlimbs coated with grey and black non-toxic tempera paint, respectively, and then allowed to walk along a paper strip placed in a 13 cm wide PVC corridor (with 5 cm high walls). A series of at least four sequential steps were used (not including the first or last strides) for manual measurement of stride length, width between forelimbs and hindlimbs and the overlap between forelimb and hindlimb for each stride (cm).

3f. Postural instability

To assess postural instability, after applying paint to the forelimbs, each rat was held upside-down from its tail, almost vertically, over a paper strip. The rat was then slowly lowered until its paws touched the paper and began to move forward, making steps while trying to regain its center of gravity, in response to the sequential weight shifts from the one forelimb to the other. A series of at least three sequential steps were used to measure the distance it takes for the animal to take a step with the forelimb to regain its balance. To avoid baseline variation between WT and BAC animals, since the transgenic animals tend to weigh less since they are hyperactive throughout their life (Polissidis et al., 2021), we calculated the overall variation among the forelimb steps the rats took trying to regain their balance rather than the length of the forelimb step.

3g. Morris water maze

The Morris water maze test was used to assess spatial learning and memory retention (Morris, 1984; D'Hooge & De Deyn, 2001; Vorhees & Williams, 2006). Briefly, spatial cues were placed on the four walls surrounding a pool filled with opaque water (colored black with non-toxic tempera paint for contrast), along with a platform submerged 1 cm below the water's surface. During the 3-day acquisition phase, the platform remained hidden in a specific quadrant of the pool. Each rat was semi-randomly introduced into the water from four different start-points over four sessions each day. For each session, the rat had to locate the platform before a 90-sec cut-off. If a rat did not succeed in reaching and mounting the hidden platform within 90 sec, the rat was gently guided by the experimenter. The average latency (s) and distance travelled (cm) to find the platform was measured. On the fourth day, the rats were subjected to a probe trial where the platform was removed. The time spent in the target quadrant (s) was measured as an index of spatial memory while the number of times each rat crossed the position where the platform used to be submerged, was used to assess memory retention. Finally, to exclude the possibility of visuomotor deficiencies in the animals, the latency to reach a visible platform emerging 1 cm from the surface of the water was evaluated (semi-random placement in the four quadrants over four trials) on the fifth day. Trials were video-recorded and measured automatically [Ethovision XT9.0, Noldus, The Netherlands].

4. Surgery and microdialysis

CMA 12 guide cannulas were stereotaxically implanted in the right striatum under a combination of sevoflurane anesthesia and ketamine (100 mg/kg)/xylazine (10 mg/kg) cocktail administered intramuscularly (IM). Atropine sulfate (0.6 mg/kg IM) was administered to reduce bronchial secretions. Briefly, after securing the rat in the stereotaxic frame, a guide cannula was implanted unilaterally in the striatum; coordinates: anterior-posterior (AP): +1.0, medio-lateral (ML): +3.0, dorsoventral (DV): -4.0, according to Paxinos & Watson (Paxinos & Watson, 2004). The cannula was secured to the skull by three stainless steel anchor screws and rapid-setting acrylic dental cement, which surrounded the assembly.

Three days after surgery, rats were placed in the microdialysis cage (CMA-120, system for freely moving animals; Canergie Medicin AB, Sweden) and CMA 12 microdialysis probes were inserted in the striatum and connected to the microdialysis pump through a

liquid swivel to a CMA 402 pump with a constant flow rate. Perfusion was performed in artificial CSF (147 mM NaCl, 2.7 mM KCl, 1.2 mM $CaCl_2$, 0.85 mM $MgCl_2$) containing 0.15% bovine serum albumin. For collection of monoamine samples, a CMA 12 Elite (molecular weight cut off: 20 kDa) probe was used and the speed of the pump was set at 1.2 µl/min. $HClO_4$ was added in the samples to a final concentration of 0.1M to prevent monoamines from oxidation. For collection of asyn samples a CMA 12 High Cut-off (molecular weight cut off: 100 kDa) probe was used and the speed of the pump was set at 0.6 µl/min. Triton-X-100 and Tween-20 [Thermo Fischer Scientific, 85115] were added in the samples to a final concentration of 0.5% to prevent asyn aggregation in the collected artificial CSF. The probes were allowed to equilibrate for 2 h with the same flow rate each time before the collection of samples. Samples were collected either every half an hour for the monoamines or hourly for asyn, using a CMA 470 refrigerated fraction collector and stored at -80 °C until analyzed by HPLC and ELISA. The average concentration of DA and asyn in the first three samples was considered as the baseline concentration. Diazoxide (60mM) - a SUR1 channel activator producing a robust increase in interstitial fluid asyn level (Emmanouilidou et al., 2016) - was infused through the dialysis membrane by changing the perfusion buffer to artificial CSF containing the compound. At the end of the experiment, the brain was excised, fixed in 4% PFA and analyzed for probe placement by 2% Evans blue staining. All efforts were made to minimize animal suffering. The animals that underwent surgeries did not participate in any behavioral tests.

5. Sacrifices

Animals were sacrificed either by decapitation or by transcardial perfusion. The use of guillotine was applied when the brain regions collected were scheduled to be analyzed by HPLC or by Western blot (WB). The key brain regions received were the following: olfactory bulbs, prefrontal cortex, amygdala, hypothalamus, midbrain, hippocampus, ventral and dorsal striatum, as well as an intestinal sample - the first 1 cm of the duodenum - were dissected, snap frozen and stored in -80°C until analysis. The animals whose brains were to be stained for immunohistochemistry (IHC) protocols were transcardially perfused with phosphate-buffered saline (PBS 1x) for 5 min followed by 4% PFA in PBS 1x for 5 min (pump speed set at 16 rpm) under isoflurane anesthesia. Finally, in the case when we planned to perform both IHC and further analyze the biochemical and transcriptional profile of the same brain regions, the animals were transcardially perfused with PBS 1x for 10 min and brain hemispheres were separated after perfusion. Left hemispheres were post fixed

overnight in 4% PFA in PBS 1x. Right hemispheres were further dissected to collect regions of interest and kept at -80^{o}C. Furthermore, adrenal glands, thymus gland and blood samples for each animal were collected during the perfusion. Adrenal glands and thymus were kept in 4% PFA at 4^{o}C and blood samples, collected in EDTA coated 1.5 mL tubes, were centrifuged for 10 min at 2000 x g at 4^{o}C and the plasmas were stored at -80^{o}C. Perfused brains were stored in increasing concentrations of sucrose (15% and 30%) in 0.1M PBS 1x, pH 7.4 at 4^{o}C and were later snap frozen with isopentane at -50^{o}C on dry ice and stored at -80^{o}C. Finally, after they were sectioned using a cryotome (35μm), brain slices were stored free floating in an antifreeze solution at -20^{o}C.

6. Determination of rat brain region-specific monoamine neurotransmitter levels using HPLC

Homogenization and sample analysis was performed according to established protocols (Polissidis et al., 2021). The assay measured the concentration of noradrenaline (NA), dopamine (DA) and its metabolites (3, 4-Dihydroxyphenylacetic acid (DOPAC), 3-Methoxytyramine (3-MT) and homovanillic acid (HVA), in brain tissue homogenates with reverse-phase ion-pair chromatography on an isocratic pump (YL9112 Instrument Co., Ltd., Gyeonggi-do, Korea) coupled with an electrochemical detector (BASi LC-EC, Bioanalytical Systems, Inc., Indianapolis, IN, USA). Briefly, the column used was YMC Triart C18 100 × 2 mm, 3-μm particle size, the mobile phase consisted of an acetonitrile (Sigma-Aldrich, 271004)-50 mM phosphate buffer (1:9 dilution; Thermo Fisher Scientific, 70011036), pH 3.0, containing 300 mg/l 5-octylsulfate sodium salt (Merck Millipore, 112268) as the ion-pair reagent and 20 mg/l Na2EDTA (Sigma-Aldrich, 03683). HPLC software (DataApex, Clarity) was used to quantify neurotransmitter levels by comparing the area under the peaks with the area of external reference standards. Final results are expressed as ng/mg of wet tissue weight. Glutamate, glutamine and gamma aminobutyric acid (GABA) levels were measured in the Department of Pharmacology, Faculty of Medicine, School of Health Sciences University of Ioannina, Ioannina in a YL9112 Plus Isocratic HPLC Pump (YOUNG IN Chromass Inc., Korea) coupled with a DECADETM Elite Electrochemical Detector (Antec@Scientific, USA). HypersilTM ODS C18, 250 mm × 10 mm × 5 μm column (Thermo Fisher ScientificTM, Massachusetts, USA) was used with pre-column derivatization, as previously described, with some minor modifications (Ntoulas et al., 2024; Kokras et al., 2020).

7. ELISAs

7a. Corticoptropin-releasing factor (CRF) measurements in rat hypothalami

Hypothalami were homogenized, diluted and analyzed to measure CRF levels using the Corticotropin Releasing Factor (CRF) (Human, Rat, Mouse, Canine, Feline) EIE Kit (Phoenix Pharmaceuticals, Inc., Catalog No. EK-019-06), following the manufacturer's instructions. The enzyme-linked immunosorbent assay (ELISA) was quantified by the SPARK® multimode microplate reader (TECAN).

7b. Corticosterone measurements in rat plasma

Trunk blood was collected from the animals upon sacrifice with the use of guillotine and collected in EDTA coated 1.5mL tubes. Animals from each group were sequentially sacrificed during morning hours (09:00-11:00) to eliminate the time factor since CORT secretion follows a diurnal rhythm. The blood was centrifuged for 10min in 2000 x g in a precooled centrifuge set at 4^{o}C. The supernatant was collected, diluted and analyzed in a commercial corticosterone ELISA Kit (Enzo, Catalog No. ADI-900-097), according to the manufacturer's instructions. The ELISA was quantified by the SPARK® multimode microplate reader (TECAN).

7c. Asyn measurements in striatal extracellular milieu

Artificial CSF samples were diluted and analyzed to measure asyn levels in the extracellular striatal milieu using the SensoLyte Anti-a-Synuclein (Human) ELISA Kit (Anaspec, Catalog No. AS-55550-H), following the manufacturer's instructions. The enzyme-linked immunosorbent assay (ELISA) was quantified by the SPARK® multimode microplate reader (TECAN).

8. Asyn pathology assessment in the rat brain

8a. Protein extraction protocol, immunoblotting and analysis

Briefly, following brain tissue harvesting by decapitation, hippocampi and striata were homogenized, lysed, centrifuged (120 000×g for 60 min) and depending on the lysis buffer (either STET (50 mM Tris [Sigma-Aldrich, T1503], pH 7.4, 150 mM NaCl [Lach-Ner, 30093], 1% Triton-X-100 [Applichem, A1388], 2 mM EDTA [Applichem, A1104], protease and phosphatase inhibitors [Roche, 11836153001, 4906845001]) or RIPA (same as STET supplemented with 1% SDS)), appropriate amounts of the supernatants containing either

the “soluble” (Tx100) or the membrane-associated and aggregated “insoluble” (SDS) protein fractions were loaded on 12% SDS polyacrylamide gels. The proteins were transferred onto nitrocellulose membranes and blocked using 5% milk in 1 × TBST. For detection of pS129 asyn, membranes were incubated overnight in PBS 1 × at 65 °C and blocked in 5% BSA. For a list of all primary and secondary antibodies used for all immunoblot/staining protocols, refer to Supplementary Table 1. Analysis was performed with Fiji/ImageJ (Schindelin et al., 2012).

8b. PS129 asyn immunohistochemistry

Perfusion, brain fixation, sectioning, and immunohistochemistry were performed according to standardized lab protocols (Xilouri et al., 2016; Polissidis et al., 2021). Briefly, the brains were sliced coronally (thickness 35 μm) on a cryotome [LEICA CM3050 S] and three representative sections from each brain region of interest were chosen per subject. The sections were placed for 10 min in 3% H2O2/10% methanol mixture and subsequently blocked with 5% normal goat serum for 1 h at room temperature (RT). The rabbit monoclonal anti-α-synuclein phospho S129 antibody was used as the primary antibody, for 48 h at 4 °C, the sections were washed three times for five min in PBS 1 × and incubated for 1 h with biotinylated goat anti-rabbit IgG secondary antibody [Vectastain ABC kit, PK-4001, Vector Laboratories]. Three washes in PBS 1 × for 5 min followed, and the sections were then treated for 1 h with ABC solution [Vectastain ABC kit, PK-4001, Vector Laboratories] at RT followed by three more washes in PBS 1x. Antibody binding was visualized by the reaction of hydrogen peroxidase with 3, 3-diaminobenzidine [DAB, Dako, K3468]. Finally, the sections were mounted on Superfrost microscope slides [Epredia, J1800 AMNZ] dehydrated and treated for 15 min with 0.5% Cresyl Violet Acetate. Following staining, the sections were rehydrated and treated with xylene. Finally, the sections were placed on slides with DPX Coverquick 2000 [VWR chemicals, 0554730-500ML] as a mounting medium.

8c. Microscopic observation

Immunohistochemistry staining was observed with a Leica DM RA2 microscope. Whole sections were scanned using Stereo Investigator software [MBF Bioscience, Version 10] using a vertiga 2000-Qimaging camera and a 10 × objective lens. For the analysis, images from the “5th edition of The Rat Brain in Stereotaxic Coordinates” (Paxinos & Watson, 2004) were overlaid with the tile scanned images of the section (three representative coronal sections per brain region with the coordinates “bregma/interaural line”; for hypothalamus: − 1.40 mm/7.60 mm, − 3.14 mm/5.86 mm and − 4.16 mm/4.84 mm and for hippocampus: −

2.56 mm/6.44 mm, − 3.14 mm/5.86 mm and − 3.80 mm/5.20 mm). Using Fiji/ImageJ, the specific regions of the hypothalamus and the hippocampus were selected. Background subtraction of the area of the pS129 was quantified as compared to the total area of the region.

8d. Confocal microscopy and analysis

A Leica TCS SP5 II on a DM 6000 CFS upright confocal microscope was used to acquire z stacks of 1024 × 1024 pixel resolution throughout the whole thickness of the midbrain sections with a 40 × 1.20 objective lens and a z step size of 0.7 microns. For each brain section, three representative images were taken to cover the whole region of the SNpc and image analysis and evaluation of the volume of the pS129 asyn was performed with Fiji/ImageJ. Briefly, the TH channel was used to create a mask of the SNpc, after applying a threshold. The total volume of the SNpc was measured in the z-projection (using the "Sum slices" option) and measured by dividing the Raw Integrated Density by 255. The pS129 channel was masked using the "Image calculator" option in the "Process" tab of Fiji/ImageJ ("Min" operation). After applying a threshold, the masked image was z-projected using the "Sum slices" option and the volume was calculated. The final values are expressed as the ratio of pS129volume/total TH volume. For the assessment of asyn pathology in dopaminergic neurons of the hypothalamus, z-stacks of 2048 × 2048 pixel resolution and a step-size 0.3 microns were generated using a water-immersion Leica HCX APO 63 × 1.20 objective on a Leica TCS SP5 confocal microscope (Wetzlar, Germany). Analysis was performed using Imaris × 64 9.1 software. To create the surface of dopaminergic cells, Imaris Surface module was utilized, and an intensity threshold was applied to distinguish between background and cell fill. The surface that was created from the TH signal was used as a mask for pS129 asyn signal and the overlap between the reconstructed surface and pS129 immunoreactivity signal created a new signal channel representing the pS129 asyn located inside the dopaminergic neurons.

9. Immunohistochemistry of the nigrostriatal pathway in the rat brain

9a. DAB staining

Representative sections (every 6th section) of the entire striatum and midbrain (containing the SNpc) were stained with the polyclonal anti-tyrosine hydroxylase (TH) antibody. The staining was visualized using DAB and the sections were further stained with

cresyl violet (Nissl stain) and dehydrated in consecutive increasing concentrations of ethanol solution.

9b. Dopaminergic cell counts in the SNpc

Stereological counts of TH + neurons in the SNpc was estimated using a stereological microscope [LEICA DMRA2] coupled with a QImaging color camera and Stereo Investigator v10.0 software [MBF Bioscience, USA], according to established protocols (Polissidis et al., 2021). For each animal, 8–10 representative sections throughout the rostro-caudal axis of the SNpc were quantified based on an unbiased method using the Optical Fractionator, employing a systematic random sampling of counting frames. Counting contours in each section were outlined with a 2.5 × objective lens while counting was performed using a 63 × 1.30 glycerol immersion objective lens with the following settings: optical dissector, grid size (150 μm) and counting frame (50 μm). A coefficient of error (Gundersen, m = 1) of ≤ 0.1 was accepted.

9c. Dopaminergic afferent densitometry in the striatum

The density of TH + axons in the striatum was measured, as previously described (Xilouri et al., 2016). Six sections for each animal, covering the whole rostrocaudal axis of the striatum, were stained for TH using DAB staining. Densitometric analysis was performed using Fiji/ImageJ. The striatum was sub-divided into three regions: dorsolateral (DL), dorsomedial (DM) and ventral (V), according to the boundary between the caudate-putamen complex and the nucleus accumbens or measured as a whole. The density of TH + neurons was measured using Fiji/ImageJ for each region.

10. Neuroinflammation assessment along the rat nigrostriatal axis

10a. Tissue processing for immunofluorescence

Immunohistochemistry was performed in free-floating sections for the assessment of neuroinflammation along the nigrostriatal axis. Midbrain and striatal sections (3 sections/brain region/subject) were selected, washed in PBS 1x, and blocked in a buffer containing 5% natural-goat-serum (NGS) and 0,1% Triton-X-100 in PBS 1x, to reduce nonspecific binding of the antibodies and background signal. Incubation overnight at 4 °C with primary antibodies followed, using anti-GFAP (glial fibrillary acidic protein) for the staining of astrocytes, anti-Iba1 (ionized calcium binding adaptor molecule 1) for microglia and anti-TH for dopaminergic neurons. The sections were washed in PBS 1 × and incubated

with secondary antibodies conjugated with fluorophores (CF488A green, CF555 red and Cy5 far-red) for 1 h at RT. After PBS 1 × washes, sections were mounted on poly-L-lysine glass microscopic slides [Epredia, J2800AMNZ] with mounting medium containing DAPI (4',6-diamidino-2-phenylindole) [Fluoromount-G™, Invitrogen].

10b. Structured illumination (SIM) confocal microscopy

For the CORT cohort, the Aurox Clarity Laser Free Structure Illumination Confocal Microscope was used to generate tile scan images of the stained brain slices which were subsequently quantified to measure the mean intensity of the GFAP and Iba1 glial cells using TH + staining to select the ROIs, in the SNpc and the striatum. The images were analyzed using Fiji/ImageJ. Briefly, images belonging to the same section were stitched together (using the "Stitching" plug-in), converted from 16-bit to 8-bit (after setting the contrast to its full range) and the background was subtracted ("Subtract background" option in the "Process" tab). ROIs were selected based on a max projected version of the image and saved for subsequent use in the workflow. Total volume of the structure of interest (SOI) was evaluated by thresholding the stitched image, z-projecting using the "Sum slices" option and measuring the integrated density statistic after overlaying the ROI on the z-projected image. The resulting value was equal to the total number of pixels comprising the structure of interest over the entire 3D volume × 255. Therefore, to extract the total volume (V), the latter value was divided by 255. To calculate the numerator of the mean volume ratio, the image was masked based on the thresholded image using the "Image calculator" option in the "Process" tab of Fiji/ImageJ ("Min" operation). The resulting image contains 0-valued pixels over background regions (0-value in the thresholded image) and the raw values over the structure of interest. The masked image was z-projected using the "Sum slices" option and once more the raw integrated density statistic giving the intensity sum (I) over the SOI was calculated after overlaying the ROI. The mean intensity of the SOI, within the ROI, is given by the ratio: I/V.

Alternatively, for CRUST a Leica TCS SP5 confocal microscope (Wetzlar, Germany) was used to acquire z stacks of 1024 x 1024 pixels throughout the whole thickness of the section with a HCX APO 40× 1.20 objective and a z step size of 0.7 microns. For each brain section, three images were captured; 20-30 stacks each, to represent all regions of the dorsal striatum and the substantia nigra (Figure 1). Analysis of the images was performed using Fiji/ImageJ software. Z-stacks were projected (using the "Max intensity" option") and after a manual threshold was applied, the area of the astrocytes and microglia was

measured. Area was divided by the area of the region of interest (ROI) (i.e., striatum or substantia nigra) and finally expressed as a percentage of the total ROI.

11. RNA extraction and cDNA synthesis from rat hippocampi

RNA was isolated from rat hippocampus samples using the Nucleospin© RNA kit [Macherey Nagel], according to manufacturer's instructions. Total RNA was quantified with NanoPhotometer [IMPLEN]. RNA integrity was assessed by loading 200 ng of each sample on a 1% agarose gel. 1 μg of total RNA was used for cDNA synthesis in a two-step cDNA synthesis protocol, according to manufacturer's instructions [GoScript™ Reverse Transcriptase, Promega].

12. RNA sequencing

RNA-sequencing experiments were carried out in the Greek Genome Center (GGC) of the Biomedical Research Foundation of the Academy of Athens (BRFAA). RNA was isolated from rat hippocampus samples using the Nucleospin RNA kit [Macherey Nagel] according to manufacturer's instructions. Total RNA was quantified with Nanodrop [IMPLEN]. RNA integrity was assessed by loading 200 ng of each sample on a 1% agarose gel. Total RNA was subsequently isolated according to manufacturer's instructions. mRNAseq libraries were prepared with the Illumina TruSeq RNA v2 kit using 1 μg of total RNA. Libraries were checked with the Agilent Bioanalyzer DNA1000 chip, quantitated with the qubit HS spectrophotometric method and pooled in equimolar amounts for Sequencing. One hundred basepair Single-End reads were generated with the Illumina NextSeq500 sequencer and for each sample, approximately 25 million were obtained.

12a. Read alignment and quantification

FASTQ files were imported into the Galaxy web platform and data were processed and analyzed using the public server usegalaxy.org (Afgan et al., 2018). Sequence quality control was performed with FastQC and MultiQC twice, once at the raw and the second time at the aligned output. Cutadapt was utilized for adapter trimming. Assembly to the rat reference genome (version 6.0; July 2014) was conducted with HISAT2, mapping successfully 96% of total reads to at least one genome region and 84.5% of total reads to a unique genome location (percentages are expressed as means over all 17 samples). Uniquely mapped reads for each sample were quantified to read counts based on the union exon model and the function featureCounts.

12b. Annotation and differential expression analysis

A table of read counts per sample and per mRNA RefSeq ID was exported from Galaxy and was directly imported into the R environment for statistical computing (version 4.0.2). Gene annotation data were obtained with the Bioconductor package biomaRt (version 2.44.1), and 17,042 out of 18,464 RefSeq IDs could successfully map to Gene Symbols. Cases where different Refseq IDs mapped to same gene, were summarized to Gene Symbol with the function *collapseRows* of the WGCNA package (version 1.69), by selecting the RefSeq ID with the highest mean of counts across all 17 samples (resulted in 16,061 Gene Symbols). Differential expression analysis was performed with the Bioconductor package edgeR (version 3.30.3). edgeR extends the standard negative binomial model (in which an overdispersion parameter is calculated globally for all genes) by implementing gene specific quasi-likelihood (QL) dispersion estimates to account for the increased variance that characterizes low expressed genes (Robinson et al., 2010). QL estimates obtained for each gene are then squeezed towards their mean value (across all genes) under an empirical Bayes approach. The squeezed estimates are finally supplied for hypothesis testing. We investigated differential expression after removing genes with very low read counts. Briefly, genes with a sum of counts per million reads lower than 2 were filtered out and the raw read counts of 12,097 genes were submitted for library size normalization using as scaling factor the trimmed mean of M-values calculated over each pair of samples (function *calcNormFactors*). Fitting and testing for differential expression were performed with the functions *glmQLFit* and *glmQLFTest*, respectively. Multidimensional scaling plot revealed the presence of an outlier which was omitted from further analysis. Diagnostic plots of the raw and the EB fitted QL dispersions are presented in Supplementary Figure 1.

12c. Gene Ontology analysis

While FDR (False Discovery Rate) is typically more strict than setting a raw p-value threshold, i.e. $p<0.05$, the p-value threshold of 0.05 applies to each individual test, rejecting the null hypothesis if the probability of the observed data under the null hypothesis is less than 0.05. However, in large-scale analyses like RNA-seq, testing for significance is performed several thousand times, one for each gene. This gives rise to the multiple comparisons problem, which posits that when multiple statistical inferences are computed simultaneously, a portion of them will be significant only by chance (Benjamini, 2010) thus increasing the chance of false positives. On the other hand, setting strict criteria for defining significance can increase the Type-II error, which signifies the false negative results, or in

other words, the error of incorrectly accepting the null hypothesis. This is particularly evident when sample sizes are low. Correcting for multiple hypotheses in such cases, more often than not leads to overly large p values, and increased risk for Type-II error. An FDR threshold of 0.1 controls the proportion of false discoveries among all significant results, allowing up to 10% of the significant results to be false positives. FDR is generally less strict in terms of discovering more hits, but when sample size is limited, it might result in very few significant hits. This is why lowering the threshold to $p<0.05$, even though stricter per test, may help find more significant results at the cost of not adjusting for the false discovery rate. Combining both approaches can help balance the number of discoveries with control over false positives.

To identify which DEGs possess the strongest discriminatory power for distinguishing the four groups, we performed unsupervised clustering analysis using various DEG combinations, comparing the clustering results to the known sample groupings. The analysis began with a minimal gene set, defined as the union of the top 20 DEGs from each of the four comparisons, based on the lowest nominal p-values. In each of the subsequent clustering iterations we expanded the input gene list by adding the next five most significant genes from each comparison to the union list. This iterative process continued until the clustering output no longer corresponded to the known group labels. A mis-clustering of maximum 1 sample was set as the stopping point of clustering. This incremental-input clustering approach resulted in a list consisting of the top 50 genes with the lowest p value from each of the aforementioned comparisons.

For the pathway analyses, genes with $p<0.05$ were screened against the complete Rattus norvegicus Gene Ontology database, comprised of the three libraries: Biological Process, Molecular Function and Cellular Component. Gene Ontology testing for significance was conducted using a two-sided hypergeometric test implemented in the functions *compareCluster and enrichGO* from the Bioconductor package clusterProfiler package (version 3.16.1). Statistically significant gene ontology terms were defined as those with Benjamini-Hochberg adjusted $p < 0.05$.

13. RT qPCR analysis of rat hippocampal gene expression

To assess changes in expression of selected genes (a list of all the primers is available in Supplementary Table 2), real time (RT) qPCR was performed in triplicates for each sample. GAPDH or b-actin were used as housekeeping genes for normalization. 2 µl of each sample

was added to a master mix preparation containing 2 µl of each primer, 7.5 µl of iTaq Universal SYBR Green Master Mix [Biorad, 1725121] and 3.5 µl nuclease-free water [Invitrogen], and loaded on a 96-well plate [Roche, Lightcycler 480 Multiwell plate 96]. Data was collected and analyzed using the LightCycler 96 System [Roche]. The value of the cycle number at which any sample crossed the threshold (Ct) was used to determine fold difference. In addition, the geometric mean of the reference gene served as a point for normalization. Fold difference was calculated with the $2^{-\Delta\Delta Ct}$ method (Livak & Schmittgen, 2001).

14. 16s RNA sequencing

Overall, fecal pellets from 47 animals were sent to our collaborator Dr. Yogesh Singh in the University of Tubingen for 16s RNA microbiome profiling, one sample before and one after the chronic stress treatments - either corticosterone administration (CORT) or stress (CRUST) - thus, 94 samples in total. Of the 47 animals, 18 animals participated in the CORT cohort while 29 animals participated in the CRUST cohort as presented in Table 3. To detect the genotypic effects of the BAC transgene on the populations of gut microbiota, data from WT and BAC animals before treatment (i.e., chronic stress) were compared for quantitative alterations. Significance was defined at $p < 0.05$, using a Mann-Whitney test adjusted with Benjamini-Hochberg. To identify the interaction effect of stress (either CORT or CRUST) on the WT and BAC, a 2x2 design was arranged involving WT CTL, WT stress, BAC CTL and BAC stress animals was estimated with a two-way ANOVA test, after transforming the data to the logarithmic scale, using the formula ~genotype*treatment. Normality of the ANOVA residuals was tested with Shapiro's test, and microbiome genera with non-normal residuals were excluded from the analysis.

Table 3. Table summarizing the fecal pellet samples shipped to the University of Tubingen for microbiome profiling

Stress protocol		**CORT**		**CRUST**	
Genotype	**WT**	4	4	6	6
	BAC	4	6	8	9
Treatment		Control	Stress	Control	Stress

15. SCFAs in rat fecal samples

15a. Reagents, lipid standards, stock and working solutions

All the solvents used were of LC-MS analytical grade. Acetonitrile was purchased from Carlo Erba (Val De Reuil, France), isopropanol and methanol from Fisher Scientific (Laughborough, UK), and formic acid 98-100% from Chem-Lab (Zedelgem, Belgium). 3-Nitrophenylhydrazine hydrochloride (97%) and *N*-(3-dimethyl aminopropyl)-*N*'-ethylcarbodiimide hydrochloride (EDC.HCl) (97%) were purchased from Fluorochem (Derbyshire, UK). *N*'-(3-nitrophenyl) acetohydrazide, *N*'-(3-nitrophenyl) propionohydrazide, *N*'-(3-nitrophenyl) butyrohydrazide and d_3-*N*'-(3-nitrophenyl) acetohydrazide were previously synthesized at the Laboratory of Organic Chemistry, National and Kapodistrian University of Athens. Stock solutions of the standard compounds (1000 mg/L in methanol) were prepared and stored at 4 °C. Working solutions (500 and 1000 ng/mL) were prepared daily by appropriate dilution.

15b. Extraction of SCFAs from fecal samples

For the fecal samples, 20 mg of freshly collected feces were homogenized in 400 µL of precooled methanol and then centrifuged at 15,000 g for 10 min at 4 °C. The supernatants were collected for further use (Wei et al., 2020).

15c. Derivatization procedure

For derivatization, 10 µL of each of the supernatants and 10 µL d_4-acetic acid (10 ppm in methanol) were mixed with 10 µL of 3-NPH (200 mM in 50% aqueous acetonitrile) and 10 µL of EDC-6% pyridine solution (120 mM in the same solvent). The mixture was incubated at 40 ^{0}C for 30 min. After reaction, this solution was diluted to 1 mL with methanol/water 1:1 in a vial and this mixture was used for the LC-MS/MS analysis (Han et al., 2015).

15d. LC-MS/MS analysis

An ABSciex Triple TOF 4600 [ABSciex, Darmstadt, Germany] combined with a micro-LC Eksigent [Eksigent, Darmstadt, Germany] and an autosampler set at 5 °C and a thermostated column compartment were used to perform the LC-MS/MS measurements. Electrospray ionization (ESI) in negative mode was used for all the MS experiments. The data acquisition method consisted of a TOF-MS full scan *m/z* 50–850 and several information-dependent acquisition (IDA)-TOF-MS/MS product ion scans using 40 V collision energy (CE)

with 15 V collision energy spread (CES) used for each candidate ion in each data acquisition cycle (1091). This workflow allows quantitation (primarily using TOF-MS) and confirmation (using IDA-TOF-MS/MS) in a single run. The MS resolution working conditions were: ion energy 1 (IE1) -2.3, vertical steering (VS1) -0.65, horizontal steering (HST) 1.15, and vertical steering 2 (VS2) 0.00. A Halo C18 2.7 µm, 90 Å, 0.5 × 50 mm^2 column from Eksigent was used for the present study. The mobile phase consisted of a gradient (A: acetonitrile/0.01% formic acid/isopropanol 80/20 *v*/*v*; B: H_2O/0.01% formic acid) and the elution gradient adopted started with 5% of phase B for 0.5 min, gradually increasing to 98% in the next 7.5 min. These conditions were kept constant for 0.5 min, and then the initial conditions (95% solvent B, 5% solvent A) were restored within 0.1 min to re-equilibrate the column for 1.5 min for the next injection (flow rate: 55 µL/min).

15e. Data processing and quantification

All chemical structures were drawn using ChemBioDraw Ultra 12.0 [PerkinElmer Informatics, Waltham, MA, USA]. The data acquisition was carried out with MultiQuant 3.0.2 and PeakView 2.1 from [ABSciex, Darmstadt, Germany]. EICs were obtained with the use of MultiQuant 3.0.2 [ABSciex, Darmstadt, Germany], which created the base peak chromatograms for the masses that achieve a 0.01 Da mass accuracy width. The relative tolerance of the retention time was set within a margin of ±2.5%.

15f. Method validation

Solutions from 5-1500 ng/mL of *N*'-(3-nitrophenyl) acetohydrazide, *N*'-(3-nitrophenyl) propionohydrazide and *N*'-(3-nitrophenyl) butyrohydrazide containing 100 ng/mL of d_3-*N*'-(3-nitrophenyl) acetohydrazide (3 replicates; 11 levels) were used to assess the linearity and the limits of detection (LOD) and quantification (LOQ). The LOD and LOQ were calculated using the signal-to-noise method. A signal-to-noise ratio (S/N) of three is generally accepted for estimating the LOD, and a signal-to-noise ratio of 10 is used for estimating the LOQ. This method is commonly applied to analytical methods that exhibit baseline noise.

16. Statistical analysis and graphic illustrations

GraphPad Prism 9 software was used for statistical analyses and Adobe Illustrator Artwork 23 was used to create figures and artwork. For two-way ANOVAs, the two factors were genotype (WT and BAC) and drug treatment (CTL and CORT/CRUST) with Bonferroni's multiple comparison tests used for post-hoc analysis. Unpaired Student's t-tests and simple

linear regression analysis were also used, where applicable. A p-value of < 0.05 was considered statistically significant. The exact p-values for all analyses are reported in Supplementary Table 3. Results are presented in graphs as mean ± SEM.

III. Results

1. Assessment of pharmacological stress: chronic CORT administration

After two weeks of CORT administration, a battery of behavioral tests (OF, EPM and motor phenotype analysis) was conducted before sacrificing the animals. Brain regions associated with the HPA axis and PD pathology, including the amygdala, hypothalamus, hippocampus, ventral midbrain and striatum, were collected for further analysis (experimental timeline summarized in Fig. 1a). In addition, the adrenal glands, thymus glands, and the first part of the small intestine (duodenum) were excised. Throughout the experiment, blood and fecal samples were collected to assess the animals' microbiota profile and investigate potential gut-brain axis dysfunction and dysbiosis. More specifically, pS129 asyn levels were measured in all the aforementioned brain regions while CRF levels and neurotransmitters related to stress response and PD pathology (NA and DA turnover) were quantified specifically in the hypothalamus. In the hippocampus, NA and total asyn protein levels were analyzed. Along the nigrostriatal pathway, we evaluated the degeneration of TH+ neurons, glial activation, and total asyn levels to determine the extent of dopaminergic dysfunction and neuroinflammation.

2. Human asyn overexpression in BAC rats confers baseline HPA axis dysregulation

The first evidence of HPA axis dysregulation was lower baseline CRF levels found in the hypothalamus of BAC rats (Fig. 1b). Next, HPA axis activity was assessed by measuring the levels of CORT circulating in the blood. The experimental groups that received CORT revealed nonsignificant elevated plasma CORT levels (Fig. 1c) and the BAC animals demonstrated decreased CORT levels, regardless of treatment (Fig. 1c). Adrenal insufficiency and relative HPA axis dysregulation was also confirmed by a significant decrease in the weight of the adrenal glands in BAC rats, regardless of treatment (Fig. 1d). Subsequently, the EPM, OF and PPI tests were used to assess behaviors sensitive to stress, specifically anxiety and sensorimotor gating. While BAC animals displayed baseline increased mobility in the EPM, CORT further increased the distance travelled in both WT and BAC rats in the EPM (SFig. 2a). As expected, CORT increased the levels of anxiety in WT rats, depicted by a decrease in the percentage of time that WT CORT animals spent in the open arms of the EPM, while the baseline anxiogenic profile of BAC rats was not further exacerbated (Fig. 1e). In the OF, CORT decreased the total time spent in the center of the arena, indicating elevated anxiety, while there was a baseline difference with BAC animals spending more time in the center of the open field (Fig. 1f) that correlated with the total distance travelled

in the arena of the OF (SFig. 2b). Assessment of sensorimotor gating revealed an increased average percentage of PPI in both WT and BAC rats following treatment with CORT (Fig. 1g). An increase in startle response amplitude following CORT treatment in BAC rats was indicative of hypervigilance (Fig. 1h). Moreover, CORT increased NA levels in the hypothalamus in both WT and BAC rats (Fig. 1i) and reversed enhanced DA turnover (DOPAC+HVA+3MT/DA) in the hypothalamus of BAC rats (Fig. 1j). In the hippocampus, BAC rats demonstrated decreased NA levels (SFig. 2c). Overall, CORT administration resulted in anticipated behavioral and neurochemical changes. Several stress endpoints, neurochemical and behavioral outcomes indicate a baseline imbalance of the stress system in BAC animals, rendering them more sensitive to the effects of CORT.

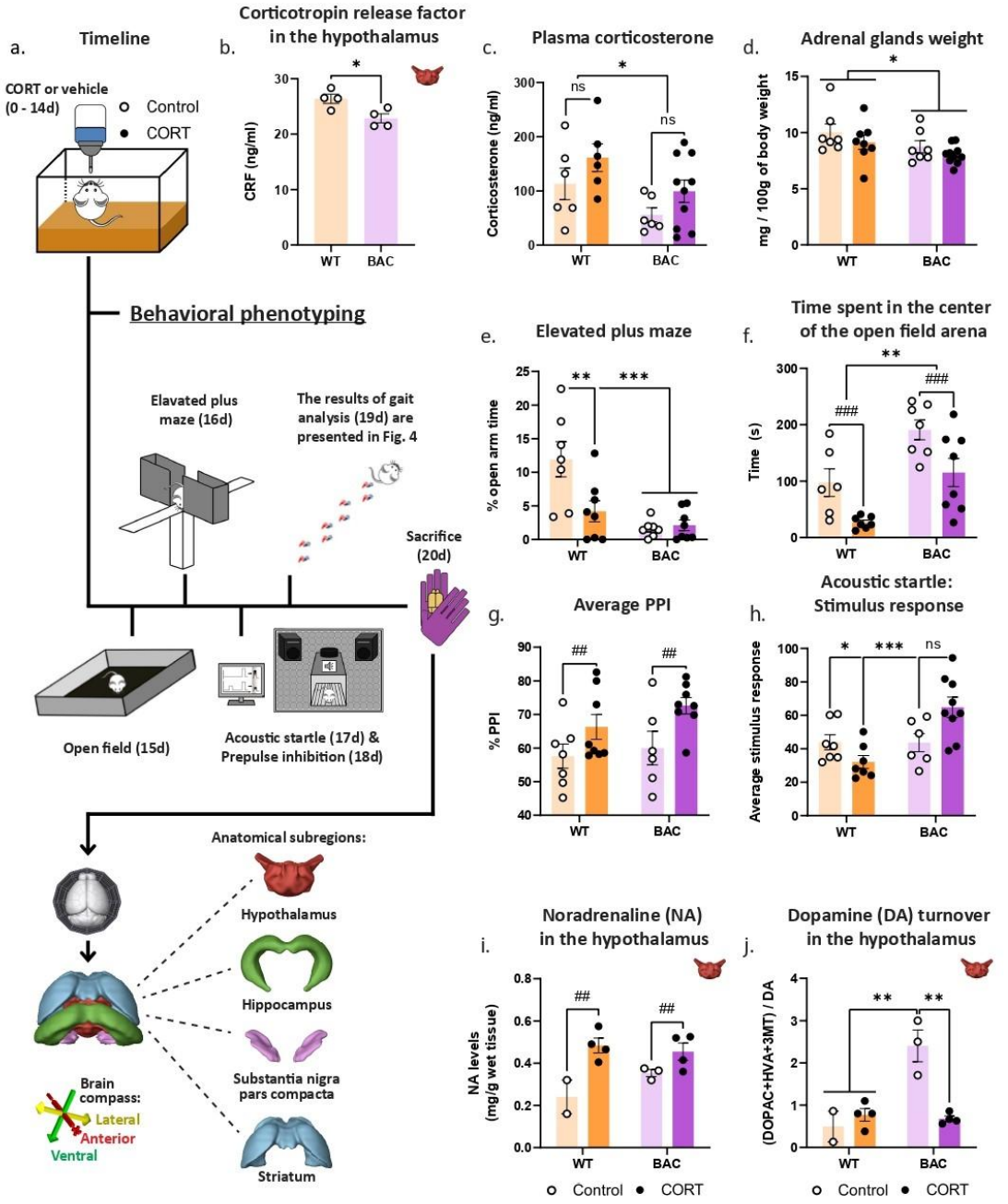

Figure 1. HPA axis dysregulation in asyn BAC rats. As depicted in the experiment outline (a), following CORT administration for 14 days and a battery of behavioral tests consisting of open field (OF), elevated plus maze (EPM), prepulse inhibition (PPI) and motor phenotype analysis, brains of BAC and WT rats were harvested and the hypothalamus, hippocampus, ventral midbrain - encompassing the SNg - and striatum were dissected. First, we evaluated (b) CRF levels (ng/ml) in the hypothalamus of 9 mo BAC animals and age-matched WT controls without treatment, (c) levels of plasma CORT (ng/ml) following CORT administration and (d) adrenal glands weight (mg/100g of body weight). For the behavioral phenotyping, we calculated (e) the percentage of time spent in the open arms of the EPM, (f) the total amount of time (s) spent in the center of the OF arena, (g) average % PPI and (h) average stimulus response in PPI test. Following neurochemical measurements in the hypothalamus, we quantified (i) NA levels (mg/g wet tissue) and (j) DA turnover (DOPAC+HVA+3MT/DA). Unpaired t-test was applied for (b) while two-way ANOVAs were applied for (c-j) with Bonferroni's multiple comparisons post-hoc tests. All data are expressed as mean ± SEM. Asterisk (*) is used to denote genotype main effects while hashtag (#) denotes main treatment effects. Significance levels: */# $p<0.05$; **/## $p<0.01$; ***/### $p<0.001$. N=4 per group for (b), N=7-10 for (c-h) and N=2-4 for (i) and (j).

3. Chronic CORT enhances asyn pathology in the hypothalamus of asyn BAC rats

The hypothalamus acts as a link between the central nervous and endocrine systems. Immunohistochemical staining in the hypothalamus (Fig. 2a) revealed extensive pS129 asyn pathology in BAC animals (Fig. 2b) which colocalizes with dopaminergic neurons (SFig. 3 for indicative images of pS129 asyn colocalization with dopaminergic neurons in the hypothalamus). In the hippocampus, BAC transgenic animals displayed approximately five-fold greater amounts of pS129 asyn than WT animals, regardless of CORT treatment, indicating a potential plateau effect (Fig. 2c). Moreover, Western immunoblot analysis showed elevated soluble and insoluble total asyn levels in the hippocampus of BAC animals, regardless of treatment (Fig. 2d, SFig. 4a,e). PS129 asyn levels in the BAC animals remained unchanged in the hippocampus after CORT treatment, in both the soluble and insoluble fractions (Fig. 2e, SFig. 4b,f). Comparing the shift in asyn species (insoluble/soluble fraction), there is an overall trend for increased total (SFig. 4i; $p=0.0939$) and pS129 (SFig. 4j; $p=0.0505$) asyn levels in BAC animals following CORT.

Analysis in the striatum revealed increased soluble and insoluble total asyn levels in the BAC animals, regardless of treatment (Fig. 2f, SFig. 4c,g). Comparing the shift in asyn species (insoluble/soluble fraction), BAC rats demonstrated increased total asyn levels with an interaction effect, indicating an increase in total asyn levels between WT CTL and BAC CTL groups (SFig. 4k). PS129 asyn levels in the striatum were unchanged in BAC animals upon CORT treatment, in both the soluble and insoluble fractions (Fig. 2g, SFig. 4h). No further differences were observed with respect to the shift in pS129 asyn species (insoluble/soluble fraction) (SFig. 4l). Taken together, our results show that chronic CORT administration

significantly enhances pS129 asyn levels in the hypothalamus, along with an apparent shift to more insoluble pS129 asyn in the hippocampus of BAC rats.

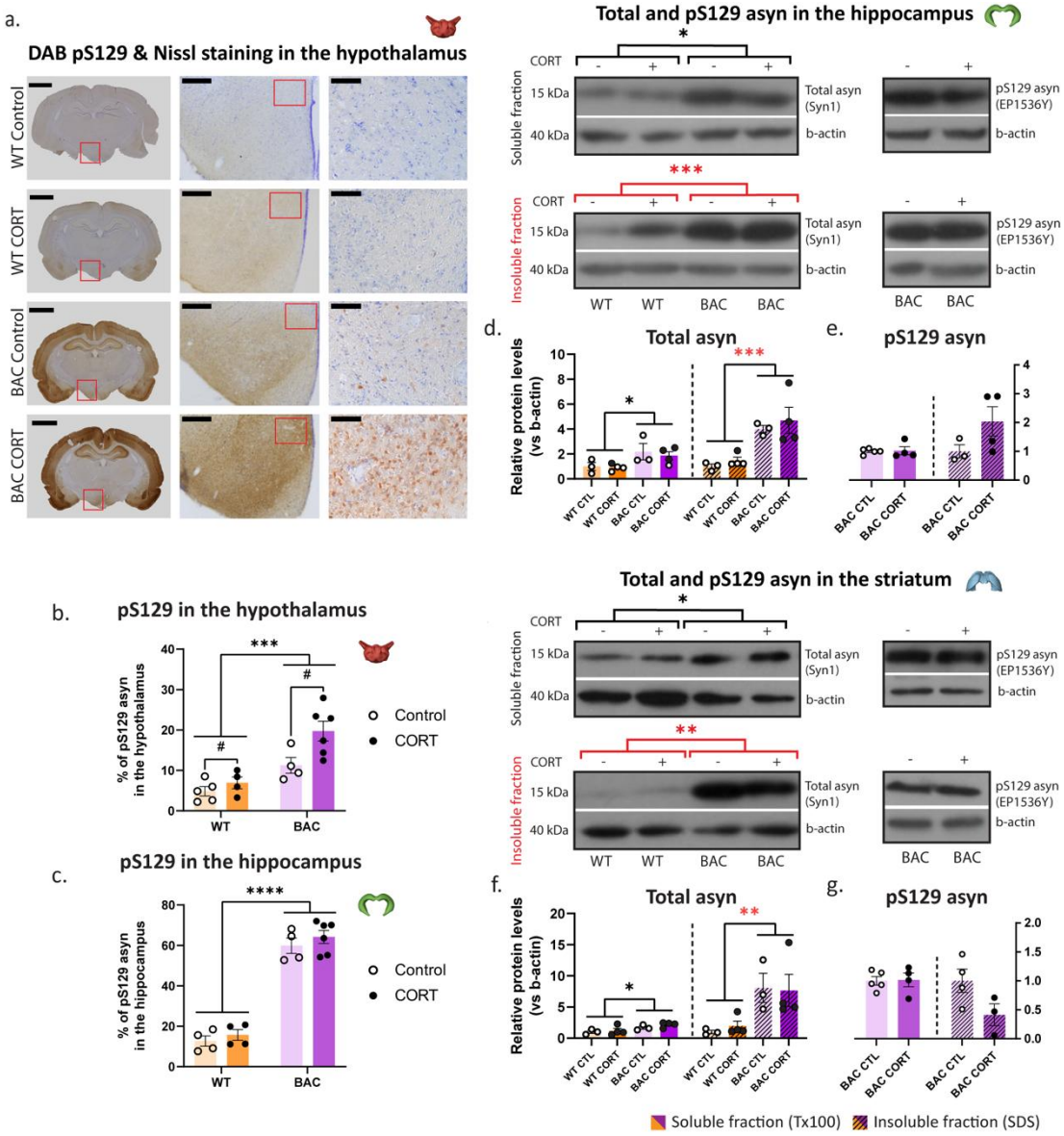

Figure 2. PS129 asyn pathology in stress-related brain regions. Asyn pathology was assessed in BAC rats following chronic CORT with (a) DAB pS129 asyn staining in the hypothalamus and hippocampus, where we calculated (b & c) the % of pS129 asyn, respectively; scale bars; 1st column: 3 mm, 2nd column (10x): 300 µm and 3rd column (40x): 75 µm). Immunoblotting quantification of total and pS129 asyn in the soluble and insoluble fractions of the hippocampus and the striatum are presented in SFig. 4. In the hippocampus, we measured the relative protein levels of (d) total soluble, total insoluble, (e) pS129 soluble and pS129 insoluble asyn. In the striatum, we measured the relative protein levels of (f) total soluble, total insoluble, (g) pS129 soluble and pS129 insoluble asyn. Protein levels were normalized against b-actin using Fiji/ImageJ for relative quantification. Two-way ANOVAs were applied for (b) and (c) with Bonferroni's multiple comparisons post-hoc tests while unpaired t-tests were applied for the comparisons of the normalized amounts of total and pS129 asyn between the soluble and the insoluble fractions in (d-g). All data are expressed as mean ± SEM. Asterisk (*) is used to denote genotype effects while hashtag (#) denotes treatment effects. Significance levels: */# p<0.05; ** p<0.01; *** p<0.001; **** p<0.0001. N=4-5 for (b) and (c) and N=3-4 per group for (d-g).

4. Chronic CORT enhances asyn phosphorylation and exacerbates nigrostriatal neurodegeneration in asyn BAC rats

Brains were collected and processed to evaluate the integrity of the dopaminergic system by quantifying the TH+ neurons in the SNpc (Fig. 3a,b) and amount of pS129 asyn in these cells (Fig. 3c,d), as well as the density of their afferents in the striatum (Fig. 3e-h). Chronic CORT administration led to a significant loss of TH+ neurons in the SNpc in both WT and BAC animals, with a loss ranging from 15% for the former to 30% for the latter (Fig. 3b), indicating an additive effect on nigral DA cell loss in BAC rats. Immunohistochemical staining in the SNpc revealed a significant increase of pS129 asyn localized in the TH+ cells of the BAC animals, while chronic CORT further increased pS129 asyn levels (significant genotype x treatment interaction), indicating a synergistic effect (Fig. 3d). Separate analysis of the three striatal subdivisions - DL, DM and V striatum - revealed a significantly decreased density of TH+ afferents only in the DL striatum following CORT (Fig. 3e). While there were no differences observed in the DM striatum (Fig. 3f), the genotype x treatment interaction effect was significant in the V striatum (Fig. 3g).

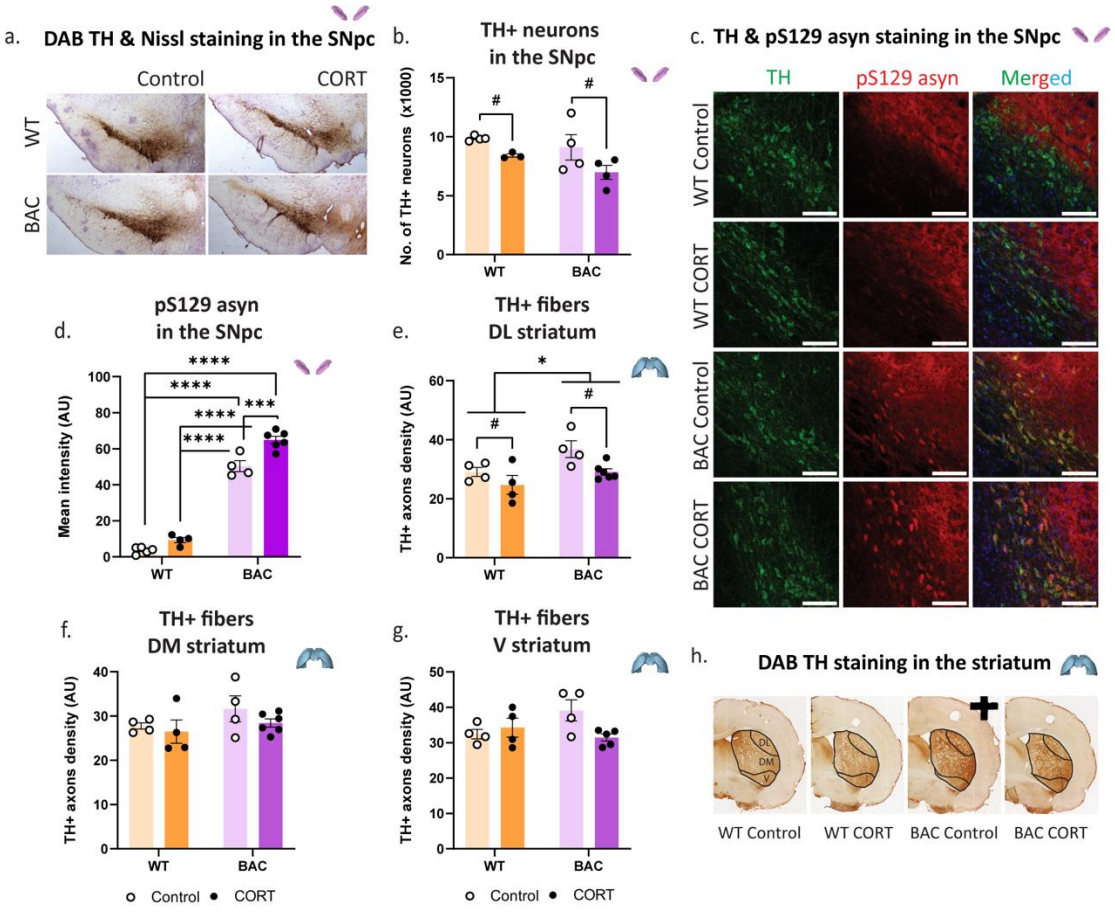

Figure 3. Nigrostriatal dopaminergic system integrity following chronic CORT administration. Nigrostriatal DA system integrity following chronic CORT administration was assessed with (a) DAB TH and Nissl staining in the SNpc to (b) calculate the number of TH+ neurons (expressed as thousands of neurons). Following (c) immunofluorescent staining against TH and pS129 asyn (scale bar: 100 μm) with DAPI in the column with the merged images, we measured (d) the mean intensity (AU) of pS129 asyn in TH+ neurons. (e) TH+ axons density in the dorsolateral (DL) striatum, (f) dorsomedial (DM) striatum and (g) ventral (V) striatum were calculated following (h) DAB TH staining. Two-way ANOVAs were applied for (b) and (d-g) with Bonferroni's multiple comparisons post-hoc tests. All data are expressed as mean ± SEM. Asterisk (*) is used to denote genotype main effects while hashtag (#) denotes treatment main effects. Significance levels: */# $p<0.05$;*** $p<0.001$; **** $p<0.0001$. N=3-4 per group for (b), N=4-6 for (b) and (d-g).

5. Chronic CORT increases neuroinflammation in WT animals along the nigrostriatal axis while asyn BAC rats display enhanced astrogliosis at baseline

In the SNpc (Fig. 4a), immunohistological evaluation of neuroinflammation, revealed a significant increase in the mean intensity of astrocytic (GFAP) cells following chronic CORT administration (Fig. 4b), while no changes were observed in the mean intensity of microglial (Iba1) cell profiles (Fig. 4c). In the striatum, a specific expression pattern for GFAP emerged; immunoblot analysis of the soluble protein fraction (Fig. 4d) demonstrated a significant genotype x treatment interaction effect on GFAP protein expression levels (Fig. 4e). This GFAP expression pattern was further supported by immunohistochemical glial staining in the striatum (Fig. 4f), which also revealed a significant genotype x treatment interaction effect on GFAP mean intensity (Fig. 4g). Iba1 mean intensity in the striatum also displayed a genotype x treatment interaction effect (Fig. 4h) and had a similar expression pattern to GFAP (Fig. 4g). Overall, the glial expression pattern was characterized by significantly increased striatal GFAP mean intensity in the BAC rats, combined with a genotype x treatment interaction effect, suggesting that BAC rats have already reached a plateau immune activation, achieved by WT animals after CORT administration. The same pattern was seen in the Iba1 mean intensity levels in the striatum.

6. Chronic CORT triggers phenoconversion in asyn BAC rats, worsening their Parkinsonian phenotype

Assessment of gross motor function supported the observed degeneration of dopaminergic neurons in the SNpc following CORT (Fig. 3b). BAC rats exhibited a characteristic baseline locomotor hyperactivity in the open field, expressed as increased distance traveled (cm) (Fig. 5a), while CORT administration decreased motor activity in WT rats and reversed hyperactivity in BAC rats (Fig. 5a). In addition, a significant increase in the total number of rearings was observed in BAC rats receiving CORT, indicative of augmented

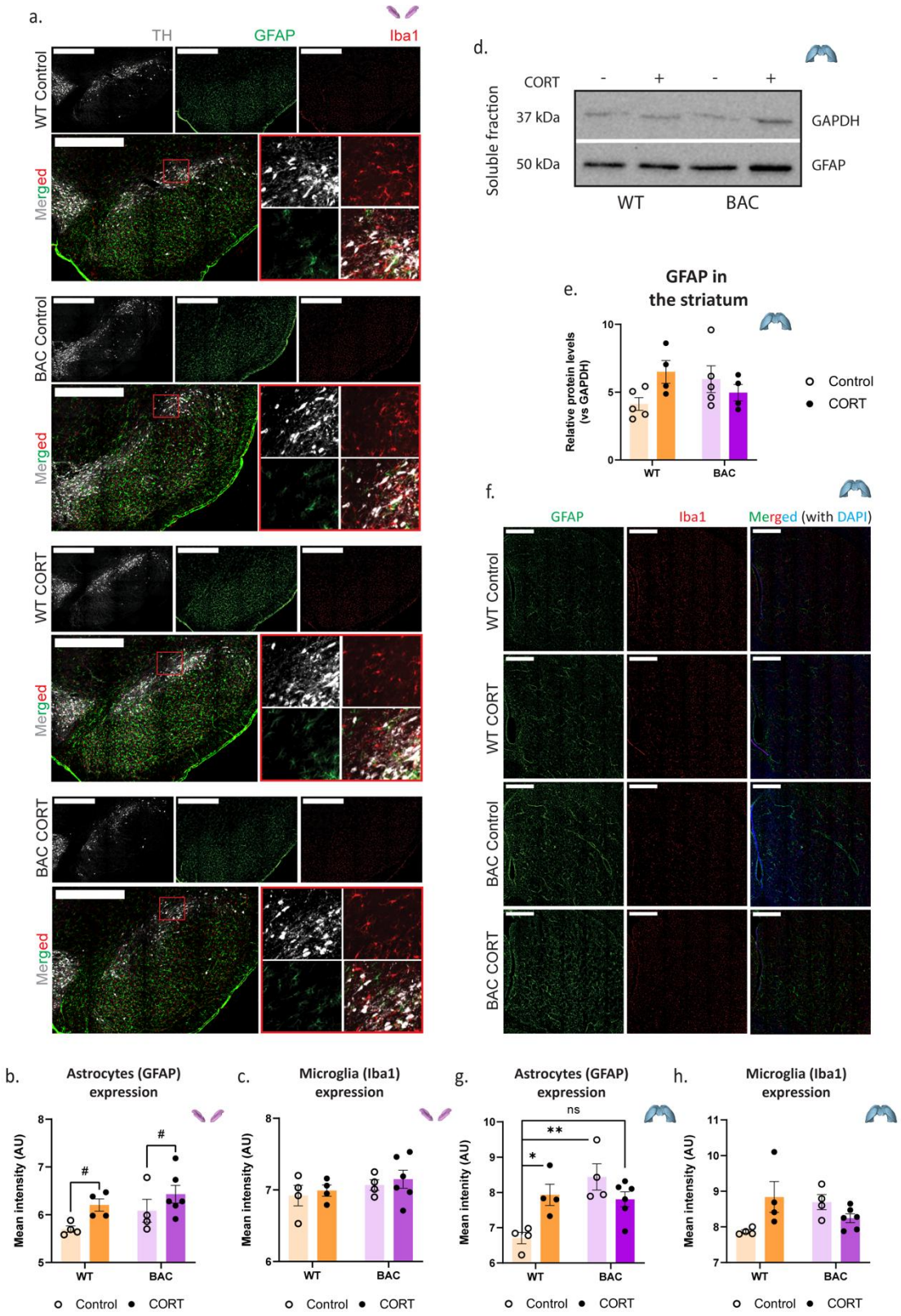

Figure 4. Neuroinflammation in the nigrostriatal axis following chronic CORT administration. Following (a) immunohistochemical staining in the SNpc we calculated the mean intensity (AU) of (b) astrocytes (GFAP) and (c) microglia (Iba1) expression. (d) Using Western immunoblot biochemical analysis, we measured (e) relative protein levels of GFAP (vs GAPDH) in the soluble fraction of the striatum. (f) By applying immunohistochemical staining in the striatum, we calculated the mean intensity (AU) of (g) astrocytes (GFAP) and (h) microglia (Ibal) expression. The relative quantification of protein levels was performed with the use of Fiji/ImageJ. Regular 2-way

ANOVAS were applied for (b), (c), (e), (g) and (h) with Bonferroni's multiple comparisons post-hoc tests. Asterisk (*) is used to denote genotype main effects while hashtag (#) denotes treatment main effects. All data are expressed as Mean ± SEM. Significance levels: */# p<0.05, ** p<0.01. N=4-6.

exploratory activity (Fig. 5b) and consistent with the hypervigilant state observed in the PPI test (Fig. 1h). Examination of fine motor function revealed that CORT triggered worse performance in the postural instability test for both genotypes (Fig. 5c). Moreover, recorded stride lengths of both forelimbs and hindlimbs revealed CORT - and genotype - dependent changes in gait; decreased right and left forelimb stride length (BAC animals have a shorter stride length, regardless of treatment) and shorter right and left hindlimb stride length (Fig. 5d). The general pattern in these fine motor tasks was for CORT to worsen performance in the WT, but in certain cases, it led to further exacerbation of BAC rats' gross and fine motor performance.

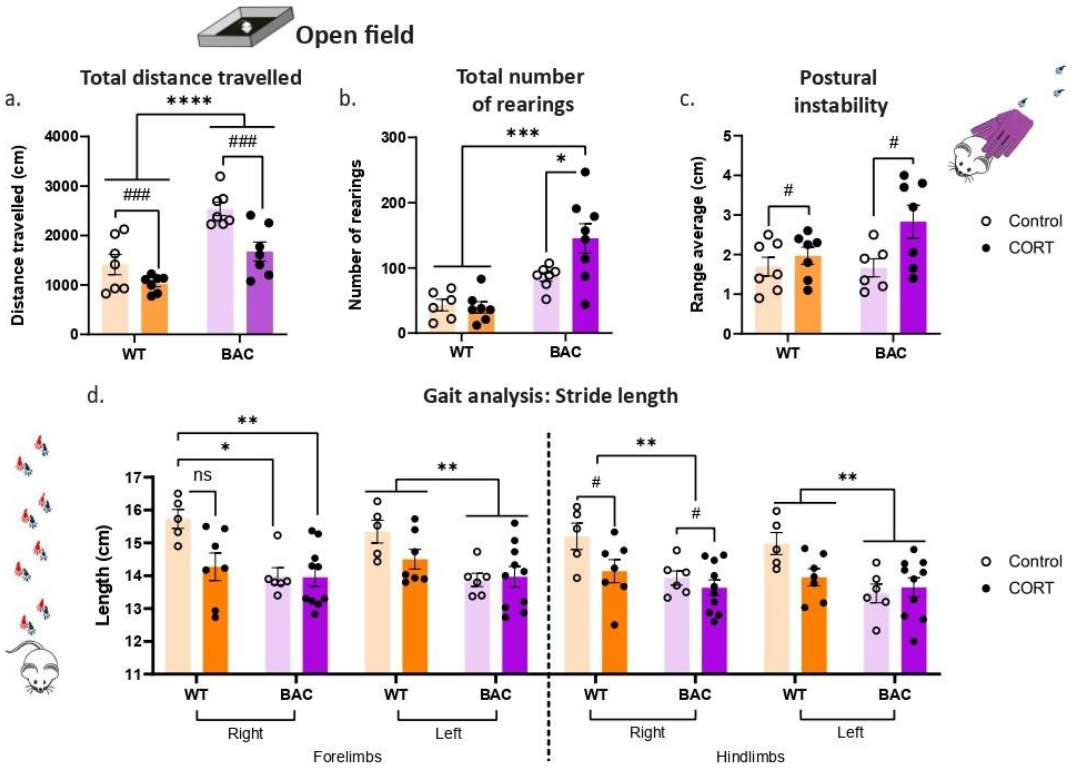

Figure 5. Motor phenotype decline after chronic CORT treatment. Behavioral testing in BAC rats following CORT administration measured (a) the total distance travelled (cm) and (b) the total number of rearings in the OF test. Fine motor function behavioral tests measured (c) the average range (cm) of forelimb steps in the postural instability test and (d) the stride length (cm) both for the forelimbs and the hindlimbs. Two-way ANOVAs were applied for (a- d) with Bonferroni's multiple comparisons post-hoc tests. All data are expressed as mean ± SEM. Asterisk (*) is used to denote genotype main effects while hashtag (#) denotes treatment main effects. Significance levels: */# p<0.05; ** p<0.01; ***/### p<0.001; **** p<0.0001. N=5-10 for (a-d).

7. Assessment of psychological stress: the CRUST protocol

After two weeks of CRUST, we performed a series of pre-motor (ODT, MWM, PPI) and motor (OF, overlap, gait analysis) behavioral tests, similar to the approach used following CORT administration, to evaluate the PD-like behavioral phenotype in the BAC animals (Fig. 6a). Upon completion of the behavioral testing, the animals were sacrificed and brain regions including the olfactory bulbs, prefrontal cortex, hippocampus, ventral midbrain, and striatum were collected for subsequent analysis (Fig. 6a). As described earlier, we collected the adrenal and thymus glands, duodenum, as well as blood and fecal samples. We quantified the levels of glutamate, glutamine, and GABA across all the aforementioned brain regions. Along the nigrostriatal pathway, we assessed the degeneration of TH+ neurons and fibers, glial activation, and the levels of total, human and pS129 asyn. Additionally, asyn levels were measured in the hippocampus, where we also performed RNA sequencing to identify potential alterations in transcriptional regulation. This region has been previously reported to express high levels of asyn (Polissidis et al., 2021) and is implicated in both stress response and PD pathology.

8. CRUST induces stress in both WT and Tg animals triggering phenoconversion in asyn BAC rats

After completing the CRUST protocol and behavioral assessments (Fig. 6a), both WT and BAC rats that underwent CRUST showed increased weight loss (Fig. 6b), as well as hypertrophy of the adrenal glands, indicative of prolonged stress exposure and thus, chronic HPA axis activation (Fig. 6c). Additionally, HPA axis and immune dysregulation was evident in BAC rats by the significant hypertrophy of the thymus gland, independent of stress protocol treatment (Fig. 6d). This finding was consistent with the BAC rats analyzed in the CORT cohort (SFig. 3d). Similar to observations in the CORT cohort, gross motor function assessments suggested DA neuron degeneration in the SNpc following CRUST treatment (Fig. 7c). BAC rats exhibited a characteristic baseline locomotor hyperactivity in the open field, expressed as increased distance traveled, while CRUST administration decreased motor activity in WT rats and reversed hyperactivity in BAC rats (Fig. 6e). In the open field test, CRUST also reduced the total time spent in the center of the arena, signifying heightened anxiety levels. Interestingly, BAC rats showed a baseline increase in time spent in the center compared to WT rats (Fig. 6f). Olfactory testing revealed a trend toward decreased olfactory function in WT rats ($p = 0.0726$; Fig. 6g), whereas BAC rats, already presenting a baseline olfactory deficit, showed no further decline (Fig. 6g). This finding was consistent with the

BAC rats in the CORT cohort (SFig. 3e). Evaluation of sensorimotor gating with the PPI revealed an increase in PPI percentage in both WT and BAC rats following CRUST (Fig. 6h), while the startle response amplitude increased only in BAC rats following CRUST, suggesting heightened alertness (Fig. 6i). Interestingly, CRUST improved performance in the long-term memory probe trial of the Morris water maze (24-hour retention), as indicated by an increase in time spent in the target quadrant and the number of platform crossings (Fig. 6j,k). Overall, stress endpoints following CRUST indicate HPA axis activation in both WT and BAC rats. The physiological and behavioral data suggest a baseline dysregulation of the stress response in BAC animals, making them more susceptible to the effects of CRUST- as was also the case with CORT.

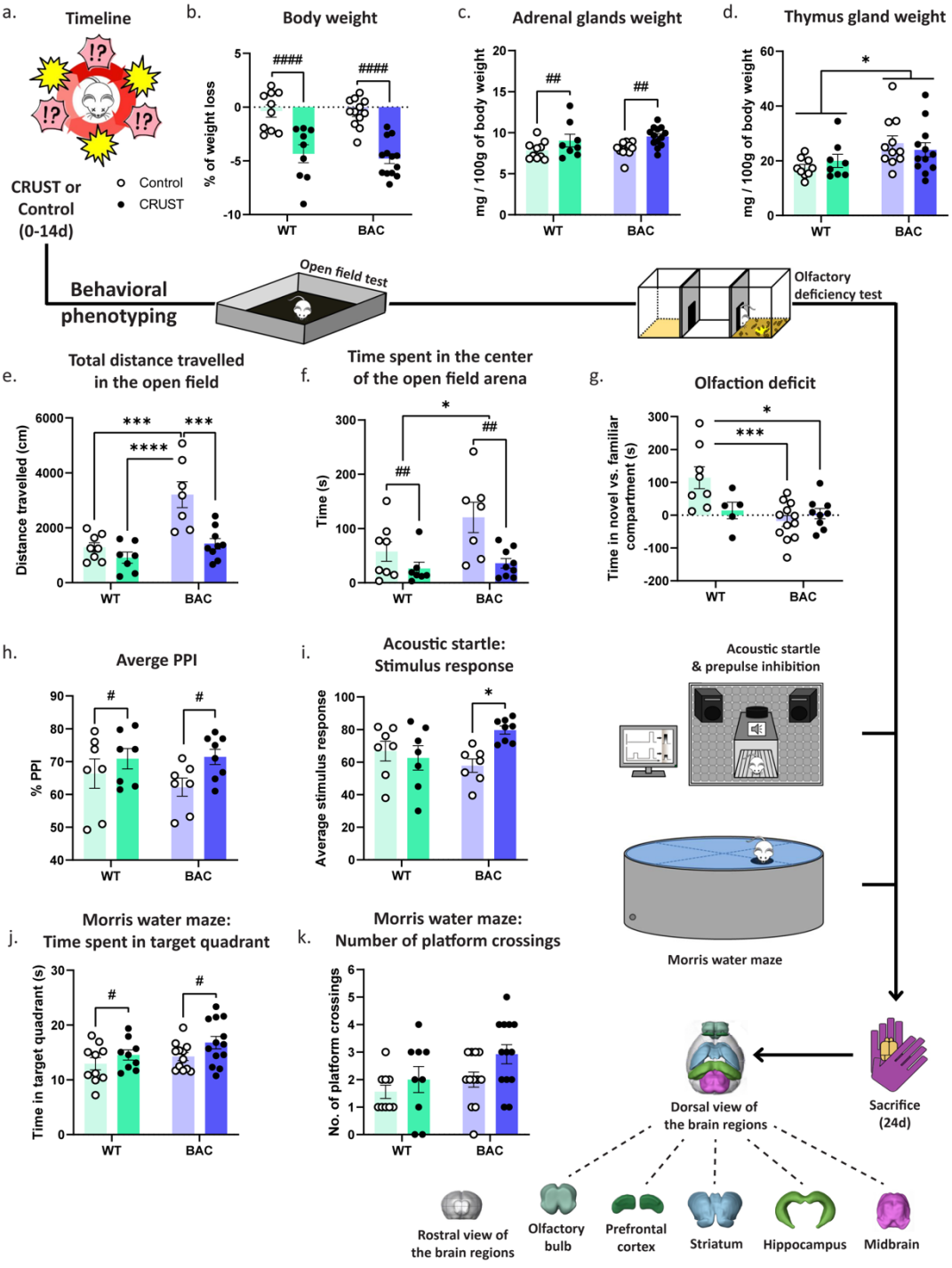

Figure 6. CRUST causes stress, behavioral phenotype alterations and leads to phenoconversion in asyn BAC rats. (a) After completing the CRUST protocol and subsequent behavioral phenotyping, stress endpoints in CRUST-exposed WT vs human asyn BAC rats were assessed (b) by calculating the % of weight loss after two weeks, (c) measuring adrenal and (d) thymus gland weights (mg/100g of body weight). In BAC rats, behavioral phenotyping post CRUST involved measuring (e) total distance travelled (cm) and (f) time spent in the center of the OF arena. (g) Olfactory function was evaluated based on the time spent in the compartment with the familiar odor, while (h) average % PPI and (i) average stimulus response were measured with the PPI protocol. Spatial learning and memory performance were assessed through the Morris water maze by measuring (j) time spent in the platform quadrant and (k) the number of platform crossings. Two-way ANOVAs were applied for (a-h) with Bonferroni's multiple comparisons post-hoc tests. All data are expressed as mean ± SEM. Asterisk (*) is used to denote genotype main effects while hashtag (#) denotes treatment main effects. Significance levels: */# $p<0.05$; ## $p<0.01$; ***/### $p<0.001$. N=8-13 per group for (b-f) and (h-k) and N=4-12 for (g).

9. CRUST worsens nigral neurodegeneration in asyn BAC rats and disrupts DA metabolism and neurotransmission

To evaluate the integrity of the dopaminergic system along the nigrostriatal axis, we collected and processed the ventral midbrain, including the SNg, and the striatum (Fig. 7a), to quantify TH+ neurons. At baseline, BAC rats exhibited fewer TH+ neurons (a representative image of neuronal degeneration is presented in Fig. 7b) and CRUST exposure resulted in a significant reduction of TH+ neurons in the SNpc in both WT and BAC rats, with a 15% loss observed in WT and a 25% loss in BAC rats (Fig. 7c). This suggests an additive effect of CRUST on nigral dopaminergic cell loss in BAC rats. However, the analysis of the striatal region did not reveal significant changes in the density of TH+ fibers (Fig. 7d).

Additionally, CRUST reduced striatal DA levels exclusively in BAC rats, which exhibited elevated baseline DA levels (Fig. 7e). DA turnover (DOPAC+HVA+3MT/DA) in the striatum was not affected by stress exposure but was influenced by genotype, as BAC rats showed decreased baseline DA turnover (Fig. 7f). To further investigate these changes and their association with asyn levels, we conducted *in vivo* microdialysis by inserting probes into the striatal region to measure extracellular DA release (Fig. 7g provides a representative image of the experimental setup). *In vivo* microdialysis measurements indicated that DA release increased in WT rats following CRUST, whereas BAC control animals displayed higher baseline DA release compared to WT controls. In contrast, DA turnover was significantly lower in WT CRUST and BAC rats, regardless of stress exposure (Fig. 7i).

Regarding asyn levels in the extracellular milieu in the striatum, administration of diazoxide resulted in an increased release of asyn. However, the findings showed only a non-significant trend toward elevated extracellular asyn release in BAC rats subjected to stress

(Fig. 7j), making it difficult to draw definitive conclusions about the effect of CRUST on extracellular asyn dynamics.

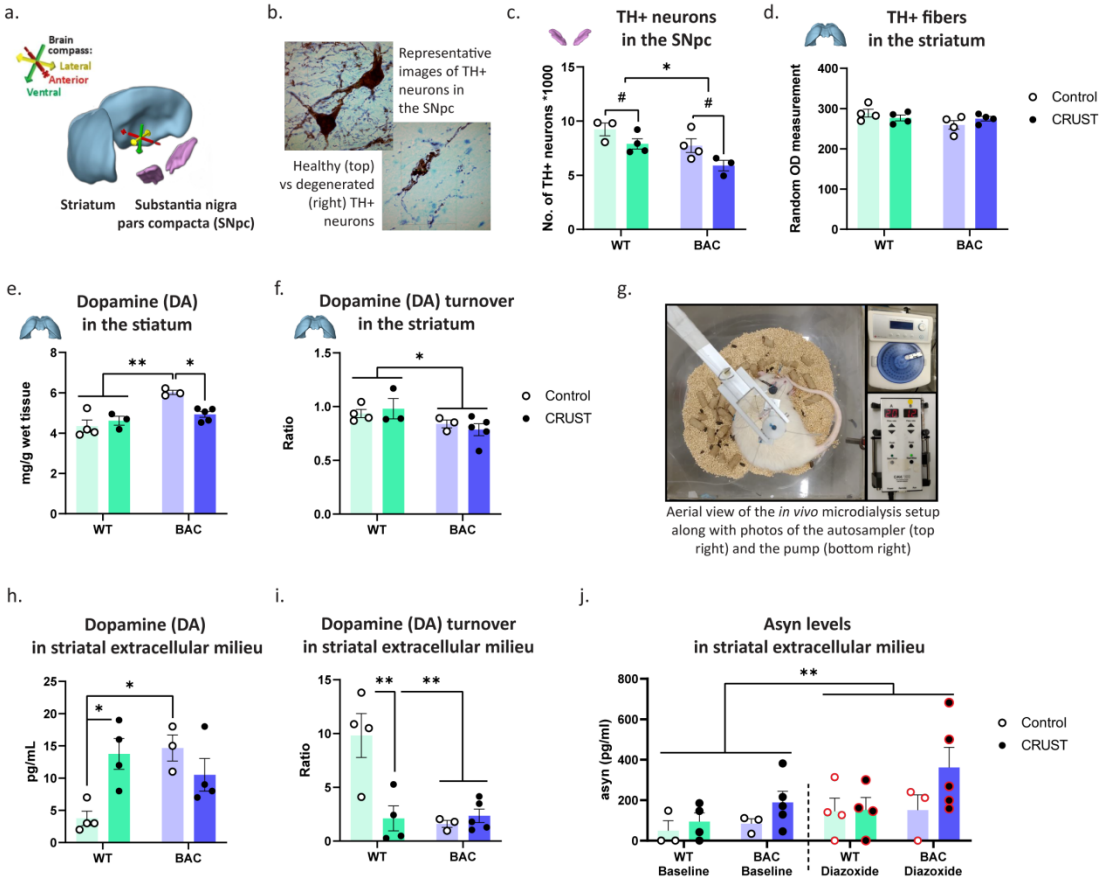

Figure 7. Dopaminergic system integrity along the nigrostriatal systems is compromised following CRUST. DA system integrity following CRUST administration was assessed (a) along the nigrostriatal axis using (b) DAB TH and Nissl staining in (c) the SNpc to quantify the number of TH+ neurons (expressed as thousands of neurons). (d) In the striatum, TH+ axon density was measured using DAB TH staining. DA levels (mg/g wet tissue) and DA turnover (DOPAC+HVA+3MT/DA) were quantified in both (e,f) *ex vivo* striatal tissue and samples collected with *in vivo* microdialysis (g) representing extracellular release (h,i). Additionally, we measured (j) asyn levels (pg/ml) in the same microdialysate samples collected from the striatal extracellular milieu. Two-way ANOVAs were applied for (a-j) with Bonferroni's multiple comparisons post-hoc tests while paired t-test was additionally applied for (j) to compare baseline asyn levels with asyn levels following diazoxide administration. All data are expressed as mean ± SEM. Asterisk (*) is used to denote genotype main effects while hashtag (#) denotes treatment main effects. Significance levels: */# p<0.05; ** p<0.01. N=3-5 per group.

10. CRUST enhances asyn truncation in the striatum of asyn BAC rats

Western blot analysis revealed elevated levels of soluble total asyn in the striatum of BAC animals, irrespective of stress exposure (Fig. 8a,c). Additionally, prolonged exposure led to the appearance of truncated forms of total asyn in BAC animals, with significantly higher levels observed in the second truncated band (Fig. 2e), but not in the first (Fig. 2d) in

stressed BAC groups. Levels of pS129 asyn in BAC animals remained unchanged in the striatum after the CRUST protocol in both the soluble (Fig. 8b,f) and insoluble (Fig. 8l,n) fractions, although there was a non-significant trend toward increased soluble pS129 asyn in the BAC CRUST group compared to their unstressed counterparts (Fig. 8f). Further biochemical analyses of asyn (Fig. 8g) did not reveal any significant differences in human asyn levels (Fig. 8h), truncated forms (Fig. 8i), or endogenous rodent asyn levels (Fig. 8j). Similarly, no changes were detected in the insoluble fraction of total asyn among the groups (Fig. 8 k,m). Collectively, these findings indicate that CRUST selectively enhances asyn truncation in the striatum of BAC rats without affecting the levels of human or endogenous rodent asyn.

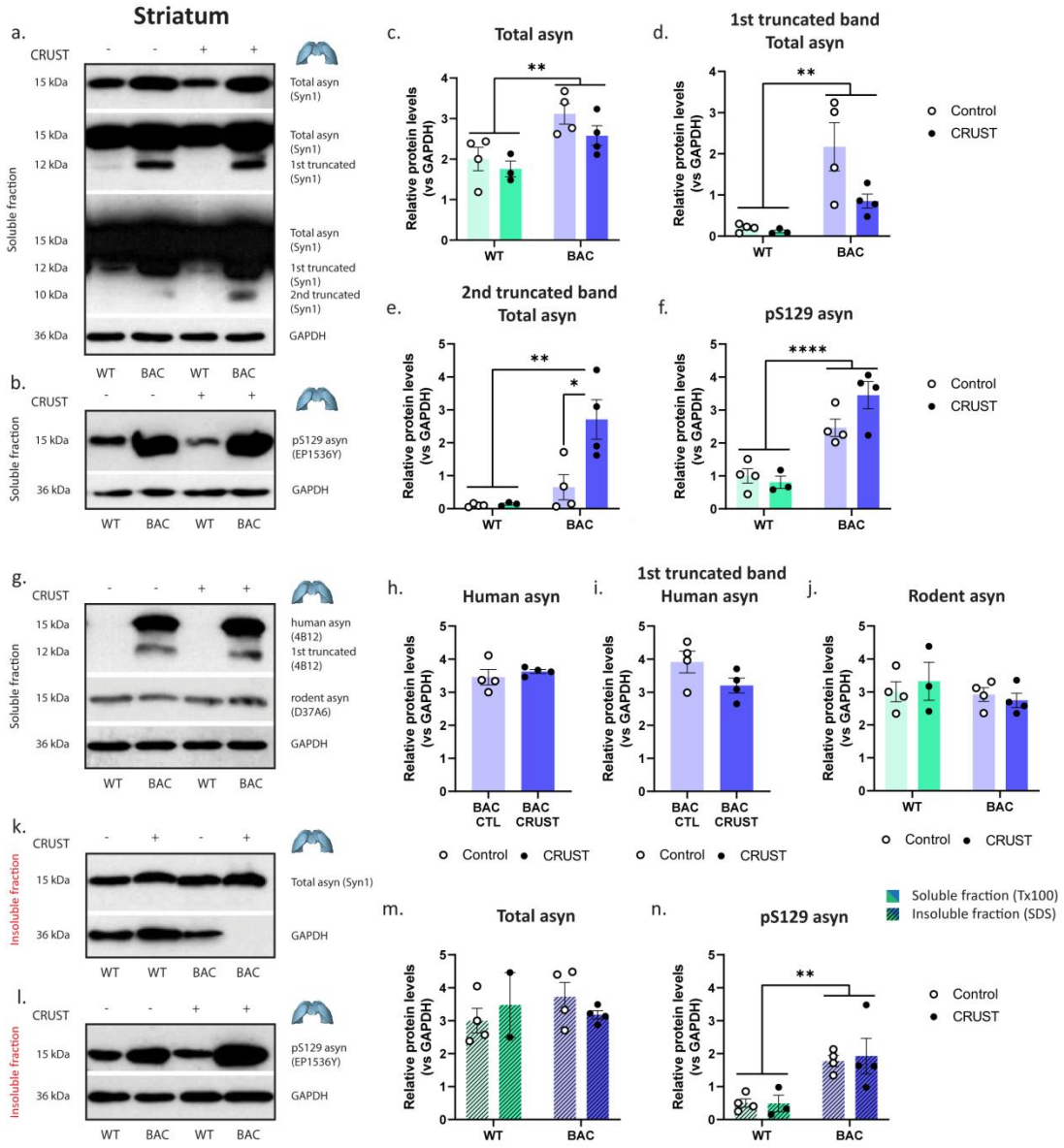

Figure 8. Soluble and insoluble asyn levels in the striatum. Using immunoblot analysis, in (a) we quantified soluble protein levels of (c) total asyn (d) 1st truncated and (e) 2nd truncated asyn band. In (b) we quantified soluble protein levels of (f) pS129 asyn while in (g) we quantified soluble protein levels of (h) human asyn, (i) 1st truncated human asyn band and (j) rodent asyn. For the insoluble fraction in (k), we quantified insoluble protein levels of (m) total asyn protein levels and in (l), we quantified (n) pS129 asyn insoluble protein levels. Protein levels were normalized against GAPDH using Fiji/ImageJ for relative quantification. Unpaired t-tests were applied for (h) and (i) while two-way ANOVAs were applied for (c-f) and (j), (m) and (n) with Bonferroni's multiple comparisons post-hoc tests. All data are expressed as mean ± SEM. Asterisk (*) is used to denote genotype main effects. Significance levels: ** p<0.01; ****p<0.0001. N=2-4 per group.

11. CRUST increases gliosis in the striatum, mostly affecting WT animals

To investigate the effect of CRUST on neuroinflammation, we performed immunofluorescence staining for GFAP, a key structural protein of astrocytes, and Iba1, a marker of reactive microglia, in sections of the SNg (Fig. 9a) and striatum (Fig. 10a). Analysis of the GFAP-positive area in the SNg revealed no significant differences (Fig. 9b,c). For Iba1 expression, a significant genotype x treatment interaction was observed (p=0.0236; Fig. 9d), although no further differences were identified in subsequent multiple comparisons.

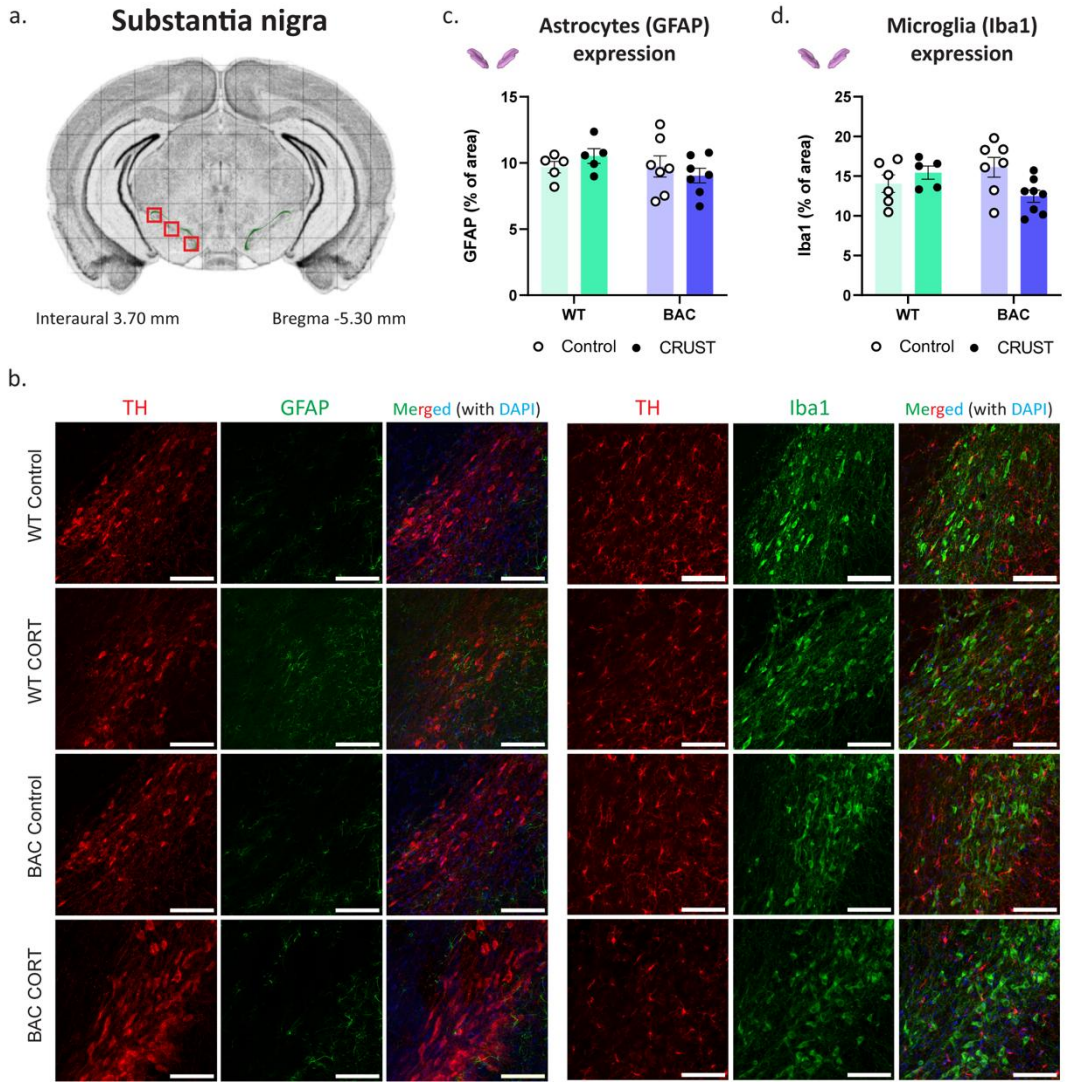

Figure 9. No evidence of gliosis in the SNg following CRUST. (a) Upon selection of three representative sites from coronal sections based on "The Rat Brain in Stereotaxic Coordinates" 5th edition atlas by Paxinos (image credit: Allen Institute for Brain Science) (b) we performed immunohistochemical staining in the SNpc with antibodies targeting GFAP or Iba1 (green), TH (red), along with merged image containing DAPI which stains cell nuclei (blue). We calculated (c) the percentage of astrocytic area (GFAP) and (d) the percentage of microglial area (Iba1). Scale bar = 100 µm. Two-way ANOVAs were applied for (c) and (d) with Bonferroni's multiple comparisons post-hoc tests. All data are expressed as mean ± SEM. N=5-7 per group.

In the striatum, our analysis revealed that CRUST exposure led to an increase in the astrocytic area (GFAP) in both BAC and WT rats compared to their unstressed counterparts (Fig. 10c). For microglial (Iba1) expression, we observed a significant effect of stress as well as a genotype x treatment interaction (p = 0.0134; Fig. 10d), indicating that BAC rats either show resistance to further stress-induced activation or have already reached a plateau of immune activation, which is then surpassed by WT animals following CRUST exposure (Fig. 10d).

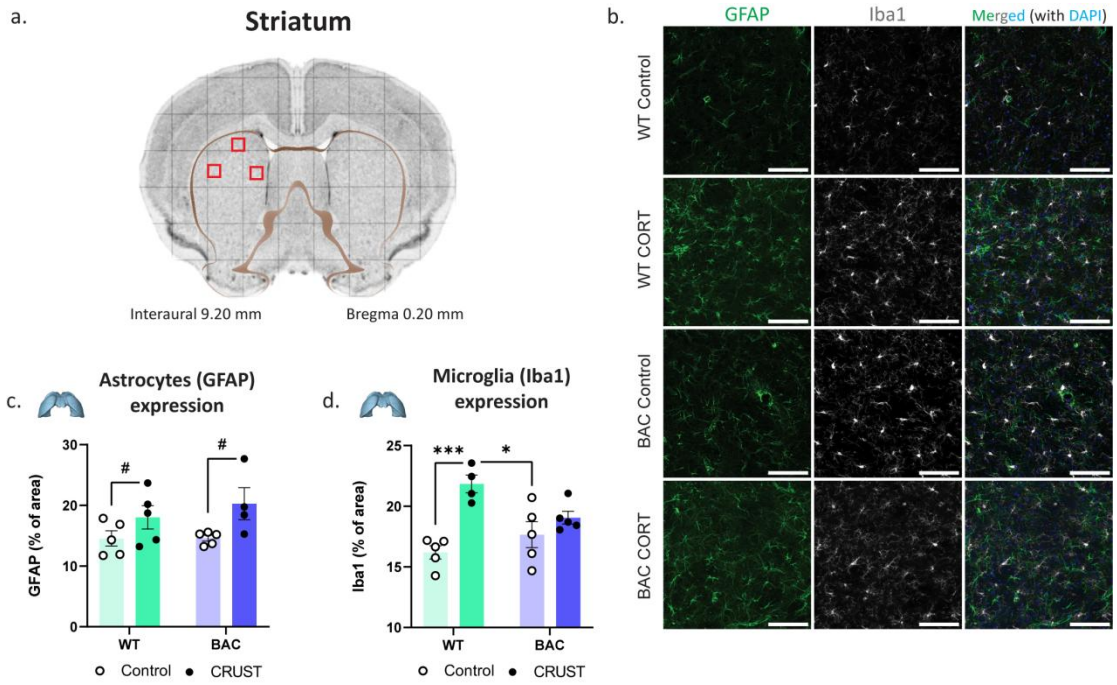

Figure 10. CRUST induces neuroinflammation in the striatum. (a) Upon selection of three representative sites from coronal sections based on "The Rat Brain in Stereotaxic Coordinates" 5th edition atlas by Paxinos (image credit: Allen Institute for Brain Science), (b) we performed immunofluorescent staining in the striatum with antibodies against GFAP (green), Iba1 (far red) and merged image containing DAPI (blue). We calculated (c) the percentage of astrocytic area (GFAP) and (d) the percentage of microglial area (Iba1). Scale bar: 100 µm. Two-way ANOVAs were applied for (c) and (d) with Bonferroni's multiple comparisons post-hoc tests. All data are expressed as mean ± SEM. Significance levels: */# p<0.05; ***p<0.001. N=4-5 per group.

12. CRUST induces excitatory and inhibitory neurotransmission alterations across multiple brain regions, while BAC rats exhibit baseline differences in areas implicated in PD pathology

Excitatory (glutamate, glutamine) and inhibitory (GABA) neurotransmission were evaluated in several brain regions affected by chronic stress and implicated in PD. In the olfactory bulb, baseline glutamate levels were elevated in BAC animals (Fig. 11a), while no changes were observed in glutamine (Fig. 11b) or GABA (Fig. 11c) levels. In the prefrontal cortex, CRUST exposure resulted in an overall reduction of excitatory and inhibitory neurotransmitters, as evidenced by decreased levels of glutamate (Fig. 11d), glutamine (Fig. 11e), and GABA (Fig. 11f). In the striatum, apart from a CRUST-induced reduction in glutamine, more pronounced in BAC animals (Fig. 11h; non-significant genotype x treatment interaction, $p=0.0911$), an overall neurotransmission imbalance was evident. There was a trend toward increased glutamate in BAC animals ($p=0.09$; Fig. 11g), while baseline elevated GABA levels in BAC rats were normalized to WT levels following CRUST (Fig. 11i). In the hippocampus, chronic stress significantly decreased glutamate (Fig. 11j) and glutamine (Fig. 11k) levels, while BAC animals exhibited consistently lower baseline GABA levels, regardless of CRUST exposure (Fig. 11l). In the ventral midbrain, CRUST significantly reduced glutamate levels (Fig. 11m), while glutamine (Fig. 11n) and GABA (Fig. 11o) levels remained unaffected.

A comprehensive examination of the glutamine-glutamate-GABA cycle - a critical metabolic pathway for maintaining excitatory and inhibitory balance - revealed that chronic stress predominantly reduced these neurotransmitters and their metabolites in most of the brain regions analyzed. BAC animals, however, displayed altered baseline levels, particularly in the striatum and olfactory bulb.

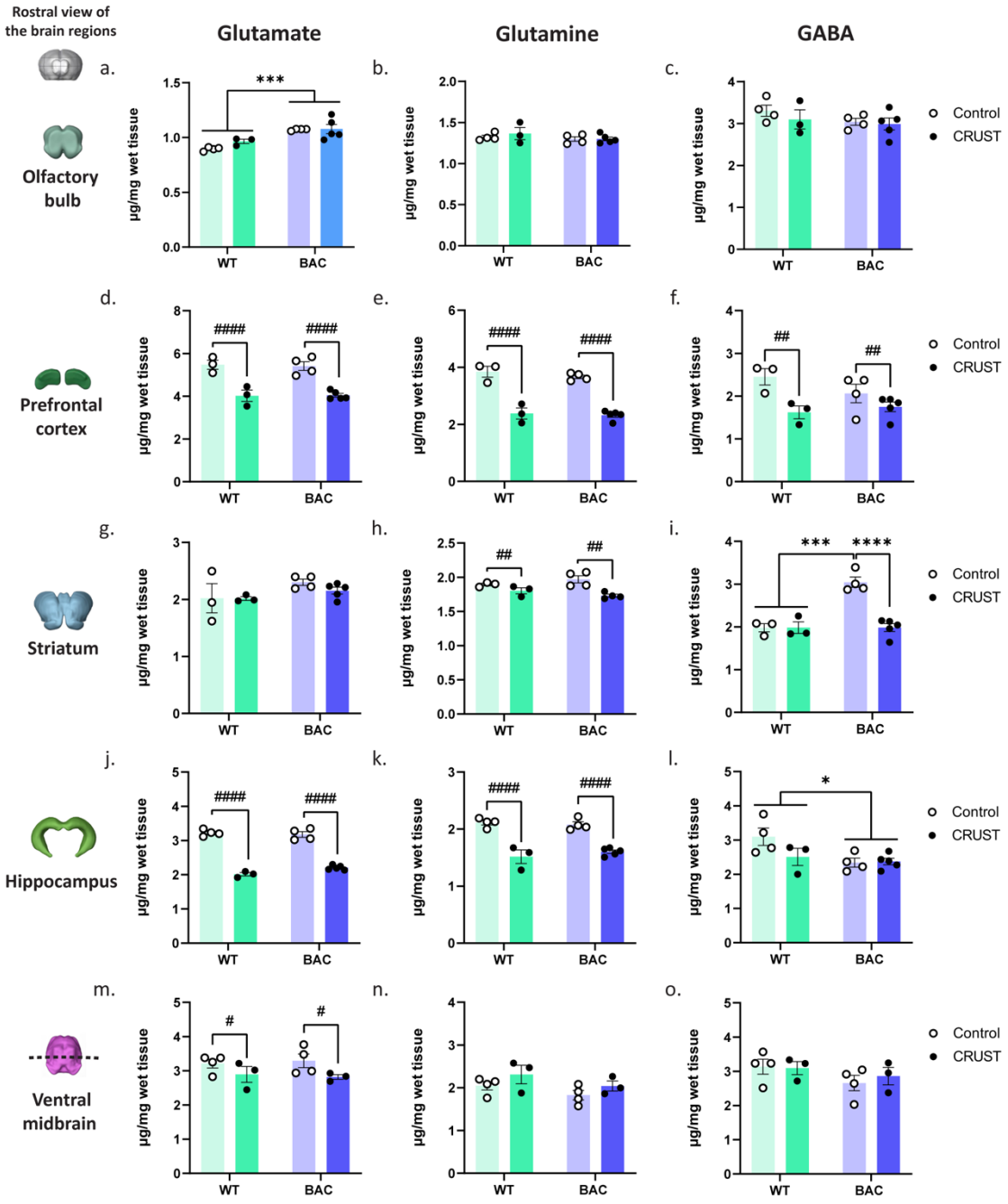

Figure 11. CRUST reduces excitatory neurotransmission while BAC animals exhibit baseline alterations in neurotransmitter levels across PD-relevant brain regions. Neurochemical measurements of glutamate, glutamine, and GABA (µg/mg wet tissue) were performed in the following regions: (a-c) olfactory bulbs; (d-f) prefrontal cortex; (g-i) striatum; (j-l) hippocampus; and (m-o) ventral midbrain. Two-way ANOVAs were applied for (a-o) with Bonferroni's multiple comparisons post-hoc tests. All data are expressed as mean ± SEM. Asterisk (*) is used to denote genotype main effects while hashtag (#) denotes treatment main effects. Significance levels: */# p<0.05; **/## p<0.01; ***/### p<0.001. N=3-5 per group.

13. CRUST increases asyn truncation in the hippocampus of asyn BAC rats

Western immunoblot analysis of the soluble protein fraction from the hippocampus (Fig. 12a) revealed no significant changes in total asyn, irrespective of CRUST treatment (Fig. 12b). However, truncated forms of total asyn were observed in both groups after chronic stress, with BAC animals exhibiting significantly higher levels of the 1st truncated band, which were further elevated following CRUST (Fig. 12c). The levels of pS129 asyn in the BAC animals remained unchanged in the soluble fraction after CRUST (Fig. 12d), despite significantly higher baseline amounts in Tg animals compared to WT (Fig. 12e). Additional biochemical analyses (Fig. 12f) did not show any differences in the levels of human asyn (Fig. 12g) or endogenous rodent asyn (Fig. 12h) in the soluble fraction of the hippocampus. Collectively, these findings indicate that CRUST selectively increases asyn truncation in the soluble protein fraction of the hippocampus in BAC rats, without altering the levels of human or endogenous asyn.

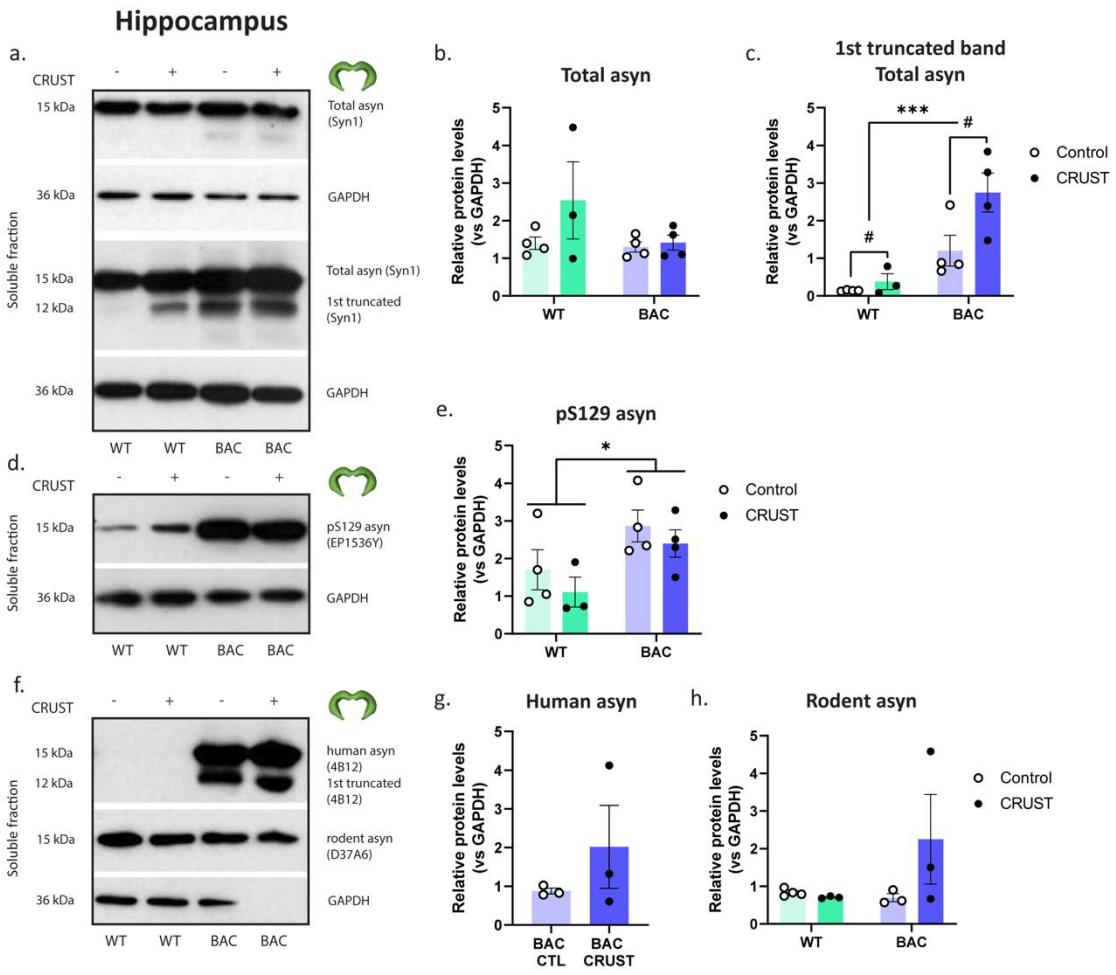

Figure 12. Soluble asyn levels in the hippocampus. In the soluble protein fraction (a) immunoblot analysis was conducted to quantify (b) total asyn and (c) the 1st truncated asyn band. Additionally, (d) pS129 asyn levels we determined (e), while in (f), the levels of (g) human asyn and (h) rodent asyn were also measured. Protein levels were normalized against GAPDH using Fiji/ImageJ for relative quantification. Unpaired t-test was applied for (g) while two-way ANOVAs were applied for (b), (c), (e) and (h) with Bonferroni's multiple comparisons post-hoc tests. All data are expressed as mean ± SEM. Asterisk (*) is used to denote genotype main effects while hashtag (#) denotes treatment main effects. Significance levels: */# p<0.05; *** p<0.001. N=3-4 per group.

14. *SNCA* overexpression alters the hippocampal transcriptome while chronic stress further triggers PD-related DEGs and neuronal pathways activation in the Tg rats

A summary of the number of differentially expressed genes (DEGs) using either FDR <0.1 (corrected p value) (Fig. 13a) or p <0.05 (nominal p value) (Fig. 13b) criteria indicates that genotype had a stronger impact on the hippocampal transcriptome than chronic stress. This is particularly evident under the stricter threshold (FDR <0.1), where DEGs were only observed in comparisons between WT and BAC groups (i.e., BAC CTL vs. CRUST CTL and BAC CRUST vs. WT CRUST) (Fig. 13a).

To identify which DEGs possess the strongest discriminatory power for distinguishing the four groups, we performed unsupervised clustering analysis using various DEG combinations, comparing the clustering results to the known sample groupings resulting in a list consisting of the top 50 genes with the lowest p value from each of the aforementioned comparisons. Since 38 genes were differentially expressed in more than one of the comparisons, this resulted a list of 162 genes (SFig. 1c) whose gene expression levels can distinguish with maximum accuracy between the 4 groups (Fig. 13c). Finally we used the DEGs that ensued using p <0.05 as an error control measure for a Gene Ontology (GO) Biological Process pathway process tool to organize and interpret our hippocampus transcriptome biological data of our experimental groups (Fig. 13d).

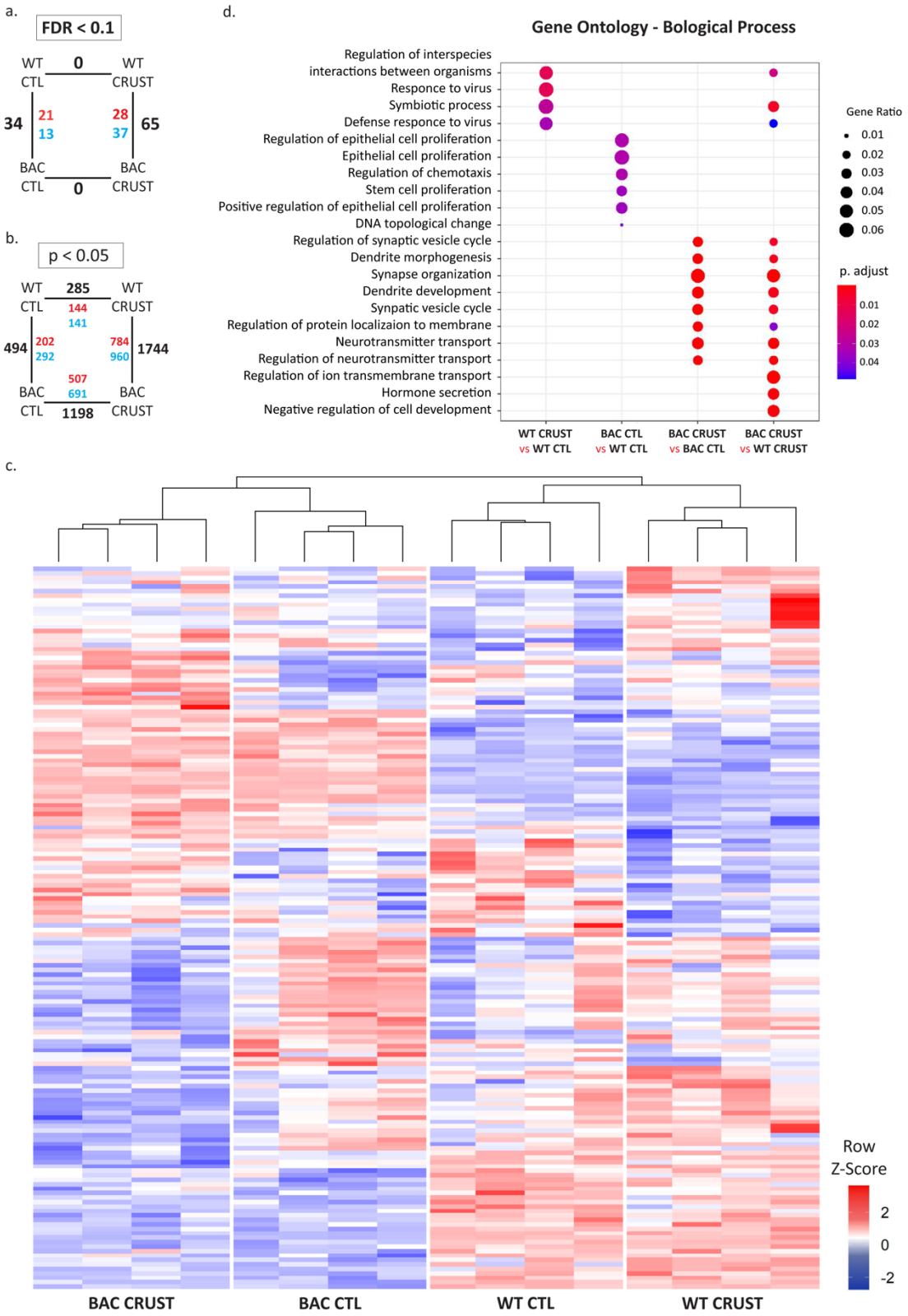

Figure 13. Hippocampal gene expression changes following *SNCA* overexpression and CRUST exposure. Summaries of the statistically significant DEGs were generated from pairwise comparisons of the four experimental groups using (a) a global error control measure of FDR<0.1 and (b) a local error control measure of p<0.05. (c) Heat map of 162 genes that distinguish the four experimental groups, generated by unsupervised clustering of the top 50 significant DEGs from each pairwise group comparison. (d) Gene Ontology (GO) Biological Process pathway analysis was performed using the DEGs identified with the local error control measure ($p < 0.05$) for all experimental groups. N=4 animals/group.

The majority of significant DEGs were identified when comparing the BAC CRUST group to BAC CTL (1198 DEGs) and WT CRUST (1744 DEGs) (Fig. 13b). These genes were implicated in disease-relevant pathways, such as synapse and neurotransmission functioning (Fig. 13d), prompting us to further investigate the transcriptional changes in the hippocampi of chronically stressed Tg animals. To gain a clearer understanding, we performed GO Biological Process analysis to identify the top 10 upregulated and downregulated pathways in the BAC CRUST vs. BAC CTL and BAC CRUST vs. WT CRUST comparisons (Fig. 14a). In both comparisons, pathways related to dendrite morphogenesis and development, neurotransmitter transport and secretion, regulation of neurotransmitter levels and postsynapse organization were downregulated in chronically stressed BAC animals (Fig. 14a). A subset of key genes previously associated with PD, such as *LRRK2* and *SCARB2*, were identified among the top DEGs in the heatmap (Fig. 13c, S2). Additionally, other genes, including *SNCG, RGS2, NQO2, P2RX4, PAK6, NEPN, MERTK, LDLR, MMP16* and *PPM1F*, were highlighted by the stricter FDR < 0.1 criterion (Fig. 13a). To validate these findings, we conducted qPCR analysis for selected genes (Fig. 14b).

For *SNCG*, qPCR confirmed a baseline downregulation in Tg rats, regardless of CRUST, while a marked upregulation was observed in chronically stressed WT rats (Fig. 14c). For *LRRK2*, we observed a genotype-specific effect, with BAC animals exhibiting lower baseline expression levels compared to WT (Fig. 14d). Although not statistically significant, qPCR for *SCARB2* ($p = 0.11$; Fig. 14e) was consistent with RNA-seq results, suggesting that CRUST increased SCARB2 expression in WT animals but decreased it in BAC rats.

RGS2 expression displayed a significant baseline decrease in BAC animals relative to WT, and a further reduction in BAC rats following chronic stress (Fig. 14f). However, contrary to RNA-seq data, qPCR did not reveal a decrease in RGS2 expression in BAC CRUST animals compared to WT CRUST (Fig. 14f). Instead, the expression levels in the WT CRUST group dropped to the same level as in the BAC CRUST group after CRUST (Fig. 14f). Additionally, *NQO2* showed significantly elevated expression in BAC CRUST animals compared to other groups, while expression levels in WT rats remained unaffected by treatment and were lower at baseline compared to BAC CTL animals (Fig. 14g).

We identified 11 genes that were differentially expressed across all four group comparisons (Fig. 14h). Of these, three genes—*RGS5, INHBA*, and *PSMD14*—are of particular interest due to their involvement in the TNF, TGF-beta, and ubiquitin-proteasome pathways, respectively. These pathways play pivotal roles in modulating inflammation, cellular growth,

and protein degradation, which are crucial processes in the pathogenesis of neurodegenerative diseases.

For *RGS5*, CRUST exposure led to increased expression in WT animals (WT CRUST vs. WT CTL: p = 0.0036; Fc = 1.37), whereas the opposite effect was observed in BAC rats overexpressing human asyn (BAC CRUST vs. BAC CTL: p = 0.0210; Fc = 0.75). At baseline, BAC rats showed higher expression levels compared to WT (BAC CTL vs. WT CTL: p = 0.047; Fc = 1.28), but after CRUST, BAC animals had a marked reduction in *RGS5* expression relative to their WT counterparts (BAC CRUST vs. WT CRUST: p = 0.0053; Fc = 0.70). A similar pattern was observed for *INHBA*, which increased significantly in WT animals after CRUST (WT CRUST vs. WT CTL: p = 0.0306; Fc = 1.56), but decreased in BAC rats (BAC CRUST vs. BAC CTL: p = 0.0027; Fc = 0.52). At baseline, *INHBA* expression was significantly higher in BAC rats compared to WT (BAC CTL vs. WT CTL: p = 0.0052; Fc = 1.83), but after CRUST, BAC animals showed a marked reduction in *INHBA* expression relative to WT animals (BAC CRUST vs. WT CRUST: p = 0.0165; Fc = 0.61). For *PSMD14*, CRUST exposure caused a decrease in expression in WT animals (WT CRUST vs. WT CTL: p = 0.0491; Fc = 0.91), while it increased in BAC rats (BAC CRUST vs. BAC CTL: p = 0.0068; Fc = 1.14). At baseline, *PSMD14* expression was higher in WT animals compared to BACs (BAC CTL vs. WT CTL: p = 0.0072; Fc = 0.88), but after CRUST, BAC animals showed a further reduction in *PSMD14* expression compared to WT animals (BAC CRUST vs. WT CRUST: p = 0.0467; Fc = 1.10).

To confirm our earlier semi-quantitative findings indicating that neither total (Fig. 12a,b) nor human asyn levels were elevated in the soluble protein fraction of the hippocampus, we re-analyzed the RNA sequences using the human genome reference (version hg38) and re-ran the analysis pipeline. As expected, human *SNCA* was significantly overexpressed in BAC transgenic animals compared to WT (N=8 animals/group), with a log fold change of 9.88 (FDR = $4.18e^{-10}$). However, human *SNCA* expression did not differ between CRUST and CTL groups in the transgenic animals (data not shown).

Overall, our findings from hippocampal RNA sequencing, DEG validation, and pathway enrichment analysis suggest that *SNCA* overexpression, in combination with CRUST exposure, induces transcriptomic alterations strongly linked to PD pathology.

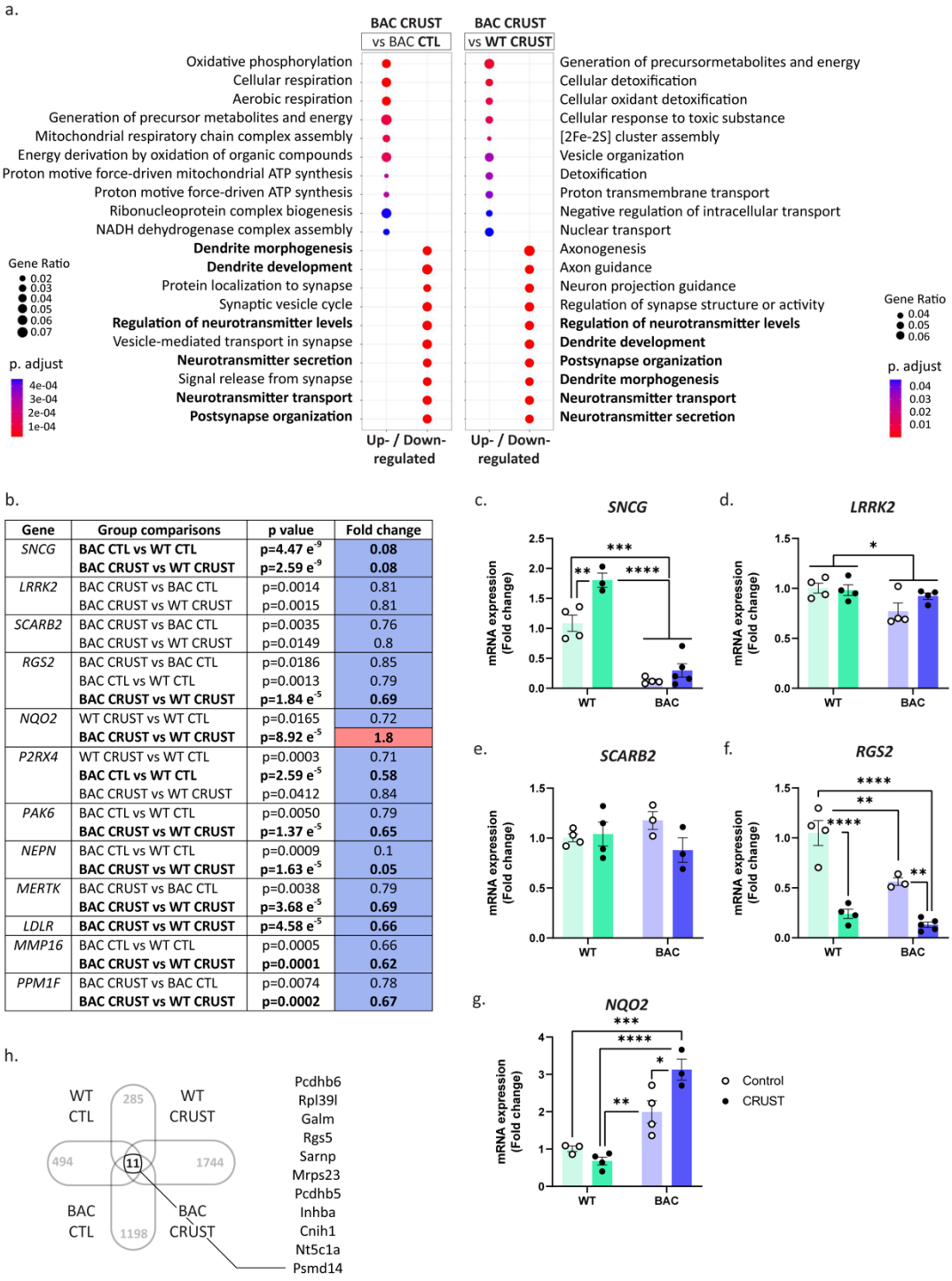

Gene	Group comparisons	p value	Fold change
SNCG	**BAC CTL vs WT CTL**	**p=4.47 e^{-9}**	**0.08**
	BAC CRUST vs WT CRUST	**p=2.59 e^{-9}**	**0.08**
LRRK2	BAC CRUST vs BAC CTL	p=0.0014	0.81
	BAC CRUST vs WT CRUST	p=0.0015	0.81
SCARB2	BAC CRUST vs BAC CTL	p=0.0035	0.76
	BAC CRUST vs WT CRUST	p=0.0149	0.8
RGS2	BAC CRUST vs BAC CTL	p=0.0186	0.85
	BAC CTL vs WT CTL	p=0.0013	0.79
	BAC CRUST vs WT CRUST	**p=1.84 e^{-5}**	**0.69**
NQO2	WT CRUST vs WT CTL	p=0.0165	0.72
	BAC CRUST vs WT CRUST	**p=8.92 e^{-5}**	**1.8**
P2RX4	WT CRUST vs WT CTL	p=0.0003	0.71
	BAC CTL vs WT CTL	**p=2.59 e^{-5}**	**0.58**
	BAC CRUST vs WT CRUST	p=0.0412	0.84
PAK6	BAC CTL vs WT CTL	p=0.0050	0.79
	BAC CRUST vs WT CRUST	**p=1.37 e^{-5}**	**0.65**
NEPN	BAC CTL vs WT CTL	p=0.0009	0.1
	BAC CRUST vs WT CRUST	**p=1.63 e^{-5}**	**0.05**
MERTK	BAC CRUST vs BAC CTL	p=0.0038	0.79
	BAC CRUST vs WT CRUST	**p=3.68 e^{-5}**	**0.69**
LDLR	**BAC CRUST vs WT CRUST**	**p=4.58 e^{-5}**	**0.66**
MMP16	BAC CTL vs WT CTL	p=0.0005	0.66
	BAC CRUST vs WT CRUST	**p=0.0001**	**0.62**
PPM1F	BAC CRUST vs BAC CTL	p=0.0074	0.78
	BAC CRUST vs WT CRUST	**p=0.0002**	**0.67**

Figure 14. Validation of altered expression levels in PD-related genes and disease-relevant neuronal pathways
(a) Gene Ontology (GO) Biological Process pathway analysis for BAC CRUST vs. BAC CTL (left) and WT CRUST (right) groups. Pathways that are significantly dysregulated in both comparisons are highlighted in bold. (b) Table of significant DEGs associated with PD. Group comparisons, p-values, and fold changes are indicated, with bolded values denoting DEGs that remained significant after applying the stricter FDR < 0.1 error control threshold. (c-g) RNA-sequencing validation of selected genes using RT-qPCR. Plots show normalized 2−ΔΔCt values for (c) SNCG, (d) *LRRK2*, (e) *SCARB2*, (f) *RGS2*, and (g) *NQO2*. (h) List of significant DEGs common across all group comparisons. Mean values ± SEMs are shown. Asterisk (*) is used to denote genotype main effects. Significance levels: *p<0.05, **p<0.01, ****p<0.0001. N=4 per group for (a), (b) and (h) and N=3-5 for (c-g).

15. Microbiota metabolites are reduced in the gut of asyn overexpressing BAC rats while the different stress paradigms interact with the BAC genotype to alter microbiota populations in the same fashion

SCFA levels in fecal matter were analyzed using Liquid Chromatography–Mass Spectrometry (LC–MS) as an indicator of inflammation-associated microbiota activity. Results revealed that, independent of the CRUST protocol, BAC rats consistently exhibited lower levels of acetic (Fig. 15a), propionic (Fig. 15b), and butyric acid (Fig. 15c). To assess the primary effects of human asyn overexpression (genotype) and the CRUST protocol (treatment) on gut microbiota populations, 16s rRNA sequencing was conducted on fecal samples from WT and BAC transgenic animals.

For evaluating the genotype effect, sequencing was performed on fecal pellets collected under sterile conditions by combining samples from both CTL and CRUST groups prior to stress exposure to enhance the robustness of the analysis (Fig. 15d). Conversely, to investigate the treatment effect of CRUST, we compared fecal samples collected before and after stress in the WT CRUST and BAC CRUST groups (Fig. 15e). This approach accounts for the observed differences in sample size between the two analyses.

In terms of differences in gut microbiome populations between WT and transgenic animals, the 15 genera with the highest raw microbiota abundance in each tested group, along with the results from statistical tests, were visualized using treemaps and volcano plots, respectively (Fig. 15d). Of the 122 microbiota genera analyzed, the top 15 genera—ranked by abundance—showed partial overlap between WT and BAC animals, as indicated by the color codes assigned to each genus in the treemaps (Fig. 15d). Within the CRUST cohort, twenty genera were significantly altered (FDR < 0.05) between WT and BAC animals, as illustrated in the corresponding volcano plot (Fig. 15d). Specifically, the genera *Escherichia, Helicobacter, Sporobacter, Lelliottia, Salmonela, Bacteroides, Alistipes, Papillibacter, Candidatus saccharimonas, Parabacteroides, Turicibacter* and *Butyrivibrio* were more abundant in WT animals. In contrast, BAC rats exhibited higher levels of *Allobaculum, Sellimonas, Faecalitalea, Candidatus stoquefichus, Fusicatenibacter, Intestinibacter, Anaeromassilibacillus, Caproiciproducens, Granulicatella* and *Muricinaculum* (Fig. 15d).

Chronic stress significantly altered the abundance of certain genera, with most of these changes not overlapping with those induced by human asyn BAC overexpression (Fig. 15e). In WT animals, *Anaeroplasma* and *Blautia* populations increased, whereas *Alistipes,*

Agathobacter and *Escherichia* populations decreased after CRUST (Fig. 15e). In BAC rats, *Muribaculum* populations decreased and *Staphylococcus* populations were no longer detectable following CRUST (Fig. 15e).

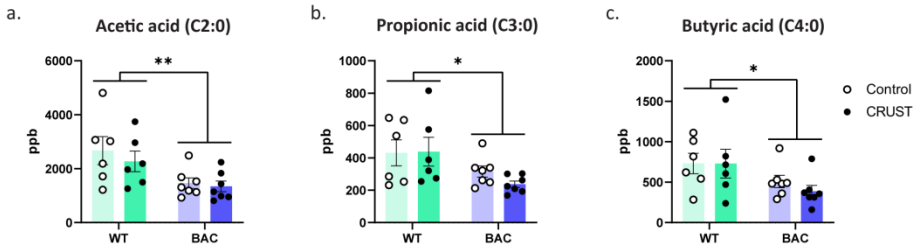

d. Main effect: **Genotype**

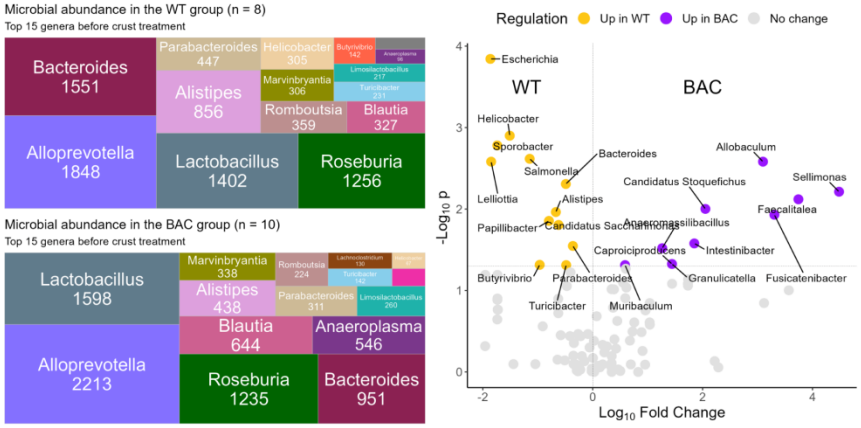

e. Main effect: **Treatment**

WT before vs after CRUST (n=6)			BAC before vs after CRUST (n=8)		
Genus	p value	Fold change	Genus	p value	Fold change
Anaeroplasma	0,0453	4,90	***Muribaculum***	0,0134	0,39
Blautia	0,0453	3,72	***Staphylococcus***	0,0339	Only detectable before CRUST
Alistipes	0,0306	0,47			
Agathobacter	0,0202	0,20			
Escherichia	0,0048	0,14			

f. Interaction effect: **Genotype x CRUST treatment**

Figure 15. Asyn overexpression reduces SCFAs and interacts with CRUST further altering gut microbiome. SCFA levels were quantified using LC-MS for (a) acetic acid, (b) propionic acid, and (c) butyric acid. 16s rRNA sequencing of fecal pellets collected under sterile conditions was conducted to examine the microbiota profile and subsequent alterations: (d) due to asyn overexpression in BAC transgenic rats, (e) following CRUST and (f) as a result of genotype x treatment interactions. Two-way ANOVAs were applied for (a-c) with Bonferroni's multiple comparisons post-hoc tests. All data are expressed as mean ± SE. M. Asterisk (*) is used to denote genotype main effects. Significance levels: * $p<0.05$; ** $p<0.01$. For the main effects (d) and (e), significance was defined at $p<0.05$, using a Mann-Whitney test adjusted with Benjamini-Hochberg. The interaction effect was estimated with a two-way ANOVA test, using the formula ~genotype*treatment and significance for the genera presented in the boxplots was defined at $p<0.1$. Data were transformed to the logarithmic scale, and normality of the ANOVA residuals was tested with Shapiro's test. Microbiome genera with non-normal residuals were excluded from the analysis. N=6-7 per group for (a-c), N=6-10 per group for (d-f).

Finally, an interaction effect between the BAC genotype and CRUST was identified for the genera *Tyzzerella, Turicibacter, Subdoligranulum, Peptococcus, Faecalibacterium* and *Dubosiella* (Fig. 15f).

In the CORT cohort, SCFA analysis showed that only acetic acid was significantly reduced at baseline in BAC rats, irrespective of CORT administration (Fig. 16a), while no differences were observed for propionic (Fig. 16b) or butyric acid levels (Fig. 16c). Similar to the CRUST cohort, the main effects of genotype and CORT treatment were assessed using 16s rRNA sequencing data from fecal samples collected under sterile conditions. For the genotype effect, the 15 most abundant genera in WT and BAC animals prior to CORT administration are visualized using color-coded treemaps (Fig. 16d). In the CORT cohort, fourteen genera were significantly altered (FDR < 0.05) between WT and BAC animals as shown in the volcano plot (Fig. 16d). Specifically, the genera *Canditus arthomitus, Helicobacter, Sporobacter, Salmonela, Escherichia, Bacteroides* were more abundant in the WT rats, while BAC rats showed a higher abundance of *Faecalitalea, Fusicatenibacter, Sellimonas, Allobaculum, Robinsoniella* and *Pygmaiobacter* (Fig. 16d).

Chronic CORT administration induced significant changes in gut microbiome populations exclusively in BAC animals. Following CORT treatment*, Desulfibrio, Akkermansia, Herbinix,* and *Anaerostripes* populations were no longer detectable in BAC rats (Fig. 16e). Interestingly, although the interaction between genotype and CORT administration resulted in only a single significant change due to limited statistical power, the alteration observed in *Subdoligranulum* populations was also detected in the CRUST cohort, following a similar pattern (Fig. 16f). Additionally, while not statistically significant, *Peptococcus* populations exhibited a trend consistent with the changes seen in the CRUST cohort (Fig. 16g).

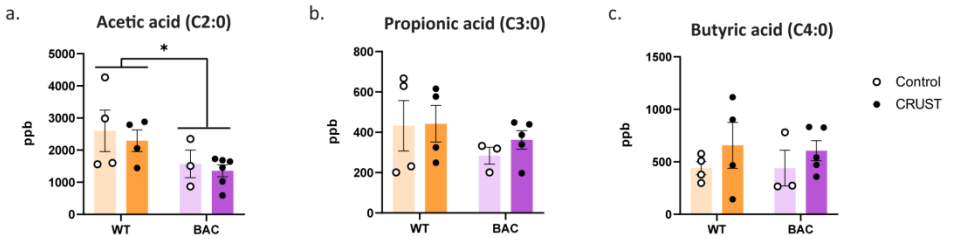

d. Main effect: **Genotype**

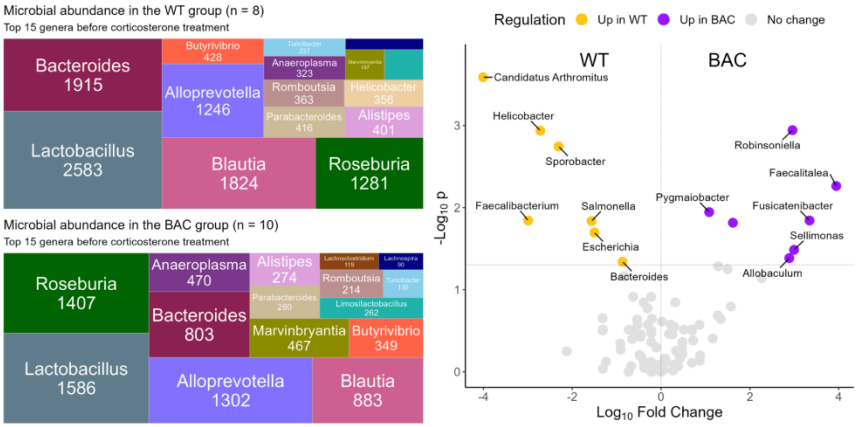

e. Main effect: **Treatment**

BAC before vs after CORT (n=4)		
Genus	p value	Fold change
Desulfovibrio	0,0028	
Akkermansia	0,0096	Only detectable before CORT
Herbinix	0,0284	
Anaerostipes	0,0341	

f. Interaction effect: **Genotype x CORT treatment**

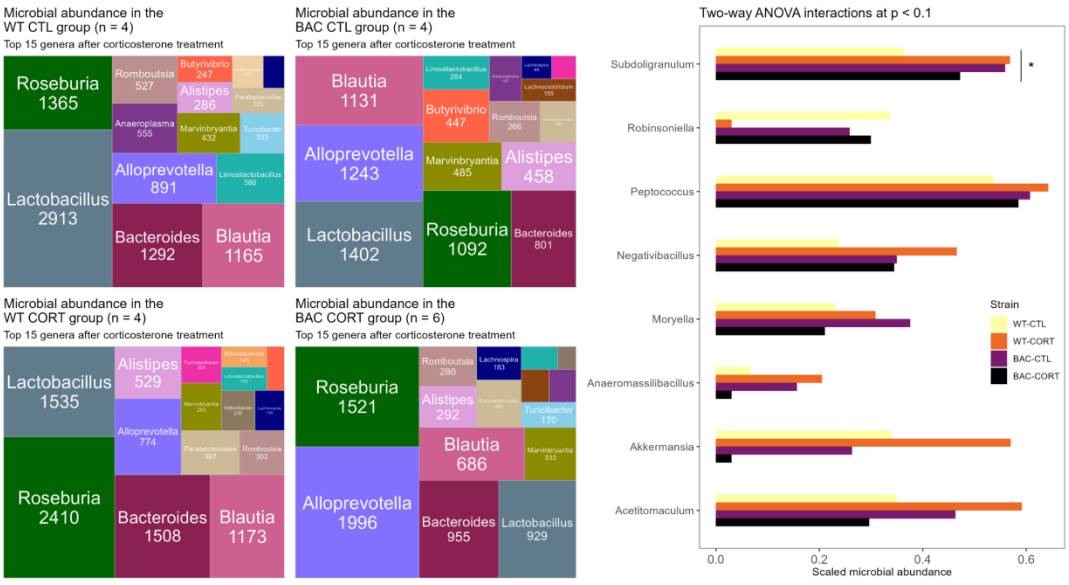

Figure 16. Asyn overexpression reduces acetic acid and interacts with chronic CORT administration further altering gut microbiome in the CORT cohort. The SCFAs (a) acetic acid, (b) propionic acid and (c) butyric acid were quantified with the use of LC-MS. Sequencing of 16s rRNA isolated from fecal pellet in sterile conditions enabled to examine the microbiota populations profile in the gut of the animals along with the subsequent alterations; (d) due to the overexpression of human asyn in the BAC transgenic rats, (e) after CRUST and (f) by the genotype x treatment interactions. Two-way ANOVAs were applied for (a-c) with Bonferroni's multiple comparisons post-hoc tests. All data are expressed as mean ± SE. M. Asterisk (*) is used to denote genotype main

effects. Significance levels: * p<0.05; ** p<0.01. For the main effects (d) and (e), significance was defined at p<0.05, using a Mann-Whitney test adjusted with Benjamini-Hochberg. The interaction effect was estimated with a two-way ANOVA test, using the formula ~genotype*treatment and significance for the genera presented in the boxplots was defined at p<0.1. Data were transformed to the logarithmic scale, and normality of the ANOVA residuals was tested with Shapiro's test. Microbiome genera with non-normal residuals were excluded from the analysis. N=6-7 per group for (a-d), N=6-10 per group for (e-g).

Overall, while neither stress paradigm appeared to significantly impact the levels of metabolites produced by gut microbes, overexpression of human *SNCA* in BAC animals consistently resulted in reduced SCFA levels in both experimental cohorts. Additionally, the same microbiota populations exhibited consistent upregulation across experiments: in BAC rats, *Faecalitalea, Fusicatenibacter, Sellimonas* and *Allobaculum* were consistently elevated, while in WT rats, *Bacteroides, Escherichia, Salmonella, Helicobacter, Candidatus sp.* and *Sporobacter* showed higher abundance. Furthermore, the distinct stress paradigms appeared to interact significantly with the BAC genotype, revealing *Subdoligranulum* and *Peptococcus* populations to be consistently altered in a similar manner across both experiments.

Discussion

There is a relative lack of depth in preclinical research assessing HPA axis pathology in PD (Bougea et al., 2022; X. Du & Pang, 2015). In this study, we provide the first evidence for asyn-linked HPA axis hypoactivation in a PD model, indicative of GC/stress hypersensitivity (Nicolaides et al., 2015; Nicolaides & Charmandari, 2021). In parallel, GC hypersensitivity leads to enhanced expression of pS129 asyn in the hypothalamus and in dopaminergic neurons of the SNg upon chronic CORT administration, suggesting direct effects of circulating GCs on asyn pathology. Chronic HPA axis activation with CRUST produced overall similar effects on behavior, recapitulating non-motor and motor symptoms, neuroinflammation, neurodegeneration and gut dysbiosis. The observed changes in CRF production and adrenal suppression as well as altered GC receptor expression (Nakos Bimpos et al., 2024b) and hippocampal transcriptomic signatures, may serve as compensatory mechanisms in response to these alterations that ultimately promote neurodegeneration. Significant disruptions in transcriptomic pathways of BAC rats related to neuronal development, synaptic function and neurotransmitter signaling, suggest impaired brain connectivity and synaptic transmission. Chronic stress further exacerbates these effects, triggering compensatory upregulation in mitochondrial and detoxification pathways, associated with heightened cellular stress that drives synaptic dysfunction and neurodegenerative processes. Alterations in the gut microbiome and their metabolites can significantly influence the gut-brain axis, and our observation of reduced fecal SCFAs in BAC animals aligns with similar reductions reported in the feces of PD patients, possibly contributing to insufficient suppression of neuroinflammation. Upregulation of the same microbiota populations is consistent across experiments in BAC rats for *Faecalitalea, Fusicatenibacter, Sellimonas* and *Allobaculum* and in WT rats for *Bacteroides, Escherichia, Salmonella, Helicobacter, Candidatus sp.* and *Sporobacter*. The different stress paradigms additionally appear to significantly interact with the BAC genotype revealing *Subdoligranulum* and *Peptococcus* populations to be significantly altered in the same fashion. These results explain, at least in part, the ability of chronic stress to trigger phenoconversion from a prodromal to a more overt motor phenotype, associated with neuroinflammation, aggravated nigrostriatal neurodegeneration, and gut dysbiosis. Taken together, our results link asyn with brain stress system hypoactivation/dysregulation that confers enhanced sensitivity to stress system; Thus, elevated circulating GCs can impact already offset brain stress homeostatic mechanisms, potentially triggering, or at least contributing to, PD-related neurodegeneration and emergence of clinical symptoms.

Although the effects of the enteric system and the nature of microbiome metabolism and population changes observed are complex and multifaceted, we can now exploit these findings to identify, isolate and test specific bacterial species for their detrimental or beneficial effects on restoration of physiologic enteric function and eubiosis and circuitously, neurodegeneration.

1. Overexpression of human wildtype asyn leads to baseline HPA axis dysregulation

The most direct measurement of HPA axis function in humans is blood cortisol levels. The directionality of these changes in PD is inconclusive with reports of decreased (Bellomo et al., 1991; Stypuła et al., 1996), increased (Rabey et al., 1990; Hartmann et al., 1997; Charlett et al., 1998) or unaltered (Volpi et al., 1994, 1997) cortisol levels. These differences can be explained by the lack of large-scale, multi-sampled, circadian studies up until today and variable inclusion criteria, including age, drug treatment and disease stage (X. Du & Pang, 2015). Strikingly, the COVID-19 pandemic, considered as an environmental stressor, did not accelerate PD progression, but exacerbated depressive symptoms in stressor-reactive (vs. stressor-resilient) PD patients (van der Heide et al., 2024).

The hypothalamus is a highly-conserved brain region involved in the regulation of core homeostatic processes, neuroendocrine integration and autonomic output required for an appropriate stress response. Asyn is present in the hypothalamus of PD patients (Fronczek et al., 2007; Thannickal et al., 2007) and Lewy bodies have been detected in all hypothalamic nuclei (Braak et al., 2011). In line with our findings (Fig. 2a,b), enhanced hypothalamic pS129asyn is observed in Thy1-asyn mice (Cuvelier et al., 2018). pS129asyn affects asyn structure and aggregation propensity (Oliveira et al., 2021) and is used as a surrogate marker of asyn aggregation and toxicity (Karampetsou et al., 2017), despite the ongoing debate as to whether this post-translational modification is associated with neurotoxicity or neuroprotection (Ramalingam et al., 2023). Furthermore, decreased CRF-like immunoreactivity has been observed in post-mortem cortical tissue from PD brains (Whitehouse et al., 1987) and MPTP treatment in mice leads to selective reduction of CRF-positive neurons in the PVN, suggesting that hypothalamic CRF neuron integrity is regulated by dopaminergic pathways (X. Du & Pang, 2015). Indeed, we observe robust expression of pS129 asyn in dopaminergic neurons of the PVN (SFig. 1). Enhanced hypothalamic DA turnover in BAC rats (Fig. 1j) - previously reported in the striatum (Polissidis et al., 2021) - is indicative of compensatory mechanisms also reported in patients (Sossi et al., 2002).

Surprisingly, CORT completely reverses this increase, suggesting that it constitutes a tipping point, leading to phenoconversion.

A critical regulator of HPA axis function is the hippocampus (Roozendaal et al., 2001; Jankord & Herman, 2008), a brain region with abundant asyn expression (Adamczyk et al., 2005; Polissidis et al., 2021). Depressed PD patients' hippocampal volumes are inversely correlated with their clinical depression scores (van Mierlo et al., 2015). Moreover, HPA axis function is affected in PD and together, these changes may help explain in part the high comorbidity with depression and anxiety (22 and 25-40%, respectively) (Pfeiffer, 2016). Finally, besides CRF's well-known role in mediating HPA axis function, hippocampal stress signaling and neurogenesis also require intact CRF signaling (Y. Chen et al., 2004; Koutmani et al., 2019). CRF neurons are predominantly regulated by GABAergic signaling, with nearly one-third of their inputs being GABAergic in origin (Miklós & Kovács, 2002). The PVN itself has a high density of GABAergic inputs stemming from the hippocampus (especially the ventral subregion), reflecting the critical role of this inhibition in modulating CRF activity. Moreover, many cortical and limbic areas that influence the HPA axis do so via GABAergic relay neurons located in the peri-PVN region (Maguire, 2019).

Our present findings of 1) enhanced pS129 asyn (particularly in DA-expressing neurons) in the hypothalamus (Fig. 2a,b), 2) an apparent shift to more insoluble pS129 in the hippocampus (Fig. 2e, S5j), 3) decreased CRF in both regions (Fig. 1b, (Nakos Bimpos et al., 2024b)), 4) lower baseline plasma CORT (Fig. 1c), 5) adrenal gland atrophy (Fig. 1d) and 6) decreased GABA levels in the hippocampus (Fig. 11i), indicate multi-level HPA axis dysfunction, including partial adrenal insufficiency associated with asyn-dependent PD pathology. We propose that asyn-dependent baseline HPA axis dysregulation leads to enhanced stress system sensitivity/responsivity, consistent with the observed anxiety-like phenotype (Fig. 1e,h, 5b, 6i) in asyn BAC rats. Notably, transcriptomic analysis in healthy control subjects revealed a four-fold increase in asyn expression in GC-sensitive subjects vs. GC-resistant subjects (Nicolaides et al., 2019). Presumably, baseline HPA axis dysregulation and stress hyper responsivity sets the stage for enhanced stress sensitivity, i.e. via altered stress signalling (discussed below), and subsequent neurodegeneration/phenoconversion upon exposure to chronic stress since as reported on multiple occasions, asyn overexpression and hyperdopaminergia are not enough to induce neurodegeneration (Polissidis et al., 2021; Moreno et al., 2024).

2. Chronic stress leads to phenoconversion from prodromal to overt motor PD

Chronic stress is a detrimental environmental factor that leads to sustained hyper- or hypo- activation of the HPA axis, GC hyper- or hypo- secretion, decreased DA levels and increased DA turnover in the hippocampus (Chrousos, 2009; Siopi et al., 2020). In rodent models, chronic stress is associated with increased anxiety and depressive-like behaviors (Watanabe et al., 1992; Conrad et al., 1996; Charney & Manji, 2004; Gong et al., 2021) and in humans, chronic stress is a major risk factor for accelerating the onset of and exacerbating symptomatology of depression and anxiety, although there is no clear link between the existence of these comorbidities with PD and accelerated or worse clinical outcome [reviewed in (Bougea et al., 2022; X. Du & Pang, 2015)]. Chronic emotional stress per se may cause dopaminergic neurodegeneration in susceptible individuals (Djamshidian & Lees, 2014) and rodents (Wu et al., 2016), and is known to accelerate dopaminergic neurodegeneration, subsequently exacerbating motor symptoms in toxin models of PD (Hemmerle et al., 2014; L. K. Smith et al., 2008). Furthermore, chronic CORT administration reduces proteostatic stress adaptation to intrastriatal asyn preformed fibril injections, lowering the threshold for asyn pathology and nigral neurodegeneration (Burtscher et al., 2019) and chronic mild stress is associated with microglial activation and cytokine release, midbrain asyn inclusion pathology, exacerbated nigrostriatal neurodegeneration, and motor worsening in A53T male mice (Q. Wu et al., 2016). Importantly, the present findings confirm the neurodegenerative potential of chronic stress to accelerate asyn pathology and nigrostriatal neurodegeneration and extend them by demonstrating its potential to act as a trigger of phenoconversion.

Patients with preclinical PD may demonstrate symptoms characteristic of severe DA deficiency following stress (Snyder et al., 1985) indicating temporary stress-induced acceleration of the disease (Gibberd & Simmonds, 1980; Goetz et al., 1990). We previously reported mild nigrostriatal neurodegeneration along with increased striatal DA, motor hyperactivity and other non-motor symptoms in asyn BAC rats; a phenotype resembling prodromal PD (Polissidis et al., 2021). Both chronic stress paradigms led to a decrease in dopaminergic cell numbers in the SNpc (Fig. 3b, 7c). Although initial analysis in the striatum showed no significant differences in TH+ fiber density in either the CRUST (Fig. 7d) or the CORT (data not shown) cohorts, subsequent subregional analysis revealed a specific reduction in dopaminergic fibers within the anatomically-connected DL striatum (Fig. 3e) in the CORT cohort. These results corroborate with neuroanatomical findings that dopaminergic neurons located in the SNpc with axonal projections to the DL striatum are

preferentially degenerated in PD (Björklund & Dunnett, 2007). Additionally, the increased density of TH+ fibers observed in the BAC rats (Fig. 3e), is in line with the striatal hyperdopaminergia we previously reported (Polissidis et al., 2021). Chronic stress appears to act as a facilitator or aggravator of PD pathogenesis as demonstrated by its "phenoconverting" ability to reverse baseline motor hyperactivity (Fig. 5a, 6e) (Polissidis et al., 2021) along with striatal DA levels and dopaminergic fiber density in asyn BAC rats (i.e., compensatory enhanced dopaminergic signalling in the striatum; Fig. 7e, 3e).

In our attempt to understand the nature of striatal hyperdopaminergia coupled with decreased DA turnover*, in vivo* microdialysis experiments reveal that baseline increased DA levels observed in the BAC rats is due to enhanced DA release (Fig. 7h). Interestingly, CRUST has an inverse effect, increasing extracellular DA levels in WT animals while lowering DA levels in the BAC rats, diminishing their robust difference with WT controls (Fig. 7h). Previous microdialysis studies report no changes in DA levels in the NAc following chronic stress (Di Chiara & Tanda, 1997; Di Chiara et al., 1999), while others find increased DA levels in the NAc but not in the dorsal striatum (Mangiavacchi et al., 2001; Stamford et al., 1991). Overall, it is hypothesized that the paradoxical hyperdopaminergia and altered DA neurotransmission, frequently observed following nigrostriatal pathway lesions (Hefti et al., 1985; Altar et al., 1987; Pifl & Hornykiewicz, 2006; Koprich et al., 2011) and in animal models overexpressing asyn (Graham & Sidhu, 2010; Kurz et al., 2010; Hunn et al., 2019; Polissidis et al., 2021), which lead to hyperlocomotion and possibly to improved motor phenotype, represent a compensatory mechanism that does not reflect the underlying progressive degeneration (Hunn et al., 2019).

The increase of extracellular DA levels in the WT animals is accompanied by a decline in DA turnover (Fig. 7i). Animal models with nigrostriatal lesions typically show increased DA turnover, possibly reflecting a compensatory rise in DA metabolism in remaining synapses (Altar et al., 1987; Hefti et al., 1985; Pifl & Hornykiewicz, 2006). However, in human asyn overexpressing BAC rats, DA turnover at 9 months was lower regardless of stress treatment both in tissue (Fig. 7f) and microdialysis (Fig. 7i) measurements. The same results, accompanied by an increase of DA turnover at 12 months, coinciding with SNg neuronal loss at that timepoint, were previously reported by our group (Polissidis et al., 2021). Notably, despite neuronal loss in the SNg and alterations in DA metabolism, increased striatal DA levels persist for up to 18 months in the BAC rats (Polissidis et al., 2021). These results confirm and extend the chronic stress-induced

phenoconversion we observe with respect to reversal of hyperlocomotion and *ex vivo* striatal DA levels.

In the first publication describing the creation of the asyn BAC rats, asyn was found to be C-terminally truncated using an antibody specific for the C-terminus of human asyn and reverse-phase chromatography (Nuber et al., 2013). Furthermore, Nuber and colleagues report increased C-terminal truncated asyn in the striatum of aged asyn BAC rats, mirroring biochemical findings seen in the striatum of PD patients with advancing Braak stages (Nuber et al., 2013). While other studies support that truncated asyn is naturally observed both in healthy and diseased brains and is not related to pathology or aging but rather correlates with the total amount of asyn, accumulated truncated asyn is located in the core of LBs (Dufty et al., 2007; Muntané et al., 2012). Combined with finding supporting that insoluble truncated asyn mediates the pathogenic conversion of soluble asyn into pathogenic fibrils (Mishizen-Eberz et al., 2005), it has been hypothesized that truncated forms of asyn might act as a 'seed' of protein aggregation (Nuber et al., 2013). In the CRUST cohort, we observed truncated forms of asyn (Fig. 8d, 12a), especially in the striatum (Fig. 8f) and the hippocampus (Fig. 12c) of asyn BAC rats following chronic stress. In terms of increased neuronal vulnerability, *in vitro* selective expression of truncated human asyn in dopaminergic neurons of the nigrostriatal pathway does not result in dopaminergic cell loss, however, it significantly lowers the levels of striatal DA and its metabolites (Daher et al., 2009). *In vivo,* in asyn-null Tg mice, truncated human asyn reduces striatal DA (Tofaris et al., 2006) and increases vulnerability of transplanted dopaminergic neurons to stress, indicating a role in dopaminergic cell loss in sporadic PD (Michell et al., 2007). Indeed, asyn BAC animals with truncated asyn (Fig. 8a), display baseline decreased DA turnover (Fig. 7f), while chronic stress further enhances asyn truncation (Fig. 8e), which coincides with a reduction in DA levels in the striatum (Fig. 7e). Truncated asyn is proposed to be the byproduct of impaired autophagy and oxidative stress (Sorrentino & Giasson, 2020).

In parallel, subtle fine motor deficits manifest upon chronic stress exposure, including worsening of postural instability (Fig. 4c) and decrease right hindlimb stride length (Fig. 4d). Thy1-aSYN mice seem to be the only Tg PD mice that naturally phenoconvert with age - their natural history evolves from a state of increased extracellular striatal DA at 6 months of age to decreased locomotion at 14 months of age, when striatal DA is significantly depleted (Lam et al., 2011; Chesselet et al., 2012). Here, we report an accelerated model of phenoconversion to a neurodegenerative state in 9 mo asyn BAC rats using chronic stress,

demonstrating the importance of gene-environment interactions in the study of PD pathogenesis.

We also observe similar dopaminergic neurotransmission imbalances in less well-characterized dopaminergic systems including the hypothalamus where we see a reversal of enhanced DA turnover in asyn BAC rats following chronic CORT treatment (Fig. 1j), further supporting phenoconversion and apparent baseline dysregulation of HPA axis at the neurotransmission level as well. 18 Fluoro-dopa PET has demonstrated reduced monoamine storage capacity in PD (Moore et al., 2008), thus, enhanced DA turnover may be a consequence of reduced storage capacity in asyn BAC rats and chronic stress may alter the metabolic activity of dopaminergic neurons, decreasing their turnover.

Neuroinflammation has a cause-effect relationship with PD. Nigrostriatal astrocytic activation is in accordance with dopaminergic neuron death (Lee et al., 2010; Walsh et al., 2011; Morales et al., 2016), while cytokines influence neurotransmitter systems, altering brain neurocircuits resulting in substantial changes in motor function, motivation, and emotional states like anxiety, arousal, and heightened vigilance (Miller et al., 2013). Reactive microglia are detected in the hippocampus of PD brains (McGeer et al., 1988; Imamura et al., 2003) and loss of GR signalling in the SNg of MPTP-treated mice and PD patients is caused by nuclear re-localization of GR in activated microglia, demonstrating their pivotal role in regulating dopaminergic neurodegeneration (Ros-Bernal et al., 2011). Microglial activation was not as prominent although it followed the same pattern as astrocytic activation (Fig. 5, 9, 10). The robust decrease in nigral dopaminergic cell number (Fig. 3b, 6c), decreased locomotor activity (Fig. 4a, 6e) and fine motor deficits (Fig. 4c,d) – a profile matched by WT only after chronic stress – indicates that, temporally, inflammation precedes dopaminergic cell loss. Additionally, BAC animals display a baseline thymus hypertrophy regardless of chronic stress (SFig. 3d & Fig. 3d). Thymus hyperplasia may occur as a compensatory mechanism to restore immune balance following initial stress-induced atrophy caused by elevated GCs. This rebound hypertrophy reflects the thymus's adaptive attempt to cope with long-term immune dysregulation (Collins et al., 2024). In light of recent finding suggesting an antigenic response to asyn in PD patients and a possible role of the adaptive immune system in PD pathogenesis (Sulzer et al., 2017), this finding suggesting a role of thymus dysfunction in PD warrants future studies.

Astrocytes play a key role in neurotransmitter metabolism and glial dysfunction has been linked to abnormal GABA and glutamate levels in mood disorder patients' brains,

particularly in the hippocampus (Middeldorp & Hol, 2011). The glutamine-glutamate-GABA cycle is a critical metabolic pathway that maintains the balance of excitatory and inhibitory neurotransmission in the brain with astrocytes playing a key role in converting glutamate back to glutamine, while GABA is converted into glutamate and subsequently into glutamine (Hertz & Zielke, 2004). This continuous cycling process is essential for replenishing neurotransmitter pools and maintaining neurotransmitter homeostasis (i.e. excitation/inhibition) in the CNS (Schousboe et al., 2014). Following chronic stress, mRNA expression of transporters and enzymes involved in the aforementioned metabolic cycle are significantly altered in the striatum and the hippocampus accompanied by a downregulation of L-glutamine levels (Xu et al., 2020), in agreement with our results (Fig. 11h,k). In the striatum, decreased GABA levels (Fig. 11i) might be related to changes in the intrinsic regulation of GABAergic medium spiny neurons due to DA depletion (Fig. 7e) and axonal loss in the dorsolateral region of the putamen (Fig. 3e) innervated by the SNg. Additionally, asyn overexpression alters synaptic communication in the corticostriatal pathway, possibly contributing to preclinical manifestations preceding neuronal loss (Wu et al., 2010) while elevated DA levels in the striatum of aged A53T mice may not be transmitted appropriately due to functional changes hampering striatal synaptic plasticity (Kurz et al., 2010). It has been confirmed that genes related to synaptic plasticity are altered in the striatum of asyn BAC mice, regardless of CUMS exposure (Wassouf et al., 2019), therefore, we focused on the hippocampal transcriptome.

3. Distinct stress response and altered hippocampal transcriptome in asyn overexpressing BAC rats

Asyn inclusions are abundant in the hippocampus and associate with cognitive dysfunction, especially in later stages of the disease (Adamowicz et al., 2017; Braak et al., 2003; G. Halliday et al., 2008; Villar-Conde et al., 2021) and asyn expression is greatest in the hippocampus in rodent overexpression models (Nuber et al., 2013; Polissidis et al., 2021). Interestingly, mild to moderate levels of chronic stress can heighten arousal state and improve spatial learning and memory by enhancing synaptic plasticity and long-term potentiation (LTP) in the hippocampus (Conrad et al., 1999; Joëls et al., 2006). That is the case with both WT and BAC animals displaying improved MWM performance following chronic stress (Fig. 6j) while the BAC animals additionally exhibit a general trend toward enhanced spatial memory (Fig. 6k). This pattern aligns with previous findings in 9 mo A53T

mice, where better MWM performance - though not related to hippocampal neurogenesis - was observed (Liu et al., 2018).

A recent review aiming to summarize transcriptomic studies on PD, examined shared biological pathways across various studies (Borrageiro et al., 2018). The most commonly reported alterations were reported in pathways involved in DA metabolism, mitochondrial function, oxidative stress, protein degradation, neuroinflammation, vesicular transport and synaptic transmission. The majority of studies were performed in the SNg and the striatum, while no studies were performed in the hippocampus (Borrageiro et al., 2018). In the hippocampus, by focusing on the chronically stressed BAC animals, the most significantly downregulated pathways - whether compared to the BAC CTL or the WT CRUST group - are largely overlapping and involve neuronal development and synaptic function (Fig. 14a). This pattern indicates extensive disruptions in brain connectivity and communication. Reduction in axonogenesis, axon guidance, neuron projection guidance, dendrite morphogenesis and development indicates compromised neuronal growth and connectivity characteristic of disrupted neural circuits. In parallel, downregulation of synaptic structure regulation, synaptic vesicle cycle and vesicle-mediated transport points to significant synaptic dysfunction, implying the neurons' inability to transmit signals effectively. Deficits in pathways involved in neurotransmitter secretion, transport and signal release suggest impaired neurotransmission, a hallmark of PD. Taken together, the pattern of pathway downregulation emerging from our results indicates that chronic stress interacts with asyn overexpression to trigger a disruption of essential processes needed for maintaining healthy neuronal networks, consequently leading to neurodegenerative progression.

On the upregulated pathways, the common denominator is mitochondrial function and energy metabolism, suggesting that cells are faced with an increased demand for energy production (Fig, 14a). This pattern typically indicates that mitochondrial activity is heightened to meet elevated energy needs, often due to stress or damage. Upregulation of mitochondria and energy production-related pathways suggests that cells are faced with disrupted energy metabolism and cellular homeostasis. Additionally, upregulation of detoxification pathways points to increased activity in neutralizing ROS and other harmful metabolites, indicating oxidative stress. Taken together, our results suggest that enhanced asyn burden leads to cellular metabolic and oxidative stress in an attempt to maintain homeostasis.

Focusing on the specific disease-relevant DEGs, among the members of the synuclein family, *SNCG* (Fig. 14b) shows baseline decreased expression in BAC rats (Fig. 14c). Pathological accumulation of *SNCG* has been found in the brains of patients with PD and DLB, (Galvin et al., 1999) while in patients with amyotrophic lateral sclerosis (ALS), gamma-synuclein-positive structures are found in the spinal cord and a rare SNP enhances the otherwise resilient amyloid formation of gamma-synuclein (Peters et al., 2015; Aubrey et al., 2024). In mice, *SNCG* overexpression results in pathology reminiscent of ALS (Peters et al., 2015, 2015). While in BAC rats *SNCG* downregulation may be an offset response to *SNCA* overexpression, *SNCG* upregulation following stress might be pathological (Fig. 14c) since alterations in *SNCG* expression and function have been associated with neurodegenerative diseases (Surgucheva et al., 2014).

Apart from changes in the synuclein family, we also examined alterations in the expression of *LRRK2* and *SCARB2*, both of which have established links to PD. Mutations in *LRRK2* lead to increased kinase activity and are implicated in neuronal degeneration and PD progression (Chang et al., 2017). Despite the conflicting results regarding *LRRK2* expression levels in the hippocampi of WT rodents (Taymans et al., 2006; Melrose et al., 2007), baseline decreased expression in BAC rats (Fig. 14 d) agrees with findings of reduced *LRRK2* mRNA in the limbic system of iPD patients (Sharma et al., 2011). *SCARB2* (*LIMP2*) plays a crucial role in GCase trafficking and stability (Reczek et al., 2007), required for cellular lipid homeostasis. In PD, *SCARB2* downregulation exacerbates lysosomal dysfunction leading to misfolded asyn accumulation (Beavan & Schapira, 2013). While the differential effect of stress – increasing expression in WTs and decreasing it in BAC animals – is not statistically significant (Fig. 14e), sequencing results are consistent with the transcription validation showing reduction of *SCARB2* expression in BAC animals following stress (Fig. 14b).

Among the most significant DEGs identified was *RGS2* which encodes a regulator of G-protein-coupled receptor (GPCR) modulating neurotransmission in pathways related to mood and anxiety. *RGS2* disruption is linked to alterations in dopaminergic pathways (Jones-Tabah, 2023) and antioxidant defenses (Salim et al., 2011). *RGS2* interacts with *LRRK2* to regulate GTPase and kinase activities and is reduced in the striatum of *LRRK2* and sporadic PD (Dusonchet et al., 2014) while a polymorphism constitutes a risk allele for schizophrenia and antipsychotic-induced Parkinsonism (Greenbaum et al., 2009; Higa et al., 2010). In the hippocampus, RNA-seq results are partially validated, showing a significant baseline

decrease in *RGS2* expression in BAC animals compared to WT, with a further reduction following chronic stress (Fig. 14f).

NQO2 encodes a cytosolic flavoprotein exerting protective action again ROS formation (W. Wang et al., 2008). A 29-bp deletion in its promoter is 3.5 times more prevalent in PD patients (Harada et al., 2001). Moreover, *NQO2* is a key modulator of autophagy, with elevated activity following 6-OHDA exposure in SH-SY5Y cells (Verbovaya et al., 2024) and increased levels in the hippocampi of rats exposed to high fluoride, while *NQO2* inhibition reduces autophagic flux and increases oxidative stress (Ran et al., 2023). Additionally, *NQO2* inhibition in 6-OHDA-treated astrocytes restores autophagic flux and lowers oxidative stress, while *NQO2* silencing diminishes 6-OHDA's toxicity (Janda et al., 2023). In early-stage PD patients, increased *NQO2* expression is observed in blood cells, whereas late-stage postmortem SNg samples show decreased mRNA levels (Janda et al., 2023). RNA-seq validation reveals baseline increased *NQO2* expression, further increased in BAC animals after CRUST (Fig. 14g), and possibly linked to an increased need for protection against oxidative stress.

Despite the lack of PCR validation, the remaining DEGs are briefly discussed since they are closely associated with PD and their expression levels is significantly altered; *P2RX4* encodes a purine receptor ligand-gated ion channel with high calcium permeability, broadly expressed in neurons and glia. Typically, *P2RX4* is found intracellularly in endosomes and lysosomes while surface expression increases under pathological conditions (Duveau et al., 2020). *P2X4R* KO mice show impaired sensorimotor gating, social interactions (Wyatt et al., 2013), and reduced L-DOPA-induced motor behaviors (Khoja et al., 2016). P2RX4 overexpression in SNg after 6-OHDA, elevates IL-6 levels, leading to neuroinflammation and neuronal loss (Ma et al., 2020). Additionally, *P2RX4* rescues motor deficits and promotes asyn degradation (R. Li et al., 2022). Intriguingly, BAC rats show decreased baseline *P2RX4* levels while stress appears to reduce expression in WT rats (Fig. 14b). *PAK6* is a kinase exerting neuroprotective roles, especially during stress responses (Kumar et al., 2017). *PAK6* was identified as a novel interactor with the GTPase/ROC domain of *LRRK2*, acting as a positive regulator of neurite outgrowth. Post-mortem studies report increased *PAK6* activation in idiopathic PD and *LRRK2* G2019S carriers, while *LRRK2* KO mice exhibit reduced *PAK6* activation (Civiero et al., 2015). Phosphorylation of 14-3-3γ by active *PAK6* disrupts binding to *LRRK2* can counteract the neurite shortening (Civiero et al., 2017). Interestingly, BAC rats are characterized by baseline reduced *PAK6* expression levels (Fig. 14 b).

Neprhrocan (*NEPN*) encodes a protein that acts as a negative regulator of the TGF-β signaling pathway. While nephrocan itself is not directly linked to PD, disruptions in TGF-β signaling have been implicated in neurodegenerative diseases, including PD, given the role of TGF-β in neuroinflammation and neuronal survival (Karampetsou et al., 2022). Surprisingly, we see an immense decrease in the expression levels of nephrocan in the hippocampus of the BAC animals (Fig. 14b). *MERTK* encodes a critical regulator of immune responses, particularly in the clearance of apoptotic cells through a process called efferocytosis. In the brain, *MERTK* helps regulate inflammation and maintain cellular homeostasis (Rothlin et al., 2015). BAC animals present decreased levels of *MERTK* after CRUST but also compared to the stressed WT animals (Fig. 14 b). *LDLR* encodes a receptor that regulates cholesterol levels. Cholesterol homeostasis has been increasingly linked to neurodegenerative diseases while lower levels of total and LDL cholesterol are associated with PD (L. Zhang et al., 2017). Additionally, *DJ-1* KO cells and mice display reduced *LDLR* mRNA and protein levels, suggesting a potential link between *LDLR* and PD pathology (Yamaguchi et al., 2012) while in our case, only after CRUST, BAC rats display reduced LDLR expression levels compared to stressed WT animals (Fig. 14 b). *MMP16* encodes a protein that plays a role in degrading components of the extracellular matrix and activating other matrix metalloproteinases (MMPs), like MMP2 (Yong, 2005). Although MMP16 has not been directly linked to PD, MMPs are known to be involved in neuroinflammation and BBB breakdown, making MMP16's role in these processes potentially relevant to PD pathology (Rosenberg, 2009; Consortium (IPDGC) & Consortium 2 (WTCCC2), 2011). MMP16 rs60298754 was associated with the presence of apathy, pain, nocturia and light sensitivity in a cohort of PD patients in southern China (Chen et al., 2021). We observe a baseline decrease of *MMP16* expression levels in the hippocampus of BAC rats (Fig. 14b). Finally, *PPM1F* is a serine/threonine phosphatase that regulates various cellular processes, including stress response. In mice, *PPM1F* is differentially expressed after immobilization stress, and in humans, mRNA levels are downregulated in individuals with comorbid PTSD and depression, suggesting a role in stress-related disorders (Wingo et al., 2018). While acute restraint stress increases *PPM1F* expression and decreases BDNF in the hippocampus (Meng et al., 2021), chronically stressed BAC rats display decreased expression levels compared either to non-stressed BAC rats or to stressed WT rats (Fig. 14 b). While the identified DEGs show potential relevance and novelty in our experimental groups, additional validation is crucial to establish the precise role of each gene in disease pathology before reaching definitive conclusions.

Two recent back-to-back studies by Wassouf and colleagues stand out; RNA sequencing of hippocampal tissue from female mice overexpressing human *SNCA* using a BAC construct, either after 8 weeks of chronic stress at 6 mo (Wassouf et al., 2019) or following 12 months of environmental enrichment (Wassouf et al., 2018) provide a valuable opportunity to corroborate the most significant DEGs identified across different studies; considering however, the independent variables of sex and species (i.e., female mice *vs.* male rats). Genome-wide DNA methylation analysis of neurons in the parietal cortex of postmortem PD patients reveal sex-specific changes in *SLC17A6, NR4A2* and other genes linked to developmental pathways, neurotransmitter release and axon guidance (Kochmanski et al., 2022). *SLC17A6* encodes the vesicular glutamate transporter 2 (VGLUT2). Loss of thalamostriatal glutamate signaling in the dorsal striatum produces a bradyphrenia-like phenotype similar to PD (Melief et al., 2018).

Bioinformatics analysis implicates *SLC17A6* in the pathogenesis of PD and DLB (Xu et al., 2023) and as a top DEG in the globus pallidus of PD patients (Lin-ya, 2024). Apart from reports of decreased *SLC17A6* expression in the hippocampus of BAC Tg mice (Wassouf et al., 2019), we see a reduction in BAC compared to WT animals only after CRUST (p=0.045; Fc 0.61). While the Tg animals are indeed characterized by altered neurotransmission (Fig. 11l), glutamate levels are not affected by asyn overexpression in the hippocampus (Fig. 11j).

NR4A2, also known as *NURR1*, encodes for a transcription factor crucial for the development, maintenance and function of dopaminergic neurons, particularly in the SNg, regulating genes involved in DA synthesis and release, such as *TH*, dopa decarboxylase (*DDC*), and *SLC6A3* (DAT) (Decressac et al., 2013). While rare mutations or altered expression of this gene are linked to familial PD, NR4A2 also reduces pro-inflammatory and neurotoxic mediator expression in microglia and astrocytes through NF-κB-p65 binding (Saijo et al., 2009). The effects of NR4A2 could also apply to the hippocampus (Wassouf et al., 2018), suggesting that enhancing *NR4A2* expression may support neuron survival by mitigation of inflammation. After CRUST, BAC animals show a significant reduction in *NR4A2* expression compared to their WT counterparts (p=0.017; Fc: 0.67).

SYT6 encodes a protein from the synaptotagmin family, which serves as a calcium sensor involved in synaptic vesicle trafficking and neurotransmitter release, playing a key role in exocytosis and synaptic transmission (Wolfes & Dean, 2020). *LRRC55* (Leucine-Rich Repeat Containing 55) encodes a regulatory subunit of large-conductance calcium-activated potassium channels that modulate neuronal activity and neurotransmitter release by

regulating membrane potential (Yan & Aldrich, 2012). RNA-seq results marked an increased baseline expression of *SYT6* in Tg animals (p=0.0057; Fc: 1.54), while *LRRC55* expression is significantly reduced after stress compared to WT animals (p=0.022; Fc: 0.74).

ALDH1A1 plays a crucial role in detoxifying harmful reactive aldehydes (Marchitti et al., 2007). The subset of DA-producing neurons in the ventral SNpc of PD patients suffering the greatest loss, is marked by selective *ALDH1A1* expression (Carmichael et al., 2021). Reduced ALDH1A1 activity or expression is linked to vulnerability of dopaminergic neurons to oxidative damage, making it a potential neuroprotective factor (Liu et al., 2014). While *ALDH1A1* iss downregulated only in 6mo BAC mice overexpressing human asyn (Wassouf et al., 2019), our findings show a significant reduction in BAC animals after CRUST compared to BAC controls (p=0.005; Fc: 0.80) and stressed WT animals (p=0.005; Fc: 0.74).

Out of the eleven common DEGs in all 4 group comparisons (Fig. 14 h), we briefly examine three, namely; *RGS5, INHBA* and *PSMD14*. Prolonged treatment with reserpine, an inhibitor of vesicular monoamine transporter (*VMAT*), used to deplete DA as a model of parkinsonism, significantly decrease mRNA levels of several regulator of G-protein signaling (RGS) proteins, including *RGS2* and *RGS5*, in the striatum (Geurts et al., 2003). Similarly, in the hippocampus, we find lower baseline *RGS5* expression in WT animals compared to BAC rats overexpressing human asyn (Fig. 14h). Recent work suggests that astrocytic RGS5 is a key regulator of TNF signaling, promoting astrocyte activation and chronic neuroinflammation (Yin et al., 2023). *INHBA*, a component of the TGF-β signaling pathway involved in inflammation and cell growth, is significantly upregulated in the striatum of a dyskinesia model following long-term L-Dopa treatment (Dyavar et al., 2020) and also increased after *LRRK2* depletion in SHSY5Y cells (Häbig et al., 2008). In the hippocampus, WT rats have lower baseline *INHBA* expression compared to BACs, but after chronic stress, BAC rats show reduced *INHBA* levels compared to WT. Finally, *PSMD14*, part of the ubiquitin-proteasome system, is found among the most dysregulated genes in aged humans (Dick et al., 2023) and differentially expressed across all experimental comparisons in our analysis (Fig. 14h).

Lastly, given that GCs are crucial for modulating the activity of stress-responsive glutamatergic synapses (Popoli et al., 2011), stress susceptible WT mice demonstrate elevated hippocampal MR transcript levels and no change in GR, compared to stress resilient mice after CUMS, resulting to a greater suppression of hippocampal mGlu2 receptors due to stress (Nasca et al., 2015). Intriguingly, both Tg BAC rats and PD patients display increased

MR expression levels (Nakos Bimpos et al., 2024b), while RNA-seq results show decreased expression of the mGlu2-encoding gene *GRM2* in the group of stressed BAC animals compared to the WT groups (BAC CRUST vs WT CTL, p=0.049; Fc: 0.75 and BAC CRUST vs WT CRUST, p=0.0037; Fc: 0.64).

4. The body-first BAC model replicates key human microbiome findings and reveals stress-responsive microbiota linked to PD

Recent studies using BAC Tg rodents expressing human asyn have shown age-dependent prodromal symptoms and dopaminergic degeneration (Nuber et al., 2013; Taguchi et al., 2020; Polissidis et al., 2021). Although asyn is widely expressed throughout the body, pathology appears in the gut before affecting the basal ganglia, making these models particularly relevant for studying body-first PD (Van Den Berge & Ulusoy, 2022). Since Braak's hypothesis proposed that the gut might serve as an entry point for the initiation and spread of PD pathology (Braak et al., 2003), this idea gained traction as more research highlighted the gut-brain axis' role in PD pathogenesis with population-based studies suggesting a potentially higher risk of PD in patients with inflammatory bowel disease (IBD) (Lee et al., 2021). However, since not all IBD patients develop PD, some researchers propose that gut inflammation might act as a "facilitator" in the spread of PD pathology (Derkinderen et al., 2021; Johnson et al., 2019). Supporting this, an analysis of serum samples from IBD patients reveals elevated tryptophan degradation, suggesting that tryptophan deficiency could influence PD risk or severity (Nikolaus et al., 2017).

Computational models analyzing the interactions between the microbiome and the metabolism of PD patients showcase decreased folate and increased homocysteine production (Rosario et al., 2021). While folate along with vitamins B12 and B6 catabolize homocysteine releasing other amino acids, high homocysteine levels is an indicator of vitamin deficiency, can disrupt methylation cycles and affect tryptophan metabolism, potentially leading to neurological and metabolic imbalances (Bottiglieri, 2005; Obeid & Herrmann, 2006). Briefly, it is hypothesized that increased levels of homocysteine lead to excitotoxicity through binding to NMDA receptors and by contribution to the release of inflammatory mediators, either by astrogliosis or by endothelial cell dysfunction which in turn stimulate the activation of MMPs leading to BBB disruption (Fan et al., 2020).

Intriguingly, *Subdoligranulum* was revealed as the main producer of homocysteine and its population is increased in PD cases compared to controls (Mao et al., 2021; Rosario

et al., 2021). Along with *Faecalibacterium*, both species produce SCFAs (Duncan et al., 2002; Holmstrøm et al., 2004) and are known to be auxotrophic (i.e. unable to synthesize) for the majority of vitamins and for tryptophan (Soto-Martin et al., 2020) and are affected following overexpression of human asyn and chronic stress interaction (Fig. 15f, 16f). While the exact mechanisms underlying the beneficial effects of SCFAs are yet to be fully understood, it is known that SCFAs exert anti-inflammatory, anti-oxidant and intestinal barrier protective properties by binding to G-protein coupled receptors (Caetano & Castelucci, 2022). Overall, in our results the asyn overexpressing BAC rats are characterized by reduced baseline SCFA levels (Fig. 15a-c, 16a).

Our findings are supported by multiple studies showing a significant decrease in *Faecalibacterium* levels that correlate with both disease severity and duration (Haikal et al., 2019; W. Li et al., 2017). Similarly, individuals with high trait anxiety exhibit reduced microbial diversity and distinct alterations in microbiota composition, including elevated *Blautia* and decreased *Faecalibacterium*. Notably, those who respond better to cognitive intervention display improved tryptophan metabolism and increased *Subdoligranulum* levels (Z. Wang et al., 2022).

Being first isolated in the 30s, the gram-positive anaerobic *Peptococcus* (Kluyver & Niel, 1936) is part of the normal flora of the human body, including the intestine tract (Murdoch, 1998). Interestingly, in two different occasions, *Peptococcus* has been associated with motor complications in PD patients (Qian et al., 2018; Baldini et al., 2020), while in both CRUST and CORT cohort *Peptococcus* populations are increased in the same fashion following chronic stress in the WT rats, reaching the higher baseline levels characterizing BAC animals (Fig. 15f, 16f).

Gut dysbiosis, known to be present in the early stages of irritable bowel syndrome (IBS), is thought to be triggered following an intestinal infection (Spiller & Garsed, 2009) or a stressful life event (L. Chang, 2011). Restraint stress triggering IBS in mice, results in elevated plasma CORT, ROS and increased abundance of the genera *Tyzzerella* and *Bacteroides* (R. Lin et al., 2021). Interestingly, chronic stress also elevates *Tyzzerella* levels in our study with BAC animals already exhibiting higher baseline levels (Fig. 15f), while *Bacteroides* is consistently reported to be the most abundant genera characterizing WT animals in both cohorts (Fig. 15d, 16d) in agreement with data from human studies reporting an almost unanimous decreased population of *Bacteroides* in PD patients (Haikal et al., 2019). Moreover, the serotonin and NA reuptake inhibitor drug venlafaxine exerts its antidepressant action by also

restoring glutamate levels with *Tyzzerella* and *Blautia* emerging, among other genera, as potential targets since their populations correlates with glutamate levels (W. Shen et al., 2023).

Treatment of animal models with PD patient medication (L-DOPA and carbidopa) alleviates depressive behaviors and ameliorates constipation symptoms through the increase of *Turicibacter* population both in the ileum and the feces and the boost of butyrate production (Radisavljevic, 2023). *Turicibacter* (Fig. 15f) is an anaerobic, gram-positive, non-spore-forming bacteria named after Zurich (Turicum in latin), the city of Switzerland, where is was first isolated (Bosshard et al., 2002). Conversely, 6-OHDA injections result in decreased abundance of *Turicibacter,* while this decrease is reversed following high dosages of phenolic antioxidants (Nurrahma et al., 2022). Finally, findings from the field of cancer research identified *Turicibacter* as a key player in overall immune activation (Hamada et al., 2023). Intriguingly, our results show lower baseline levels in the BAC rats and *Turicibacter* population decrease following after CRUST in the WT animals (Fig. 15f).

Our results show a lower baseline population of the *Helicobacter* genus in BAC animals (Fig. 15d, 16d), while much of the research attention has focused on *Helicobacter pylori*. The literature is brimming with studies, meta-analyses and reviews exploring the potential links between this pathogen and increased PD risk and pathogenesis, the worsening of motor symptoms and the alteration of L-DOPA pharmacokinetics with many studies highlight the potential benefits of *H. pylori* eradication (Huang et al., 2018; McGee et al., 2018; Shen et al., 2017; Tan et al., 2020; Zhong et al., 2022).

Escherichia, a gram-negative, non-spore forming, facultatively anaerobic bacteria inhabiting the GI tract (Escherich, 1988), has lower baseline abundance in the BAC animals of both cohorts (Fig. 15d, 16d) and is further decreased after CRUST (Fig. 15e). 16S rRNA gene sequencing from a big group of PD patients reported that *Sporobacter, Escherichia* and other genera has higher linear discriminant analysis scores in the PD patient group (Jo et al., 2022) while in a different human study *Sporobacter* and *Blautia* – among other genera – shows negative correlation with UPDRS scores (W. Li et al., 2017). Interestingly, vitamin K2, primarily produced by *Escherichia* bacteria (Kang et al., 2022), has been shown to function as an electron carrier in mitochondria successfully rescuing a *Drosophila* model of PD with mitochondrial dysfunction (Vos et al., 2012). Additionally, *in vitro* studies indicate that vitamin K can delay asyn fibrillization by interacting with the N-terminus of the protein (da Silva et al., 2013) and directly suppress ROS production and p38 activation in a rotenone-

activated microglial cell line (Y. Yu et al., 2016). In PD patients, decreased vitamin K2 levels in the serum are associated with disease progression, dysregulated inflammatory responses and coagulation cascades (Y.-X. Yu et al., 2020). In 2020 a clinical trial was launched to investigate the potentially beneficial effects of vitamin K2 in genetic cases of PD associated with mitochondria dysfunction, e.g. with *PINK1* gene mutations (Prasuhn et al., 2020). Finally, in agreement with our results, a group using a similar animal model also reports significantly increased *Faecalitalea* population in the cecum of their BAC transgenic mice (Singh et al., 2019) while studies in human PD patients have shown that the severity of constipation (evaluated by the Wexner score) positively correlates with *Faecalitalea* and *Sellimonas* (Fig. 15d, 16d) among other microbiota genera populations (W. Chen et al., 2021).

As a concluding remark, it is crucial to highlight that sequencing results and correlation studies often produce vast amounts of data, which, when analyzed through varying pipelines, may not always reflect disease relevance. Therefore, utilizing large sample sizes processed through consistent analytical methods is essential. Most importantly, understanding the precise mechanisms by which microbial communities contribute to disease pathogenesis should be a primary focus to translate findings into meaningful insights. A seminal meta-analysis published in 2020 combined data from over 1,000 PD patients across diverse populations in Japan, the United States, Finland, Russia and Germany. This large-scale study reported a decrease in SCFA-producing *Roseburia* and *Faecalibacterium*, alongside an increase in *Akkermansia*, a bacterium known to disrupt gut integrity and increase oxidative stress in the ENS (Nishiwaki et al., 2020).

In relation to the second part of my remark, a study assessing the impact of *Akkermansia* on obesity and diabetes through microbiota transplantation reported no significant effects on these markers in colonized mice, despite prior correlative evidence suggesting such a role (Depommier et al., 2020), underscoring the importance of *in vivo* studies to validate microbial contributions to disease beyond correlations (Van Hul et al., 2020).

Overall, our body-first PD animal model recapitulates the most important finding from PD human studies, including the recently reviewed levels of *Faecalibacterium* which show a lower baseline in BAC animals regardless of treatment and a decrease in WT animals after CRUST (Fig. 15f), as well as the decreased SCFAs (Fig. 15a-c, 16a). Apart from the diversity stemming from the asyn overexpression, interaction with chronic stress revealed a

plethora of altered microbiota genera which constitute promising targets for therapeutic interventions.

5. Conclusions

This study demonstrates HPA axis dysregulation prior to overt neurodegeneration in human-asyn BAC overexpression Tg rats. Chronic stress, by enhancing asyn pathological changes, appears to supersede compensatory mechanisms leading to more overt neurodegeneration and subsequent emergence of full-blown Parkinsonian phenotypes. Thus, under conditions of enhanced asyn burden/pathology, chronic stress as an environmental factor can potentially "trigger" PD phenoconversion on multiple levels in the brain and gut. Chronic stress protocols could therefore be used as critical research tools to study the underlying mechanisms of phenoconversion in PD.

References

Abeliovich, A., Schmitz, Y., Fariñas, I., Choi-Lundberg, D., Ho, W. H., Castillo, P. E., Shinsky, N., Verdugo, J. M., Armanini, M., Ryan, A., Hynes, M., Phillips, H., Sulzer, D., & Rosenthal, A. (2000). Mice lacking alpha-synuclein display functional deficits in the nigrostriatal dopamine system. *Neuron*, *25*(1), 239–252. https://doi.org/10.1016/s0896-6273(00)80886-7

Adamczyk, A., Solecka, J., & Strosznajder, J. B. (2005). Expression of alpha-synuclein in different brain parts of adult and aged rats. *Journal of Physiology and Pharmacology: An Official Journal of the Polish Physiological Society*, *56*(1), 29–37.

Adamowicz, D. H., Roy, S., Salmon, D. P., Galasko, D. R., Hansen, L. A., Masliah, E., & Gage, F. H. (2017). Hippocampal α-Synuclein in Dementia with Lewy Bodies Contributes to Memory Impairment and Is Consistent with Spread of Pathology. *Journal of Neuroscience*, *37*(7), 1675–1684. https://doi.org/10.1523/JNEUROSCI.3047-16.2016

Adams-Carr, K. L., Bestwick, J. P., Shribman, S., Lees, A., Schrag, A., & Noyce, A. J. (2016). Constipation preceding Parkinson's disease: A systematic review and meta-analysis. *Journal of Neurology, Neurosurgery, and Psychiatry*, *87*(7), 710–716. https://doi.org/10.1136/jnnp-2015-311680

Afgan, E., Baker, D., Batut, B., van den Beek, M., Bouvier, D., Cech, M., Chilton, J., Clements, D., Coraor, N., Grüning, B. A., Guerler, A., Hillman-Jackson, J., Hiltemann, S., Jalili, V., Rasche, H., Soranzo, N., Goecks, J., Taylor, J., Nekrutenko, A., & Blankenberg, D. (2018). The Galaxy platform for accessible, reproducible and collaborative biomedical analyses: 2018 update. *Nucleic Acids Research*, *46*(W1), W537–W544. https://doi.org/10.1093/nar/gky379

Aho, V. T. E., Houser, M. C., Pereira, P. A. B., Chang, J., Rudi, K., Paulin, L., Hertzberg, V., Auvinen, P., Tansey, M. G., & Scheperjans, F. (2021). Relationships of gut microbiota, short-chain fatty acids, inflammation, and the gut barrier in Parkinson's disease. *Molecular Neurodegeneration*, *16*(1), 6. https://doi.org/10.1186/s13024-021-00427-6

Altar, C. A., Marien, M. R., & Marshall, J. F. (1987). Time course of adaptations in dopamine biosynthesis, metabolism, and release following nigrostriatal lesions: Implications for behavioral recovery from brain injury. *Journal of Neurochemistry*, *48*(2), 390–399. https://doi.org/10.1111/j.1471-4159.1987.tb04106.x

Alvarez-Erviti, L., Seow, Y., Schapira, A. H., Gardiner, C., Sargent, I. L., Wood, M. J. A., & Cooper, J. M. (2011). Lysosomal dysfunction increases exosome-mediated alpha-synuclein release and transmission. *Neurobiology of Disease*, *42*(3), 360–367. https://doi.org/10.1016/j.nbd.2011.01.029

Alvarez-Fischer, D., Noelker, C., Grünewald, A., Vulinović, F., Guerreiro, S., Fuchs, J., Lu, L., Lombès, A., Hirsch, E. C., Oertel, W. H., Michel, P. P., & Hartmann, A. (2013). Probenecid potentiates MPTP/MPP+ toxicity by interference with cellular energy metabolism. *Journal of Neurochemistry*, *127*(6), 782–792. https://doi.org/10.1111/jnc.12343

Alwani, A., Maziarz, K., Burda, G., Jankowska-Kiełtyka, M., Roman, A., Łyszczarz, G., Er, S., Barut, J., Barczyk-Woźnicka, O., Pyza, E., Kreiner, G., Nalepa, I., & Chmielarz, P. (2023). Investigating the potential effects of α-synuclein aggregation on susceptibility to chronic stress in a mouse Parkinson's disease model. *Pharmacological Reports: PR*. https://doi.org/10.1007/s43440-023-00530-z

Amadeo, A., Pizzi, S., Comincini, A., Modena, D., Calogero, A. M., Madaschi, L., Faustini, G., Rolando, C., Bellucci, A., Pezzoli, G., Mazzetti, S., & Cappelletti, G. (2021). The Association between α-Synuclein and α-Tubulin in Brain Synapses. *International Journal of Molecular Sciences*, *22*(17), 9153. https://doi.org/10.3390/ijms22179153

Anderson, J. P., Walker, D. E., Goldstein, J. M., de Laat, R., Banducci, K., Caccavello, R. J., Barbour, R., Huang, J., Kling, K., Lee, M., Diep, L., Keim, P. S., Shen, X., Chataway, T., Schlossmacher, M. G., Seubert, P., Schenk, D., Sinha, S., Gai, W. P., & Chilcote, T. J. (2006). Phosphorylation of Ser-129 is the dominant pathological modification of alpha-synuclein in familial and sporadic Lewy body disease. *The Journal of Biological Chemistry*, *281*(40), 29739–29752. https://doi.org/10.1074/jbc.M600933200

Anwar, S., Peters, O., Millership, S., Ninkina, N., Doig, N., Connor-Robson, N., Threlfell, S., Kooner, G., Deacon, R. M., Bannerman, D. M., Bolam, J. P., Chandra, S. S., Cragg, S. J., Wade-Martins, R., & Buchman, V. L. (2011). Functional alterations to the nigrostriatal system in mice lacking all three members of the synuclein family. *The Journal of Neuroscience: The Official Journal of the Society for Neuroscience*, *31*(20), 7264–7274. https://doi.org/10.1523/JNEUROSCI.6194-10.2011

Appel-Cresswell, S., Vilarino-Guell, C., Encarnacion, M., Sherman, H., Yu, I., Shah, B., Weir, D., Thompson, C., Szu-Tu, C., Trinh, J., Aasly, J. O., Rajput, A., Rajput, A. H., Jon Stoessl, A., & Farrer, M. J. (2013). Alpha-synuclein p.H50Q, a novel pathogenic mutation for Parkinson's disease. *Movement Disorders*, *28*(6), 811–813. https://doi.org/10.1002/mds.25421

Arotcarena, M.-L., Dovero, S., Prigent, A., Bourdenx, M., Camus, S., Porras, G., Thiolat, M.-L., Tasselli, M., Aubert, P., Kruse, N., Mollenhauer, B., Trigo Damas, I., Estrada, C., Garcia-Carrillo, N., Vaikath, N. N., El-Agnaf, O. M. A., Herrero, M. T., Vila, M., Obeso, J. A., … Bezard, E. (2020). Bidirectional gut-to-brain and brain-to-gut propagation of

synucleinopathy in non-human primates. *Brain: A Journal of Neurology*, *143*(5), 1462–1475. https://doi.org/10.1093/brain/awaa096

Arsac, J.-N., Sedru, M., Dartiguelongue, M., Vulin, J., Davoust, N., Baron, T., & Mollereau, B. (2021). Chronic Exposure to Paraquat Induces Alpha-Synuclein Pathogenic Modifications in Drosophila. *International Journal of Molecular Sciences*, *22*(21), 11613. https://doi.org/10.3390/ijms222111613

Askanas, V., Engel, W. K., Alvarez, R. B., McFerrin, J., & Broccolini, A. (2000). Novel immunolocalization of alpha-synuclein in human muscle of inclusion-body myositis, regenerating and necrotic muscle fibers, and at neuromuscular junctions. *Journal of Neuropathology and Experimental Neurology*, *59*(7), 592–598. https://doi.org/10.1093/jnen/59.7.592

Aubrey, L. D., Ninkina, N., Ulamec, S. M., Abramycheva, N. Y., Vasili, E., Devine, O. M., Wilkinson, M., Mackinnon, E., Limorenko, G., Walko, M., Muwanga, S., Amadio, L., Peters, O. M., Illarioshkin, S. N., Outeiro, T. F., Ranson, N. A., Brockwell, D. J., Buchman, V. L., & Radford, S. E. (2024). Substitution of Met-38 to Ile in γ-synuclein found in two patients with amyotrophic lateral sclerosis induces aggregation into amyloid. *Proceedings of the National Academy of Sciences*, *121*(2), e2309700120. https://doi.org/10.1073/pnas.2309700120

Bae, E.-J., Yang, N. Y., Lee, C., Lee, H.-J., Kim, S., Sardi, S. P., & Lee, S.-J. (2015). Loss of glucocerebrosidase 1 activity causes lysosomal dysfunction and α-synuclein aggregation. *Experimental & Molecular Medicine*, *47*(3), e153–e153. https://doi.org/10.1038/emm.2014.128

Bains, J. S., Cusulin, J. I. W., & Inoue, W. (2015). Stress-related synaptic plasticity in the hypothalamus. *Nature Reviews Neuroscience*, *16*(7), 377–388. https://doi.org/10.1038/nrn3881

Baldini, F., Hertel, J., Sandt, E., Thinnes, C. C., Neuberger-Castillo, L., Pavelka, L., Betsou, F., Krüger, R., Thiele, I., Aguayo, G., Allen, D., Ammerlann, W., Aurich, M., Balling, R., Banda, P., Beaumont, K., Becker, R., Berg, D., Binck, S., … on behalf of the NCER-PD Consortium. (2020). Parkinson's disease-associated alterations of the gut microbiome predict disease-relevant changes in metabolic functions. *BMC Biology*, *18*(1), 62. https://doi.org/10.1186/s12915-020-00775-7

Barbour, R., Kling, K., Anderson, J. P., Banducci, K., Cole, T., Diep, L., Fox, M., Goldstein, J. M., Soriano, F., Seubert, P., & Chilcote, T. J. (2008). Red Blood Cells Are the Major Source of Alpha-Synuclein in Blood. *Neurodegenerative Diseases*, *5*(2), 55–59. https://doi.org/10.1159/000112832

Barnum, C. J., Eskow, K. L., Dupre, K., Blandino, P., Deak, T., & Bishop, C. (2008). EXOGENOUS CORTICOSTERONE REDUCES L-DOPA-INDUCED DYSKINESIA IN THE HEMI-PARKINSONIAN RAT: ROLE FOR INTERLEUKIN-1β. *Neuroscience*, *156*(1), 30–41. https://doi.org/10.1016/j.neuroscience.2008.07.016

Beach, T. G., Adler, C. H., Lue, L., Sue, L. I., Bachalakuri, J., Henry-Watson, J., Sasse, J., Boyer, S., Shirohi, S., Brooks, R., Eschbacher, J., White, C. L., Akiyama, H., Caviness, J., Shill, H. A., Connor, D. J., Sabbagh, M. N., & Walker, D. G. (2009). Unified Staging System for Lewy Body Disorders: Correlation with Nigrostriatal Degeneration, Cognitive Impairment and Motor Dysfunction. *Acta Neuropathologica*, *117*(6), 613–634. https://doi.org/10.1007/s00401-009-0538-8

Beavan, M. S., & Schapira, A. H. V. (2013). Glucocerebrosidase mutations and the pathogenesis of Parkinson disease. *Annals of Medicine*, *45*(8), 511–521. https://doi.org/10.3109/07853890.2013.849003

Bell, R., & Vendruscolo, M. (2021). Modulation of the Interactions Between α-Synuclein and Lipid Membranes by Post-translational Modifications. *Frontiers in Neurology*, *12*. https://doi.org/10.3389/fneur.2021.661117

Bellani, S., Mescola, A., Ronzitti, G., Tsushima, H., Tilve, S., Canale, C., Valtorta, F., & Chieregatti, E. (2014). GRP78 clustering at the cell surface of neurons transduces the action of exogenous alpha-synuclein. *Cell Death & Differentiation*, *21*(12), 1971–1983. https://doi.org/10.1038/cdd.2014.111

Bellomo, G., Santambrogio, L., Fiacconi, M., Scarponi, A. M., & Ciuffetti, G. (1991). Plasma profiles of adrenocorticotropic hormone, cortisol, growth hormone and prolactin in patients with untreated parkinson's disease. *Journal of Neurology*, *238*(1), 19–22. https://doi.org/10.1007/BF00319704

Bellucci, A., Navarria, L., Falarti, E., Zaltieri, M., Bono, F., Collo, G., Grazia, M., Missale, C., & Spano, P. (2011). Redistribution of DAT/α-Synuclein Complexes Visualized by "In Situ" Proximity Ligation Assay in Transgenic Mice Modelling Early Parkinson's Disease. *PLOS ONE*, *6*(12), e27959. https://doi.org/10.1371/journal.pone.0027959

Ben Gedalya, T., Loeb, V., Israeli, E., Altschuler, Y., Selkoe, D. J., & Sharon, R. (2009). α-Synuclein and Polyunsaturated Fatty Acids Promote Clathrin-Mediated Endocytosis and Synaptic Vesicle Recycling. *Traffic*, *10*(2), 218–234. https://doi.org/10.1111/j.1600-0854.2008.00853.x

Benjamini, Y. (2010). Simultaneous and selective inference: Current successes and future challenges. *Biometrical Journal. Biometrische Zeitschrift*, *52*(6), 708–721. https://doi.org/10.1002/bimj.200900299

Bentivenga, G. M., Mammana, A., Baiardi, S., Rossi, M., Ticca, A., Magliocchetti, F., Mastrangelo, A., Poleggi, A., Ladogana, A., Capellari, S., & Parchi, P. (2024). Performance of a seed amplification assay for misfolded alpha-synuclein in

cerebrospinal fluid and brain tissue in relation to Lewy body disease stage and pathology burden. *Acta Neuropathologica*, *147*(1), 18. https://doi.org/10.1007/s00401-023-02663-0

Béraud, D., Hathaway, H. A., Trecki, J., Chasovskikh, S., Johnson, D. A., Johnson, J. A., Federoff, H. J., Shimoji, M., Mhyre, T. R., & Maguire-Zeiss, K. A. (2013). Microglial activation and antioxidant responses induced by the Parkinson's disease protein α-synuclein. *Journal of Neuroimmune Pharmacology: The Official Journal of the Society on NeuroImmune Pharmacology*, *8*(1), 94–117. https://doi.org/10.1007/s11481-012-9401-0

Berg, D., Postuma, R. B., Bloem, B., Chan, P., Dubois, B., Gasser, T., Goetz, C. G., Halliday, G. M., Hardy, J., Lang, A. E., Litvan, I., Marek, K., Obeso, J., Oertel, W., Olanow, C. W., Poewe, W., Stern, M., & Deuschl, G. (2014). Time to Redefine PD? Introductory Statement of the MDS Task Force on the Definition of Parkinson's Disease. *Movement Disorders*, *29*(4), 454–462. https://doi.org/10.1002/mds.25844

Berridge, M. J., Bootman, M. D., & Roderick, H. L. (2003). Calcium signalling: Dynamics, homeostasis and remodelling. *Nature Reviews. Molecular Cell Biology*, *4*(7), 517–529. https://doi.org/10.1038/nrm1155

Betarbet, R., Sherer, T. B., MacKenzie, G., Garcia-Osuna, M., Panov, A. V., & Greenamyre, J. T. (2000). Chronic systemic pesticide exposure reproduces features of Parkinson's disease. *Nature Neuroscience*, *3*(12), 1301–1306. https://doi.org/10.1038/81834

Björklund, A., & Dunnett, S. B. (2007). Dopamine neuron systems in the brain: An update. *Trends in Neurosciences*, *30*(5), 194–202. https://doi.org/10.1016/j.tins.2007.03.006

Blauwendraat, C., Heilbron, K., Vallerga, C. L., Bandres-Ciga, S., von Coelln, R., Pihlstrøm, L., Simón-Sánchez, J., Schulte, C., Sharma, M., Krohn, L., Siitonen, A., Iwaki, H., Leonard, H., Noyce, A. J., Tan, M., Gibbs, J. R., Hernandez, D. G., Scholz, S. W., Jankovic, J., … International Parkinson's Disease Genomics Consortium (IPDGC). (2019). Parkinson's disease age at onset genome-wide association study: Defining heritability, genetic loci, and α-synuclein mechanisms. *Movement Disorders: Official Journal of the Movement Disorder Society*, *34*(6), 866–875. https://doi.org/10.1002/mds.27659

Bloem, B. R., Okun, M. S., & Klein, C. (2021). Parkinson's disease. *The Lancet*, *397*(10291), 2284–2303. https://doi.org/10.1016/S0140-6736(21)00218-X

Bonifati, V. (2012). Autosomal recessive parkinsonism. *Parkinsonism & Related Disorders*, *18*, S4–S6. https://doi.org/10.1016/S1353-8020(11)70004-9

Borghammer, P., Horsager, J., Andersen, K., Van Den Berge, N., Raunio, A., Murayama, S., Parkkinen, L., & Myllykangas, L. (2021). Neuropathological evidence of body-first vs. Brain-first Lewy body disease. *Neurobiology of Disease*, *161*, 105557. https://doi.org/10.1016/j.nbd.2021.105557

Borrageiro, G., Haylett, W., Seedat, S., Kuivaniemi, H., & Bardien, S. (2018). A review of genome-wide transcriptomics studies in Parkinson's disease. *European Journal of Neuroscience*, *47*(1), 1–16. https://doi.org/10.1111/ejn.13760

Bosshard, P. P., Zbinden, R., & Altwegg, M. (2002). Turicibacter sanguinis gen. Nov., sp. Nov., a novel anaerobic, Gram-positive bacterium. *International Journal of Systematic and Evolutionary Microbiology*, *52*(4), 1263–1266. https://doi.org/10.1099/00207713-52-4-1263

Bottiglieri, T. (2005). Homocysteine and folate metabolism in depression. *Progress in Neuro-Psychopharmacology and Biological Psychiatry*, *29*(7), 1103–1112. https://doi.org/10.1016/j.pnpbp.2005.06.021

Bougea, A., Stefanis, L., & Chrousos, G. (2022). Stress system and related biomarkers in Parkinson's disease. *Advances in Clinical Chemistry*, *111*, 177–215. https://doi.org/10.1016/bs.acc.2022.07.004

Bouillot, S., Reboud, E., & Huber, P. (2018). Functional Consequences of Calcium Influx Promoted by Bacterial Pore-Forming Toxins. *Toxins*, *10*(10), 387. https://doi.org/10.3390/toxins10100387

Bové, J., & Perier, C. (2012). Neurotoxin-based models of Parkinson's disease. *Neuroscience*, *211*, 51–76. https://doi.org/10.1016/j.neuroscience.2011.10.057

Braak, H., de Vos, R. A. I., Bohl, J., & Del Tredici, K. (2006). Gastric alpha-synuclein immunoreactive inclusions in Meissner's and Auerbach's plexuses in cases staged for Parkinson's disease-related brain pathology. *Neuroscience Letters*, *396*(1), 67–72. https://doi.org/10.1016/j.neulet.2005.11.012

Braak, H., Ghebremedhin, E., Rüb, U., Bratzke, H., & Del Tredici, K. (2004). Stages in the development of Parkinson's disease-related pathology. *Cell and Tissue Research*, *318*(1), 121–134. https://doi.org/10.1007/s00441-004-0956-9

Braak, H., Thal, D. R., & Del Tredici, K. (2011). Nerve cells immunoreactive for p62 in select hypothalamic and brainstem nuclei of controls and Parkinson's disease cases. *Journal of Neural Transmission (Vienna, Austria: 1996)*, *118*(5), 809–819. https://doi.org/10.1007/s00702-010-0508-2

Braak, H., Tredici, K. D., Rüb, U., de Vos, R. A. I., Jansen Steur, E. N. H., & Braak, E. (2003). Staging of brain pathology related to sporadic Parkinson's disease. *Neurobiology of Aging*, *24*(2), 197–211. https://doi.org/10.1016/S0197-4580(02)00065-9

Bridi, J. C., Bereczki, E., Smith, S. K., Poças, G. M., Kottler, B., Domingos, P. M., Elliott, C. J., Aarsland, D., & Hirth, F. (2021). Presynaptic accumulation of α-synuclein causes synaptopathy and progressive neurodegeneration in Drosophila. *Brain Communications*, *3*(2), fcab049. https://doi.org/10.1093/braincomms/fcab049

Brooks, A. I., Chadwick, C. A., Gelbard, H. A., Cory-Slechta, D. A., & Federoff, H. J. (1999). Paraquat elicited neurobehavioral syndrome caused by dopaminergic neuron loss. *Brain Research*, *823*(1–2), 1–10. https://doi.org/10.1016/s0006-8993(98)01192-5

Brown, K. J., & Grunberg, N. E. (1995). Effects of housing on male and female rats: Crowding stresses male but calm females. *Physiology & Behavior*, *58*(6), 1085–1089. https://doi.org/10.1016/0031-9384(95)02043-8

Burns, M. E., Sasaki, T., Takai, Y., & Augustine, G. J. (1998). Rabphilin-3A: A Multifunctional Regulator of Synaptic Vesicle Traffic. *Journal of General Physiology*, *111*(2), 243–255. https://doi.org/10.1085/jgp.111.2.243

Burré, J., Edwards, R. H., Halliday, G., Lang, A. E., Lashuel, H. A., Melki, R., Murayama, S., Outeiro, T. F., Papa, S. M., Stefanis, L., Woerman, A. L., Surmeier, D. J., Kalia, L. V., Takahashi, R., & Committee, the M. S. I. (n.d.). Research Priorities on the Role of α-Synuclein in Parkinson's Disease Pathogenesis. *Movement Disorders*, *n/a*(n/a). https://doi.org/10.1002/mds.29897

Burré, J., Sharma, M., & Südhof, T. C. (2018). Cell Biology and Pathophysiology of α-Synuclein. *Cold Spring Harbor Perspectives in Medicine*, *8*(3), a024091. https://doi.org/10.1101/cshperspect.a024091

Burré, J., Sharma, M., Tsetsenis, T., Buchman, V., Etherton, M., & Südhof, T. C. (2010). α-Synuclein Promotes SNARE-Complex Assembly in vivo and in vitro. *Science (New York, N.Y.)*, *329*(5999), 1663–1667. https://doi.org/10.1126/science.1195227

Burtscher, J., Copin, J.-C., Rodrigues, J., Kumar, S. T., Chiki, A., Guillot de Suduiraut, I., Sandi, C., & Lashuel, H. A. (2019). Chronic corticosterone aggravates behavioral and neuronal symptomatology in a mouse model of alpha-synuclein pathology. *Neurobiology of Aging*, *83*, 11–20. https://doi.org/10.1016/j.neurobiolaging.2019.08.007

Butler, B., Saha, K., Rana, T., Becker, J. P., Sambo, D., Davari, P., Goodwin, J. S., & Khoshbouei, H. (2015). Dopamine Transporter Activity Is Modulated by α-Synuclein *. *Journal of Biological Chemistry*, *290*(49), 29542–29554. https://doi.org/10.1074/jbc.M115.691592

Cadet, J. L., & Krasnova, I. N. (2009). Molecular bases of methamphetamine-induced neurodegeneration. *International Review of Neurobiology*, *88*, 101–119. https://doi.org/10.1016/S0074-7742(09)88005-7

Caetano, M. A. F., & Castelucci, P. (2022). Role of short chain fatty acids in gut health and possible therapeutic approaches in inflammatory bowel diseases. *World Journal of Clinical Cases*, *10*(28), 9985–10003. https://doi.org/10.12998/wjcc.v10.i28.9985

Calabresi, P., Di Lazzaro, G., Marino, G., Campanelli, F., & Ghiglieri, V. (2023). Advances in understanding the function of alpha-synuclein: Implications for Parkinson's disease. *Brain*, *146*(9), 3587–3597. https://doi.org/10.1093/brain/awad150

Cali, F., Cantone, M., Cosentino, F. I. I., Lanza, G., Ruggeri, G., Chiavetta, V., Salluzzo, R., Ragalmuto, A., Vinci, M., & Ferri, R. (2019). Interpreting Genetic Variants: Hints from a Family Cluster of Parkinson's Disease. *Journal of Parkinson's Disease*, *9*(1), 203–206. https://doi.org/10.3233/JPD-171292

Carmichael, K., Evans, R. C., Lopez, E., Sun, L., Kumar, M., Ding, J., Khaliq, Z. M., & Cai, H. (2021). Function and Regulation of ALDH1A1-Positive Nigrostriatal Dopaminergic Neurons in Motor Control and Parkinson's Disease. *Frontiers in Neural Circuits*, *15*. https://doi.org/10.3389/fncir.2021.644776

Carr, W. J., Yee, L., Gable, D., & Marasco, E. (1976). Olfactory recognition of conspecifics by domestic Norway rats. *Journal of Comparative and Physiological Psychology*, *90*(9), 821–828. https://doi.org/10.1037/h0077266

Carroll, J. C., Iba, M., Bangasser, D. A., Valentino, R. J., James, M. J., Brunden, K. R., Lee, V. M.-Y., & Trojanowski, J. Q. (2011). Chronic Stress Exacerbates Tau Pathology, Neurodegeneration, and Cognitive Performance through a Corticotropin-Releasing Factor Receptor-Dependent Mechanism in a Transgenic Mouse Model of Tauopathy. *The Journal of Neuroscience*, *31*(40), 14436–14449. https://doi.org/10.1523/JNEUROSCI.3836-11.2011

Carroll, W. M. (2019). The global burden of neurological disorders. *The Lancet Neurology*, *18*(5), 418–419. https://doi.org/10.1016/S1474-4422(19)30029-8

Castaño, A., Herrera, A. J., Cano, J., & Machado, A. (1998). Lipopolysaccharide intranigral injection induces inflammatory reaction and damage in nigrostriatal dopaminergic system. *Journal of Neurochemistry*, *70*(4), 1584–1592. https://doi.org/10.1046/j.1471-4159.1998.70041584.x

Chan, C. S., Guzman, J. N., Ilijic, E., Mercer, J. N., Rick, C., Tkatch, T., Meredith, G. E., & Surmeier, D. J. (2007). "Rejuvenation" protects neurons in mouse models of Parkinson's disease. *Nature*, *447*(7148), 1081–1086. https://doi.org/10.1038/nature05865

Chandra, R., Hiniker, A., Kuo, Y.-M., Nussbaum, R. L., & Liddle, R. A. (2017). α-Synuclein in gut endocrine cells and its implications for Parkinson's disease. *JCI Insight*, *2*(12), e92295, 92295. https://doi.org/10.1172/jci.insight.92295

Chandra, S., Fornai, F., Kwon, H.-B., Yazdani, U., Atasoy, D., Liu, X., Hammer, R. E., Battaglia, G., German, D. C., Castillo, P. E., & Südhof, T. C. (2004). Double-knockout mice for alpha- and beta-synucleins: Effect on synaptic functions. *Proceedings of the National Academy of Sciences of the United States of America*, *101*(41), 14966–14971. https://doi.org/10.1073/pnas.0406283101

Chang, D., Nalls, M. A., Hallgrímsdóttir, I. B., Hunkapiller, J., van der Brug, M., Cai, F., Kerchner, G. A., Ayalon, G., Bingol, B., Sheng, M., Hinds, D., Behrens, T. W., Singleton, A. B., Bhangale, T. R., & Graham, R. R. (2017). A meta-analysis of genome-wide association studies identifies 17 new Parkinson's disease risk loci. *Nature Genetics*, *49*(10), 1511–1516. https://doi.org/10.1038/ng.3955

Chang, L. (2011). The Role of Stress on Physiological Responses and Clinical Symptoms in Irritable Bowel Syndrome. *Gastroenterology*, *140*(3), 761–765. https://doi.org/10.1053/j.gastro.2011.01.032

Charlett, A., Dobbs, R. J., Purkiss, A. G., Wrighe, D. J., Peterson, D. W., Weller, C., & Dobbs, S. M. (1998). Cortisol is higher in parkinsonism and associated with gait deficit. *Acta Neurologica Scandinavica*, *97*(2), 77–85. https://doi.org/10.1111/j.1600-0404.1998.tb00614.x

Charney, D. S., & Manji, H. K. (2004). Life Stress, Genes, and Depression: Multiple Pathways Lead to Increased Risk and New Opportunities for Intervention. *Science's STKE*, *2004*(225), re5–re5. https://doi.org/10.1126/stke.2252004re5

Chartier-Harlin, M.-C., Kachergus, J., Roumier, C., Mouroux, V., Douay, X., Lincoln, S., Levecque, C., Larvor, L., Andrieux, J., Hulihan, M., Waucquier, N., Defebvre, L., Amouyel, P., Farrer, M., & Destée, A. (2004). Alpha-synuclein locus duplication as a cause of familial Parkinson's disease. *Lancet (London, England)*, *364*(9440), 1167–1169. https://doi.org/10.1016/S0140-6736(04)17103-1

Chen, K., Guo, M.-R., Zhang, Y., Li, G., Liu, Y., & Zhang, B. (2021). Association between MMP16 rs60298754 and clinical phenotypes of Parkinson's disease in southern Chinese. *Neurological Sciences*, *42*(8), 3211–3215. https://doi.org/10.1007/s10072-020-04894-5

Chen, L., Jin, J., Davis, J., Zhou, Y., Wang, Y., Liu, J., Lockhart, P. J., & Zhang, J. (2007). Oligomeric α-synuclein inhibits tubulin polymerization. *Biochemical and Biophysical Research Communications*, *356*(3), 548–553. https://doi.org/10.1016/j.bbrc.2007.02.163

Chen, S.-J., Chen, C.-C., Liao, H.-Y., Lin, Y.-T., Wu, Y.-W., Liou, J.-M., Wu, M.-S., Kuo, C.-H., & Lin, C.-H. (2022). Association of Fecal and Plasma Levels of Short-Chain Fatty Acids With Gut Microbiota and Clinical Severity in Patients With Parkinson Disease. *Neurology*, *98*(8), e848–e858. https://doi.org/10.1212/WNL.0000000000013225

Chen, W., Bi, Z., Zhu, Q., Gao, H., Fan, Y., Zhang, C., Liu, X., & Ye, M. (2021). An analysis of the characteristics of the intestinal flora in patients with Parkinson's disease complicated with constipation. *American Journal of Translational Research*, *13*(12), 13710–13722.

Chen, Y., Brunson, K. L., Adelmann, G., Bender, R. A., Frotscher, M., & Baram, T. Z. (2004). Hippocampal corticotropin releasing hormone: Pre- and postsynaptic location and release by stress. *Neuroscience*, *126*(3), 533–540. https://doi.org/10.1016/j.neuroscience.2004.03.036

Cheng, F., Li, X., Li, Y., Wang, C., Wang, T., Liu, G., Baskys, A., Uéda, K., Chan, P., & Yu, S. (2011). α-Synuclein promotes clathrin-mediated NMDA receptor endocytosis and attenuates NMDA-induced dopaminergic cell death. *Journal of Neurochemistry*, *119*(4), 815–825. https://doi.org/10.1111/j.1471-4159.2011.07460.x

Chesselet, M.-F., Richter, F., Zhu, C., Magen, I., Watson, M. B., & Subramaniam, S. R. (2012). A Progressive Mouse Model of Parkinson's Disease: The Thy1-aSyn ("Line 61") Mice. *Neurotherapeutics*, *9*(2), 297–314. https://doi.org/10.1007/s13311-012-0104-2

Chinta, S. J., Mallajosyula, J. K., Rane, A., & Andersen, J. K. (2010). Mitochondrial α-synuclein accumulation impairs complex I function in dopaminergic neurons and results in increased mitophagy in vivo. *Neuroscience Letters*, *486*(3), 235–239. https://doi.org/10.1016/j.neulet.2010.09.061

Chong, C., Hamid, A., Yao, T., Garza, A. E., Pojoga, L. H., Adler, G. K., Romero, J. R., & Williams, G. H. (2017). Regulation of aldosterone secretion by mineralocorticoid receptor–mediated signaling. *Journal of Endocrinology*, *232*(3), 525–534. https://doi.org/10.1530/JOE-16-0452

Choubey, V., Safiulina, D., Vaarmann, A., Cagalinec, M., Wareski, P., Kuum, M., Zharkovsky, A., & Kaasik, A. (2011). Mutant A53T α-Synuclein Induces Neuronal Death by Increasing Mitochondrial Autophagy. *The Journal of Biological Chemistry*, *286*(12), 10814–10824. https://doi.org/10.1074/jbc.M110.132514

Chrousos, G. P. (2009). Stress and disorders of the stress system. *Nature Reviews Endocrinology*, *5*(7), 374–381. https://doi.org/10.1038/nrendo.2009.106

Civiero, L., Cirnaru, M. D., Beilina, A., Rodella, U., Russo, I., Belluzzi, E., Lobbestael, E., Reyniers, L., Hondhamuni, G., Lewis, P. A., Van den Haute, C., Baekelandt, V., Bandopadhyay, R., Bubacco, L., Piccoli, G., Cookson, M. R., Taymans, J., & Greggio, E. (2015). Leucine-rich repeat kinase 2 interacts with p21-activated kinase 6 to control neurite

complexity in mammalian brain. *Journal of Neurochemistry*, *135*(6), 1242–1256. https://doi.org/10.1111/jnc.13369

Civiero, L., Cogo, S., Kiekens, A., Morganti, C., Tessari, I., Lobbestael, E., Baekelandt, V., Taymans, J.-M., Chartier-Harlin, M.-C., Franchin, C., Arrigoni, G., Lewis, P. A., Piccoli, G., Bubacco, L., Cookson, M. R., Pinton, P., & Greggio, E. (2017). PAK6 Phosphorylates 14-3-3γ to Regulate Steady State Phosphorylation of LRRK2. *Frontiers in Molecular Neuroscience*, *10*. https://doi.org/10.3389/fnmol.2017.00417

Clark, I. E., Dodson, M. W., Jiang, C., Cao, J. H., Huh, J. R., Seol, J. H., Yoo, S. J., Hay, B. A., & Guo, M. (2006). Drosophila pink1 is required for mitochondrial function and interacts genetically with parkin. *Nature*, *441*(7097), 1162–1166. https://doi.org/10.1038/nature04779

Cole, A. B., Montgomery, K., Bale, T. L., & Thompson, S. M. (2022). What the hippocampus tells the HPA axis: Hippocampal output attenuates acute stress responses via disynaptic inhibition of CRF+ PVN neurons. *Neurobiology of Stress*, *20*, 100473. https://doi.org/10.1016/j.ynstr.2022.100473

Collier, T. J., Kanaan, N. M., & Kordower, J. H. (2011). Ageing as a primary risk factor for Parkinson's disease: Evidence from studies of non-human primates. *Nature Reviews. Neuroscience*, *12*(6), 359–366. https://doi.org/10.1038/nrn3039

Collins, C. P., Khuat, L. T., Sckisel, G. D., Vick, L. V., Minnar, C. M., Dunai, C., Le, C. T., Curti, B. D., Crittenden, M., Merleev, A., Sheng, M., Chao, N. J., Maverakis, E., Rosario, S. R., Monjazeb, A. M., Blazar, B. R., Longo, D. L., Canter, R. J., & Murphy, W. J. (2024). Systemic immunostimulation induces glucocorticoid-mediated thymic involution succeeded by rebound hyperplasia which is impaired in aged recipients. *Frontiers in Immunology*, *15*. https://doi.org/10.3389/fimmu.2024.1429912

Conrad, C. D., Galea, L. A., Kuroda, Y., & McEwen, B. S. (1996). Chronic stress impairs rat spatial memory on the Y maze, and this effect is blocked by tianeptine pretreatment. *Behavioral Neuroscience*, *110*(6), 1321–1334. https://doi.org/10.1037//0735-7044.110.6.1321

Conrad, C. D., LeDoux, J. E., Magariños, A. M., & McEwen, B. S. (1999). Repeated restraint stress facilitates fear conditioning independently of causing hippocampal CA3 dendritic atrophy. *Behavioral Neuroscience*, *113*(5), 902–913. https://doi.org/10.1037//0735-7044.113.5.902

Consortium (IPDGC), I. P. D. G., & Consortium 2 (WTCCC2), W. T. C. C. (2011). A Two-Stage Meta-Analysis Identifies Several New Loci for Parkinson's Disease. *PLOS Genetics*, *7*(6), e1002142. https://doi.org/10.1371/journal.pgen.1002142

Cooper, A. A., Gitler, A. D., Cashikar, A., Haynes, C. M., Hill, K. J., Bhullar, B., Liu, K., Xu, K., Strathearn, K. E., Liu, F., Cao, S., Caldwell, K. A., Caldwell, G. A., Marsischky, G., Kolodner, R. D., Labaer, J., Rochet, J.-C., Bonini, N. M., & Lindquist, S. (2006). Alpha-synuclein blocks ER-Golgi traffic and Rab1 rescues neuron loss in Parkinson's models. *Science (New York, N.Y.)*, *313*(5785), 324–328. https://doi.org/10.1126/science.1129462

Courte, J., Bousset, L., Boxberg, Y. V., Villard, C., Melki, R., & Peyrin, J.-M. (2020). The expression level of alpha-synuclein in different neuronal populations is the primary determinant of its prion-like seeding. *Scientific Reports*, *10*, 4895. https://doi.org/10.1038/s41598-020-61757-x

Cryan, J. F., O'Riordan, K. J., Sandhu, K., Peterson, V., & Dinan, T. G. (2020). The gut microbiome in neurological disorders. *The Lancet. Neurology*, *19*(2), 179–194. https://doi.org/10.1016/S1474-4422(19)30356-4

Cuervo, A. M., Stefanis, L., Fredenburg, R., Lansbury, P. T., & Sulzer, D. (2004). Impaired Degradation of Mutant α-Synuclein by Chaperone-Mediated Autophagy. *Science*, *305*(5688), 1292–1295. https://doi.org/10.1126/science.1101738

Cummings, J. H., Pomare, E. W., Branch, W. J., Naylor, C. P., & Macfarlane, G. T. (1987). Short chain fatty acids in human large intestine, portal, hepatic and venous blood. *Gut*, *28*(10), 1221–1227. https://doi.org/10.1136/gut.28.10.1221

Cuvelier, E., Méquinion, M., Leghay, C., Sibran, W., Stievenard, A., Sarchione, A., Bonte, M.-A., Vanbesien-Mailliot, C., Viltart, O., Saitoski, K., Caron, E., Labarthe, A., Comptdaer, T., Semaille, P., Carrié, H., Mutez, E., Gressier, B., Destée, A., Chartier-Harlin, M.-C., & Belarbi, K. (2018). Overexpression of Wild-Type Human Alpha-Synuclein Causes Metabolism Abnormalities in Thy1-aSYN Transgenic Mice. *Frontiers in Molecular Neuroscience*, *11*. https://www.frontiersin.org/articles/10.3389/fnmol.2018.00321

da Silva, F. L., Coelho Cerqueira, E., de Freitas, M. S., Gonçalves, D. L., Costa, L. T., & Follmer, C. (2013). Vitamins K interact with N-terminus α-synuclein and modulate the protein fibrillization in vitro. Exploring the interaction between quinones and α-synuclein. *Neurochemistry International*, *62*(1), 103–112. https://doi.org/10.1016/j.neuint.2012.10.001

Daher, J. P. L., Ying, M., Banerjee, R., McDonald, R. S., Hahn, M. D., Yang, L., Flint Beal, M., Thomas, B., Dawson, V. L., Dawson, T. M., & Moore, D. J. (2009). Conditional transgenic mice expressing C-terminally truncated human α-synuclein (αSyn119) exhibit reduced striatal dopamine without loss of nigrostriatal pathway dopaminergic neurons. *Molecular Neurodegeneration*, *4*(1), 34. https://doi.org/10.1186/1750-1326-4-34

Dalile, B., Van Oudenhove, L., Vervliet, B., & Verbeke, K. (2019). The role of short-chain fatty acids in microbiota–gut–brain communication. *Nature Reviews Gastroenterology & Hepatology*, *16*(8), 461–478. https://doi.org/10.1038/s41575-019-0157-3

Danzer, K. M., Haasen, D., Karow, A. R., Moussaud, S., Habeck, M., Giese, A., Kretzschmar, H., Hengerer, B., & Kostka, M. (2007). Different Species of α-Synuclein Oligomers Induce Calcium Influx and Seeding. *Journal of Neuroscience*, *27*(34), 9220–9232. https://doi.org/10.1523/JNEUROSCI.2617-07.2007

de Kloet, E. R., Joëls, M., & Holsboer, F. (2005). Stress and the brain: From adaptation to disease. *Nature Reviews Neuroscience*, *6*(6), 463–475. https://doi.org/10.1038/nrn1683

de la Fuente-Fernández, R. (2012). Role of DaTSCAN and clinical diagnosis in Parkinson disease. *Neurology*, *78*(10), 696–701. https://doi.org/10.1212/WNL.0b013e318248e520

de Pablos, R. M., Herrera, A. J., Espinosa-Oliva, A. M., Sarmiento, M., Muñoz, M. F., Machado, A., & Venero, J. L. (2014). Chronic stress enhances microglia activation and exacerbates death of nigral dopaminergic neurons under conditions of inflammation. *Journal of Neuroinflammation*, *11*, 34. https://doi.org/10.1186/1742-2094-11-34

Decressac, M., Volakakis, N., Björklund, A., & Perlmann, T. (2013). NURR1 in Parkinson disease—From pathogenesis to therapeutic potential. *Nature Reviews. Neurology*, *9*(11), 629–636. https://doi.org/10.1038/nrneurol.2013.209

Depommier, C., Van Hul, M., Everard, A., Delzenne, N. M., De Vos, W. M., & Cani, P. D. (2020). Pasteurized Akkermansia muciniphila increases whole-body energy expenditure and fecal energy excretion in diet-induced obese mice. *Gut Microbes*, *11*(5), 1231–1245. https://doi.org/10.1080/19490976.2020.1737307

Derkinderen, P., Noble, W., Neunlist, M., & Rolli-Derkinderen, M. (2021). Upregulation of enteric alpha-synuclein as a possible link between inflammatory bowel disease and Parkinson's disease. *Gut*, *70*(10), 2010–2012. https://doi.org/10.1136/gutjnl-2020-323482

Desplats, P., Lee, H.-J., Bae, E.-J., Patrick, C., Rockenstein, E., Crews, L., Spencer, B., Masliah, E., & Lee, S.-J. (2009). Inclusion formation and neuronal cell death through neuron-to-neuron transmission of alpha-synuclein. *Proceedings of the National Academy of Sciences of the United States of America*, *106*(31), 13010–13015. https://doi.org/10.1073/pnas.0903691106

Devi, L., Raghavendran, V., Prabhu, B. M., Avadhani, N. G., & Anandatheerthavarada, H. K. (2008). Mitochondrial Import and Accumulation of α-Synuclein Impair Complex I in Human Dopaminergic Neuronal Cultures and Parkinson Disease Brain. *The Journal of Biological Chemistry*, *283*(14), 9089–9100. https://doi.org/10.1074/jbc.M710012200

Df, L., Ef, R., R, L., H, S., T, R., P, G., E, G., K, K., J, K., Md, P., B, P., N, K., B, M., So, R., Gh, B., Km, D., & Tf, O. (2014). Systematic comparison of the effects of alpha-synuclein mutations on its oligomerization and aggregation. *PLoS Genetics*, *10*(11). https://doi.org/10.1371/journal.pgen.1004741

D'Hooge, R., & De Deyn, P. P. (2001). Applications of the Morris water maze in the study of learning and memory. *Brain Research Reviews*, *36*(1), 60–90. https://doi.org/10.1016/S0165-0173(01)00067-4

Di Chiara, G., Loddo, P., & Tanda, G. (1999). Reciprocal changes in prefrontal and limbic dopamine responsiveness to aversive and rewarding stimuli after chronic mild stress: Implications for the psychobiology of depression. *Biological Psychiatry*, *46*(12), 1624–1633. https://doi.org/10.1016/s0006-3223(99)00236-x

Di Chiara, G., & Tanda, G. (1997). Blunting of reactivity of dopamine transmission to palatable food: A biochemical marker of anhedonia in the CMS model? *Psychopharmacology*, *134*(4), 351–353. https://doi.org/10.1007/s002130050465

Di, S., Malcher-Lopes, R., Halmos, K. C., & Tasker, J. G. (2003). Nongenomic Glucocorticoid Inhibition via Endocannabinoid Release in the Hypothalamus: A Fast Feedback Mechanism. *Journal of Neuroscience*, *23*(12), 4850–4857. https://doi.org/10.1523/JNEUROSCI.23-12-04850.2003

Dick, F., Tysnes, O.-B., Alves, G. W., Nido, G. S., & Tzoulis, C. (2023). Altered transcriptome-proteome coupling indicates aberrant proteostasis in Parkinson's disease. *iScience*, *26*(2). https://doi.org/10.1016/j.isci.2023.105925

Ding, H., Cui, X.-Y., Cui, S.-Y., Ye, H., Hu, X., Zhao, H.-L., Liu, Y.-T., & Zhang, Y.-H. (2018). Depression-like behaviors induced by chronic corticosterone exposure via drinking water: Time-course analysis. *Neuroscience Letters*, *687*, 202–206. https://doi.org/10.1016/j.neulet.2018.09.059

Diorio, D., Viau, V., & Meaney, M. (1993). The role of the medial prefrontal cortex (cingulate gyrus) in the regulation of hypothalamic-pituitary-adrenal responses to stress. *The Journal of Neuroscience*, *13*(9), 3839–3847. https://doi.org/10.1523/JNEUROSCI.13-09-03839.1993

Diwakarla, S., Finkelstein, D. I., Constable, R., Artaiz, O., Di Natale, M., McQuade, R. M., Lei, E., Chai, X., Ringuet, M. T., Fothergill, L. J., Lawson, V. A., Ellett, L. J., Berger, J. P., & Furness, J. B. (2020). Chronic isolation stress is associated with increased colonic and motor symptoms in the A53T mouse model of Parkinson's disease. *Neurogastroenterology & Motility*, *32*(3), e13755. https://doi.org/10.1111/nmo.13755

Djamshidian, A., & Lees, A. J. (2014). Can stress trigger Parkinson's disease? *Journal of Neurology, Neurosurgery & Psychiatry*, *85*(8), 878–881. https://doi.org/10.1136/jnnp-2013-305911

Dodiya, H. B., Forsyth, C. B., Voigt, R. M., Engen, P. A., Patel, J., Shaikh, M., Green, S. J., Naqib, A., Roy, A., Kordower, J. H., Pahan, K., Shannon, K. M., & Keshavarzian, A. (2020). Chronic stress-induced gut dysfunction exacerbates Parkinson's disease phenotype and pathology in a rotenone-induced mouse model of Parkinson's disease. *Neurobiology of Disease*, *135*, 104352. https://doi.org/10.1016/j.nbd.2018.12.012

Doherty, K. M., Silveira-Moriyama, L., Parkkinen, L., Healy, D. G., Farrell, M., Mencacci, N. E., Ahmed, Z., Brett, F. M., Hardy, J., Quinn, N., Counihan, T. J., Lynch, T., Fox, Z. V., Revesz, T., Lees, A. J., & Holton, J. L. (2013). Parkin disease: A clinicopathologic entity? *JAMA Neurology*, *70*(5), 571–579. https://doi.org/10.1001/jamaneurol.2013.172

Dorsey, E. R., Sherer, T., Okun, M. S., & Bloem, B. R. (2018). The Emerging Evidence of the Parkinson Pandemic. *Journal of Parkinson's Disease*, *8*(s1), S3–S8. https://doi.org/10.3233/JPD-181474

Du, T., Li, G., Zong, Q., Luo, H., Pan, Y., & Ma, K. (2024). Nuclear alpha-synuclein accelerates cell senescence and neurodegeneration. *Immunity & Ageing*, *21*(1), 47. https://doi.org/10.1186/s12979-024-00429-0

Du, X., & Pang, T. Y. (2015). Is Dysregulation of the HPA-Axis a Core Pathophysiology Mediating Co-Morbid Depression in Neurodegenerative Diseases? *Frontiers in Psychiatry*, *6*, 32. https://doi.org/10.3389/fpsyt.2015.00032

Duan, W.-X., Wang, F., Liu, J.-Y., & Liu, C.-F. (2024). Relationship Between Short-chain Fatty Acids and Parkinson's Disease: A Review from Pathology to Clinic. *Neuroscience Bulletin*, *40*(4), 500–516. https://doi.org/10.1007/s12264-023-01123-9

Duda, J. E., Giasson, B. I., Mabon, M. E., Miller, D. C., Golbe, L. I., Lee, V. M.-Y., & Trojanowski, J. Q. (2002). Concurrence of α-synuclein and tau brain pathology in the Contursi kindred. *Acta Neuropathologica*, *104*(1), 7–11. https://doi.org/10.1007/s00401-002-0563-3

Dufty, B. M., Warner, L. R., Hou, S. T., Jiang, S. X., Gomez-Isla, T., Leenhouts, K. M., Oxford, J. T., Feany, M. B., Masliah, E., & Rohn, T. T. (2007). Calpain-cleavage of alpha-synuclein: Connecting proteolytic processing to disease-linked aggregation. *The American Journal of Pathology*, *170*(5), 1725–1738. https://doi.org/10.2353/ajpath.2007.061232

Duka, T., Rusnak, M., Drolet, R. E., Duka, V., Wersinger, C., Goudreau, J. L., & Sidhu, A. (2006). Alpha-Synuclein induces hyperphosphorylation of Tau in the MPTP model of Parkinsonism. *The FASEB Journal*, *20*(13), 2302–2312. https://doi.org/10.1096/fj.06-6092com

Duncan, S. H., Hold, G. L., Harmsen, H. J. M., Stewart, C. S., & Flint, H. J. (2002). Growth requirements and fermentation products of Fusobacterium prausnitzii, and a proposal to reclassify it as Faecalibacterium prausnitzii gen. Nov., comb. Nov. *International Journal of Systematic and Evolutionary Microbiology*, *52*(Pt 6), 2141–2146. https://doi.org/10.1099/00207713-52-6-2141

Durante, V., de Iure, A., Loffredo, V., Vaikath, N., De Risi, M., Paciotti, S., Quiroga-Varela, A., Chiasserini, D., Mellone, M., Mazzocchetti, P., Calabrese, V., Campanelli, F., Mechelli, A., Di Filippo, M., Ghiglieri, V., Picconi, B., El-Agnaf, O. M., De Leonibus, E., Gardoni, F., … Calabresi, P. (2019). Alpha-synuclein targets GluN2A NMDA receptor subunit causing striatal synaptic dysfunction and visuospatial memory alteration. *Brain*, *142*(5), 1365–1385. https://doi.org/10.1093/brain/awz065

Dusonchet, J., Li, H., Guillily, M., Liu, M., Stafa, K., Derada Troletti, C., Boon, J. Y., Saha, S., Glauser, L., Mamais, A., Citro, A., Youmans, K. L., Liu, L., Schneider, B. L., Aebischer, P., Yue, Z., Bandopadhyay, R., Glicksman, M. A., Moore, D. J., … Wolozin, B. (2014). A Parkinson's disease gene regulatory network identifies the signaling protein RGS2 as a modulator of LRRK2 activity and neuronal toxicity. *Human Molecular Genetics*, *23*(18), 4887–4905. https://doi.org/10.1093/hmg/ddu202

Duveau, A., Bertin, E., & Boué-Grabot, E. (2020). Implication of Neuronal Versus Microglial P2X4 Receptors in Central Nervous System Disorders. *Neuroscience Bulletin*, *36*(11), 1327–1343. https://doi.org/10.1007/s12264-020-00570-y

Dyavar, S. R., Potts, L. F., Beck, G., Dyavar Shetty, B. L., Lawson, B., Podany, A. T., Fletcher, C. V., Amara, R. R., & Papa, S. M. (2020). Transcriptomic approach predicts a major role for transforming growth factor beta type 1 pathway in L-Dopa-induced dyskinesia in parkinsonian rats. *Genes, Brain and Behavior*, *19*(8), e12690. https://doi.org/10.1111/gbb.12690

Dzamko, N., Gysbers, A., Perera, G., Bahar, A., Shankar, A., Gao, J., Fu, Y., & Halliday, G. M. (2017). Toll-like receptor 2 is increased in neurons in Parkinson's disease brain and may contribute to alpha-synuclein pathology. *Acta Neuropathologica*, *133*(2), 303–319. https://doi.org/10.1007/s00401-016-1648-8

El-Agnaf, O. M. A., Salem, S. A., Paleologou, K. E., Cooper, L. J., Fullwood, N. J., Gibson, M. J., Curran, M. D., Court, J. A., Mann, D. M. A., Ikeda, S.-I., Cookson, M. R., Hardy, J., & Allsop, D. (2003). α-Synuclein implicated in Parkinson's

disease is present in extracellular biological fluids, including human plasma. *The FASEB Journal*, *17*(13), 1–16. https://doi.org/10.1096/fj.03-0098fje

Emmanouilidou, E., Melachroinou, K., Roumeliotis, T., Garbis, S. D., Ntzouni, M., Margaritis, L. H., Stefanis, L., & Vekrellis, K. (2010). Cell-Produced α-Synuclein Is Secreted in a Calcium-Dependent Manner by Exosomes and Impacts Neuronal Survival. *Journal of Neuroscience*, *30*(20), 6838–6851. https://doi.org/10.1523/JNEUROSCI.5699-09.2010

Emmanouilidou, E., Minakaki, G., Keramioti, M. V., Xylaki, M., Balafas, E., Chrysanthou-Piterou, M., Kloukina, I., & Vekrellis, K. (2016). GABA transmission via ATP-dependent K + channels regulates α-synuclein secretion in mouse striatum. *Brain*, *139*(3), 871–890. https://doi.org/10.1093/brain/awv403

Escherich, Th. (1988). The Intestinal Bacteria of the Neonate and Breast-Fed Infant. *Reviews of Infectious Diseases*, *10*(6), 1220–1225. https://doi.org/10.1093/clinids/10.6.1220

Esteves, A. R., Arduino, D. M., Swerdlow, R. H., Oliveira, C., & Cardoso, S. M. (2010). Microtubule depolymerization potentiates alpha-synuclein oligomerization. *Frontiers in Aging Neuroscience*, *1*. https://doi.org/10.3389/neuro.24.005.2009

Fan, X., Zhang, L., Li, H., Chen, G., Qi, G., Ma, X., & Jin, Y. (2020). Role of homocysteine in the development and progression of Parkinson's disease. *Annals of Clinical and Translational Neurology*, *7*(11), 2332–2338. https://doi.org/10.1002/acn3.51227

Farrer, M., Maraganore, D. M., Lockhart, P., Singleton, A., Lesnick, T. G., de Andrade, M., West, A., de Silva, R., Hardy, J., & Hernandez, D. (2001). Alpha-Synuclein gene haplotypes are associated with Parkinson's disease. *Human Molecular Genetics*, *10*(17), 1847–1851. https://doi.org/10.1093/hmg/10.17.1847

Fellner, L., Irschick, R., Schanda, K., Reindl, M., Klimaschewski, L., Poewe, W., Wenning, G. K., & Stefanova, N. (2013). Toll-like receptor 4 is required for α-synuclein dependent activation of microglia and astroglia. *Glia*, *61*(3), 349–360. https://doi.org/10.1002/glia.22437

Fellner, L., Jellinger, K. A., Wenning, G. K., & Stefanova, N. (2011). Glial dysfunction in the pathogenesis of α-synucleinopathies: Emerging concepts. *Acta Neuropathologica*, *121*(6), 675–693. https://doi.org/10.1007/s00401-011-0833-z

Ferrari, E., Scheggia, D., Zianni, E., Italia, M., Brumana, M., Palazzolo, L., Parravicini, C., Pilotto, A., Padovani, A., Marcello, E., Eberini, I., Calabresi, P., Diluca, M., & Gardoni, F. (2022). Rabphilin-3A as a novel target to reverse α-synuclein-induced synaptic loss in Parkinson's disease. *Pharmacological Research*, *183*, 106375. https://doi.org/10.1016/j.phrs.2022.106375

Flora, G., Lee, Y. W., Nath, A., Maragos, W., Hennig, B., & Toborek, M. (2002). Methamphetamine-induced TNF-alpha gene expression and activation of AP-1 in discrete regions of mouse brain: Potential role of reactive oxygen intermediates and lipid peroxidation. *Neuromolecular Medicine*, *2*(1), 71–85. https://doi.org/10.1385/NMM:2:1:71

Foehring, R. C., Zhang, X. F., Lee, J. C. F., & Callaway, J. C. (2009). Endogenous calcium buffering capacity of substantia nigral dopamine neurons. *Journal of Neurophysiology*, *102*(4), 2326–2333. https://doi.org/10.1152/jn.00038.2009

Fronczek, R., Overeem, S., Lee, S. Y. Y., Hegeman, I. M., van Pelt, J., van Duinen, S. G., Lammers, G. J., & Swaab, D. F. (2007). Hypocretin (orexin) loss in Parkinson's disease. *Brain: A Journal of Neurology*, *130*(Pt 6), 1577–1585. https://doi.org/10.1093/brain/awm090

Fujishiro, H., Frigerio, R., Burnett, M., Klos, K. J., Josephs, K. A., Delledonne, A., Parisi, J. E., Ahlskog, J. E., & Dickson, D. W. (2008). Cardiac sympathetic denervation correlates with clinical and pathologic stages of Parkinson's disease. *Movement Disorders: Official Journal of the Movement Disorder Society*, *23*(8), 1085–1092. https://doi.org/10.1002/mds.21989

Fujiwara, H., Hasegawa, M., Dohmae, N., Kawashima, A., Masliah, E., Goldberg, M. S., Shen, J., Takio, K., & Iwatsubo, T. (2002). Alpha-Synuclein is phosphorylated in synucleinopathy lesions. *Nature Cell Biology*, *4*(2), 160–164. https://doi.org/10.1038/ncb748

Furay, A. R., Bruestle, A. E., & Herman, J. P. (2008). The Role of the Forebrain Glucocorticoid Receptor in Acute and Chronic Stress. *Endocrinology*, *149*(11), 5482–5490. https://doi.org/10.1210/en.2008-0642

Galvin, J. E., Uryu, K., Lee, V. M., & Trojanowski, J. Q. (1999). Axon pathology in Parkinson's disease and Lewy body dementia hippocampus contains alpha-, beta-, and gamma-synuclein. *Proceedings of the National Academy of Sciences of the United States of America*, *96*(23), 13450–13455. https://doi.org/10.1073/pnas.96.23.13450

Ganjam, G. K., Bolte, K., Matschke, L. A., Neitemeier, S., Dolga, A. M., Höllerhage, M., Höglinger, G. U., Adamczyk, A., Decher, N., Oertel, W. H., & Culmsee, C. (2019). Mitochondrial damage by α-synuclein causes cell death in human dopaminergic neurons. *Cell Death & Disease*, *10*(11), 1–16. https://doi.org/10.1038/s41419-019-2091-2

Gao, H.-M., Jiang, J., Wilson, B., Zhang, W., Hong, J.-S., & Liu, B. (2002). Microglial activation-mediated delayed and progressive degeneration of rat nigral dopaminergic neurons: Relevance to Parkinson's disease. *Journal of Neurochemistry*, *81*(6), 1285–1297. https://doi.org/10.1046/j.1471-4159.2002.00928.x

Gasser, T. (2009). Mendelian forms of Parkinson's disease. *Biochimica et Biophysica Acta (BBA) - Molecular Basis of Disease*, *1792*(7), 587–596. https://doi.org/10.1016/j.bbadis.2008.12.007

Geurts, M., Maloteaux, J.-M., & Hermans, E. (2003). Altered expression of regulators of G-protein signaling (RGS) mRNAs in the striatum of rats undergoing dopamine depletion. *Biochemical Pharmacology*, *66*(7), 1163–1170. https://doi.org/10.1016/S0006-2952(03)00447-7

Ghanem, S. S., Majbour, N. K., Vaikath, N. N., Ardah, M. T., Erskine, D., Jensen, N. M., Fayyad, M., Sudhakaran, I. P., Vasili, E., Melachroinou, K., Abdi, I. Y., Poggiolini, I., Santos, P., Dorn, A., Carloni, P., Vekrellis, K., Attems, J., McKeith, I., Outeiro, T. F., … El-Agnaf, O. M. A. (2022). α-Synuclein phosphorylation at serine 129 occurs after initial protein deposition and inhibits seeded fibril formation and toxicity. *Proceedings of the National Academy of Sciences*, *119*(15), e2109617119. https://doi.org/10.1073/pnas.2109617119

Ghio, S., Kamp, F., Cauchi, R., Giese, A., & Vassallo, N. (2016). Interaction of α-synuclein with biomembranes in Parkinson's disease—Role of cardiolipin. *Progress in Lipid Research*, *61*, 73–82. https://doi.org/10.1016/j.plipres.2015.10.005

Giasson, B. I., Duda, J. E., Quinn, S. M., Zhang, B., Trojanowski, J. Q., & Lee, V. M.-Y. (2002). Neuronal alpha-synucleinopathy with severe movement disorder in mice expressing A53T human alpha-synuclein. *Neuron*, *34*(4), 521–533. https://doi.org/10.1016/s0896-6273(02)00682-7

Gibb, W. R., & Lees, A. J. (1988). The relevance of the Lewy body to the pathogenesis of idiopathic Parkinson's disease. *Journal of Neurology, Neurosurgery, and Psychiatry*, *51*(6), 745–752. https://doi.org/10.1136/jnnp.51.6.745

Gibberd, F. B., & Simmonds, J. P. (1980). NEUROLOGICAL DISEASE IN EX-FAR-EAST PRISONERS OF WAR. *The Lancet*, *316*(8186), 135–137. https://doi.org/10.1016/S0140-6736(80)90015-X

Gillies, G. E., Pienaar, I. S., Vohra, S., & Qamhawi, Z. (2014). Sex differences in Parkinson's disease. *Frontiers in Neuroendocrinology*, *35*(3), 370–384. https://doi.org/10.1016/j.yfrne.2014.02.002

Giráldez-Pérez, R. M., Antolín-Vallespín, M., Muñoz, M. D., & Sánchez-Capelo, A. (2014). Models of α-synuclein aggregation in Parkinson's disease. *Acta Neuropathologica Communications*, *2*(1), 176. https://doi.org/10.1186/s40478-014-0176-9

Goetz, C. G., Tanner, C., Penn, R. D., Stebbins, G. T., Gilley, D. W., Shannon, K. M., Klawans, H. L., Comelia, C. L., Wilson, R. S., & Witt, T. (1990). Adrenal medullary transplant to the striatum of patients with advanced Parkinson's disease: 1-year motor and psychomotor data. *Neurology*, *40*(2), 273–273. https://doi.org/10.1212/WNL.40.2.273

Gong, W., Liao, W., Fang, C., Liu, Y., Xie, H., Yi, F., Huang, R., Wang, L., & Zhou, J. (2021). Analysis of Chronic Mild Stress-Induced Hypothalamic Proteome: Identification of Protein Dysregulations Associated With Vulnerability and Resiliency to Depression or Anxiety. *Frontiers in Molecular Neuroscience*, *14*, 633398. https://doi.org/10.3389/fnmol.2021.633398

Gorbatyuk, O. S., Li, S., Sullivan, L. F., Chen, W., Kondrikova, G., Manfredsson, F. P., Mandel, R. J., & Muzyczka, N. (2008). The phosphorylation state of Ser-129 in human alpha-synuclein determines neurodegeneration in a rat model of Parkinson disease. *Proceedings of the National Academy of Sciences of the United States of America*, *105*(2), 763–768. https://doi.org/10.1073/pnas.0711053105

Gowers, W. R. (1887). A Manual of Diseases of the Nervous System. *The Journal of Nervous and Mental Disease*, *14*(2), 123.

Grace, A. A., & Bunney, B. S. (1984). The control of firing pattern in nigral dopamine neurons: Burst firing. *The Journal of Neuroscience: The Official Journal of the Society for Neuroscience*, *4*(11), 2877–2890. https://doi.org/10.1523/JNEUROSCI.04-11-02877.1984

Graham, D. R., & Sidhu, A. (2010). Mice Expressing the A53T Mutant Form of Human Alpha-Synuclein Exhibit Hyperactivity and Reduced Anxiety-Like Behavior. *Journal of Neuroscience Research*, *88*(8), 1777–1783. https://doi.org/10.1002/jnr.22331

Granseth, B., Odermatt, B., Royle, S. J., & Lagnado, L. (2006). Clathrin-Mediated Endocytosis Is the Dominant Mechanism of Vesicle Retrieval at Hippocampal Synapses. *Neuron*, *51*(6), 773–786. https://doi.org/10.1016/j.neuron.2006.08.029

Grassi, D., Howard, S., Zhou, M., Diaz-Perez, N., Urban, N. T., Guerrero-Given, D., Kamasawa, N., Volpicelli-Daley, L. A., LoGrasso, P., & Lasmézas, C. I. (2018). Identification of a highly neurotoxic α-synuclein species inducing mitochondrial damage and mitophagy in Parkinson's disease. *Proceedings of the National Academy of Sciences*, *115*(11), E2634–E2643. https://doi.org/10.1073/pnas.1713849115

Greenbaum, L., Smith, R. C., Rigbi, A., Strous, R., Teltsh, O., Kanyas, K., Korner, M., Lancet, D., Ben-Asher, E., & Lerer, B. (2009). Further evidence for association of the RGS2 gene with antipsychotic-induced parkinsonism: Protective

role of a functional polymorphism in the 3'-untranslated region. *The Pharmacogenomics Journal*, *9*(2), 103–110. https://doi.org/10.1038/tpj.2008.6

Greten-Harrison, B., Polydoro, M., Morimoto-Tomita, M., Diao, L., Williams, A. M., Nie, E. H., Makani, S., Tian, N., Castillo, P. E., Buchman, V. L., & Chandra, S. S. (2010). Aβγ-Synuclein triple knockout mice reveal age-dependent neuronal dysfunction. *Proceedings of the National Academy of Sciences of the United States of America*, *107*(45), 19573–19578. https://doi.org/10.1073/pnas.1005005107

Grigoruţă, M., Martínez-Martínez, A., Dagda, R. Y., & Dagda, R. K. (2020). Psychological stress phenocopies brain mitochondrial dysfunction and motor deficits as observed in a Parkinsonian rat model. *Molecular Neurobiology*, *57*(4), 1781–1798. https://doi.org/10.1007/s12035-019-01838-9

Grissom, N., & Bhatnagar, S. (2009). Habituation to repeated stress: Get used to it. *Neurobiology of Learning and Memory*, *92*(2), 215–224. https://doi.org/10.1016/j.nlm.2008.07.001

Gründemann, J., Schlaudraff, F., Haeckel, O., & Liss, B. (2008). Elevated α-synuclein mRNA levels in individual UV-laser-microdissected dopaminergic substantia nigra neurons in idiopathic Parkinson's disease. *Nucleic Acids Research*, *36*(7), e38. https://doi.org/10.1093/nar/gkn084

Gureviciene, I., Gurevicius, K., & Tanila, H. (2007). Role of alpha-synuclein in synaptic glutamate release. *Neurobiology of Disease*, *28*(1), 83–89. https://doi.org/10.1016/j.nbd.2007.06.016

Guzman, J. N., Sánchez-Padilla, J., Chan, C. S., & Surmeier, D. J. (2009). Robust pacemaking in substantia nigra dopaminergic neurons. *The Journal of Neuroscience: The Official Journal of the Society for Neuroscience*, *29*(35), 11011–11019. https://doi.org/10.1523/JNEUROSCI.2519-09.2009

Häbig, K., Walter, M., Poths, S., Riess, O., & Bonin, M. (2008). RNA interference of LRRK2–microarray expression analysis of a Parkinson's disease key player. *Neurogenetics*, *9*(2), 83–94. https://doi.org/10.1007/s10048-007-0114-0

Haggerty, T., Credle, J., Rodriguez, O., Wills, J., Oaks, A. W., Masliah, E., & Sidhu, A. (2011). Hyperphosphorylated Tau in an α-synuclein-overexpressing transgenic model of Parkinson's disease. *The European Journal of Neuroscience*, *33*(9), 1598–1610. https://doi.org/10.1111/j.1460-9568.2011.07660.x

Haikal, C., Chen, Q.-Q., & Li, J.-Y. (2019). Microbiome changes: An indicator of Parkinson's disease? *Translational Neurodegeneration*, *8*(1), 38. https://doi.org/10.1186/s40035-019-0175-7

Halliday, G., Hely, M., Reid, W., & Morris, J. (2008). The progression of pathology in longitudinally followed patients with Parkinson's disease. *Acta Neuropathologica*, *115*(4), 409–415. https://doi.org/10.1007/s00401-008-0344-8

Halliday, G. M., & Stevens, C. H. (2011). Glia: Initiators and progressors of pathology in Parkinson's disease. *Movement Disorders*, *26*(1), 6–17. https://doi.org/10.1002/mds.23455

Halliday, G., McCann, H., & Shepherd, C. (2012). Evaluation of the Braak hypothesis: How far can it explain the pathogenesis of Parkinson's disease? *Expert Review of Neurotherapeutics*, *12*(6), 673–686. https://doi.org/10.1586/ern.12.47

Hamada, K., Isobe, J., Hattori, K., Hosonuma, M., Baba, Y., Murayama, M., Narikawa, Y., Toyoda, H., Funayama, E., Tajima, K., Shida, M., Hirasawa, Y., Tsurui, T., Ariizumi, H., Ishiguro, T., Suzuki, R., Ohkuma, R., Kubota, Y., Sambe, T., … Yoshimura, K. (2023). Turicibacter and Acidaminococcus predict immune-related adverse events and efficacy of immune checkpoint inhibitor. *Frontiers in Immunology*, *14*. https://www.frontiersin.org/journals/immunology/articles/10.3389/fimmu.2023.1164724

Hamamah, S., Aghazarian, A., Nazaryan, A., Hajnal, A., & Covasa, M. (2022). Role of Microbiota-Gut-Brain Axis in Regulating Dopaminergic Signaling. *Biomedicines*, *10*(2), 436. https://doi.org/10.3390/biomedicines10020436

Han, J., Lin, K., Sequeira, C., & Borchers, C. H. (2015). An isotope-labeled chemical derivatization method for the quantitation of short-chain fatty acids in human feces by liquid chromatography–tandem mass spectrometry. *Analytica Chimica Acta*, *854*, 86–94. https://doi.org/10.1016/j.aca.2014.11.015

Han, W., Tellez, L. A., Perkins, M. H., Perez, I. O., Qu, T., Ferreira, J., Ferreira, T. L., Quinn, D., Liu, Z.-W., Gao, X.-B., Kaelberer, M. M., Bohórquez, D. V., Shammah-Lagnado, S. J., de Lartigue, G., & de Araujo, I. E. (2018). A Neural Circuit for Gut-Induced Reward. *Cell*, *175*(3), 665-678.e23. https://doi.org/10.1016/j.cell.2018.08.049

Hao, Y., Shabanpoor, A., & Metz, G. A. (2017). Stress and Corticosterone Alter Synaptic Plasticity in a Rat Model of Parkinson's Disease. *Neuroscience Letters*, *651*, 79–87. https://doi.org/10.1016/j.neulet.2017.04.063

Harada, S., Fujii, C., Hayashi, A., & Ohkoshi, N. (2001). An association between idiopathic Parkinson's disease and polymorphisms of phase II detoxification enzymes: Glutathione S-transferase M1 and quinone oxidoreductase 1 and 2. *Biochemical and Biophysical Research Communications*, *288*(4), 887–892. https://doi.org/10.1006/bbrc.2001.5868

Hartmann, A., Veldhuis, J. D., Deuschle, M., Standhardt, H., & Heuser, I. (1997). Twenty-Four Hour Cortisol Release Profiles in Patients With Alzheimer's and Parkinson's Disease Compared to Normal Controls: Ultradian Secretory

Pulsatility and Diurnal Variation. *Neurobiology of Aging*, *18*(3), 285–289. https://doi.org/10.1016/S0197-4580(97)80309-0

Hefti, F., Enz, A., & Melamed, E. (1985). Partial lesions of the nigrostriatal pathway in the rat: Acceleration of transmitter synthesis and release of surviving dopaminergic neurones by drugs. *Neuropharmacology*, *24*(1), 19–23. https://doi.org/10.1016/0028-3908(85)90090-5

Hemmerle, A. M., Dickerson, J. W., Herman, J. P., & Seroogy, K. B. (2014). Stress exacerbates experimental Parkinson's disease. *Molecular Psychiatry*, *19*(6), Article 6. https://doi.org/10.1038/mp.2013.108

Henrich, M. T., Geibl, F. F., Lakshminarasimhan, H., Stegmann, A., Giasson, B. I., Mao, X., Dawson, V. L., Dawson, T. M., Oertel, W. H., & Surmeier, D. J. (2020). Determinants of seeding and spreading of α-synuclein pathology in the brain. *Science Advances*, *6*(46), eabc2487. https://doi.org/10.1126/sciadv.abc2487

Herman, J. P., McKlveen, J. M., Ghosal, S., Kopp, B., Wulsin, A., Makinson, R., Scheimann, J., & Myers, B. (2016). Regulation of the hypothalamic-pituitary-adrenocortical stress response. *Comprehensive Physiology*, *6*(2), 603–621. https://doi.org/10.1002/cphy.c150015

Hermanowicz, N., Jones, S. A., & Hauser, R. A. (2019). Impact of non-motor symptoms in Parkinson's disease: A PMDAlliance survey. *Neuropsychiatric Disease and Treatment*, *15*, 2205–2212. https://doi.org/10.2147/NDT.S213917

Hertz, L., & Zielke, H. R. (2004). Astrocytic control of glutamatergic activity: Astrocytes as stars of the show. *Trends in Neurosciences*, *27*(12), 735–743. https://doi.org/10.1016/j.tins.2004.10.008

Higa, M., Ohnuma, T., Maeshima, H., Hatano, T., Hanzawa, R., Shibata, N., Sakai, Y., Suzuki, T., & Arai, H. (2010). Association analysis between functional polymorphism of the rs4606 SNP in the RGS2 gene and antipsychotic-induced Parkinsonism in Japanese patients with schizophrenia: Results from the Juntendo University Schizophrenia Projects (JUSP). *Neuroscience Letters*, *469*(1), 55–59. https://doi.org/10.1016/j.neulet.2009.11.043

Hill, M. N., Hellemans, K. G. C., Verma, P., Gorzalka, B. B., & Weinberg, J. (2012). Neurobiology of chronic mild stress: Parallels to major depression. *Neuroscience and Biobehavioral Reviews*, *36*(9), 2085–2117. https://doi.org/10.1016/j.neubiorev.2012.07.001

Hilton, D., Stephens, M., Kirk, L., Edwards, P., Potter, R., Zajicek, J., Broughton, E., Hagan, H., & Carroll, C. (2014). Accumulation of α-synuclein in the bowel of patients in the pre-clinical phase of Parkinson's disease. *Acta Neuropathologica*, *127*(2), 235–241. https://doi.org/10.1007/s00401-013-1214-6

Holmqvist, S., Chutna, O., Bousset, L., Aldrin-Kirk, P., Li, W., Björklund, T., Wang, Z.-Y., Roybon, L., Melki, R., & Li, J.-Y. (2014). Direct evidence of Parkinson pathology spread from the gastrointestinal tract to the brain in rats. *Acta Neuropathologica*, *128*(6), 805–820. https://doi.org/10.1007/s00401-014-1343-6

Holmstrøm, K., Collins, M. D., Møller, T., Falsen, E., & Lawson, P. A. (2004). *Subdoligranulum variabile* gen. Nov., sp. Nov. From human feces. *Anaerobe*, *10*(3), 197–203. https://doi.org/10.1016/j.anaerobe.2004.01.004

Howells, F. M., Russell, V. A., Mabandla, M. V., & Kellaway, L. A. (2005). Stress reduces the neuroprotective effect of exercise in a rat model for Parkinson's disease. *Behavioural Brain Research*, *165*(2), 210–220. https://doi.org/10.1016/j.bbr.2005.06.044

Huang, H.-K., Wang, J.-H., Lei, W.-Y., Chen, C.-L., Chang, C.-Y., & Liou, L.-S. (2018). *Helicobacter pylori* infection is associated with an increased risk of Parkinson's disease: A population-based retrospective cohort study. *Parkinsonism & Related Disorders*, *47*, 26–31. https://doi.org/10.1016/j.parkreldis.2017.11.331

Hüls, S., Högen, T., Vassallo, N., Danzer, K. M., Hengerer, B., Giese, A., & Herms, J. (2011). AMPA-receptor-mediated excitatory synaptic transmission is enhanced by iron-induced α-synuclein oligomers. *Journal of Neurochemistry*, *117*(5), 868–878. https://doi.org/10.1111/j.1471-4159.2011.07254.x

Hunn, B. H., Vingill, S., Threlfell, S., Alegre-Abarrategui, J., Magdelyns, M., Deltheil, T., Bengoa-Vergniory, N., Oliver, P. L., Cioroch, M., Doig, N. M., Bannerman, D. M., Cragg, S. J., & Wade-Martins, R. (2019). Impairment of Macroautophagy in Dopamine Neurons Has Opposing Effects on Parkinsonian Pathology and Behavior. *Cell Reports*, *29*(4), 920. https://doi.org/10.1016/j.celrep.2019.09.029

Hutmacher, F. (2021). Putting Stress in Historical Context: Why It Is Important That Being Stressed Out Was Not a Way to Be a Person 2,000 Years Ago. *Frontiers in Psychology*, *12*. https://www.frontiersin.org/journals/psychology/articles/10.3389/fpsyg.2021.539799

Hyland, B. I., Reynolds, J. N. J., Hay, J., Perk, C. G., & Miller, R. (2002). Firing modes of midbrain dopamine cells in the freely moving rat. *Neuroscience*, *114*(2), 475–492. https://doi.org/10.1016/S0306-4522(02)00267-1

Idrissi, S. E., Fath, N., Ibork, H., Taghzouti, K., Alamy, M., & Abboussi, O. (2023). Restraint Stress Exacerbates Apoptosis in a 6-OHDA Animal Model of Parkinson Disease. *Neurotoxicity Research*, *41*(2), 166–176. https://doi.org/10.1007/s12640-022-00630-3

Imamura, K., Hishikawa, N., Sawada, M., Nagatsu, T., Yoshida, M., & Hashizume, Y. (2003). Distribution of major histocompatibility complex class II-positive microglia and cytokine profile of Parkinson's disease brains. *Acta Neuropathologica*, *106*(6), 518–526. https://doi.org/10.1007/s00401-003-0766-2

Iwai, A., Masliah, E., Yoshimoto, M., Ge, N., Flanagan, L., de Silva, H. A., Kittel, A., & Saitoh, T. (1995). The precursor protein of non-A beta component of Alzheimer's disease amyloid is a presynaptic protein of the central nervous system. *Neuron*, *14*(2), 467–475. https://doi.org/10.1016/0896-6273(95)90302-x

Iwanaga, K., Wakabayashi, K., Yoshimoto, M., Tomita, I., Satoh, H., Takashima, H., Satoh, A., Seto, M., Tsujihata, M., & Takahashi, H. (1999). Lewy body-type degeneration in cardiac plexus in Parkinson's and incidental Lewy body diseases. *Neurology*, *52*(6), 1269–1271. https://doi.org/10.1212/wnl.52.6.1269

Janakiraman, U., Manivasagam, T., Justin Thenmozhi, A., Dhanalakshmi, C., Essa, M. M., Song, B.-J., & Guillemin, G. J. (2017). Chronic mild stress augments MPTP induced neurotoxicity in a murine model of Parkinson's disease. *Physiology & Behavior*, *173*, 132–143. https://doi.org/10.1016/j.physbeh.2017.01.046

Janda, E., Parafati, M., Martino, C., Crupi, F., George William, J. N., Reybier, K., Arbitrio, M., Mollace, V., & Boutin, J. A. (2023). Autophagy and neuroprotection in astrocytes exposed to 6-hydroxydopamine is negatively regulated by NQO2: Relevance to Parkinson's disease. *Scientific Reports*, *13*(1), 21624. https://doi.org/10.1038/s41598-023-44666-7

Janezic, S., Threlfell, S., Dodson, P. D., Dowie, M. J., Taylor, T. N., Potgieter, D., Parkkinen, L., Senior, S. L., Anwar, S., Ryan, B., Deltheil, T., Kosillo, P., Cioroch, M., Wagner, K., Ansorge, O., Bannerman, D. M., Bolam, J. P., Magill, P. J., Cragg, S. J., & Wade-Martins, R. (2013). Deficits in dopaminergic transmission precede neuron loss and dysfunction in a new Parkinson model. *Proceedings of the National Academy of Sciences of the United States of America*, *110*(42), E4016-4025. https://doi.org/10.1073/pnas.1309143110

Jankord, R., & Herman, J. P. (2008). Limbic Regulation of Hypothalamo-Pituitary-Adrenocortical Function during Acute and Chronic Stress. *Annals of the New York Academy of Sciences*, *1148*(1), 64–73. https://doi.org/10.1196/annals.1410.012

Jensen, P. H., Hager, H., Nielsen, M. S., Hojrup, P., Gliemann, J., & Jakes, R. (1999). Alpha-synuclein binds to Tau and stimulates the protein kinase A-catalyzed tau phosphorylation of serine residues 262 and 356. *The Journal of Biological Chemistry*, *274*(36), 25481–25489. https://doi.org/10.1074/jbc.274.36.25481

Jo, S., Kang, W., Hwang, Y. S., Lee, S. H., Park, K. W., Kim, M. S., Lee, H., Yoon, H. J., Park, Y. K., Chalita, M., Lee, J. H., Sung, H., Lee, J.-Y., Bae, J.-W., & Chung, S. J. (2022). Oral and gut dysbiosis leads to functional alterations in Parkinson's disease. *Npj Parkinson's Disease*, *8*(1), 1–12. https://doi.org/10.1038/s41531-022-00351-6

Joëls, M., Pu, Z., Wiegert, O., Oitzl, M. S., & Krugers, H. J. (2006). Learning under stress: How does it work? *Trends in Cognitive Sciences*, *10*(4), 152–158. https://doi.org/10.1016/j.tics.2006.02.002

Johnson, M. E., Stecher, B., Labrie, V., Brundin, L., & Brundin, P. (2019). Triggers, Facilitators, and Aggravators: Redefining Parkinson's Disease Pathogenesis. *Trends in Neurosciences*, *42*(1), 4–13. https://doi.org/10.1016/j.tins.2018.09.007

Jones-Tabah, J. (2023). Targeting G Protein-Coupled Receptors in the Treatment of Parkinson's Disease. *Journal of Molecular Biology*, *435*(12), 167927. https://doi.org/10.1016/j.jmb.2022.167927

Joniec, I., Ciesielska, A., Kurkowska-Jastrzebska, I., Przybylkowski, A., Czlonkowska, A., & Czlonkowski, A. (2009). Age- and sex-differences in the nitric oxide synthase expression and dopamine concentration in the murine model of Parkinson's disease induced by 1-methyl-4-phenyl-1,2,3,6-tetrahydropyridine. *Brain Research*, *1261*, 7–19. https://doi.org/10.1016/j.brainres.2008.12.081

Kaelberer, M. M., Buchanan, K. L., Klein, M. E., Barth, B. B., Montoya, M. M., Shen, X., & Bohórquez, D. V. (2018). A gut-brain neural circuit for nutrient sensory transduction. *Science (New York, N.Y.)*, *361*(6408), eaat5236. https://doi.org/10.1126/science.aat5236

Kalaitzakis, M. E., Graeber, M. B., Gentleman, S. M., & Pearce, R. K. B. (2008). The dorsal motor nucleus of the vagus is not an obligatory trigger site of Parkinson's disease: A critical analysis of alpha-synuclein staging. *Neuropathology and Applied Neurobiology*, *34*(3), 284–295. https://doi.org/10.1111/j.1365-2990.2007.00923.x

Kamp, F., Exner, N., Lutz, A. K., Wender, N., Hegermann, J., Brunner, B., Nuscher, B., Bartels, T., Giese, A., Beyer, K., Eimer, S., Winklhofer, K. F., & Haass, C. (2010). Inhibition of mitochondrial fusion by α-synuclein is rescued by PINK1, Parkin and DJ-1. *The EMBO Journal*, *29*(20), 3571–3589. https://doi.org/10.1038/emboj.2010.223

Kang, M.-J., Baek, K.-R., Lee, Y.-R., Kim, G.-H., & Seo, S.-O. (2022). Production of Vitamin K by Wild-Type and Engineered Microorganisms. *Microorganisms*, *10*(3), 554. https://doi.org/10.3390/microorganisms10030554

Karampetsou, M., Ardah, M. T., Semitekolou, M., Polissidis, A., Samiotaki, M., Kalomoiri, M., Majbour, N., Xanthou, G., El-Agnaf, O. M. A., & Vekrellis, K. (2017). Phosphorylated exogenous alpha-synuclein fibrils exacerbate pathology

and induce neuronal dysfunction in mice. *Scientific Reports*, *7*(1), Article 1. https://doi.org/10.1038/s41598-017-15813-8

Karampetsou, M., Vekrellis, K., & Melachroinou, K. (2022). The promise of the TGF-β superfamily as a therapeutic target for Parkinson's disease. *Neurobiology of Disease*, *171*, 105805. https://doi.org/10.1016/j.nbd.2022.105805

Keefe, K. A., Stricker, E. M., Zigmond, M. J., & Abercrombie, E. D. (1990). Environmental stress increases extracellular dopamine in striatum of 6-hydroxydopamine-treated rats: In vivo microdialysis studies. *Brain Research*, *527*(2), 350–353. https://doi.org/10.1016/0006-8993(90)91158-D

Kelly, K. A., Miller, D. B., Bowyer, J. F., & O'Callaghan, J. P. (2012). Chronic exposure to corticosterone enchances the neuroinflammatory and neurotoxic responses to methamphetamine. *Journal of Neurochemistry*, *122*(5), 995–1009. https://doi.org/10.1111/j.1471-4159.2012.07864.x

Khoja, S., Shah, V., Garcia, D., Asatryan, L., Jakowec, M. W., & Davies, D. L. (2016). Role of Purinergic P2X4 Receptors in Regulating Striatal Dopamine Homeostasis and Dependent Behaviors. *Journal of Neurochemistry*, *139*(1), 134–148. https://doi.org/10.1111/jnc.13734

Kim, C., Ho, D.-H., Suk, J.-E., You, S., Michael, S., Kang, J., Joong Lee, S., Masliah, E., Hwang, D., Lee, H.-J., & Lee, S.-J. (2013). Neuron-released oligomeric α-synuclein is an endogenous agonist of TLR2 for paracrine activation of microglia. *Nature Communications*, *4*(1), 1562. https://doi.org/10.1038/ncomms2534

Kim, C., Rockenstein, E., Spencer, B., Kim, H.-K., Adame, A., Trejo, M., Stafa, K., Lee, H.-J., Lee, S.-J., & Masliah, E. (2015). Antagonizing Neuronal Toll-like Receptor 2 Prevents Synucleinopathy by Activating Autophagy. *Cell Reports*, *13*(4), 771–782. https://doi.org/10.1016/j.celrep.2015.09.044

Kim, S., Kwon, S.-H., Kam, T.-I., Panicker, N., Karuppagounder, S. S., Lee, S., Lee, J. H., Kim, W. R., Kook, M., Foss, C. A., Shen, C., Lee, H., Kulkarni, S., Pasricha, P. J., Lee, G., Pomper, M. G., Dawson, V. L., Dawson, T. M., & Ko, H. S. (2019). Transneuronal Propagation of Pathologic α-Synuclein from the Gut to the Brain Models Parkinson's Disease. *Neuron*, *103*(4), 627-641.e7. https://doi.org/10.1016/j.neuron.2019.05.035

Kisos, H., Ben-Gedalya, T., & Sharon, R. (2014). The Clathrin-Dependent Localization of Dopamine Transporter to Surface Membranes Is Affected by α-Synuclein. *Journal of Molecular Neuroscience*, *52*(2), 167–176. https://doi.org/10.1007/s12031-013-0118-1

Kita, T., Wagner, G. C., & Nakashima, T. (2003). Current research on methamphetamine-induced neurotoxicity: Animal models of monoamine disruption. *Journal of Pharmacological Sciences*, *92*(3), 178–195. https://doi.org/10.1254/jphs.92.178

Klæstrup, I. H., Just, M. K., Holm, K. L., Alstrup, A. K. O., Romero-Ramos, M., Borghammer, P., & Van Den Berge, N. (2022). Impact of aging on animal models of Parkinson's disease. *Frontiers in Aging Neuroscience*, *14*, 909273. https://doi.org/10.3389/fnagi.2022.909273

Klegeris, A., Giasson, B. I., Zhang, H., Maguire, J., Pelech, S., & McGeer, P. L. (2006). Alpha-synuclein and its disease-causing mutants induce ICAM-1 and IL-6 in human astrocytes and astrocytoma cells. *The FASEB Journal*, *20*(12), 2000–2008. https://doi.org/10.1096/fj.06-6183com

Kluyver, A. J., & Niel, C. B. van. (1936). *Prospects for a natural system of classification of bacteria*. G. Fischer.

Kochmanski, J., Kuhn, N. C., & Bernstein, A. I. (2022). Parkinson's disease-associated, sex-specific changes in DNA methylation at PARK7 (DJ-1), SLC17A6 (VGLUT2), PTPRN2 (IA-2β), and NR4A2 (NURR1) in cortical neurons. *Npj Parkinson's Disease*, *8*(1), 1–13. https://doi.org/10.1038/s41531-022-00355-2

Kokras, N., Dioli, C., Paravatou, R., Sotiropoulos, M. G., Delis, F., Antoniou, K., Calogeropoulou, T., Charalampopoulos, I., Gravanis, A., & Dalla, C. (2020). Psychoactive properties of BNN27, a novel neurosteroid derivate, in male and female rats. *Psychopharmacology*, *237*(8), 2435–2449. https://doi.org/10.1007/s00213-020-05545-5

Kong, H., Yang, L., He, C., Zhou, J.-W., Li, W.-Z., Wu, W.-N., Chen, H.-Q., & Yin, Y.-Y. (2019). Chronic unpredictable mild stress accelerates lipopolysaccharide- induced microglia activation and damage of dopaminergic neurons in rats. *Pharmacology Biochemistry and Behavior*, *179*, 142–149. https://doi.org/10.1016/j.pbb.2019.01.004

Koolhaas, J. M., Bartolomucci, A., Buwalda, B., de Boer, S. F., Flügge, G., Korte, S. M., Meerlo, P., Murison, R., Olivier, B., Palanza, P., Richter-Levin, G., Sgoifo, A., Steimer, T., Stiedl, O., van Dijk, G., Wöhr, M., & Fuchs, E. (2011). Stress revisited: A critical evaluation of the stress concept. *Neuroscience and Biobehavioral Reviews*, *35*(5), 1291–1301. https://doi.org/10.1016/j.neubiorev.2011.02.003

Koprich, J. B., Johnston, T. H., Huot, P., Reyes, M. G., Espinosa, M., & Brotchie, J. M. (2011). Progressive Neurodegeneration or Endogenous Compensation in an Animal Model of Parkinson's Disease Produced by Decreasing Doses of Alpha-Synuclein. *PLOS ONE*, *6*(3), e17698. https://doi.org/10.1371/journal.pone.0017698

Kordower, J. H., Chu, Y., Hauser, R. A., Freeman, T. B., & Olanow, C. W. (2008). Lewy body-like pathology in long-term embryonic nigral transplants in Parkinson's disease. *Nature Medicine*, *14*(5), 504–506. https://doi.org/10.1038/nm1747

Kotzbauer, P. T., Giasson, B. I., Kravitz, A. V., Golbe, L. I., Mark, M. H., Trojanowski, J. Q., & Lee, V. M.-Y. (2004). Fibrillization of α-synuclein and tau in familial Parkinson's disease caused by the A53T α-synuclein mutation. *Experimental Neurology*, *187*(2), 279–288. https://doi.org/10.1016/j.expneurol.2004.01.007

Koutmani, Y., Gampierakis, I. A., Polissidis, A., Ximerakis, M., Koutsoudaki, P. N., Polyzos, A., Agrogiannis, G., Karaliota, S., Thomaidou, D., Rubin, L. L., Politis, P. K., & Karalis, K. P. (2019). CRH Promotes the Neurogenic Activity of Neural Stem Cells in the Adult Hippocampus. *Cell Reports*, *29*(4), 932-945.e7. https://doi.org/10.1016/j.celrep.2019.09.037

Krüger, R., Kuhn, W., Müller, T., Woitalla, D., Graeber, M., Kösel, S., Przuntek, H., Epplen, J. T., Schöls, L., & Riess, O. (1998). Ala30Pro mutation in the gene encoding alpha-synuclein in Parkinson's disease. *Nature Genetics*, *18*(2), 106–108. https://doi.org/10.1038/ng0298-106

Krzisch, M., Yuan, B., Chen, W., Osaki, T., Fu, D., Garrett-Engele, C. M., Svoboda, D. S., Andrykovich, K. R., Gallagher, M. D., Sur, M., & Jaenisch, R. (2024). The A53T mutation in α-synuclein enhances pro-inflammatory activation in human microglia upon inflammatory stimulus. *Biological Psychiatry*, *0*(0). https://doi.org/10.1016/j.biopsych.2024.07.011

Kumar, R., Sanawar, R., Li, X., & Li, F. (2017). Structure, biochemistry, and biology of PAK kinases. *Gene*, *605*, 20–31. https://doi.org/10.1016/j.gene.2016.12.014

Kurz, A., Double, K. L., Lastres-Becker, I., Tozzi, A., Tantucci, M., Bockhart, V., Bonin, M., García-Arencibia, M., Nuber, S., Schlaudraff, F., Liss, B., Fernández-Ruiz, J., Gerlach, M., Wüllner, U., Lüddens, H., Calabresi, P., Auburger, G., & Gispert, S. (2010). A53T-Alpha-Synuclein Overexpression Impairs Dopamine Signaling and Striatal Synaptic Plasticity in Old Mice. *PLOS ONE*, *5*(7), e11464. https://doi.org/10.1371/journal.pone.0011464

L, C., & Mb, F. (2005). Alpha-synuclein phosphorylation controls neurotoxicity and inclusion formation in a Drosophila model of Parkinson disease. *Nature Neuroscience*, *8*(5). https://doi.org/10.1038/nn1443

Lam, H. A., Wu, N., Cely, I., Kelly, R. L., Hean, S., Richter, F., Magen, I., Cepeda, C., Ackerson, L. C., Walwyn, W., Masliah, E., Chesselet, M.-F., Levine, M. S., & Maidment, N. T. (2011). Elevated tonic extracellular dopamine concentration and altered dopamine modulation of synaptic activity precede dopamine loss in the striatum of mice overexpressing human α-synuclein. *Journal of Neuroscience Research*, *89*(7), 1091–1102. https://doi.org/10.1002/jnr.22611

Langston, J. W., Ballard, P., Tetrud, J. W., & Irwin, I. (1983). Chronic Parkinsonism in humans due to a product of meperidine-analog synthesis. *Science (New York, N.Y.)*, *219*(4587), 979–980. https://doi.org/10.1126/science.6823561

Lashuel, H. A., & Lansbury, P. T. (2006). Are amyloid diseases caused by protein aggregates that mimic bacterial pore-forming toxins? *Quarterly Reviews of Biophysics*, *39*(2), 167–201. https://doi.org/10.1017/S0033583506004422

Lashuel, H. A., Petre, B. M., Wall, J., Simon, M., Nowak, R. J., Walz, T., & Lansbury, P. T. (2002). Alpha-synuclein, especially the Parkinson's disease-associated mutants, forms pore-like annular and tubular protofibrils. *Journal of Molecular Biology*, *322*(5), 1089–1102. https://doi.org/10.1016/s0022-2836(02)00735-0

Lauretti, E., Di Meco, A., Merali, S., & Praticò, D. (2016). Chronic behavioral stress exaggerates motor deficit and neuroinflammation in the MPTP mouse model of Parkinson's disease. *Translational Psychiatry*, *6*(2), e733. https://doi.org/10.1038/tp.2016.1

Lautenschläger, J., Stephens, A. D., Fusco, G., Ströhl, F., Curry, N., Zacharopoulou, M., Michel, C. H., Laine, R., Nespovitaya, N., Fantham, M., Pinotsi, D., Zago, W., Fraser, P., Tandon, A., St George-Hyslop, P., Rees, E., Phillips, J. J., De Simone, A., Kaminski, C. F., & Schierle, G. S. K. (2018). C-terminal calcium binding of α-synuclein modulates synaptic vesicle interaction. *Nature Communications*, *9*(1), 712. https://doi.org/10.1038/s41467-018-03111-4

Leandrou, E., Chalatsa, I., Anagnostou, D., Machalia, C., Semitekolou, M., Filippa, V., Makridakis, M., Vlahou, A., Anastasiadou, E., Vekrellis, K., & Emmanouilidou, E. (2024). α-Synuclein oligomers potentiate neuroinflammatory NF-κB activity and induce Cav3.2 calcium signaling in astrocytes. *Translational Neurodegeneration*, *13*(1), 11. https://doi.org/10.1186/s40035-024-00401-4

Lee, E.-J., Woo, M.-S., Moon, P.-G., Baek, M.-C., Choi, I.-Y., Kim, W.-K., Junn, E., & Kim, H.-S. (2010). Alpha-synuclein activates microglia by inducing the expressions of matrix metalloproteinases and the subsequent activation of protease-activated receptor-1. *Journal of Immunology (Baltimore, Md.: 1950)*, *185*(1), 615–623. https://doi.org/10.4049/jimmunol.0903480

Lee, H.-J., Khoshaghideh, F., Lee, S., & Lee, S.-J. (2006). Impairment of microtubule-dependent trafficking by overexpression of α-synuclein. *European Journal of Neuroscience*, *24*(11), 3153–3162. https://doi.org/10.1111/j.1460-9568.2006.05210.x

Lee, H.-J., Suk, J.-E., Patrick, C., Bae, E.-J., Cho, J.-H., Rho, S., Hwang, D., Masliah, E., & Lee, S.-J. (2010). Direct transfer of alpha-synuclein from neuron to astroglia causes inflammatory responses in synucleinopathies. *The Journal of Biological Chemistry*, *285*(12), 9262–9272. https://doi.org/10.1074/jbc.M109.081125

Lee, H.-S., Lobbestael, E., Vermeire, S., Sabino, J., & Cleynen, I. (2021). Inflammatory bowel disease and Parkinson's disease: Common pathophysiological links. *Gut*, *70*(2), 408–417. https://doi.org/10.1136/gutjnl-2020-322429

Lee, Y. H., Cha, J., Chung, S. J., Yoo, H. S., Sohn, Y. H., Ye, B. S., & Lee, P. H. (2019). Beneficial effect of estrogen on nigrostriatal dopaminergic neurons in drug-naïve postmenopausal Parkinson's disease. *Scientific Reports*, *9*(1), 10531. https://doi.org/10.1038/s41598-019-47026-6

Lesage, S., Anheim, M., Letournel, F., Bousset, L., Honoré, A., Rozas, N., Pieri, L., Madiona, K., Dürr, A., Melki, R., Verny, C., Brice, A., & Group, for the F. P. D. G. S. (2013). G51D α-synuclein mutation causes a novel Parkinsonian–pyramidal syndrome. *Annals of Neurology*, *73*(4), 459–471. https://doi.org/10.1002/ana.23894

Li, J.-Y., Englund, E., Holton, J. L., Soulet, D., Hagell, P., Lees, A. J., Lashley, T., Quinn, N. P., Rehncrona, S., Björklund, A., Widner, H., Revesz, T., Lindvall, O., & Brundin, P. (2008). Lewy bodies in grafted neurons in subjects with Parkinson's disease suggest host-to-graft disease propagation. *Nature Medicine*, *14*(5), 501–503. https://doi.org/10.1038/nm1746

Li, R., Lu, Y., Zhang, Q., Liu, W., Yang, R., Jiao, J., Liu, J., Gao, G., & Yang, H. (2022). Piperine promotes autophagy flux by P2RX4 activation in SNCA/α-synuclein-induced Parkinson disease model. *Autophagy*, *18*(3), 559–575. https://doi.org/10.1080/15548627.2021.1937897

Li, W., West, N., Colla, E., Pletnikova, O., Troncoso, J. C., Marsh, L., Dawson, T. M., Jäkälä, P., Hartmann, T., Price, D. L., & Lee, M. K. (2005). Aggregation promoting C-terminal truncation of α-synuclein is a normal cellular process and is enhanced by the familial Parkinson's disease-linked mutations. *Proceedings of the National Academy of Sciences*, *102*(6), 2162–2167. https://doi.org/10.1073/pnas.0406976102

Li, W., Wu, X., Hu, X., Wang, T., Liang, S., Duan, Y., Jin, F., & Qin, B. (2017). Structural changes of gut microbiota in Parkinson's disease and its correlation with clinical features. *Science China Life Sciences*, *60*(11), 1223–1233. https://doi.org/10.1007/s11427-016-9001-4

Lim, S., Chun, Y., Lee, J. S., & Lee, S.-J. (2016). Neuroinflammation in Synucleinopathies. *Brain Pathology (Zurich, Switzerland)*, *26*(3), 404–409. https://doi.org/10.1111/bpa.12371

Lim, Y., Kehm, V. M., Lee, E. B., Soper, J. H., Li, C., Trojanowski, J. Q., & Lee, V. M.-Y. (2011). α-Syn Suppression Reverses Synaptic and Memory Defects in a Mouse Model of Dementia with Lewy Bodies. *The Journal of Neuroscience*, *31*(27), 10076–10087. https://doi.org/10.1523/JNEUROSCI.0618-11.2011

Lin, R., Wang, Z., Cao, J., Gao, T., Dong, Y., & Chen, Y. (2021). Role of melatonin in murine "restraint stress"-induced dysfunction of colonic microbiota. *Journal of Microbiology*, *59*(5), 500–512. https://doi.org/10.1007/s12275-021-0305-7

Lin, X., Parisiadou, L., Gu, X.-L., Wang, L., Shim, H., Sun, L., Xie, C., Long, C.-X., Yang, W.-J., Ding, J., Chen, Z. Z., Gallant, P. E., Tao-Cheng, J.-H., Rudow, G., Troncoso, J. C., Liu, Z., Li, Z., & Cai, H. (2009). Leucine-Rich Repeat Kinase 2 Regulates the Progression of Neuropathology Induced by Parkinson's-Disease-Related Mutant α-synuclein. *Neuron*, *64*(6), 807–827. https://doi.org/10.1016/j.neuron.2009.11.006

Lin-ya, Z. G. L. F. X. W. G. Y. Z. B. L. W. Y. (2024). Differential expression analysis of the transcriptome for human basal ganglia from normal donors and Parkinson's disease patients. *Acta Anatomica Sinica*, *55*(4), 482. https://doi.org/10.16098/j.issn.0529-1356.2024.04.015

Liu, B., Fang, F., Pedersen, N. L., Tillander, A., Ludvigsson, J. F., Ekbom, A., Svenningsson, P., Chen, H., & Wirdefeldt, K. (2017). Vagotomy and Parkinson disease. *Neurology*, *88*(21), 1996–2002. https://doi.org/10.1212/WNL.0000000000003961

Liu, G., Yu, J., Ding, J., Xie, C., Sun, L., Rudenko, I., Zheng, W., Sastry, N., Luo, J., Rudow, G., Troncoso, J. C., & Cai, H. (2014). Aldehyde dehydrogenase 1 defines and protects a nigrostriatal dopaminergic neuron subpopulation. *The Journal of Clinical Investigation*, *124*(7), 3032–3046. https://doi.org/10.1172/JCI72176

Liu, G., Zhang, C., Yin, J., Li, X., Cheng, F., Li, Y., Yang, H., Uéda, K., Chan, P., & Yu, S. (2009). Alpha-Synuclein is differentially expressed in mitochondria from different rat brain regions and dose-dependently down-regulates complex I activity. *Neuroscience Letters*, *454*(3), 187–192. https://doi.org/10.1016/j.neulet.2009.02.056

Liu, H., Koros, C., Strohäker, T., Schulte, C., Bozi, M., Varvaresos, S., Ibáñez de Opakua, A., Simitsi, A. M., Bougea, A., Voumvourakis, K., Maniati, M., Papageorgiou, S. G., Hauser, A.-K., Becker, S., Zweckstetter, M., Stefanis, L., & Gasser, T. (2021). A Novel SNCA A30G Mutation Causes Familial Parkinson's Disease. *Movement Disorders*, *36*(7), 1624–1633. https://doi.org/10.1002/mds.28534

Liu, Q., Xu, Y., Wan, W., & Ma, Z. (2018). An unexpected improvement in spatial learning and memory ability in alpha-synuclein A53T transgenic mice. *Journal of Neural Transmission*, *125*(2), 203–210. https://doi.org/10.1007/s00702-017-1819-3

Livak, K. J., & Schmittgen, T. D. (2001). Analysis of relative gene expression data using real-time quantitative PCR and the 2(-Delta Delta C(T)) Method. *Methods (San Diego, Calif.)*, *25*(4), 402–408. https://doi.org/10.1006/meth.2001.1262

Loftis, J. M., & Janowsky, A. (2014). Neuroimmune Basis of Methamphetamine Toxicity. *International Review of Neurobiology*, *118*, 165–197. https://doi.org/10.1016/B978-0-12-801284-0.00007-5

Longhena, F., Faustini, G., Spillantini, M. G., & Bellucci, A. (2019). Living in Promiscuity: The Multiple Partners of Alpha-Synuclein at the Synapse in Physiology and Pathology. *International Journal of Molecular Sciences*, *20*(1), Article 1. https://doi.org/10.3390/ijms20010141

Lu, Y., Prudent, M., Fauvet, B., Lashuel, H. A., & Girault, H. H. (2011). Phosphorylation of α-Synuclein at Y125 and S129 Alters Its Metal Binding Properties: Implications for Understanding the Role of α-Synuclein in the Pathogenesis of Parkinson's Disease and Related Disorders. *ACS Chemical Neuroscience*, *2*(11), 667–675. https://doi.org/10.1021/cn200074d

Luk, K. C., Kehm, V., Carroll, J., Zhang, B., O'Brien, P., Trojanowski, J. Q., & Lee, V. M.-Y. (2012). Pathological α-Synuclein Transmission Initiates Parkinson-like Neurodegeneration in Nontransgenic Mice. *Science*, *338*(6109), 949–953. https://doi.org/10.1126/science.1227157

Luna, E., Decker, S. C., Riddle, D. M., Caputo, A., Zhang, B., Cole, T., Caswell, C., Xie, S. X., Lee, V. M. Y., & Luk, K. C. (2018). Differential α-synuclein expression contributes to selective vulnerability of hippocampal neuron subpopulations to fibril-induced toxicity. *Acta Neuropathologica*, *135*(6), 855–875. https://doi.org/10.1007/s00401-018-1829-8

Lwin, A., Orvisky, E., Goker-Alpan, O., LaMarca, M. E., & Sidransky, E. (2004). Glucocerebrosidase mutations in subjects with parkinsonism. *Molecular Genetics and Metabolism*, *81*(1), 70–73. https://doi.org/10.1016/j.ymgme.2003.11.004

Ma, J., Gao, J., Niu, M., Zhang, X., Wang, J., & Xie, A. (2020). P2X4R Overexpression Upregulates Interleukin-6 and Exacerbates 6-OHDA-Induced Dopaminergic Degeneration in a Rat Model of PD. *Frontiers in Aging Neuroscience*, *12*. https://doi.org/10.3389/fnagi.2020.580068

Maguire, J. (2019). Neuroactive Steroids and GABAergic Involvement in the Neuroendocrine Dysfunction Associated With Major Depressive Disorder and Postpartum Depression. *Frontiers in Cellular Neuroscience*, *13*, 83. https://doi.org/10.3389/fncel.2019.00083

Mangiavacchi, S., Masi, F., Scheggi, S., Leggio, B., De Montis, M. G., & Gambarana, C. (2001). Long-term behavioral and neurochemical effects of chronic stress exposure in rats. *Journal of Neurochemistry*, *79*(6), 1113–1121. https://doi.org/10.1046/j.1471-4159.2001.00665.x

Manning-Bog, A. B., McCormack, A. L., Li, J., Uversky, V. N., Fink, A. L., & Di Monte, D. A. (2002). The herbicide paraquat causes up-regulation and aggregation of alpha-synuclein in mice: Paraquat and alpha-synuclein. *The Journal of Biological Chemistry*, *277*(3), 1641–1644. https://doi.org/10.1074/jbc.C100560200

Mansour, M. A., Rahman, M., Ayad, A. A., Warrington, A. E., & Burns, T. C. (2023). P21 Overexpression Promotes Cell Death and Induces Senescence in Human Glioblastoma. *Cancers*, *15*(4), Article 4. https://doi.org/10.3390/cancers15041279

Mao, L., Zhang, Y., Tian, J., Sang, M., Zhang, G., Zhou, Y., & Wang, P. (2021). Cross-Sectional Study on the Gut Microbiome of Parkinson's Disease Patients in Central China. *Frontiers in Microbiology*, *12*. https://www.frontiersin.org/articles/10.3389/fmicb.2021.728479

Marchitti, S. A., Deitrich, R. A., & Vasiliou, V. (2007). Neurotoxicity and metabolism of the catecholamine-derived 3,4-dihydroxyphenylacetaldehyde and 3,4-dihydroxyphenylglycolaldehyde: The role of aldehyde dehydrogenase. *Pharmacological Reviews*, *59*(2), 125–150. https://doi.org/10.1124/pr.59.2.1

Maroteaux, L., Campanelli, J. T., & Scheller, R. H. (1988). Synuclein: A neuron-specific protein localized to the nucleus and presynaptic nerve terminal. *The Journal of Neuroscience: The Official Journal of the Society for Neuroscience*, *8*(8), 2804–2815. https://doi.org/10.1523/JNEUROSCI.08-08-02804.1988

Martinez-Vicente, M., Talloczy, Z., Kaushik, S., Massey, A. C., Mazzulli, J., Mosharov, E. V., Hodara, R., Fredenburg, R., Wu, D.-C., Follenzi, A., Dauer, W., Przedborski, S., Ischiropoulos, H., Lansbury, P. T., Sulzer, D., & Cuervo, A. M. (2008). Dopamine-modified alpha-synuclein blocks chaperone-mediated autophagy. *The Journal of Clinical Investigation*, *118*(2), 777–788. https://doi.org/10.1172/JCI32806

Masliah, E., Rockenstein, E., Veinbergs, I., Mallory, M., Hashimoto, M., Takeda, A., Sagara, Y., Sisk, A., & Mucke, L. (2000). Dopaminergic loss and inclusion body formation in alpha-synuclein mice: Implications for neurodegenerative disorders. *Science (New York, N.Y.)*, *287*(5456), 1265–1269. https://doi.org/10.1126/science.287.5456.1265

Masuda-Suzukake, M., Nonaka, T., Hosokawa, M., Oikawa, T., Arai, T., Akiyama, H., Mann, D. M. A., & Hasegawa, M. (2013). Prion-like spreading of pathological α-synuclein in brain. *Brain: A Journal of Neurology*, *136*(Pt 4), 1128–1138. https://doi.org/10.1093/brain/awt037

Mazzulli, J. R., Xu, Y.-H., Sun, Y., Knight, A. L., McLean, P. J., Caldwell, G. A., Sidransky, E., Grabowski, G. A., & Krainc, D. (2011). Gaucher disease glucocerebrosidase and α-synuclein form a bidirectional pathogenic loop in synucleinopathies. *Cell*, *146*(1), 37–52. https://doi.org/10.1016/j.cell.2011.06.001

Mazzulli, J. R., Zunke, F., Isacson, O., Studer, L., & Krainc, D. (2016). α-Synuclein–induced lysosomal dysfunction occurs through disruptions in protein trafficking in human midbrain synucleinopathy models. *Proceedings of the National Academy of Sciences*, *113*(7), 1931–1936. https://doi.org/10.1073/pnas.1520335113

McCormick, C. M., Robarts, D., Kopeikina, K., & Kelsey, J. E. (2005). Long-lasting, sex- and age-specific effects of social stressors on corticosterone responses to restraint and on locomotor responses to psychostimulants in rats. *Hormones and Behavior*, *48*(1), 64–74. https://doi.org/10.1016/j.yhbeh.2005.01.008

McEwen, B. S. (2007). Physiology and neurobiology of stress and adaptation: Central role of the brain. *Physiological Reviews*, *87*(3), 873–904. https://doi.org/10.1152/physrev.00041.2006

McFarland, N. R., Fan, Z., Xu, K., Schwarzschild, M. A., Feany, M. B., Hyman, B. T., & McLean, P. J. (2009). Alpha-synuclein S129 phosphorylation mutants do not alter nigrostriatal toxicity in a rat model of Parkinson disease. *Journal of Neuropathology and Experimental Neurology*, *68*(5), 515–524. https://doi.org/10.1097/NEN.0b013e3181a24b53

McGee, D. J., Lu, X.-H., & Disbrow, E. A. (2018). Stomaching the Possibility of a Pathogenic Role for Helicobacter pylori in Parkinson's Disease. *Journal of Parkinson's Disease*, *8*(3), 367–374. https://doi.org/10.3233/JPD-181327

McGeer, P. L., Itagaki, S., Boyes, B. E., & McGeer, E. G. (1988). Reactive microglia are positive for HLA-DR in the substantia nigra of Parkinson's and Alzheimer's disease brains. *Neurology*, *38*(8), 1285–1291. https://doi.org/10.1212/wnl.38.8.1285

Melachroinou, K., Divolis, G., Tsafaras, G., Karampetsou, M., Fortis, S., Stratoulias, Y., Papadopoulou, G., Kriebardis, A. G., Samiotaki, M., & Vekrellis, K. (2024). Endogenous Alpha-Synuclein is Essential for the Transfer of Pathology by Exosome-Enriched Extracellular Vesicles, Following Inoculation with Preformed Fibrils in vivo. *Aging and Disease*, *15*(2), 869–892. https://doi.org/10.14336/AD.2023.0614

Melief, E. J., McKinley, J. W., Lam, J. Y., Whiteley, N. M., Gibson, A. W., Neumaier, J. F., Henschen, C. W., Palmiter, R. D., Bamford, N. S., & Darvas, M. (2018). Loss of glutamate signaling from the thalamus to dorsal striatum impairs motor function and slows the execution of learned behaviors. *Npj Parkinson's Disease*, *4*(1), 1–11. https://doi.org/10.1038/s41531-018-0060-6

Melrose, H. L., Kent, C. B., Taylor, J. P., Dachsel, J. C., Hinkle, K. M., Lincoln, S. J., Mok, S. S., Culvenor, J. G., Masters, C. L., Tyndall, G. M., Bass, D. I., Ahmed, Z., Andorfer, C. A., Ross, O. A., Wszolek, Z. K., Delldonne, A., Dickson, D. W., & Farrer, M. J. (2007). A comparative analysis of leucine-rich repeat kinase 2 (Lrrk2) expression in mouse brain and Lewy body disease. *Neuroscience*, *147*(4), 1047–1058. https://doi.org/10.1016/j.neuroscience.2007.05.027

Meng, F., Liu, J., Dai, J., Lian, H., Jiang, S., Li, Q., Wu, M., Wang, W., Wang, D., Zhao, D., Liu, C., Qiu, C., & Li, C. (2021). PPM1F in Dentate Gyrus Modulates Anxiety-Related Behaviors by Regulating BDNF Expression via AKT/JNK/p-H3S10 Pathway. *Molecular Neurobiology*, *58*(7), 3529–3544. https://doi.org/10.1007/s12035-021-02340-x

Meoni, S., Macerollo, A., & Moro, E. (2020). Sex differences in movement disorders. *Nature Reviews Neurology*, *16*(2), 84–96. https://doi.org/10.1038/s41582-019-0294-x

Metz, G. A. (2007). Stress as a modulator of motor system function and pathology. *Reviews in the Neurosciences*, *18*(3–4), 209–222. https://doi.org/10.1515/revneuro.2007.18.3-4.209

Mezias, C., Rey, N., Brundin, P., & Raj, A. (2020). Neural connectivity predicts spreading of alpha-synuclein pathology in fibril-injected mouse models: Involvement of retrograde and anterograde axonal propagation. *Neurobiology of Disease*, *134*, 104623. https://doi.org/10.1016/j.nbd.2019.104623

Michell, A. W., Tofaris, G. K., Gossage, H., Tyers, P., Spillantini, M. G., & Barker, R. A. (2007). The Effect of Truncated Human α-Synuclein (1–120) on Dopaminergic Cells in a Transgenic Mouse Model of Parkinson's Disease. *Cell Transplantation*, *16*(5), 461–474. https://doi.org/10.3727/000000007783464911

Middeldorp, J., & Hol, E. M. (2011). GFAP in health and disease. *Progress in Neurobiology*, *93*(3), 421–443. https://doi.org/10.1016/j.pneurobio.2011.01.005

Miklós, I. H., & Kovács, K. J. (2002). GABAergic innervation of corticotropin-releasing hormone (CRH)-secreting parvocellular neurons and its plasticity as demonstrated by quantitative immunoelectron microscopy. *Neuroscience*, *113*(3), 581–592. https://doi.org/10.1016/s0306-4522(02)00147-1

Miller, A. H., Haroon, E., Raison, C. L., & Felger, J. C. (2013). Cytokine Targets in the Brain: Impact on Neurotransmitters and Neurocircuits. *Depression and Anxiety*, *30*(4), 297. https://doi.org/10.1002/da.22084

Mishizen-Eberz, A. J., Norris, E. H., Giasson, B. I., Hodara, R., Ischiropoulos, H., Lee, V. M.-Y., Trojanowski, J. Q., & Lynch, D. R. (2005). Cleavage of alpha-synuclein by calpain: Potential role in degradation of fibrillized and nitrated species of alpha-synuclein. *Biochemistry*, *44*(21), 7818–7829. https://doi.org/10.1021/bi047846q

Misiak, M., Beyer, C., & Arnold, S. (2010). Gender-specific role of mitochondria in the vulnerability of 6-hydroxydopamine-treated mesencephalic neurons. *Biochimica Et Biophysica Acta*, *1797*(6–7), 1178–1188. https://doi.org/10.1016/j.bbabio.2010.04.009

Mitsumoto, Y., & Mori, A. (2018). Acute Restraint Stress Augments 1-Methyl-4-phenyl-1,2,3,6-tetrahydropyridine Neurotoxicity via Increased Toxin Uptake into the Brain in C57BL/6 Mice. *Neuroscience Bulletin*, *34*(5), 849–853. https://doi.org/10.1007/s12264-018-0254-2

Mitsumoto, Y., Takamori, S., & Kishida, K. (2019). Psychosocial stress enhances susceptibility to 1-methyl-4-phenyl-1,2,3,6-tetrahydropyridine neurotoxicity in C57BL/6N mice. *Biomedical Research*, *40*(6), 251–255. https://doi.org/10.2220/biomedres.40.251

Moore, R. Y., Whone, A. L., & Brooks, D. J. (2008). Extrastriatal monoamine neuron function in Parkinson's disease: An 18F-dopa PET study. *Neurobiology of Disease*, *29*(3), 381–390. https://doi.org/10.1016/j.nbd.2007.09.004

Morales, I., Sanchez, A., Rodriguez-Sabate, C., & Rodriguez, M. (2016). The astrocytic response to the dopaminergic denervation of the striatum. *Journal of Neurochemistry*, *139*(1), 81–95. https://doi.org/10.1111/jnc.13684

Moreno, S. I. G., Limani, F., Ludwig, I., Gilbert, C., Pifl, C., Hnasko, T. S., & Steinkellner, T. (2024). Viral overexpression of human alpha-synuclein in mouse substantia nigra dopamine neurons results in hyperdopaminergia but no neurodegeneration. *bioRxiv: The Preprint Server for Biology*, 2024.05.03.592188. https://doi.org/10.1101/2024.05.03.592188

Morris, R. (1984). Developments of a water-maze procedure for studying spatial learning in the rat. *Journal of Neuroscience Methods*, *11*(1), 47–60. https://doi.org/10.1016/0165-0270(84)90007-4

Mosharov, E. V., Staal, R. G. W., Bové, J., Prou, D., Hananiya, A., Markov, D., Poulsen, N., Larsen, K. E., Moore, C. M. H., Troyer, M. D., Edwards, R. H., Przedborski, S., & Sulzer, D. (2006). α-Synuclein Overexpression Increases Cytosolic Catecholamine Concentration. *The Journal of Neuroscience*, *26*(36), 9304–9311. https://doi.org/10.1523/JNEUROSCI.0519-06.2006

Muntané, G., Ferrer, I., & Martinez-Vicente, M. (2012). α-synuclein phosphorylation and truncation are normal events in the adult human brain. *Neuroscience*, *200*, 106–119. https://doi.org/10.1016/j.neuroscience.2011.10.042

Murdoch, D. A. (1998). Gram-Positive Anaerobic Cocci. *Clinical Microbiology Reviews*, *11*(1), 81–120.

Nakamura, K., Nemani, V. M., Azarbal, F., Skibinski, G., Levy, J. M., Egami, K., Munishkina, L., Zhang, J., Gardner, B., Wakabayashi, J., Sesaki, H., Cheng, Y., Finkbeiner, S., Nussbaum, R. L., Masliah, E., & Edwards, R. H. (2011). Direct membrane association drives mitochondrial fission by the Parkinson disease-associated protein alpha-synuclein. *The Journal of Biological Chemistry*, *286*(23), 20710–20726. https://doi.org/10.1074/jbc.M110.213538

Nakos Bimpos, M., Karali, K., Antoniou, C., Palermos, D., Fouka, M., Delis, A., Tzieras, I., Chrousos, G. P., Koutmani, Y., Stefanis, L., & Polissidis, A. (2024a). Alpha-synuclein-induced stress sensitivity renders the Parkinson's disease brain susceptible to neurodegeneration. *Acta Neuropathologica Communications*, *12*(1), Article 1. https://doi.org/10.1186/s40478-024-01797-w

Nakos Bimpos, M., Karali, K., Antoniou, C., Palermos, D., Fouka, M., Delis, A., Tzieras, I., Chrousos, G. P., Koutmani, Y., Stefanis, L., & Polissidis, A. (2024b). Alpha-synuclein-induced stress sensitivity renders the Parkinson's disease brain susceptible to neurodegeneration. *Acta Neuropathologica Communications*, *12*(1), 100. https://doi.org/10.1186/s40478-024-01797-w

Nandi, A., Yan, L.-J., Jana, C. K., & Das, N. (2019). Role of Catalase in Oxidative Stress- and Age-Associated Degenerative Diseases. *Oxidative Medicine and Cellular Longevity*, *2019*(1), 9613090. https://doi.org/10.1155/2019/9613090

Nasca, C., Bigio, B., Zelli, D., Nicoletti, F., & McEwen, B. S. (2015). Mind the gap: Glucocorticoids modulate hippocampal glutamate tone underlying individual differences in stress susceptibility. *Molecular Psychiatry*, *20*(6), 755–763. https://doi.org/10.1038/mp.2014.96

Nemani, V. M., Lu, W., Berge, V., Nakamura, K., Onoa, B., Lee, M. K., Chaudhry, F. A., Nicoll, R. A., & Edwards, R. H. (2010). Increased Expression of α-Synuclein Reduces Neurotransmitter Release by Inhibiting Synaptic Vesicle Reclustering after Endocytosis. *Neuron*, *65*(1), 66–79. https://doi.org/10.1016/j.neuron.2009.12.023

Nesse, R. M. (2005). Natural selection and the regulation of defenses: A signal detection analysis of the smoke detector principle. *Evolution and Human Behavior*, *26*(1), 88–105. https://doi.org/10.1016/j.evolhumbehav.2004.08.002

Nesse, R. M., Bhatnagar, S., & Ellis, B. (2016). Chapter 11—Evolutionary Origins and Functions of the Stress Response System. In G. Fink (Ed.), *Stress: Concepts, Cognition, Emotion, and Behavior* (pp. 95–101). Academic Press. https://doi.org/10.1016/B978-0-12-800951-2.00011-X

Neudorfer, O., Giladi, N., Elstein, D., Abrahamov, A., Turezkite, T., Aghai, E., Reches, A., Bembi, B., & Zimran, A. (1996). Occurrence of Parkinson's syndrome in type I Gaucher disease. *QJM: Monthly Journal of the Association of Physicians*, *89*(9), 691–694. https://doi.org/10.1093/qjmed/89.9.691

Neumann, J., Bras, J., Deas, E., O'Sullivan, S. S., Parkkinen, L., Lachmann, R. H., Li, A., Holton, J., Guerreiro, R., Paudel, R., Segarane, B., Singleton, A., Lees, A., Hardy, J., Houlden, H., Revesz, T., & Wood, N. W. (2009). Glucocerebrosidase mutations in clinical and pathologically proven Parkinson's disease. *Brain*, *132*(7), 1783–1794. https://doi.org/10.1093/brain/awp044

Nicolaides, N. C., & Charmandari, E. (2021). Primary Generalized Glucocorticoid Resistance and Hypersensitivity Syndromes: A 2021 Update. *International Journal of Molecular Sciences*, *22*(19), 10839. https://doi.org/10.3390/ijms221910839

Nicolaides, N. C., Lamprokostopoulou, A., Polyzos, A., Kino, T., Katsantoni, E., Triantafyllou, P., Christophoridis, A., Katzos, G., Dracopoulou, M., Sertedaki, A., Chrousos, G. P., & Charmandari, E. (2015). Transient generalized glucocorticoid hypersensitivity. *European Journal of Clinical Investigation*, *45*(12), 1306–1315. https://doi.org/10.1111/eci.12554

Nicolaides, N. C., Polyzos, A., Koniari, E., Lamprokostopoulou, A., Papageorgiou, I., Golfinopoulou, E., Papathanasiou, C., Sertedaki, A., Thanos, D., Chrousos, G. P., & Charmandari, E. (2019). Transcriptomics in tissue glucocorticoid sensitivity. *European Journal of Clinical Investigation*, *49*(8), e13129. https://doi.org/10.1111/eci.13129

Nikolaus, S., Schulte, B., Al-Massad, N., Thieme, F., Schulte, D. M., Bethge, J., Rehman, A., Tran, F., Aden, K., Häsler, R., Moll, N., Schütze, G., Schwarz, M. J., Waetzig, G. H., Rosenstiel, P., Krawczak, M., Szymczak, S., & Schreiber, S. (2017). Increased Tryptophan Metabolism Is Associated With Activity of Inflammatory Bowel Diseases. *Gastroenterology*, *153*(6), 1504-1516.e2. https://doi.org/10.1053/j.gastro.2017.08.028

Ninkina, N., Tarasova, T. V., Chaprov, K. D., Roman, A. Y., Kukharsky, M. S., Kolik, L. G., Ovchinnikov, R., Ustyugov, A. A., Durnev, A. D., & Buchman, V. L. (2020). Alterations in the nigrostriatal system following conditional inactivation of α-synuclein in neurons of adult and aging mice. *Neurobiology of Aging*, *91*, 76–87. https://doi.org/10.1016/j.neurobiolaging.2020.02.026

Nishiwaki, H., Ito, M., Ishida, T., Hamaguchi, T., Maeda, T., Kashihara, K., Tsuboi, Y., Ueyama, J., Shimamura, T., Mori, H., Kurokawa, K., Katsuno, M., Hirayama, M., & Ohno, K. (2020). Meta-Analysis of Gut Dysbiosis in Parkinson's Disease. *Movement Disorders*, *35*(9), 1626–1635. https://doi.org/10.1002/mds.28119

Nonaka, T., Iwatsubo, T., & Hasegawa, M. (2005). Ubiquitination of α-Synuclein. *Biochemistry*, *44*(1), 361–368. https://doi.org/10.1021/bi0485528

Ntoulas, G., Brakatselos, C., Nakas, G., Asprogerakas, M.-Z., Delis, F., Leontiadis, L. J., Trompoukis, G., Papatheodoropoulos, C., Gkikas, D., Valakos, D., Vatsellas, G., Politis, P. K., Polissidis, A., & Antoniou, K. (2024). Multi-level profiling of the Fmr1 KO rat unveils altered behavioral traits along with aberrant glutamatergic function. *Translational Psychiatry*, *14*(1), 1–12. https://doi.org/10.1038/s41398-024-02815-0

Nuber, S., Harmuth, F., Kohl, Z., Adame, A., Trejo, M., Schönig, K., Zimmermann, F., Bauer, C., Casadei, N., Giel, C., Calaminus, C., Pichler, B. J., Jensen, P. H., Müller, C. P., Amato, D., Kornhuber, J., Teismann, P., Yamakado, H., Takahashi, R., … Riess, O. (2013). A progressive dopaminergic phenotype associated with neurotoxic conversion of α-synuclein in BAC-transgenic rats. *Brain*, *136*(2), 412–432. https://doi.org/10.1093/brain/aws358

Nurrahma, B. A., Yeh, T.-H., Hsieh, R.-H., Tsao, S.-P., Chen, C.-W., Lee, Y.-P., Pan, C.-H., & Huang, H.-Y. (2022). Mangosteen Pericarp Extract Supplementation Boosts Antioxidant Status via Rebuilding Gut Microbiota to Attenuate Motor Deficit in 6-OHDA-Induced Parkinson's Disease. *Antioxidants*, *11*(12), Article 12. https://doi.org/10.3390/antiox11122396

Obeid, R., & Herrmann, W. (2006). Mechanisms of homocysteine neurotoxicity in neurodegenerative diseases with special reference to dementia. *FEBS Letters*, *580*(13), 2994–3005. https://doi.org/10.1016/j.febslet.2006.04.088

Olanow, C. W., & Brundin, P. (2013). Parkinson's Disease and Alpha Synuclein: Is Parkinson's Disease a Prion-Like Disorder? *Movement Disorders*, *28*(1), 31–40. https://doi.org/10.1002/mds.25373

Olanow, C. W., & Prusiner, S. B. (2009). Is Parkinson's disease a prion disorder? *Proceedings of the National Academy of Sciences*, *106*(31), 12571–12572. https://doi.org/10.1073/pnas.0906759106

Oldendorf, W. H. (1973). Carrier-mediated blood-brain barrier transport of short-chain monocarboxylic organic acids. *The American Journal of Physiology*, *224*(6), 1450–1453. https://doi.org/10.1152/ajplegacy.1973.224.6.1450

Oliveira, L. M. A., Gasser, T., Edwards, R., Zweckstetter, M., Melki, R., Stefanis, L., Lashuel, H. A., Sulzer, D., Vekrellis, K., Halliday, G. M., Tomlinson, J. J., Schlossmacher, M., Jensen, P. H., Schulze-Hentrich, J., Riess, O., Hirst, W. D., El-Agnaf, O., Mollenhauer, B., Lansbury, P., & Outeiro, T. F. (2021). Alpha-synuclein research: Defining strategic moves in the battle against Parkinson's disease. *Npj Parkinson's Disease*, *7*(1), Article 1. https://doi.org/10.1038/s41531-021-00203-9

Ordonez, D. G., Lee, M. K., & Feany, M. B. (2018). α-synuclein Induces Mitochondrial Dysfunction through Spectrin and the Actin Cytoskeleton. *Neuron*, *97*(1), 108-124.e6. https://doi.org/10.1016/j.neuron.2017.11.036

Orimo, S., Uchihara, T., Nakamura, A., Mori, F., Kakita, A., Wakabayashi, K., & Takahashi, H. (2008). Axonal alpha-synuclein aggregates herald centripetal degeneration of cardiac sympathetic nerve in Parkinson's disease. *Brain: A Journal of Neurology*, *131*(Pt 3), 642–650. https://doi.org/10.1093/brain/awm302

Oueslati, A., Fournier, M., & Lashuel, H. A. (2010). Chapter 7 - Role of post-translational modifications in modulating the structure, function and toxicity of α-synuclein: Implications for Parkinson's disease pathogenesis and therapies. In A. Björklund & M. A. Cenci (Eds.), *Progress in Brain Research* (Vol. 183, pp. 115–145). Elsevier. https://doi.org/10.1016/S0079-6123(10)83007-9

Paleologou, K. E., Oueslati, A., Shakked, G., Rospigliosi, C. C., Kim, H.-Y., Lamberto, G. R., Fernandez, C. O., Schmid, A., Chegini, F., Gai, W. P., Chiappe, D., Moniatte, M., Schneider, B. L., Aebischer, P., Eliezer, D., Zweckstetter, M., Masliah, E., & Lashuel, H. A. (2010). Phosphorylation at S87 Is Enhanced in Synucleinopathies, Inhibits α-Synuclein Oligomerization, and Influences Synuclein-Membrane Interactions. *Journal of Neuroscience*, *30*(9), 3184–3198. https://doi.org/10.1523/JNEUROSCI.5922-09.2010

Pang, S. Y.-Y., Ho, P. W.-L., Liu, H.-F., Leung, C.-T., Li, L., Chang, E. E. S., Ramsden, D. B., & Ho, S.-L. (2019). The interplay of aging, genetics and environmental factors in the pathogenesis of Parkinson's disease. *Translational Neurodegeneration*, *8*(1), 23. https://doi.org/10.1186/s40035-019-0165-9

Park, J.-H., Burgess, J. D., Faroqi, A. H., DeMeo, N. N., Fiesel, F. C., Springer, W., Delenclos, M., & McLean, P. J. (2020). Alpha-synuclein-induced mitochondrial dysfunction is mediated via a sirtuin 3-dependent pathway. *Molecular Neurodegeneration*, *15*(1), 5. https://doi.org/10.1186/s13024-019-0349-x

Parra-Rivas, L. A., Madhivanan, K., Aulston, B. D., Wang, L., Prakashchand, D. D., Boyer, N. P., Saia-Cereda, V. M., Branes-Guerrero, K., Pizzo, D. P., Bagchi, P., Sundar, V. S., Tang, Y., Das, U., Scott, D. A., Rangamani, P., Ogawa, Y., & Roy, S. (2023). Serine-129 phosphorylation of α-synuclein is an activity-dependent trigger for physiologic protein-protein interactions and synaptic function. *Neuron*, *111*(24), 4006-4023.e10. https://doi.org/10.1016/j.neuron.2023.11.020

Pasanen, P., Myllykangas, L., Siitonen, M., Raunio, A., Kaakkola, S., Lyytinen, J., Tienari, P. J., Pöyhönen, M., & Paetau, A. (2014). A novel α-synuclein mutation A53E associated with atypical multiple system atrophy and Parkinson's disease-type pathology. *Neurobiology of Aging*, *35*(9), 2180.e1-2180.e5. https://doi.org/10.1016/j.neurobiolaging.2014.03.024

Paxinos, G., & Watson, C. (2004). *The Rat Brain in Stereotaxic Coordinates—The New Coronal Set*. Elsevier.

Paxinou, E., Chen, Q., Weisse, M., Giasson, B. I., Norris, E. H., Rueter, S. M., Trojanowski, J. Q., Lee, V. M.-Y., & Ischiropoulos, H. (2001). Induction of α-Synuclein Aggregation by Intracellular Nitrative Insult. *Journal of Neuroscience*, *21*(20), 8053–8061. https://doi.org/10.1523/JNEUROSCI.21-20-08053.2001

Peelaerts, W., Bousset, L., Van der Perren, A., Moskalyuk, A., Pulizzi, R., Giugliano, M., Van den Haute, C., Melki, R., & Baekelandt, V. (2015). α-Synuclein strains cause distinct synucleinopathies after local and systemic administration. *Nature*, *522*(7556), 340–344. https://doi.org/10.1038/nature14547

Perez, R. G., Waymire, J. C., Lin, E., Liu, J. J., Guo, F., & Zigmond, M. J. (2002). A role for alpha-synuclein in the regulation of dopamine biosynthesis. *The Journal of Neuroscience: The Official Journal of the Society for Neuroscience*, *22*(8), 3090–3099. https://doi.org/10.1523/JNEUROSCI.22-08-03090.2002

Periquet, M., Latouche, M., Lohmann, E., Rawal, N., De Michele, G., Ricard, S., Teive, H., Fraix, V., Vidailhet, M., Nicholl, D., Barone, P., Wood, N. W., Raskin, S., Deleuze, J.-F., Agid, Y., Dürr, A., Brice, A., French Parkinson's Disease Genetics Study Group, & European Consortium on Genetic Susceptibility in Parkinson's Disease. (2003). Parkin mutations are frequent in patients with isolated early-onset parkinsonism. *Brain: A Journal of Neurology*, *126*(Pt 6), 1271–1278. https://doi.org/10.1093/brain/awg136

Peters, O. M., Shelkovnikova, T., Highley, J. R., Cooper-Knock, J., Hortobágyi, T., Troakes, C., Ninkina, N., & Buchman, V. L. (2015). Gamma-synuclein pathology in amyotrophic lateral sclerosis. *Annals of Clinical and Translational Neurology*, *2*(1), 29–37. https://doi.org/10.1002/acn3.143

Pfeiffer, R. F. (2016). Non-motor symptoms in Parkinson's disease. *Parkinsonism & Related Disorders*, *22 Suppl 1*, S119-122. https://doi.org/10.1016/j.parkreldis.2015.09.004

Philippart, F., Destreel, G., Merino-Sepúlveda, P., Henny, P., Engel, D., & Seutin, V. (2016). Differential Somatic Ca2+ Channel Profile in Midbrain Dopaminergic Neurons. *The Journal of Neuroscience: The Official Journal of the Society for Neuroscience*, *36*(27), 7234–7245. https://doi.org/10.1523/JNEUROSCI.0459-16.2016

Picillo, M., Nicoletti, A., Fetoni, V., Garavaglia, B., Barone, P., & Pellecchia, M. T. (2017). The relevance of gender in Parkinson's disease: A review. *Journal of Neurology*, *264*(8), 1583–1607. https://doi.org/10.1007/s00415-016-8384-9

Pifl, C., & Hornykiewicz, O. (2006). Dopamine turnover is upregulated in the caudate/putamen of asymptomatic MPTP-treated rhesus monkeys. *Neurochemistry International*, *49*(5), 519–524. https://doi.org/10.1016/j.neuint.2006.03.013

Pinho, R., Paiva, I., Jercic, K. G., Fonseca-Ornelas, L., Gerhardt, E., Fahlbusch, C., Garcia-Esparcia, P., Kerimoglu, C., Pavlou, M. A. S., Villar-Piqué, A., Szego, É., Lopes da Fonseca, T., Odoardi, F., Soeroes, S., Rego, A. C., Fischle, W., Schwamborn, J. C., Meyer, T., Kügler, S., … Outeiro, T. F. (2019). Nuclear localization and phosphorylation modulate pathological effects of alpha-synuclein. *Human Molecular Genetics*, *28*(1), 31–50. https://doi.org/10.1093/hmg/ddy326

Polissidis, A., Koronaiou, M., Kollia, V., Koronaiou, E., Nakos-Bimpos, M., Bogiongko, M., Vrettou, S., Karali, K., Casadei, N., Riess, O., Sardi, S. P., Xilouri, M., & Stefanis, L. (2021). Psychosis-Like Behavior and Hyperdopaminergic Dysregulation in Human α-Synuclein BAC Transgenic Rats. *Movement Disorders*, *36*(3), 716–728. https://doi.org/10.1002/mds.28383

Polissidis, A., Petropoulou-Vathi, L., Nakos-Bimpos, M., & Rideout, H. J. (2020). The Future of Targeted Gene-Based Treatment Strategies and Biomarkers in Parkinson's Disease. *Biomolecules*, *10*(6), Article 6. https://doi.org/10.3390/biom10060912

Polymeropoulos, M. H., Lavedan, C., Leroy, E., Ide, S. E., Dehejia, A., Dutra, A., Pike, B., Root, H., Rubenstein, J., Boyer, R., Stenroos, E. S., Chandrasekharappa, S., Athanassiadou, A., Papapetropoulos, T., Johnson, W. G., Lazzarini, A. M., Duvoisin, R. C., Di Iorio, G., Golbe, L. I., & Nussbaum, R. L. (1997). Mutation in the alpha-synuclein gene identified in families with Parkinson's disease. *Science (New York, N.Y.)*, *276*(5321), 2045–2047. https://doi.org/10.1126/science.276.5321.2045

Popoli, M., Yan, Z., McEwen, B., & Sanacora, G. (2011). The stressed synapse: The impact of stress and glucocorticoids on glutamate transmission. *Nature Reviews. Neuroscience*, *13*(1), 22–37. https://doi.org/10.1038/nrn3138

Prakash, K. M., Nadkarni, N. V., Lye, W.-K., Yong, M.-H., & Tan, E.-K. (2016). The impact of non-motor symptoms on the quality of life of Parkinson's disease patients: A longitudinal study. *European Journal of Neurology*, *23*(5), 854–860. https://doi.org/10.1111/ene.12950

Prasuhn, J., Kasten, M., Vos, M., König, I. R., Schmid, S. M., Wilms, B., Klein, C., & Brüggemann, N. (2020). The Use of Vitamin K2 in Patients With Parkinson's Disease and Mitochondrial Dysfunction (PD-K2): A Theranostic Pilot Study in a Placebo-Controlled Parallel Group Design. *Frontiers in Neurology*, *11*, 592104. https://doi.org/10.3389/fneur.2020.592104

Prediger, R. D. S., Batista, L. C., Medeiros, R., Pandolfo, P., Florio, J. C., & Takahashi, R. N. (2006). The risk is in the air: Intranasal administration of MPTP to rats reproducing clinical features of Parkinson's disease. *Experimental Neurology*, *202*(2), 391–403. https://doi.org/10.1016/j.expneurol.2006.07.001

Qian, Y., Yang, X., Xu, S., Wu, C., Song, Y., Qin, N., Chen, S.-D., & Xiao, Q. (2018). Alteration of the fecal microbiota in Chinese patients with Parkinson's disease. *Brain, Behavior, and Immunity*, *70*, 194–202. https://doi.org/10.1016/j.bbi.2018.02.016

Qualman, S. J., Haupt, H. M., Yang, P., & Hamilton, S. R. (1984). Esophageal Lewy bodies associated with ganglion cell loss in achalasia. Similarity to Parkinson's disease. *Gastroenterology*, *87*(4), 848–856.

Qureshi, H. Y., & Paudel, H. K. (2011). Parkinsonian neurotoxin 1-methyl-4-phenyl-1,2,3,6-tetrahydropyridine (MPTP) and alpha-synuclein mutations promote Tau protein phosphorylation at Ser262 and destabilize microtubule cytoskeleton in vitro. *The Journal of Biological Chemistry*, *286*(7), 5055–5068. https://doi.org/10.1074/jbc.M110.178905

Rabey, J. M., Scharf, M., Oberman, Z., Zohar, M., & Graff, E. (1990). Cortisol, ACTH, and beta-endorphin after dexamethasone administration in Parkinson's dementia. *Biological Psychiatry*, *27*(6), 581–591. https://doi.org/10.1016/0006-3223(90)90525-7

Radisavljevic, N. (2023). *The role of gut microbiota in Parkinson's disease* [University of British Columbia]. https://doi.org/10.14288/1.0435926

Ramalingam, N., Jin, S.-X., Moors, T. E., Fonseca-Ornelas, L., Shimanaka, K., Lei, S., Cam, H. P., Watson, A. H., Brontesi, L., Ding, L., Hacibaloglu, D. Y., Jiang, H., Choi, S. J., Kanter, E., Liu, L., Bartels, T., Nuber, S., Sulzer, D., Mosharov, E. V., … Dettmer, U. (2023). Dynamic physiological α-synuclein S129 phosphorylation is driven by neuronal activity. *NPJ Parkinson's Disease*, *9*(1), 4. https://doi.org/10.1038/s41531-023-00444-w

Ran, L., Xiang, J., Zeng, X., He, W., Dong, Y., Yu, W., Qi, X., Xiao, Y., Cao, K., Zou, J., & Guan, Z. (2023). The influence of NQO2 on the dysfunctional autophagy and oxidative stress induced in the hippocampus of rats and in SH-SY5Y cells by fluoride. *CNS Neuroscience & Therapeutics*, *29*(4), 1129–1141. https://doi.org/10.1111/cns.14090

Recasens, A., Dehay, B., Bové, J., Carballo-Carbajal, I., Dovero, S., Pérez-Villalba, A., Fernagut, P.-O., Blesa, J., Parent, A., Perier, C., Fariñas, I., Obeso, J. A., Bezard, E., & Vila, M. (2014). Lewy body extracts from Parkinson disease brains

trigger α-synuclein pathology and neurodegeneration in mice and monkeys. *Annals of Neurology*, *75*(3), 351–362. https://doi.org/10.1002/ana.24066

Reczek, D., Schwake, M., Schröder, J., Hughes, H., Blanz, J., Jin, X., Brondyk, W., Van Patten, S., Edmunds, T., & Saftig, P. (2007). LIMP-2 is a receptor for lysosomal mannose-6-phosphate-independent targeting of beta-glucocerebrosidase. *Cell*, *131*(4), 770–783. https://doi.org/10.1016/j.cell.2007.10.018

Robinson, M. D., McCarthy, D. J., & Smyth, G. K. (2010). edgeR: A Bioconductor package for differential expression analysis of digital gene expression data. *Bioinformatics*, *26*(1), 139–140. https://doi.org/10.1093/bioinformatics/btp616

Robotta, M., Gerding, H. R., Vogel, A., Hauser, K., Schildknecht, S., Karreman, C., Leist, M., Subramaniam, V., & Drescher, M. (2014). Alpha-Synuclein Binds to the Inner Membrane of Mitochondria in an α-Helical Conformation. *ChemBioChem*, *15*(17), 2499–2502. https://doi.org/10.1002/cbic.201402281

Rocca, W. A., Bower, J. H., Maraganore, D. M., Ahlskog, J. E., Grossardt, B. R., de Andrade, M., & Melton, L. J. (2008). Increased risk of parkinsonism in women who underwent oophorectomy before menopause. *Neurology*, *70*(3), 200–209. https://doi.org/10.1212/01.wnl.0000280573.30975.6a

Rojanathammanee, L., Murphy, E. J., & Combs, C. K. (2011). Expression of mutant alpha-synuclein modulates microglial phenotype in vitro. *Journal of Neuroinflammation*, *8*(1), 44. https://doi.org/10.1186/1742-2094-8-44

Roodveldt, C., Labrador-Garrido, A., Gonzalez-Rey, E., Fernandez-Montesinos, R., Caro, M., Lachaud, C. C., Waudby, C. A., Delgado, M., Dobson, C. M., & Pozo, D. (2010). Glial innate immunity generated by non-aggregated alpha-synuclein in mouse: Differences between wild-type and Parkinson's disease-linked mutants. *PloS One*, *5*(10), e13481. https://doi.org/10.1371/journal.pone.0013481

Roozendaal, B., Phillips, R. G., Power, A. E., Brooke, S. M., Sapolsky, R. M., & McGaugh, J. L. (2001). Memory retrieval impairment induced by hippocampal CA3 lesions is blocked by adrenocortical suppression. *Nature Neuroscience*, *4*(12), 1169–1171. https://doi.org/10.1038/nn766

Rosario, D., Bidkhori, G., Lee, S., Bedarf, J., Hildebrand, F., Chatelier, E. L., Uhlen, M., Ehrlich, S. D., Proctor, G., Wüllner, U., Mardinoglu, A., & Shoaie, S. (2021). Systematic analysis of gut microbiome reveals the role of bacterial folate and homocysteine metabolism in Parkinson's disease. *Cell Reports*, *34*(9). https://doi.org/10.1016/j.celrep.2021.108807

Ros-Bernal, F., Hunot, S., Herrero, M. T., Parnadeau, S., Corvol, J.-C., Lu, L., Alvarez-Fischer, D., Carrillo-de Sauvage, M. A., Saurini, F., Coussieu, C., Kinugawa, K., Prigent, A., Höglinger, G., Hamon, M., Tronche, F., Hirsch, E. C., & Vyas, S. (2011). Microglial glucocorticoid receptors play a pivotal role in regulating dopaminergic neurodegeneration in parkinsonism. *Proceedings of the National Academy of Sciences of the United States of America*, *108*(16), 6632–6637. https://doi.org/10.1073/pnas.1017820108

Rosenberg, G. A. (2009). Matrix metalloproteinases and their multiple roles in neurodegenerative diseases. *The Lancet Neurology*, *8*(2), 205–216. https://doi.org/10.1016/S1474-4422(09)70016-X

Rothlin, C. V., Carrera-Silva, E. A., Bosurgi, L., & Ghosh, S. (2015). TAM Receptor Signaling in Immune Homeostasis. *Annual Review of Immunology*, *33*, 355–391. https://doi.org/10.1146/annurev-immunol-032414-112103

Rudyk, C., Dwyer, Z., McNeill, J., Salmaso, N., Farmer, K., Prowse, N., & Hayley, S. (2019). Chronic unpredictable stress influenced the behavioral but not the neurodegenerative impact of paraquat. *Neurobiology of Stress*, *11*, 100179. https://doi.org/10.1016/j.ynstr.2019.100179

Saijo, K., Winner, B., Carson, C. T., Collier, J. G., Boyer, L., Rosenfeld, M. G., Gage, F. H., & Glass, C. K. (2009). A Nurr1/CoREST Pathway in Microglia and Astrocytes Protects Dopaminergic Neurons from Inflammation-Induced Death. *Cell*, *137*(1), 47–59. https://doi.org/10.1016/j.cell.2009.01.038

Salim, S., Asghar, M., Taneja, M., Hovatta, I., Wu, Y.-L., Saha, K., Sarraj, N., & Hite, B. (2011). Novel Role of RGS2 in Regulation of Antioxidant Homeostasis in Neuronal Cells. *FEBS Letters*, *585*(9), 1375–1381. https://doi.org/10.1016/j.febslet.2011.04.023

Salosensaari, A., Laitinen, V., Havulinna, A. S., Meric, G., Cheng, S., Perola, M., Valsta, L., Alfthan, G., Inouye, M., Watrous, J. D., Long, T., Salido, R. A., Sanders, K., Brennan, C., Humphrey, G. C., Sanders, J. G., Jain, M., Jousilahti, P., Salomaa, V., … Niiranen, T. (2021). Taxonomic signatures of cause-specific mortality risk in human gut microbiome. *Nature Communications*, *12*, 2671. https://doi.org/10.1038/s41467-021-22962-y

Sampson, T. R., Debelius, J. W., Thron, T., Janssen, S., Shastri, G. G., Ilhan, Z. E., Challis, C., Schretter, C. E., Rocha, S., Gradinaru, V., Chesselet, M.-F., Keshavarzian, A., Shannon, K. M., Krajmalnik-Brown, R., Wittung-Stafshede, P., Knight, R., & Mazmanian, S. K. (2016). Gut Microbiota Regulate Motor Deficits and Neuroinflammation in a Model of Parkinson's Disease. *Cell*, *167*(6), 1469-1480.e12. https://doi.org/10.1016/j.cell.2016.11.018

Sapolsky, R. M. (1992). Cortisol concentrations and the social significance of rank instability among wild baboons. *Psychoneuroendocrinology*, *17*(6), 701–709. https://doi.org/10.1016/0306-4530(92)90029-7

Schapansky, J., Khasnavis, S., DeAndrade, M. P., Nardozzi, J. D., Falkson, S. R., Boyd, J. D., Sanderson, J. B., Bartels, T., Melrose, H. L., & LaVoie, M. J. (2018). Familial knockin mutation of LRRK2 causes lysosomal dysfunction and accumulation of endogenous insoluble α-synuclein in neurons. *Neurobiology of Disease*, *111*, 26–35. https://doi.org/10.1016/j.nbd.2017.12.005

Schapira, A. H. V. (2015). Glucocerebrosidase and Parkinson disease: Recent advances. *Molecular and Cellular Neuroscience*, *66*, 37–42. https://doi.org/10.1016/j.mcn.2015.03.013

Schapira, A. H. V., Chaudhuri, K. R., & Jenner, P. (2017). Non-motor features of Parkinson disease. *Nature Reviews Neuroscience*, *18*(7), Article 7. https://doi.org/10.1038/nrn.2017.62

Schaser, A. J., Stackhouse, T. L., Weston, L. J., Kerstein, P. C., Osterberg, V. R., López, C. S., Dickson, D. W., Luk, K. C., Meshul, C. K., Woltjer, R. L., & Unni, V. K. (2020). Trans-synaptic and retrograde axonal spread of Lewy pathology following pre-formed fibril injection in an in vivo A53T alpha-synuclein mouse model of synucleinopathy. *Acta Neuropathologica Communications*, *8*. https://doi.org/10.1186/s40478-020-01026-0

Schindelin, J., Arganda-Carreras, I., Frise, E., Kaynig, V., Longair, M., Pietzsch, T., Preibisch, S., Rueden, C., Saalfeld, S., Schmid, B., Tinevez, J.-Y., White, D. J., Hartenstein, V., Eliceiri, K., Tomancak, P., & Cardona, A. (2012). Fiji—An Open Source platform for biological image analysis. *Nature Methods*, *9*(7), 10.1038/nmeth.2019. https://doi.org/10.1038/nmeth.2019

Schousboe, A., Scafidi, S., Bak, L. K., Waagepetersen, H. S., & McKenna, M. C. (2014). Glutamate Metabolism in the Brain Focusing on Astrocytes. *Advances in Neurobiology*, *11*, 13–30. https://doi.org/10.1007/978-3-319-08894-5_2

Sender, R., Fuchs, S., & Milo, R. (2016). Revised Estimates for the Number of Human and Bacteria Cells in the Body. *PLoS Biology*, *14*(8), e1002533. https://doi.org/10.1371/journal.pbio.1002533

Shannon, K. M., Keshavarzian, A., Dodiya, H. B., Jakate, S., & Kordower, J. H. (2012). Is alpha-synuclein in the colon a biomarker for premotor Parkinson's disease? Evidence from 3 cases. *Movement Disorders: Official Journal of the Movement Disorder Society*, *27*(6), 716–719. https://doi.org/10.1002/mds.25020

Sharma, S., Bandopadhyay, R., Lashley, T., Renton, A. E. M., Kingsbury, A. E., Kumaran, R., Kallis, C., Vilariño-Güell, C., O'Sullivan, S. S., Lees, A. J., Revesz, T., Wood, N. W., & Holton, J. L. (2011). LRRK2 expression in idiopathic and G2019S positive Parkinson's disease subjects: A morphological and quantitative study. *Neuropathology and Applied Neurobiology*, *37*(7), 777–790. https://doi.org/10.1111/j.1365-2990.2011.01187.x

Sharma, S., Taliyan, R., & Singh, S. (2015). Beneficial effects of sodium butyrate in 6-OHDA induced neurotoxicity and behavioral abnormalities: Modulation of histone deacetylase activity. *Behavioural Brain Research*, *291*, 306–314. https://doi.org/10.1016/j.bbr.2015.05.052

Shen, W., Tao, Y., Zheng, F., Zhou, H., Wu, H., Shi, H., Huang, F., & Wu, X. (2023). The alteration of gut microbiota in venlafaxine-ameliorated chronic unpredictable mild stress-induced depression in mice. *Behavioural Brain Research*, *446*, 114399. https://doi.org/10.1016/j.bbr.2023.114399

Shen, X., Yang, H., Wu, Y., Zhang, D., & Jiang, H. (2017). Meta-analysis: Association of Helicobacter pylori infection with Parkinson's diseases. *Helicobacter*, *22*(5), e12398. https://doi.org/10.1111/hel.12398

Sherer, T. B., Betarbet, R., Testa, C. M., Seo, B. B., Richardson, J. R., Kim, J. H., Miller, G. W., Yagi, T., Matsuno-Yagi, A., & Greenamyre, J. T. (2003). Mechanism of toxicity in rotenone models of Parkinson's disease. *The Journal of Neuroscience: The Official Journal of the Society for Neuroscience*, *23*(34), 10756–10764. https://doi.org/10.1523/JNEUROSCI.23-34-10756.2003

Shughrue, P. J. (2004). Estrogen attenuates the MPTP-induced loss of dopamine neurons from the mouse SNc despite a lack of estrogen receptors (ERα and ERβ). *Experimental Neurology*, *190*(2), 468–477. https://doi.org/10.1016/j.expneurol.2004.08.009

Shulman, L. M., & Bhat, V. (2006). Gender disparities in Parkinson's disease. *Expert Review of Neurotherapeutics*, *6*(3), 407–416. https://doi.org/10.1586/14737175.6.3.407

Siani, F., Greco, R., Levandis, G., Ghezzi, C., Daviddi, F., Demartini, C., Vegeto, E., Fuzzati-Armentero, M.-T., & Blandini, F. (2017). Influence of Estrogen Modulation on Glia Activation in a Murine Model of Parkinson's Disease. *Frontiers in Neuroscience*, *11*. https://doi.org/10.3389/fnins.2017.00306

Siderowf, A., Concha-Marambio, L., Lafontant, D.-E., Farris, C. M., Ma, Y., Urenia, P. A., Nguyen, H., Alcalay, R. N., Chahine, L. M., Foroud, T., Galasko, D., Kieburtz, K., Merchant, K., Mollenhauer, B., Poston, K. L., Seibyl, J., Simuni, T., Tanner, C. M., Weintraub, D., … Soto, C. (2023). Assessment of heterogeneity among participants in the Parkinson's Progression Markers Initiative cohort using α-synuclein seed amplification: A cross-sectional study. *The Lancet Neurology*, *22*(5), 407–417. https://doi.org/10.1016/S1474-4422(23)00109-6

Sidransky, E., & Lopez, G. (2012). The link between the *GBA* gene and parkinsonism. *The Lancet Neurology*, *11*(11), 986–998. https://doi.org/10.1016/S1474-4422(12)70190-4

Sidransky, E., Nalls, M. A., Aasly, J. O., Aharon-Peretz, J., Annesi, G., Barbosa, E. R., Bar-Shira, A., Berg, D., Bras, J., Brice, A., Chen, C.-M., Clark, L. N., Condroyer, C., Marco, E. V. D., Dürr, A., Eblan, M. J., Fahn, S., Farrer, M. J., Fung, H.-C., … Ziegler, S. G. (2009). Multicenter Analysis of Glucocerebrosidase Mutations in Parkinson's Disease. *New England Journal of Medicine*, *361*(17), 1651–1661. https://doi.org/10.1056/NEJMoa0901281

Simón-Sánchez, J., Schulte, C., Bras, J. M., Sharma, M., Gibbs, J. R., Berg, D., Paisan-Ruiz, C., Lichtner, P., Scholz, S. W., Hernandez, D. G., Krüger, R., Federoff, M., Klein, C., Goate, A., Perlmutter, J., Bonin, M., Nalls, M. A., Illig, T., Gieger, C., … Gasser, T. (2009). Genome-wide association study reveals genetic risk underlying Parkinson's disease. *Nature Genetics*, *41*(12), 1308–1312. https://doi.org/10.1038/ng.487

Singh, Y., El-Hadidi, M., Admard, J., Wassouf, Z., Schulze-Hentrich, J. M., Kohlhofer, U., Quintanilla-Martinez, L., Huson, D., Riess, O., & Casadei, N. (2019). Enriched Environmental Conditions Modify the Gut Microbiome Composition and Fecal Markers of Inflammation in Parkinson's Disease. *Frontiers in Neuroscience*, *13*. https://doi.org/10.3389/fnins.2019.01032

Singleton, A. B., Farrer, M. J., & Bonifati, V. (2013). The genetics of Parkinson's disease: Progress and therapeutic implications. *Movement Disorders : Official Journal of the Movement Disorder Society*, *28*(1), 14–23. https://doi.org/10.1002/mds.25249

Singleton, A. B., Farrer, M., Johnson, J., Singleton, A., Hague, S., Kachergus, J., Hulihan, M., Peuralinna, T., Dutra, A., Nussbaum, R., Lincoln, S., Crawley, A., Hanson, M., Maraganore, D., Adler, C., Cookson, M. R., Muenter, M., Baptista, M., Miller, D., … Gwinn-Hardy, K. (2003). α-Synuclein Locus Triplication Causes Parkinson's Disease. *Science*, *302*(5646), 841–841. https://doi.org/10.1126/science.1090278

Siopi, E., Chevalier, G., Katsimpardi, L., Saha, S., Bigot, M., Moigneu, C., Eberl, G., & Lledo, P.-M. (2020). Changes in Gut Microbiota by Chronic Stress Impair the Efficacy of Fluoxetine. *Cell Reports*, *30*(11), 3682-3690.e6. https://doi.org/10.1016/j.celrep.2020.02.099

Smith, A. D., Castro, S. L., & Zigmond, M. J. (2002). Stress-induced Parkinson's disease: A working hypothesis. *Physiology & Behavior*, *77*(4), 527–531. https://doi.org/10.1016/S0031-9384(02)00939-3

Smith, L. K., Jadavji, N. M., Colwell, K. L., Katrina Perehudoff, S., & Metz, G. A. (2008). Stress accelerates neural degeneration and exaggerates motor symptoms in a rat model of Parkinson's disease. *European Journal of Neuroscience*, *27*(8), 2133–2146. https://doi.org/10.1111/j.1460-9568.2008.06177.x

Snyder, A. M., Stricker, E. M., & Zigmond, M. J. (1985). Stress-induced neurological impairments in an animal model of parkinsonism. *Annals of Neurology*, *18*(5), 544–551. https://doi.org/10.1002/ana.410180506

Solana-Manrique, C., Muñoz-Soriano, V., Sanz, F. J., & Paricio, N. (2021). Oxidative modification impairs SERCA activity in *Drosophila* and human cell models of Parkinson's disease. *Biochimica et Biophysica Acta (BBA) - Molecular Basis of Disease*, *1867*(7), 166152. https://doi.org/10.1016/j.bbadis.2021.166152

Soldner, F., Stelzer, Y., Shivalila, C. S., Abraham, B. J., Latourelle, J. C., Barrasa, M. I., Goldmann, J., Myers, R. H., Young, R. A., & Jaenisch, R. (2016). Parkinson-associated risk variant in distal enhancer of α-synuclein modulates target gene expression. *Nature*, *533*(7601), 95–99. https://doi.org/10.1038/nature17939

Somayaji, M., Cataldi, S., Choi, S. J., Edwards, R. H., Mosharov, E. V., & Sulzer, D. (2020). A dual role for α-synuclein in facilitation and depression of dopamine release from substantia nigra neurons in vivo. *Proceedings of the National Academy of Sciences*, *117*(51), 32701–32710. https://doi.org/10.1073/pnas.2013652117

Sorrentino, Z. A., & Giasson, B. I. (2020). The emerging role of α-synuclein truncation in aggregation and disease. *The Journal of Biological Chemistry*, *295*(30), 10224–10244. https://doi.org/10.1074/jbc.REV120.011743

Sossi, V., de La Fuente-Fernández, R., Holden, J. E., Doudet, D. J., McKenzie, J., Stoessl, A. J., & Ruth, T. J. (2002). Increase in dopamine turnover occurs early in Parkinson's disease: Evidence from a new modeling approach to PET 18 F-fluorodopa data. *Journal of Cerebral Blood Flow and Metabolism: Official Journal of the International Society of Cerebral Blood Flow and Metabolism*, *22*(2), 232–239. https://doi.org/10.1097/00004647-200202000-00011

Soto-Martin, E. C., Warnke, I., Farquharson, F. M., Christodoulou, M., Horgan, G., Derrien, M., Faurie, J.-M., Flint, H. J., Duncan, S. H., & Louis, P. (2020). Vitamin Biosynthesis by Human Gut Butyrate-Producing Bacteria and Cross-Feeding in Synthetic Microbial Communities. *mBio*, *11*(4), e00886-20. https://doi.org/10.1128/mBio.00886-20

Sousa, V. L., Bellani, S., Giannandrea, M., Yousuf, M., Valtorta, F., Meldolesi, J., & Chieregatti, E. (2009). α-Synuclein and Its A30P Mutant Affect Actin Cytoskeletal Structure and Dynamics. *Molecular Biology of the Cell*, *20*(16), 3725–3739. https://doi.org/10.1091/mbc.e08-03-0302

Spencer, R. L., & Deak, T. (2017). A users guide to HPA axis research. *Physiology & Behavior*, *178*, 43–65. https://doi.org/10.1016/j.physbeh.2016.11.014

Spillantini, M. G., Schmidt, M. L., Lee, V. M.-Y., Trojanowski, J. Q., Jakes, R., & Goedert, M. (1997). α-Synuclein in Lewy bodies. *Nature*, *388*(6645), Article 6645. https://doi.org/10.1038/42166

Spiller, R., & Garsed, K. (2009). Postinfectious Irritable Bowel Syndrome. *Gastroenterology*, *136*(6), 1979–1988. https://doi.org/10.1053/j.gastro.2009.02.074

Stamford, J. A., Muscat, R., O'Connor, J. J., Patel, J., Trout, S. J., Wieczorek, W. J., Kruk, Z. L., & Willner, P. (1991). Voltammetric evidence that subsensitivity to reward following chronic mild stress is associated with increased release of mesolimbic dopamine. *Psychopharmacology*, *105*(2), 275–282. https://doi.org/10.1007/BF02244322

Stefanova, N., Fellner, L., Reindl, M., Masliah, E., Poewe, W., & Wenning, G. K. (2011). Toll-like receptor 4 promotes α-synuclein clearance and survival of nigral dopaminergic neurons. *The American Journal of Pathology*, *179*(2), 954–963. https://doi.org/10.1016/j.ajpath.2011.04.013

Stichel, C. C., Zhu, X.-R., Bader, V., Linnartz, B., Schmidt, S., & Lübbert, H. (2007). Mono- and double-mutant mouse models of Parkinson's disease display severe mitochondrial damage. *Human Molecular Genetics*, *16*(20), 2377–2393. https://doi.org/10.1093/hmg/ddm083

Stypuła, G., Kunert-Radek, J., Stepień, H., Zylińska, K., & Pawlikowski, M. (1996). Evaluation of interleukins, ACTH, cortisol and prolactin concentrations in the blood of patients with parkinson's disease. *Neuroimmunomodulation*, *3*(2–3), 131–134. https://doi.org/10.1159/000097237

Sugama, S., Sekiyama, K., Kodama, T., Takamatsu, Y., Takenouchi, T., Hashimoto, M., Bruno, C., & Kakinuma, Y. (2016). Chronic restraint stress triggers the dopaminergic and noradrenergic neurodegeneration: Possible role of chronic stress for the onset of Parkinson's disease. *Brain, Behavior, and Immunity*, *51*, 39–46. https://doi.org/10.1016/j.bbi.2015.08.015

Sui, Y.-T., Bullock, K. M., Erickson, M. A., Zhang, J., & Banks, W. A. (2014). Alpha Synuclein is Transported Into and Out of the Brain by the Blood-brain Barrier. *Peptides*, *62*, 197–202. https://doi.org/10.1016/j.peptides.2014.09.018

Sulzer, D. (2007). Multiple hit hypotheses for dopamine neuron loss in Parkinson's disease. *Trends in Neurosciences*, *30*(5), 244–250. https://doi.org/10.1016/j.tins.2007.03.009

Sulzer, D., Alcalay, R. N., Garretti, F., Cote, L., Kanter, E., Agin-Liebes, J. P., Liong, C., McMurtrey, C., Hildebrand, W. H., Mao, X., Dawson, V. L., Dawson, T. M., Oseroff, C., Pham, J., Sidney, J., Dillon, M. B., Carpenter, C., Weiskopf, D., Phillips, E., … Sette, A. (2017). T cells of Parkinson's disease patients recognize α–synuclein peptides. *Nature*, *546*(7660), 656. https://doi.org/10.1038/nature22815

Sundar Boyalla, S., Barbara Victor, M., Roemgens, A., Beyer, C., & Arnold, S. (2011). Sex- and brain region-specific role of cytochrome c oxidase in 1-methyl-4-phenylpyridinium-mediated astrocyte vulnerability. *Journal of Neuroscience Research*, *89*(12), 2068–2082. https://doi.org/10.1002/jnr.22669

Surgucheva, I., He, S., Rich, M. C., Sharma, R., Ninkina, N. N., Stahel, P. F., & Surguchov, A. (2014). Role of synucleins in traumatic brain injury—An experimental in vitro and in vivo study in mice. *Molecular and Cellular Neurosciences*, *63*, 114–123. https://doi.org/10.1016/j.mcn.2014.10.005

Surmeier, D. J., Guzman, J. N., Sanchez, J., & Schumacker, P. T. (2012). Physiological phenotype and vulnerability in Parkinson's disease. *Cold Spring Harbor Perspectives in Medicine*, *2*(7), a009290. https://doi.org/10.1101/cshperspect.a009290

Surmeier, D. J., Obeso, J. A., & Halliday, G. M. (2017). Selective neuronal vulnerability in Parkinson disease. *Nature Reviews. Neuroscience*, *18*(2), 101. https://doi.org/10.1038/nrn.2016.178

Svensson, E., Horváth-Puhó, E., Thomsen, R. W., Djurhuus, J. C., Pedersen, L., Borghammer, P., & Sørensen, H. T. (2015). Vagotomy and subsequent risk of Parkinson's disease. *Annals of Neurology*, *78*(4), 522–529. https://doi.org/10.1002/ana.24448

Swant, J., Goodwin, J. S., North, A., Ali, A. A., Gamble-George, J., Chirwa, S., & Khoshbouei, H. (2011). α-Synuclein Stimulates a Dopamine Transporter-dependent Chloride Current and Modulates the Activity of the Transporter *. *Journal of Biological Chemistry*, *286*(51), 43933–43943. https://doi.org/10.1074/jbc.M111.241232

Taguchi, T., Ikuno, M., Hondo, M., Parajuli, L. K., Taguchi, K., Ueda, J., Sawamura, M., Okuda, S., Nakanishi, E., Hara, J., Uemura, N., Hatanaka, Y., Ayaki, T., Matsuzawa, S., Tanaka, M., El-Agnaf, O. M. A., Koike, M., Yanagisawa, M., Uemura, M. T., … Takahashi, R. (2020). α-Synuclein BAC transgenic mice exhibit RBD-like behaviour and hyposmia: A prodromal Parkinson's disease model. *Brain*, *143*(1), 249–265. https://doi.org/10.1093/brain/awz380

Tan, A. H., Lim, S.-Y., Mahadeva, S., Loke, M. F., Tan, J. Y., Ang, B. H., Chin, K. P., Mohammad Adnan, A. F., Ong, S. M. C., Ibrahim, A. I., Zulkifli, N., Lee, J. K., Lim, W. T., Teo, Y. T., Kok, Y. L., Ng, T. Y., Tan, A. G. S., Zulkifle, I. M., Ng, C. K., … Lang, A. E. (2020). Helicobacter pylori Eradication in Parkinson's Disease: A Randomized Placebo-Controlled Trial. *Movement Disorders*, *35*(12), 2250–2260. https://doi.org/10.1002/mds.28248

Tansey, M. G., Wallings, R. L., Houser, M. C., Herrick, M. K., Keating, C. E., & Joers, V. (2022). Inflammation and immune dysfunction in Parkinson disease. *Nature Reviews. Immunology*, *22*(11), 657–673. https://doi.org/10.1038/s41577-022-00684-6

Tanudjojo, B., Shaikh, S. S., Fenyi, A., Bousset, L., Agarwal, D., Marsh, J., Zois, C., Heman-Ackah, S., Fischer, R., Sims, D., Melki, R., & Tofaris, G. K. (2021). Phenotypic manifestation of α-synuclein strains derived from Parkinson's disease and multiple system atrophy in human dopaminergic neurons. *Nature Communications*, *12*, 3817. https://doi.org/10.1038/s41467-021-23682-z

Taymans, J.-M., Van den Haute, C., & Baekelandt, V. (2006). Distribution of PINK1 and LRRK2 in rat and mouse brain. *Journal of Neurochemistry*, *98*(3), 951–961. https://doi.org/10.1111/j.1471-4159.2006.03919.x

Thannickal, T. C., Lai, Y.-Y., & Siegel, J. M. (2007). Hypocretin (orexin) cell loss in Parkinson's disease*. *Brain*, *130*(6), 1586–1595. https://doi.org/10.1093/brain/awm097

Thomas, D. M., Walker, P. D., Benjamins, J. A., Geddes, T. J., & Kuhn, D. M. (2004). Methamphetamine neurotoxicity in dopamine nerve endings of the striatum is associated with microglial activation. *The Journal of Pharmacology and Experimental Therapeutics*, *311*(1), 1–7. https://doi.org/10.1124/jpet.104.070961

Tierney, B., He, Y., Church, G., Segal, E., Kostic, A., & Patel, C. (2020). *The predictive power of the microbiome exceeds that of genome-wide association studies in the discrimination of complex human diseas*. https://doi.org/10.1101/2019.12.31.891978

Tofaris, G. K., Garcia Reitböck, P., Humby, T., Lambourne, S. L., O'Connell, M., Ghetti, B., Gossage, H., Emson, P. C., Wilkinson, L. S., Goedert, M., & Spillantini, M. G. (2006). Pathological changes in dopaminergic nerve cells of the substantia nigra and olfactory bulb in mice transgenic for truncated human alpha-synuclein(1-120): Implications for Lewy body disorders. *The Journal of Neuroscience: The Official Journal of the Society for Neuroscience*, *26*(15), 3942–3950. https://doi.org/10.1523/JNEUROSCI.4965-05.2006

Tuon, T., Meirelles, S. S., de Moura, A. B., Rosa, T., Borba, L. A., Botelho, M. E. M., Abelaira, H. M., de Mathia, G. B., Danielski, L. G., Fileti, M. E., Petronilho, F., Ignácio, Z. M., Quevedo, J., & Réus, G. Z. (2021). Behavior and oxidative stress parameters in rats subjected to the animal's models induced by chronic mild stress and 6-hydroxydopamine. *Behavioural Brain Research*, *406*, 113226. https://doi.org/10.1016/j.bbr.2021.113226

Uemura, N., Ueda, J., Yoshihara, T., Ikuno, M., Uemura, M. T., Yamakado, H., Asano, M., Trojanowski, J. Q., & Takahashi, R. (2021). α-Synuclein Spread from Olfactory Bulb Causes Hyposmia, Anxiety, and Memory Loss in BAC-SNCA Mice. *Movement Disorders*, *36*(9), 2036–2047. https://doi.org/10.1002/mds.28512

Unger, M. M., Spiegel, J., Dillmann, K.-U., Grundmann, D., Philippeit, H., Bürmann, J., Faßbender, K., Schwiertz, A., & Schäfer, K.-H. (2016). Short chain fatty acids and gut microbiota differ between patients with Parkinson's disease and age-matched controls. *Parkinsonism & Related Disorders*, *32*, 66–72. https://doi.org/10.1016/j.parkreldis.2016.08.019

Ungerstedt, U. (1968). 6-Hydroxy-dopamine induced degeneration of central monoamine neurons. *European Journal of Pharmacology*, *5*(1), 107–110. https://doi.org/10.1016/0014-2999(68)90164-7

Urakami, K., Masaki, N., Shimoda, K., Nishikawa, S., & Takahashi, K. (1988). Increase of striatal dopamine turnover by stress in MPTP-treated mice. *Clinical Neuropharmacology*, *11*(4), 360–368. https://doi.org/10.1097/00002826-198808000-00004

Valente, E. M., Abou-Sleiman, P. M., Caputo, V., Muqit, M. M. K., Harvey, K., Gispert, S., Ali, Z., Del Turco, D., Bentivoglio, A. R., Healy, D. G., Albanese, A., Nussbaum, R., González-Maldonado, R., Deller, T., Salvi, S., Cortelli, P., Gilks, W. P., Latchman, D. S., Harvey, R. J., … Wood, N. W. (2004). Hereditary Early-Onset Parkinson's Disease Caused by Mutations in PINK1. *Science*, *304*(5674), 1158–1160. https://doi.org/10.1126/science.1096284

Van Den Berge, N., & Ulusoy, A. (2022). Animal models of brain-first and body-first Parkinson's disease. *Neurobiology of Disease*, *163*, 105599. https://doi.org/10.1016/j.nbd.2021.105599

Van Den Eeden, S. K., Tanner, C. M., Bernstein, A. L., Fross, R. D., Leimpeter, A., Bloch, D. A., & Nelson, L. M. (2003). Incidence of Parkinson's Disease: Variation by Age, Gender, and Race/Ethnicity. *American Journal of Epidemiology*, *157*(11), 1015–1022. https://doi.org/10.1093/aje/kwg068

van der Heide, A., Dommershuijsen, L. J., Puhlmann, L. M. C., Kalisch, R., Bloem, B. R., Speckens, A. E. M., & Helmich, R. C. (2024). Predictors of stress resilience in Parkinson's disease and associations with symptom progression. *NPJ Parkinson's Disease*, *10*, 81. https://doi.org/10.1038/s41531-024-00692-4

Van Hul, M., Le Roy, T., Prifti, E., Dao, M. C., Paquot, A., Zucker, J.-D., Delzenne, N. M., Muccioli, G. G., Clément, K., & Cani, P. D. (2020). From correlation to causality: The case of Subdoligranulum. *Gut Microbes*, *12*(1), 1849998. https://doi.org/10.1080/19490976.2020.1849998

van Mierlo, T. J., Chung, C., Foncke, E. M., Berendse, H. W., & van den Heuvel, O. A. (2015). Depressive symptoms in Parkinson's disease are related to decreased hippocampus and amygdala volume. *Movement Disorders*, *30*(2), 245–252. https://doi.org/10.1002/mds.26112

Vasili, E., Dominguez-Meijide, A., Flores-León, M., Al-Azzani, M., Kanellidi, A., Melki, R., Stefanis, L., & Outeiro, T. F. (2022). Endogenous Levels of Alpha-Synuclein Modulate Seeding and Aggregation in Cultured Cells. *Molecular Neurobiology*, *59*(2), 1273–1284. https://doi.org/10.1007/s12035-021-02713-2

Vekrellis, K., Xilouri, M., Emmanouilidou, E., Rideout, H. J., & Stefanis, L. (2011). Pathological roles of α-synuclein in neurological disorders. *The Lancet Neurology*, *10*(11), 1015–1025. https://doi.org/10.1016/S1474-4422(11)70213-7

Vekrellis, K., Xilouri, M., Emmanouilidou, E., & Stefanis, L. (2009). Inducible over-expression of wild type alpha-synuclein in human neuronal cells leads to caspase-dependent non-apoptotic death. *Journal of Neurochemistry*, *109*(5), 1348–1362. https://doi.org/10.1111/j.1471-4159.2009.06054.x

Verbovaya, E. R., Kadnikov, I. A., Logvinov, I. O., Antipova, T. A., Voronin, M. V., & Seredenin, S. B. (2024). In vitro modelling of Parkinson's disease using 6-OHDA is associated with increased NQO2 activity. *Toxicology in Vitro*, *101*, 105940. https://doi.org/10.1016/j.tiv.2024.105940

Vicario, M., Cieri, D., Brini, M., & Calì, T. (2018). The Close Encounter Between Alpha-Synuclein and Mitochondria. *Frontiers in Neuroscience*, *12*. https://doi.org/10.3389/fnins.2018.00388

Villar-Conde, S., Astillero-Lopez, V., Gonzalez-Rodriguez, M., Villanueva-Anguita, P., Saiz-Sanchez, D., Martinez-Marcos, A., Flores-Cuadrado, A., & Ubeda-Bañon, I. (2021). The Human Hippocampus in Parkinson's Disease: An Integrative Stereological and Proteomic Study. *Journal of Parkinson's Disease*, *11*(3), 1345–1365. https://doi.org/10.3233/JPD-202465

Volles, M. J., Lee, S.-J., Rochet, J.-C., Shtilerman, M. D., Ding, T. T., Kessler, J. C., & Lansbury, P. T. (2001). Vesicle Permeabilization by Protofibrillar α-Synuclein: Implications for the Pathogenesis and Treatment of Parkinson's Disease. *Biochemistry*, *40*(26), 7812–7819. https://doi.org/10.1021/bi0102398

Volpi, R., Caffarra, P., Boni, S., Scaglioni, A., Malvezzi, L., Saginario, A., Chiodera, P., & Coiro, V. (1997). ACTH/cortisol involvement in the serotonergic disorder affecting the parkinsonian brain. *Neuropsychobiology*, *35*(2), 73–78. https://doi.org/10.1159/000119394

Volpi, R., Caffarra, P., Scaglioni, A., Maestri, D., Chiodera, P., & Coiro, V. (1994). Restoration of ACTH/cortisol and LH responses to naloxone by chronic dopaminergic treatment in Parkinson's disease. *Journal of Neural Transmission - Parkinson's Disease and Dementia Section*, *7*(1), 1–11. https://doi.org/10.1007/BF02252658

Volpicelli-Daley, L. A., Luk, K. C., Patel, T. P., Tanik, S. A., Riddle, D. M., Stieber, A., Meaney, D. F., Trojanowski, J. Q., & Lee, V. M.-Y. (2011). Exogenous α-Synuclein Fibrils Induce Lewy Body Pathology Leading to Synaptic Dysfunction and Neuron Death. *Neuron*, *72*(1), 57–71. https://doi.org/10.1016/j.neuron.2011.08.033

Vorhees, C. V., & Williams, M. T. (2006). Morris water maze: Procedures for assessing spatial and related forms of learning and memory. *Nature Protocols*, *1*(2), 848–858. https://doi.org/10.1038/nprot.2006.116

Vos, M., Esposito, G., Edirisinghe, J. N., Vilain, S., Haddad, D. M., Slabbaert, J. R., Van Meensel, S., Schaap, O., De Strooper, B., Meganathan, R., Morais, V. A., & Verstreken, P. (2012). Vitamin K2 is a mitochondrial electron carrier that rescues pink1 deficiency. *Science (New York, N.Y.)*, *336*(6086), 1306–1310. https://doi.org/10.1126/science.1218632

Wakabayashi, K., Takahashi, H., Ohama, E., & Ikuta, F. (1990). Parkinson's disease: An immunohistochemical study of Lewy body-containing neurons in the enteric nervous system. *Acta Neuropathologica*, *79*(6), 581–583. https://doi.org/10.1007/BF00294234

Wakabayashi, K., Takahashi, H., Takeda, S., Ohama, E., & Ikuta, F. (1988). Parkinson's disease: The presence of Lewy bodies in Auerbach's and Meissner's plexuses. *Acta Neuropathologica*, *76*(3), 217–221. https://doi.org/10.1007/BF00687767

Walsh, S., Finn, D. P., & Dowd, E. (2011). Time-course of nigrostriatal neurodegeneration and neuroinflammation in the 6-hydroxydopamine-induced axonal and terminal lesion models of Parkinson's disease in the rat. *Neuroscience*, *175*, 251–261. https://doi.org/10.1016/j.neuroscience.2010.12.005

Wang, W., Le, W.-D., Pan, T., Stringer, J. L., & Jaiswal, A. K. (2008). Association of NRH:Quinone Oxidoreductase 2 Gene Promoter Polymorphism With Higher Gene Expression and Increased Susceptibility to Parkinson's Disease. *The Journals of Gerontology: Series A*, *63*(2), 127–134. https://doi.org/10.1093/gerona/63.2.127

Wang, X., Becker, K., Levine, N., Zhang, M., Lieberman, A. P., Moore, D. J., & Ma, J. (2019). Pathogenic alpha-synuclein aggregates preferentially bind to mitochondria and affect cellular respiration. *Acta Neuropathologica Communications*, *7*(1), 41. https://doi.org/10.1186/s40478-019-0696-4

Wang, X., Shinkai, Y., & Doi, M. (2021). Retrogradely transmitted α-synuclein is taken up by the endophilin-independent endocytosis in the *C. elegans* neural circuit. *Biochemical and Biophysical Research Communications*, *552*, 176–182. https://doi.org/10.1016/j.bbrc.2021.03.029

Wang, X., Xu, J., Wang, Q., Ding, D., Wu, L., Li, Y., Wu, C., & Meng, H. (2021). Chronic stress induced depressive-like behaviors in a classical murine model of Parkinson's disease. *Behavioural Brain Research*, *399*, 112816. https://doi.org/10.1016/j.bbr.2020.112816

Wang, Z., Liu, S., Xu, X., Xiao, Y., Yang, M., Zhao, X., Jin, C., Hu, F., Yang, S., Tang, B., Song, C., & Wang, T. (2022). Gut Microbiota Associated With Effectiveness And Responsiveness to Mindfulness-Based Cognitive Therapy in Improving Trait Anxiety. *Frontiers in Cellular and Infection Microbiology*, *12*. https://www.frontiersin.org/articles/10.3389/fcimb.2022.719829

Wassouf, Z., Hentrich, T., Casadei, N., Jaumann, M., Knipper, M., Riess, O., & Schulze-Hentrich, J. M. (2019). Distinct Stress Response and Altered Striatal Transcriptome in Alpha-Synuclein Overexpressing Mice. *Frontiers in Neuroscience*, *12*, 1033. https://doi.org/10.3389/fnins.2018.01033

Wassouf, Z., Hentrich, T., Samer, S., Rotermund, C., Kahle, P. J., Ehrlich, I., Riess, O., Casadei, N., & Schulze-Hentrich, J. M. (2018). Environmental Enrichment Prevents Transcriptional Disturbances Induced by Alpha-Synuclein Overexpression. *Frontiers in Cellular Neuroscience*, *12*, 112. https://doi.org/10.3389/fncel.2018.00112

Watabe-Uchida, M., Zhu, L., Ogawa, S. K., Vamanrao, A., & Uchida, N. (2012). Whole-brain mapping of direct inputs to midbrain dopamine neurons. *Neuron*, *74*(5), 858–873. https://doi.org/10.1016/j.neuron.2012.03.017

Watanabe, Y., Gould, E., Daniels, D. C., Cameron, H., & McEwen, B. S. (1992). Tianeptine attenuates stress-induced morphological changes in the hippocampus. *European Journal of Pharmacology*, *222*(1), 157–162. https://doi.org/10.1016/0014-2999(92)90830-W

Wei, J., Xiang, L., Li, X., Song, Y., Yang, C., Ji, F., Chung, A. C. K., Li, K., Lin, Z., & Cai, Z. (2020). Derivatization strategy combined with parallel reaction monitoring for the characterization of short-chain fatty acids and their hydroxylated derivatives in mouse. *Analytica Chimica Acta*, *1100*, 66–74. https://doi.org/10.1016/j.aca.2019.11.009

Weiss, F., Labrador-Garrido, A., Dzamko, N., & Halliday, G. (2022). Immune responses in the Parkinson's disease brain. *Neurobiology of Disease*, *168*, 105700. https://doi.org/10.1016/j.nbd.2022.105700

Wersinger, C., & Sidhu, A. (2005). Disruption of the interaction of alpha-synuclein with microtubules enhances cell surface recruitment of the dopamine transporter. *Biochemistry*, *44*(41), 13612–13624. https://doi.org/10.1021/bi050402p

Westenbroek, C., Den Boer, J. A., & Ter Horst, G. J. (2003). Gender-specific effects of social housing on chronic stress-induced limbic Fos expression. *Neuroscience*, *121*(1), 189–199. https://doi.org/10.1016/s0306-4522(03)00367-1

Whitehouse, P. J., Vale, W. W., Zweig, R. M., Singer, H. S., Mayeux, R., Kuhar, M. J., Price, D. L., & De Souza, E. B. (1987). Reductions in corticotropin releasing factor-like immunoreactivity in cerebral cortex in Alzheimer's disease, Parkinson's disease, and progressive supranuclear palsy. *Neurology*, *37*(6), 905–909. https://doi.org/10.1212/wnl.37.6.905

Wingo, A. P., Velasco, E., Florido, A., Lori, A., Choi, D. C., Jovanovic, T., Ressler, K. J., & Andero, R. (2018). Expression of the PPM1F gene is regulated by stress and associated with anxiety and depression. *Biological Psychiatry*, *83*(3), 284–295. https://doi.org/10.1016/j.biopsych.2017.08.013

Winslow, A. R., Chen, C.-W., Corrochano, S., Acevedo-Arozena, A., Gordon, D. E., Peden, A. A., Lichtenberg, M., Menzies, F. M., Ravikumar, B., Imarisio, S., Brown, S., O'Kane, C. J., & Rubinsztein, D. C. (2010). α-Synuclein impairs macroautophagy: Implications for Parkinson's disease. *The Journal of Cell Biology*, *190*(6), 1023–1037. https://doi.org/10.1083/jcb.201003122

Wolfes, A. C., & Dean, C. (2020). The diversity of synaptotagmin isoforms. *Current Opinion in Neurobiology*, *63*, 198–209. https://doi.org/10.1016/j.conb.2020.04.006

Wu, G., Jiang, Z., Pu, Y., Chen, S., Wang, T., Wang, Y., Xu, X., Wang, S., Jin, M., Yao, Y., Liu, Y., Ke, S., & Liu, S. (2022). Serum short-chain fatty acids and its correlation with motor and non-motor symptoms in Parkinson's disease patients. *BMC Neurology*, *22*(1), 13. https://doi.org/10.1186/s12883-021-02544-7

Wu, N., Joshi, P. R., Cepeda, C., Masliah, E., & Levine, M. S. (2010). Alpha-synuclein overexpression in mice alters synaptic communication in the corticostriatal pathway. *Journal of Neuroscience Research*, *88*(8), 1764–1776. https://doi.org/10.1002/jnr.22327

Wu, Q., Yang, X., Zhang, Y., Zhang, L., & Feng, L. (2016). Chronic mild stress accelerates the progression of Parkinson's disease in A53T α-synuclein transgenic mice. *Experimental Neurology*, *285*, 61–71. https://doi.org/10.1016/j.expneurol.2016.09.004

Wyatt, L. R., Godar, S. C., Khoja, S., Jakowec, M. W., Alkana, R. L., Bortolato, M., & Davies, D. L. (2013). Sociocommunicative and sensorimotor impairments in male P2X4-deficient mice. *Neuropsychopharmacology: Official Publication of the American College of Neuropsychopharmacology*, *38*(10), 1993–2002. https://doi.org/10.1038/npp.2013.98

Xilouri, M., Brekk, O. R., Landeck, N., Pitychoutis, P. M., Papasilekas, T., Papadopoulou-Daifoti, Z., Kirik, D., & Stefanis, L. (2013). Boosting chaperone-mediated autophagy in vivo mitigates α-synuclein-induced neurodegeneration. *Brain*, *136*(7), 2130–2146. https://doi.org/10.1093/brain/awt131

Xilouri, M., Brekk, O. R., Polissidis, A., Chrysanthou-Piterou, M., Kloukina, I., & Stefanis, L. (2016). Impairment of chaperone-mediated autophagy induces dopaminergic neurodegeneration in rats. *Autophagy*, *12*(11), 2230–2247. https://doi.org/10.1080/15548627.2016.1214777

Xilouri, M., Vogiatzi, T., Vekrellis, K., Park, D., & Stefanis, L. (2009). Abberant alpha-synuclein confers toxicity to neurons in part through inhibition of chaperone-mediated autophagy. *PloS One*, *4*(5), e5515. https://doi.org/10.1371/journal.pone.0005515

Xu, J., Li, J., Sun, Y., Quan, W., Liu, L., Zhang, Q., Qin, Y., Pei, X., Su, H., & Chen, J. (2023). Identification of key genes and signaling pathways associated with dementia with Lewy bodies and Parkinson's disease dementia using bioinformatics. *Frontiers in Neurology*, *14*. https://doi.org/10.3389/fneur.2023.1029370

Xu, S., Liu, Y., Pu, J., Gui, S., Zhong, X., Tian, L., Song, X., Qi, X., Wang, H., & Xie, P. (2020). Chronic Stress in a Rat Model of Depression Disturbs the Glutamine–Glutamate–GABA Cycle in the Striatum, Hippocampus, and Cerebellum. *Neuropsychiatric Disease and Treatment*, *16*, 557–570. https://doi.org/10.2147/NDT.S245282

Yamaguchi, S., Yamane, T., Takahashi-Niki, K., Kato, I., Niki, T., Goldberg, M. S., Shen, J., Ishimoto, K., Doi, T., Iguchi-Ariga, S. M. M., & Ariga, H. (2012). Transcriptional activation of low-density lipoprotein receptor gene by DJ-1 and effect of DJ-1 on cholesterol homeostasis. *PloS One*, *7*(5), e38144. https://doi.org/10.1371/journal.pone.0038144

Yang, W., Yu, W., Li, X., Li, X., & Yu, S. (2020). Alpha-synuclein differentially reduces surface expression of *N*-methyl-d-aspartate receptors in the aging human brain. *Neurobiology of Aging*, *90*, 24–32. https://doi.org/10.1016/j.neurobiolaging.2020.02.015

Yang, X., Ai, P., He, X., Mo, C., Zhang, Y., Xu, S., Lai, Y., Qian, Y., & Xiao, Q. (2022). Parkinson's Disease Is Associated with Impaired Gut–Blood Barrier for Short-Chain Fatty Acids. *Movement Disorders*, *37*(8), 1634–1643. https://doi.org/10.1002/mds.29063

Yavich, L., Jäkälä, P., & Tanila, H. (2006). Abnormal compartmentalization of norepinephrine in mouse dentate gyrus in alpha-synuclein knockout and A30P transgenic mice. *Journal of Neurochemistry*, *99*(3), 724–732. https://doi.org/10.1111/j.1471-4159.2006.04098.x

Yin, S., Ma, X., Sun, Y., Yin, Y., Long, Y., Zhao, C., Ma, J., Li, S., Hu, Y., Li, M., Hu, G., & Zhou, J. (2023). RGS5 augments astrocyte activation and facilitates neuroinflammation via TNF signaling. *Journal of Neuroinflammation*, *20*(1), 203. https://doi.org/10.1186/s12974-023-02884-w

Yong, V. W. (2005). Metalloproteinases: Mediators of Pathology and Regeneration in the CNS. *Nature Reviews Neuroscience*, *6*(12), 931–944. https://doi.org/10.1038/nrn1807

Yoshino, H., Hirano, M., Stoessl, A. J., Imamichi, Y., Ikeda, A., Li, Y., Funayama, M., Yamada, I., Nakamura, Y., Sossi, V., Farrer, M. J., Nishioka, K., & Hattori, N. (2017). Homozygous alpha-synuclein p.A53V in familial Parkinson's disease. *Neurobiology of Aging*, *57*, 248.e7-248.e12. https://doi.org/10.1016/j.neurobiolaging.2017.05.022

Yu, W., Yang, W., Li, X., Li, X., & Yu, S. (2019). Alpha-synuclein oligomerization increases its effect on promoting NMDA receptor internalization. *International Journal of Clinical and Experimental Pathology*, *12*(1), 87–100.

Yu, Y., Li, Y., Gao, F., Hu, Q., Zhang, Y., Chen, D., & Wang, G. (2016). Vitamin K2 suppresses rotenone-induced microglial activation in vitro. *Acta Pharmacologica Sinica*, *37*(9), 1178–1189. https://doi.org/10.1038/aps.2016.68

Yu, Y.-X., Yu, X.-D., Cheng, Q., Tang, L., & Shen, M.-Q. (2020). The association of serum vitamin K2 levels with Parkinson's disease: From basic case-control study to big data mining analysis. *Aging (Albany NY)*, *12*(16), 16410–16419. https://doi.org/10.18632/aging.103691

Zarranz, J. J., Alegre, J., Gómez-Esteban, J. C., Lezcano, E., Ros, R., Ampuero, I., Vidal, L., Hoenicka, J., Rodriguez, O., Atarés, B., Llorens, V., Gomez Tortosa, E., del Ser, T., Muñoz, D. G., & de Yebenes, J. G. (2004). The new mutation, E46K, of alpha-synuclein causes Parkinson and Lewy body dementia. *Annals of Neurology*, *55*(2), 164–173. https://doi.org/10.1002/ana.10795

Zhang, L., Wang, X., Wang, M., Sterling, N. W., Du, G., Lewis, M. M., Yao, T., Mailman, R. B., Li, R., & Huang, X. (2017). Circulating Cholesterol Levels May Link to the Factors Influencing Parkinson's Risk. *Frontiers in Neurology*, *8*. https://doi.org/10.3389/fneur.2017.00501

Zhang, Z., Chu, S., Wang, S., Jiang, Y., Gao, Y., Yang, P., Ai, Q., & Chen, N. (2018). RTP801 is a critical factor in the neurodegeneration process of A53T α-synuclein in a mouse model of Parkinson's disease under chronic restraint stress. *British Journal of Pharmacology*, *175*(4), 590–605. https://doi.org/10.1111/bph.14091

Zhong, R., Chen, Q., Zhang, X., Li, M., & Lin, W. (2022). Helicobacter pylori infection is associated with a poor response to levodopa in patients with Parkinson's disease: A systematic review and meta-analysis. *Journal of Neurology*, *269*(2), 703–711. https://doi.org/10.1007/s00415-021-10473-1

Zhou, R. M., Huang, Y. X., Li, X. L., Chen, C., Shi, Q., Wang, G. R., Tian, C., Wang, Z. Y., Jing, Y. Y., Gao, C., & Dong, X. P. (2010). Molecular interaction of α-synuclein with tubulin influences on the polymerization of microtubule in vitro and structure of microtubule in cells. *Molecular Biology Reports*, *37*(7), 3183–3192. https://doi.org/10.1007/s11033-009-9899-2

Zou, K., Guo, W., Tang, G., Zheng, B., & Zheng, Z. (2013). A Case of early onset Parkinson's disease after major stress. *Neuropsychiatric Disease and Treatment*, *9*, 1067–1069. https://doi.org/10.2147/NDT.S48455

Supplementary Figures

a.

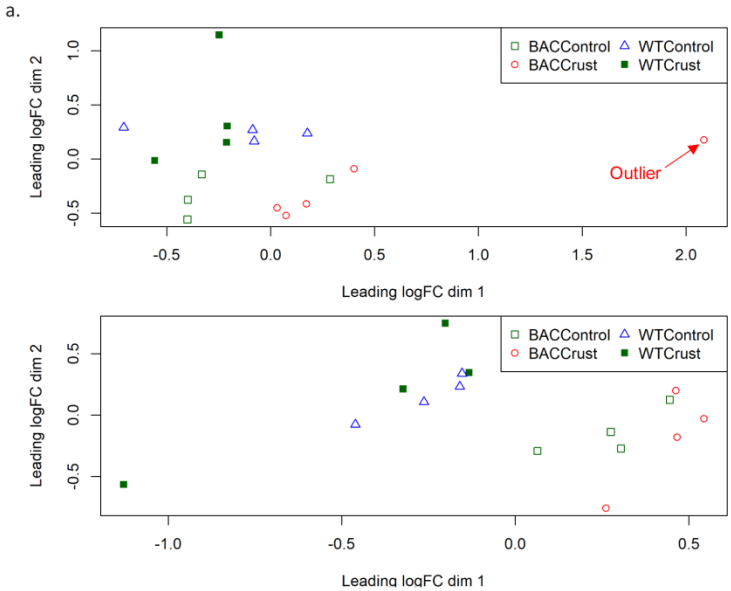

b.

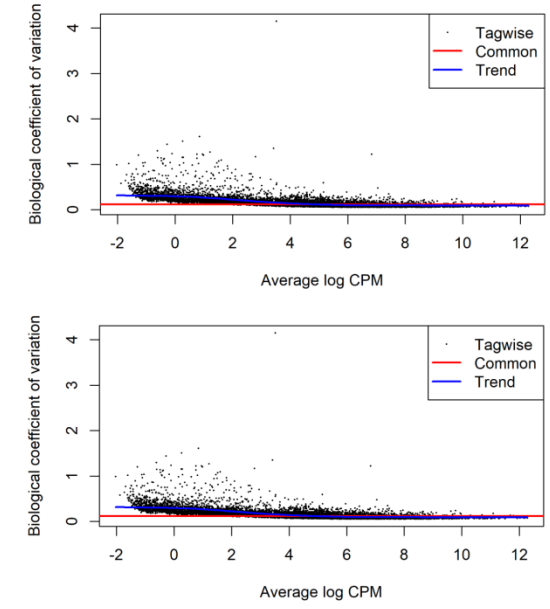

c.

No.	Top DEGs	No.	Top DEGs	No.	Top DEGs	No.	Top DEGs
1	*PCDHB6*	42	*VGLL4*	83	*RAB28*	124	*TAPBPL*
2	*MN1*	43	*IWS1*	84	*OAS1A*	125	*ABHD14A*
3	*NT5C1A*	44	*KLF7*	85	*CHCHD10*	126	*EPHB6*
4	*TMEM120A*	45	*PSD4*	86	*PIR*	127	*LOC679149*
5	*CASK*	46	*B3GNT3*	87	*TES*	128	*TOP3B*
6	*DUSP8*	47	*MERTK*	88	*TM2D1*	129	*NOTCH4*
7	*SPATA13*	48	*RPS6*	89	*LOC300308*	130	*RGS10*
8	*CABP1*	49	*CARD6*	90	*ANO1*	131	*RPL6*
9	*RBX1*	50	*FOSB*	91	*RGS5*	132	*ORAI2*
10	*VOM2R80*	51	*EXOC7*	92	*RGD1309748*	133	*SLC8B1*
11	*RASA3*	52	*CXCL1*	93	*RSAD2*	134	*DLL3*
12	*COPS6*	53	*P2RX4*	94	*SIPA1L2*	135	*KCNC2*
13	*PDXK*	54	*MPZL3*	95	*ACTA2*	136	*MZT2B*
14	*ZBTB3*	55	*CLCN2*	96	*LOC100911453*	137	*MMP16*
15	*LRRK2*	56	*IFITM3*	97	*LOC108348172*	138	*PXYLP1*
16	*ITPRIPL2*	57	*SLFN2*	98	*PARP14*	139	*SPAG6L*
17	*PRDX1*	58	*CMKLR1*	99	*G4*	140	*ZP2*
18	*MYOG*	59	*OCM2*	100	*ALDOA*	141	*TBXAS1*
19	*GFOD2*	60	*IL17RB*	101	*FREM3*	142	*DPH6*
20	*LOC108348161*	61	*MARF1*	102	*SPINT1*	143	*CARTPT*
21	*LOC103690054*	62	*MFSD3*	103	*SNCG*	144	*SMOC2*
22	*MYORG*	63	*OAS1F*	104	*VWA3A*	145	*NEPN*
23	*IRF2BPL*	64	*SDCBP2*	105	*EFCAB1*	146	*PAK6*
24	*FGFR3*	65	*TAS1R1*	106	*PNPLA1*	147	*RGS2*
25	*NDUFAF8*	66	*USP18*	107	*LILRB3A*	148	*LDLR*
26	*RIMS1*	67	*RPL39L*	108	*LILRB2*	149	*SERPINB6A*
27	*CHRDL1*	68	*MYCBP*	109	*CHCHD5*	150	*NQO2*
28	*INHBA*	69	*KCNA4*	110	*LYRM1*	151	*ALB*
29	*LIN7C*	70	*AC1576*	111	*SEC23IP*	152	*CBX6*
30	*PFKFB3*	71	*WIPI2*	112	*RTN4IP1*	153	*STEAP1*
31	*SEC11C*	72	*NEWGENE_1304700*	113	*CLIC2*	154	*POLR1B*
32	*MBIP*	73	*LOC100911402*	114	*SLC37A3*	155	*HSF2BP*
33	*ARSG*	74	*LGALS9*	115	*SPNS1*	156	*PPM1F*
34	*CDC25A*	75	*PARP16*	116	*CYP4V3*	157	*SRP14*
35	*TNFRSF19*	76	*GALM*	117	*MAN1A1*	158	*LOC361646*
36	*MRPL1*	77	*NPY5R*	118	*XKR5*	159	*SLC24A4*
37	*TAF10*	78	*CYP1B1*	119	*UBASH3A*	160	*ZC3HAV1*
38	*PENK*	79	*MOB4*	120	*RT1-M6-2*	161	*CCDC85A*
39	*DPAGT1*	80	*LRTM2*	121	*TTC30A1*	162	*RPS6KA2*
40	*KCNJ10*	81	*SUV39H1L1*	122	*CCNDBP1*		
41	*SCARB2*	82	*UFM1*	123	*LSM6*		

Supplementary Figure 1. (a) Multidimensional scaling plot of sample relationships before (top) and after (bottom) removal of the outlier. (b) Biological coefficients of variation (BCV) estimated with the edgeR pipeline. BCV measures the percentage difference of gene expression from replicate to replicate; tagwise = BCVs are calculated separately for each gene; Common = a common value of BCV calculated fo all genes; Trend = abundance-dependent fit, towards which, tagwise BCVs are squeezed via an empirical Bayes process. (c) List of top 162 DEGs among all the group comparisons.

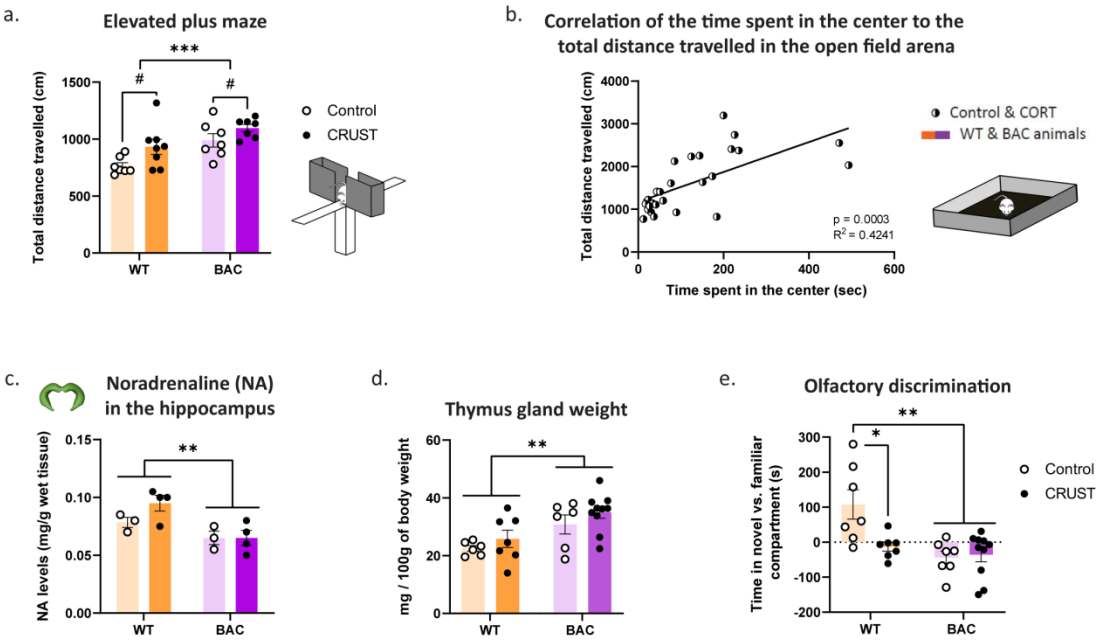

Supplementary Figure 2. (a) Total distance travelled (cm) in the EPM by WT and BAC animals after two weeks of CORT administration. (b) Simple linear regression correlation analysis of the time (s) spent in the center of the OF arena to the total distance travelled (cm) in the OF arena for the animals of all the experimental groups, regardless of genotype and treatment group. Linear regression analysis was applied. (c) NA levels (mg/g wet tissue) in the hippocampusof WT and BAC animals after two weeks of CORT administration. Two-way ANOVA was applied with Bonferroni's multiple comparisons post-hoc tests for (a) and (c-e). All data are expressed as Mean ± SEM. Asterisk (*) is used to denote genotype main effects while hashtag (#) denotes treatment main effects. Significance levels: */# p<0.05; ** p<0.01; *** p<0.001. N=7-8 per group for (a), (b) N=26, (c) N=3-4 per group, (d) and (e) N=6-10 per group.

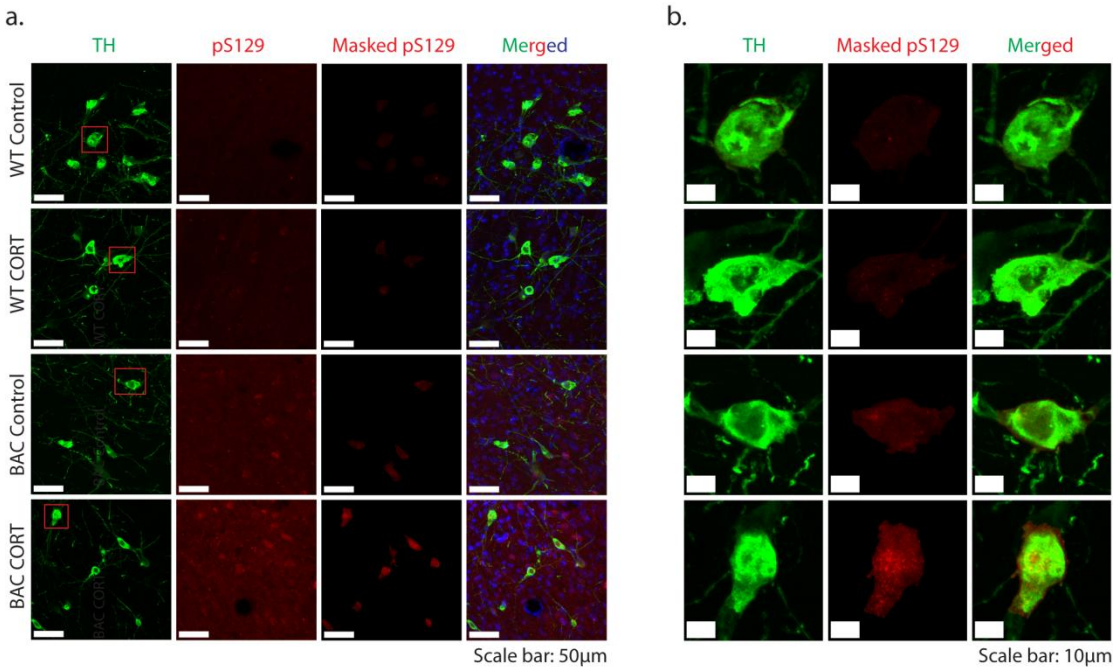

Supplementary Figure 3. Immunofluorescence staining against TH and pS129 asyn in the hypothalamus. In (a) the pictures that were captured with the 40x 1.20 objective and in (b) the pictures were captured with the 63x 1.30 objective.

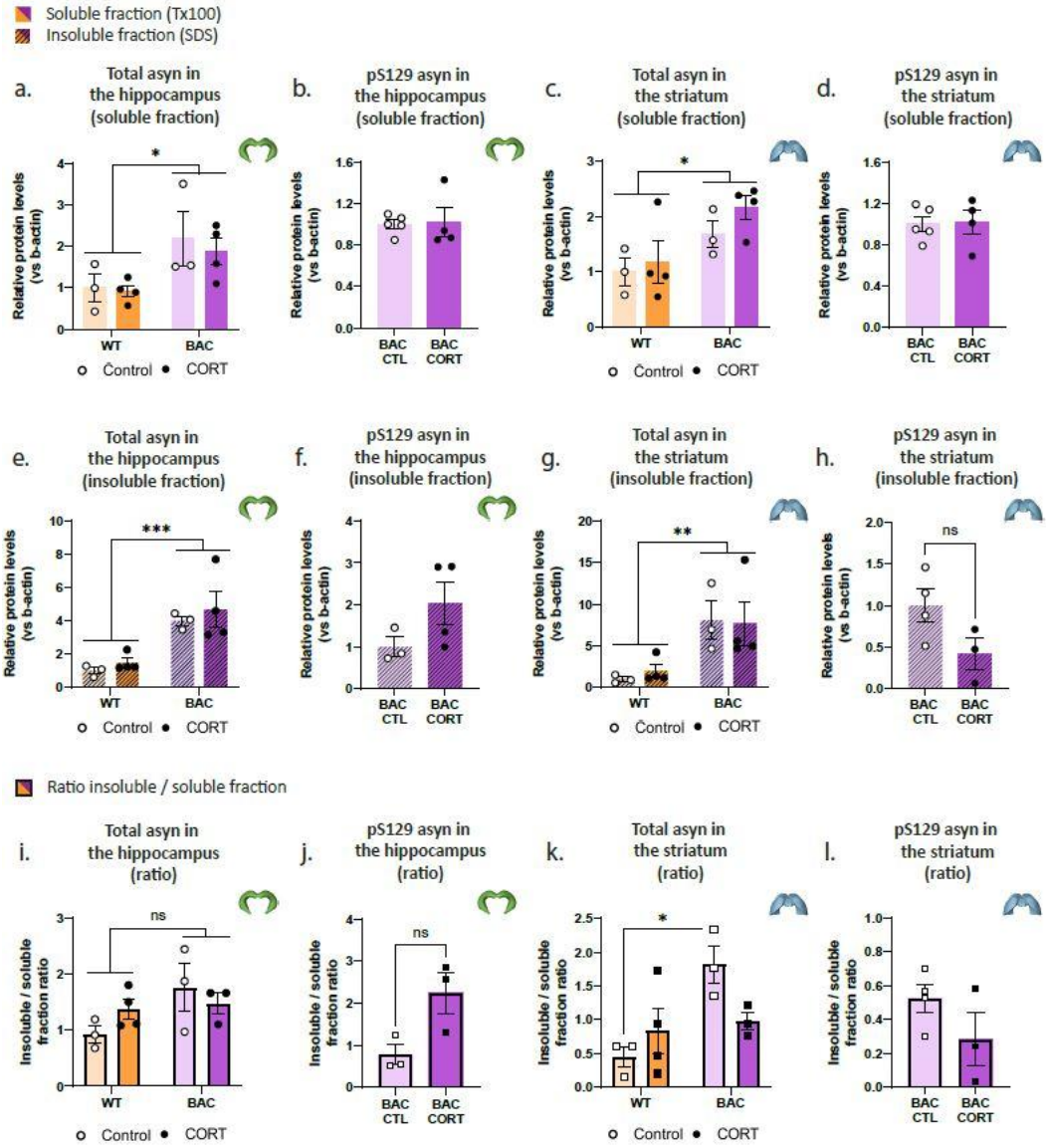

Supplementary Figure 4. By immunoblot biochemical analysis we measured relative protein levels (vs b-actin) of (a) total asyn levels in the soluble fraction of hippocampus, (b) pS129 asyn levels in the soluble fraction of hippocampus, (c) total asyn levels in the soluble fraction of striatum, (d) pS129 asyn levels in the soluble fraction of striatum, (e) total asyn levels in the insoluble fraction of hippocampus, (f) pS129 asyn levels in the insoluble fraction of hippocampus (g) total asyn levels in the insoluble fraction of striatum and (h) pS129 asyn levels in the insoluble fraction of striatum. We calculated insoluble to soluble fraction ratios of (i) total asyn levels in hippocampus, (j) pS129 asyn levels in hippocampus, (k) total asyn levels in striatum and (l) pS129 asyn levels in striatum. The relative quantification of protein levels was performed with the use of Fiji/ImageJ. Two-way ANOVAs were applied for (a), (c), (e), (g), (i) and (k) with Bonferroni's multiple comparisons post-hoc tests while unpaired t-tests were applied for the comparisons (b), (d), (f), (h), (j) and (l). Asterisk (*) is used to denote genotype effects. All data are expressed as Mean ± SEM. Significance levels: * $p<0.05$; ** $p<0.01$; *** $p<0.001$. N=3-5

Supplementary Tables

Supplementary Table 1. Lists of primary and secondary antibodies

Primary Antibody against	Clone	Catalog number	Working dilutions (WB)	Working dilutions (IHC)	Host species	Company
b-actin	C4	MAB1501	1/5000	-	mouse	EMD Millipore
	-	TA309077	1/2000	-	mouse	OriGene
GAPDH	6C5	MAB374	1/5000	-	mouse	EMD Millipore
GFAP (GA5)	-	3670	1/1000	1/1000	mouse	Cell Signaling Technology
Iba1/AIF-1	-	17198	-	1/400	rabbit	Cell Signaling Technology
	-	0199741	-	1/2000	rabbit	WAKO
Phospho S129	EP1536Y	ab51253	1/1000	1/2000	rabbit	Abcam
	-	23706	-	1/1000	rabbit	Cell signaling
Total asyn	SYN1	610786	1/1000	1/1000	mouse	BD Transduction Laboratories
Human asyn	4B12	GTX21904	1/1000	-	mouse	GeneTex
Rodent asyn	D37A6*	4179	1/1000	-	rabbit	Cell Signaling
Tyrosine Hydroxylase	LNC1	MAB318	-	1/1000	mouse	EMD Millipore
	-	ab76442	-	1/1000	chicken	Abcam
	-	657012	-	1/2000	rabbit	Calbiochem

Secondary antibody	Catalog number	Working dilutions (ICC or WB)	Company
CF488A green	-	1/2000	Biotium
CF555 red	-	1/2000	Biotium
Cy5	128-175-160	1/400	Jackson Imm. Affinipure

Supplementary Table 2. List of RT qPCR primers

Gene	**Forward (5'→ 3')**	**Reverse (5'→ 3')**
Rat GAPDH	ATGACTCTACCCACGGCAAG	CTGGAAGATGGTGATGGGTT
Rat b-actin	AGCCATGTACGTAGCCATCCA	TCTCCGGAGTCCATCACAATG
Rat SNCG	AAGGGGTCATGTATGTGGGC	TCTTCTCAGCCACCGAGGTT
Rat LRRK2	CCACTTCTGCCCAGGTCTTT	TCGCTCGCTTGCTATTGAGG
Rat SCARB2	CTGACTTCTGCAGGTCCGTC	TACCGAAAAGCAGGCAGTCC
Rat RGS2	GAAGCCCAAAACTGGCAAGA	TGAATGCAGCAAGCCCATATTT
Rat NQO2	TCCAGGAGGCAGAGACTGTT	GGAGCACTTTCTTACCTGCCA

Supplementary Table 3. Exact p-values for the results presented in Figures and Supplementary files

Fig.	Title	Statistical test	P value	P value summary	Significantly different	Multiple comparisons
1b	Corticotropin release factor in the hypothalamus	Unpaired t-test	0.0229	*	Yes	Does not apply
1c	Plasma corticosterone	Two-way ANOVA	Genotype effect: 0.0182 Treatment effect: 0.0628	* ns	Yes No	-
1d	Adrenal glands weight	Two-way ANOVA	Genotype effect: 0.0342	*	Yes	-
1e	Elevated plus maze	Two-way ANOVA	Interaction effect: 0.0135 Genotype effect: 0.0005 Treatment effect: 0.0282	* *** #	Yes Yes Yes	WT CTL vs WT CORT: p=0.0098 (**) WT CTL vs BAC CTL: p=0.0007 (***) WT CTL vs BAC CORT: p=0.0008 (***)
1f	Time spent in the center of the open field arena	Two-way ANOVA	Genotype effect: 0.0001 Treatment effect: 0.0013	** ###	Yes Yes	-
1g	Average PPI	Two-way ANOVA	Treatment effect: 0.0075	##	Yes	-
1h	Acoustic startle: Stimulus response	Two-way ANOVA	Interaction effect: 0.0047 Genotype effect: 0.0053	** ##	Yes Yes	WT CTL vs BAC CORT: p=0.0423 (*) WT CORT vs BAC CORT: p=0.0007 (***) BAC CTL vs BAC CORT: p=0.0532 (ns)
1i	Noradrenaline (NA) in the hypothalamus	Two-way ANOVA	Treatment effect: 0.0029	##	Yes	-
1j	Dopamine (DA) turnover in the hypothalamus	Two-way ANOVA	Interaction effect: 0.0019 Genotype effect: 0.0033 Treatment effect: 0.0117	** ** #	Yes Yes Yes	WT CTL vs BAC CTL: p=0.0031 (**) WT CORT vs BAC CTL: p=0.0027 (**) BAC CTL vs BAC CORT: p=0.0018 (**)
2b	pS129 in the hypothalamus	Two-way ANOVA	Genotype effect: 0.0002 Treatment effect: 0.0183	*** #	Yes Yes	-
2c	pS129 in the hippocampus	Two-way ANOVA	Genotype effect <0.0001	****	Yes	-
2d	Total asyn in the hippocampus (soluble fraction)	Two-way ANOVA	Genotype effect: 0.0165	*	Yes	-
2d	Total asyn in the hippocampus (insoluble fraction)	Two-way ANOVA	Genotype effect: 0.0008	***	Yes	-
2f	Total asyn in the striatum (soluble fraction)	Two-way ANOVA	Genotype effect: 0.0175	*	Yes	-
2f	Total asyn in the striatum (insoluble fraction)	Two-way ANOVA	Genotype effect: 0.0066	**	Yes	-
3b	TH+ neurons in the SNpc	Two-way ANOVA	Treatment effect: 0.0223	*	Yes	-

Fig.	Title	Statistical test	P value	P value summary	Significantly different	Multiple comparisons
3d	pS129 asyn in the SNpc	Two-way ANOVA	Interaction effect: 0.0403 Genotype effect<0.0001 Treatment effect: 0.0001	* **** ###	Yes Yes Yes	WT CTL vs BAC CTL & BAC CORT: p<0.0001 (****) WT CORT vs BAC CTL & BAC CORT: p<0.0001 (****) BAC CTL vs BAC CORT: p=0.0005 (***)
3e	TH+ fibers DL striatum	Two-way ANOVA	Genotype effect: 0.0138 Treatment effect: 0.0137	* #	Yes Yes	-
3g	TH+ fibers V striatum	Two-way ANOVA	Interaction effect: 0.0399	*	Yes	ns
4b	Astrocytes (GFAP) expression (in the SNpc)	Two-way ANOVA	Treatment effect:0.0327	#	Yes	-
4e	GFAP in the striatum	Two-way ANOVA	Interaction effect: 0.0449	*	Yes	ns
4g	Astrocytes (GFAP) expression (in the striatum)	Two-way ANOVA	Interaction effect: 0.0039 Genotype effect: 0.01	** *	Yes Yes	WT CTL vs WT CORT p=0.0489 (*) WT CTL vs BAC CTL p=0.004 (**) WT CTL vs BAC CORT p=0.0547 (ns)
4h	Microglia (Iba1) expression (in the striatum)	Two-way ANOVA	Interaction effect: 0.0086	**	Yes	WT CTL vs WT CORT p=0.0809 (ns)
5a	Total distance travelled (Open Field)	Two-way ANOVA	Genotype effect <0.0001 Treatment effect:0.0006	**** ###	Yes Yes	-
5b	Total number of rearings (Open Field)	Two-way ANOVA	Interaction effect: 0.0426 Genotype effect<0.0001	* ****	Yes Yes	WT CTL vs BAC CORT: p=0.0003 (***) WT CORT vs BAC CORT: p=0.0001 (***) BAC CTL vs BAC CORT: p=0.0404 (*)
5c	Postural instability	Two-way ANOVA	Treatment effect: 0.0215	#	Yes	-
5d	Gait analysis: Stride length (Right Forelimb)	Two-way ANOVA	Interaction effect: 0.0494 Genotype effect: 0.0064 Treatment effect:0.04	* ** #	Yes Yes Yes	WT CTL vs WT CORT: P=0.0558 (ns) WT CTL vs BAC CTL: P=0.0199 (*) WT CTL vs BAC CORT: P=0.0071 (**)
5d	Gait analysis: Stride length (Left Forelimb)	Two-way ANOVA	Genotype effect: 0.0047	**	Yes	-
5d	Gait analysis: Stride length (Right Backlimb)	Two-way ANOVA	Genotype effect: 0.0083 Treatment effect: 0.0378	** #	Yes Yes	-
5d	Gait analysis: Stride length (Right Backlimb)	Two-way ANOVA	Genotype effect: 0.007	**	Yes	-
6b	Body weight	Two-way ANOVA	Treatment effect <0.0001	####	Yes	-
6c	Adrenal glands weight	Two-way ANOVA	Treatment effect: 0.025	##	Yes	-
6d	Thymus gland weight	Two-way ANOVA	Genotype effect: 0.0136	*	Yes	-

Fig.	Title	Statistical test	P value	P value summary	Significantly different	Multiple comparisons
6e	Total distance travelled in the open field	Two-way ANOVA	Interaction effect: 0.0148 Genotype effect: 0.0001 Treatment effect: 0.0005	* *** ###	Yes Yes Yes	WT CTL vs BAC CTL p=0.0002 (***) WT CRUST vs BAC CTL p <0.0001 (****) BAC CTL vs BAC CRUST p=0.0004 (***)
6f	Time spent in the center of the open field arena	Two-way ANOVA	Genotype effect: 0.0462 Treatment effect: 0.0025	* ##	Yes Yes	-
6g	Olfactory discrimination	Two-way ANOVA	Interaction effect: 0.0145 Genotype effect: 0.0055	* **	Yes Yes	WT CTL vs BAC CTL: p=0.0007 (***) WT CTL vs BAC CRUST p=0.0107 (*)
6h	Average PPI	Two-way ANOVA	Interaction effect: 0.02	*	Yes	BAC CTL vs BAC CRUST p=0.0368 (*)
6i	Acoustic startle: Stimulus response	Two-way ANOVA	Treatment effect: 0.0429	#	Yes	-
6j	Morris water maze: Time spent in target quadrant	Two-way ANOVA	Genotype effect: 0.0857 Treatment effect: 0.0472	ns #	No Yes	-
6k	Morris water maze: Number of platform crossings	Two-way ANOVA	Genotype effect: 0.056 Treatment effect: 0.056	ns ns	No No	-
7c	TH+ neurons in the SNpc	Two-way ANOVA	Genotype effect: 0.0111 Treatment effect:0.0183	* #	Yes Yes	-
7e	Dopamine (DA) in the striatum	Two-way ANOVA	Interaction effect: 0.0069 Genotype effect: 0.0008	** ***	Yes Yes	WT CTL vs BAC CTL p=0.0015 (**) WT CRUST vs BAC CTL p=0.0091 (**) WT CRUST vs BAC CRUST p=0.0231 (*)
7f	Dopamine (DA) turnover in the striatum	Two-way ANOVA	Genotype effect: 0.0321	*	Yes	-
7h	Dopamine (DA) in striatal extracellular milieu	Two-way ANOVA	Interaction effect: 0.0069 Genotype effect: 0.01	** ns	Yes No	WT CTL vs WT CRUST p=0.0327 (*) WT CTL vs BAC CTL p=0.0307 (*)
7i	Dopamine (DA) turnover in striatal extracellular milieu	Two-way ANOVA	Interaction effect: 0.059 Genotype effect: 0.0084 Treatment effect: 0.0178	** ** #	Yes Yes Yes	WT CTL vs WT CRUST p=0.0055 (**) WT CTL vs BAC CTL p=0.006 (**) WT CTL vs BAC CRUST p=0.0046 (**)
7j	Asyn levels in striatal extracellular milieu	Paired t-test	0.058	**	Yes	Does not apply
8c	Total asyn (Striatum soluble fraction)	Two-way ANOVA	Treatment effect: 0.0032	**	Yes	-
8d	1st truncated band Total asyn (Striatum soluble fraction)	Two-way ANOVA	Interaction effect: 0.09 Genotype effect: 0.0018 Treatment effect:0.0586	ns ** ns	No Yes No	-

Fig.	Title	Statistical test	P value	P value summary	Significantly different	Multiple comparisons
8e	2nd truncated band Total asyn (Striatum soluble fraction)	Two-way ANOVA	Interaction effect: 0.0237 Genotype effect: 0.0019 Treatment effect:0.0197	* ** #	Yes Yes Yes	WT CTL vs BAC CRUST p=0.0024 (**) WT CRUST vs BAC CRUST p=0.005 (**) BAC CTL vs BAC CRUST p=0.0139 (*)
8f	pS129 asyn (Striatum soluble fraction)	Two-way ANOVA	Interaction effect: 0.0747 Genotype effect <0.0001	ns ****	No Yes	-
8n	pS129 asyn (Striatum insoluble fraction)	Two-way ANOVA	Genotype effect: 0.0017	**	Yes	-
10 c	Astrocytes (GFAP) expression	Two-way ANOVA	Treatment effect:0.0144	#	Yes	-
10 d	Microglia (Iba1) expression	Two-way ANOVA	Interaction effect: 0.0134 Treatment effect:0.0003	* ###	Yes Yes	WT CTL vs WT CRUST p=0.0008 (***) WT CTL vs BAC CRUST p=0.0888 (ns) WT CRUST vs BAC CTL p=0.0107 (*)
11a	Glutamate in olfactory bulb	Two-way ANOVA	Genotype effect: 0.0003	***	Yes	-
11d	Glutamate in prefrontal cortex	Two-way ANOVA	Treatment effect <0.0001	####	Yes	-
11e	Glutamine in prefrontal cortex	Two-way ANOVA	Treatment effect <0.0001	####	Yes	-
11f	GABA in prefrontal cortex	Two-way ANOVA	Treatment effect: 0.0178	##	Yes	-
11g	Glutamate in striatum	Two-way ANOVA	Treatment effect: 0.0911	ns	No	-
11h	Glutamine in striatum	Two-way ANOVA	Interaction effect: 0.09 Treatment effect: 0.0019	ns ##	No Yes	-
11i	GABA in striatum	Two-way ANOVA	Interaction effect: 0.0007 Genotype effect: 0.0006 Treatment effect: 0.0007	*** *** ###	Yes Yes Yes	WT CTL vs BAC CTL p=0.0003 (***) WT CRUST vs BAC CTL p=0.0003 (***) BAC CTL vs BAC CRUST p <0.0001
11j	Glutamate in hippocampus	Two-way ANOVA	Interaction effect: 0.05 Treatment effect: 0.0007	ns ####	No Yes	-
11k	Glutamine in hippocampus	Two-way ANOVA	Treatment effect <0.0001	####	Yeap	-
11l	GABA in hippocampus	Two-way ANOVA	Genotype effect: 0.031	*	Yes	-
11m	Glutamate in ventral midbrain	Two-way ANOVA	Treatment effect: 0.046	#	Yes	-
11n	Glutamine in ventral midbrain	Two-way ANOVA	Genotype effect: 0.1002 Treatment effect: 0.1096	ns ns	No No	-
12c	1st truncated band Total asyn (Hippocampus soluble fraction)	Two-way ANOVA	Interaction effect: 0.1021 Genotype effect: 0.0007 Treatment effect: 0.0336	ns *** #	No Yes Yes	
12e	pS129 asyn (Hippocampus soluble fraction)	Two-way ANOVA	Genotype effect: 0.0189	*	Yes	-

Fig.	Title	Statistical test	P value	P value summary	Significantly different	Multiple comparisons
14 c	SNCG	Two-way ANOVA	Interaction effect: 0.0287 Genotype effect < 0.0001 Treatment effect: 0.0017	* **** ##	Yes Yes Yes	WT CTL vs WT CRUST p=0.0058 (**) WT CTL vs BAC CTL p=0.0002 (***) WT CTL vs BAC CRUST p=0.0009 (***) WT CRUST vs BAC CRUST p<0.0001 (****) WT CRUST vs BAC CRUST p<0.0001 (****)
14 d	LRRK2	Two-way ANOVA	Genotype effect: 0.0269	*	Yes	-
14 f	RGS2	Two-way ANOVA	Interaction effect: 0.0208 Genotype effect: 0.0013 Treatment effect <0.0001	* ** ####	Yes Yes Yes	WT CTL vs WT CRUST p<0.0001 (****) WT CTL vs BAC CTL p=0.0040 (**) WT CTL vs BAC CRUST p<0.0001 (****) WT CRUST vs BAC CTL p=0.0657 (ns) BAC CTL vs BAC CRUST p=0.0074 (**)
14 g	NQO2	Two-way ANOVA	Interaction effect: 0.0086 Genotype effect: <0.0001 Treatment effect: 0.1016	** **** ##	Yes Yes ns	WT CTL vs BAC CTL p=0.0061 (ns) WT CTL vs BAC CRUST p=0.0006 (***) WT CRUST vs BAC CRUST p< 0.0071 (**) WT CRUST vs BAC CRUST p< 0.0001 (****) BAC CTL vs BAC CRUST p=0.030 (*)
16b	Acetic acid (C2:0)	Two-way ANOVA	Genotype effect: 0.0041	**	Yes	-
16c	Propionic acid (C3:0)	Two-way ANOVA	Genotype effect: 0.0137	*	Yes	-
16d	Butyric acid (C4:0)	Two-way ANOVA	Genotype effect: 0.0232	*	Yes	-
17a	Acetic acid (C2:0)	Two-way ANOVA	Genotype effect: 0.0303	*	Yes	-
S2a	Elevated Plus Maze (total distance travelled)	Two-way ANOVA	Genotype effect: 0.0008 Treatment effect: 0.0127	*** #	Yes Yes	-
S2c	Noradrenaline (NA) in the hippocampus	Two-way ANOVA	Genotype effect: 0.0064	**	Yes	-
S2d	Thymus gland weight	Two-way ANOVA	Genotype effect: 0.0020	**	Yes	-
S2e	Olfactory discrimination	Two-way ANOVA	Interaction effect: 0.0176 Genotype effect: 0.0019 Treatment effect: 0.0355	* ** ##	Yes Yes Yes	WT CTL vs WT CORT: p=0.0198 (*) WT CTL vs BAC CTL: p=0.0023 (**) WT CTL vs BAC CORT: p=0.0017 (**)

Fig.	Title	Statistical test	P value	P value summary	Significantly different	Multiple comparisons
S4i	Total asyn in the hippocampus (ratio)	Two-way ANOVA	Genotype effect: 0.0939	ns	No	-
S4j	pS129 asyn in the hippocampus (ratio)	Unpaired t-test	Genotype effect: 0.0505	ns	No	Does not apply
S4k	Total asyn in the striatum (ratio)	Two-way ANOVA	Interaction effect: 0.0490 Genotype effect: 0.0204	* *	Yes Yes	WT CTL vs BAC CTL: P=0.0416 (*)